Ankara Üniversitesi Veteriner Fakültesi Dergisi

Veterinary Journal of Ankara University

ISSN 1300-0861 • E-ISSN 1308-2817 Volume 70 • Number 1 • Year 2023

Ankara Univ Vet Fak Derg - vetjournal.ankara.edu.tr - Open Acsess

Ankara Üniversitesi Veteriner Fakültesi Dergisi

Veterinary Journal of Ankara University

ISSN 1300-0861 ● E-ISSN 1308-2817 Volume 70 ● Number 1 ● Year 2023

Ankara Univ Vet Fak Derg - vetjournal.ankara.edu.tr - Open Access

Ankara Üniversitesi Veteriner Fakültesi Dergisi
Volume: 70 • *Number*: 1 • *Year*: 2023
Veterinary Journal of Ankara University
Quarterly Scientific Journal
ISSN 1300-0861 E-ISSN 1308-2817

Publisher
On behalf of Ankara University, Faculty of Veterinary Medicine
Prof. Dr. Ender YARSAN
Dean

Publisher
Address
Ankara University, Faculty of Veterinary Medicine
Publication Subcommittee
06 110 Ankara, Türkiye
Tel: 90 312 317 03 15, **Fax:** 90 312 316 44 72
E-mail: vfdergi@veterinary.ankara.edu.tr
URL: http://vetjournal.ankara.edu.tr
Publication Type: Peer- reviewed and published quarterly online by DergiPark Akademik

This journal is covered by **SCI-EXP** and **JCR** of Thomson Reuters®, **CAB Abstracts**, **Global Health**, **CAB Direct, Database Subsets; Scopus** and **TR Dizin** database systems.

Web Address
http://vetjournal.ankara.edu.tr

Ankara Üniversitesi Basımevi / *Ankara University Press*
İncitaşı Sokak No:10 06510 Beşevler / ANKARA
Tel: 0 (312) 213 66 55
Basım Tarihi: 30/12/2022

Ankara Üniversitesi Veteriner Fakültesi Dergisi
Volume: 70 • *Number*: 1 • *Year*: 2023
Veterinary Journal of Ankara University

CONTENTS

Research Article

Short Communication

Case Report

Review

EDITORIAL

Dear Readers,

On behalf of the Editorial Board, it is my great pleasure to share the new issue of Veterinary Journal of Ankara University. The first issue of our journal appeared in 1954. Since then, it has been published four times a year and indexed in major indexing databases such as SCIE, Scopus, TR Index. The journal will begin to be published in a new format as of this issue and we hope you enjoy this new layout. In this issue, there are 12 research articles, 1 short article, 1 case report and 1 review article. Article publishing processes are operated at 5 main steps. The first step is the “Preliminary Review” stage. At this stage, the preliminary report on the submitted arricle is prepared by the relevant field editors. These reports are evaluated at the weekly meeting held by the Editorial Board; where the decision to initiate the further evaluation steps are confirmed. Rejected articles are returned to the author with their preliminary evaluation reports. Articles that passed this stage are then moved to the second stage, which is names as the “Pre-Evaluation” stage. In this stage, English language, fluency, spellings, plegiarism, ethics committee requisities and statistics are carefully examined. At this stage, necessary corrections and adjustments, if any, are recommended to the author. This stage is followed by the third stage which is the “Referee Evaluation”. Each article is subjected to double-blind review. Articles that successfully complete this stage are taken to the fourth stage, which is the "Proofreader" stage. The paper is now finalized and arranged by the journal editors in accordance with the rules for journal writing, and the layout is completed by getting the DOI number. The fifth stage is the "Pre-press Control" stage; where the article is sent to the authors for final control before printing and their approval for publication and the article publication process is completed. I would like to extend a very warm welcome to the readers and academics; and would like to conclude as an open invitation that you will join us as authors.

Wishing out readers all the very best,

Sincerely.

Dr. Levent ALTINTAŞ
Editor in Chief
Ankara Üniversitesi Veteriner Fakültesi Dergisi

Assessment of the feather score and health score in laying hens reared at different cage densities

Uğur ÖZENTÜRK[1,a, ✉], Ahmet YILDIZ[1,b], Murat GENÇ[1,c]

[1]Ataturk University, Faculty of Veterinary Medicine, Department of Animal Science, Erzurum, Türkiye

[a]ORCID: 0000-0002-2037-9340; [b]ORCID: 0000-0002-4812-6089; [c]ORCID: 0000-0002-9565-0887

ARTICLE INFO

Article History
Received : 21.04.2021
Accepted : 24.10.2021
DOI: 10.33988/auvfd.925177

Keywords
Cage density
Feather score
Health score
Laying hen

✉Corresponding author
ugur.ozenturk@atauni.edu.tr

How to cite this article: Özentürk U, Yıldız A, Genç M (2023): Assessment of the feather score and health score in laying hens reared at different cage densities. Ankara Univ Vet Fak Derg, 70 (1), 1-8. DOI: 10.33988/auvfd.925177.

ABSTRACT

This study aimed to investigate plumage conditions, injuries in the comb, cloaca, and feet at the end of the laying period (73 weeks of age) in native Atak-S (A-S) and foreign Isa Brown (IB) and Novogen White (NW) genotypes reared at two different cage densities. A total of 480 hens, including 160 of each hybrid, were used in the present study. Each hybrid group was divided into subgroups containing eight (468.75 cm^2/hen) and 12 animals (312.50 cm^2/hen) each with eight replications. The feathering status in six different regions of the body (neck, breast, back, wing, tail, and cloaca) was assessed by scoring these regions both separately and as a whole. To detect injuries in the body, the comb, cloaca, and foot regions were examined. In the study, the effect of genotype on the feather score was found to be significant in all body regions except for the tail region (P<0.05). In all hybrids, the highest plumage loss was in the tail region, while the lowest was in the cloaca region in IB and the neck and wing regions in NW and A-S. The best results were obtained from the IB hybrid in terms of the total plumage condition. Genotype had a significant effect on the health scores in all body regions except for the comb (P<0.05). In terms of the feather score, the effect of cage density was determined to be significant in all body regions (P<0.01). It was observed that plumage loss increased as the cage density increased.

Introduction

The integument of hens is associated with animal health (16) and behavior (33). In the assessment of the effects of factors that influence the health and welfare levels of hens such as genotype, breeding systems, cage density, and nutrition on integument, the scoring method is extensively used. Integument is frequently determined based on scoring the feathers, feet and skin (30). Feathers protect hens from the abrasive effect of the cage material and injuries (14). The feather score is a relatively neglected parameter in commercial laying poultry in comparison to some other classical performance data such as egg yield and feed consumption. Nevertheless, feathering status is an important indicator in interpreting health, performance and welfare (21). This is because a disruption occurring in feathers may lead to injuries and deaths by triggering cannibalistic behavior (14). In addition to the economic loss brought about by deaths, the increase in feed consumption observed for the preservation of body temperature due to plumage loss also raises economic costs (14, 38). It was also reported that the egg yield of hens decreases in relation to increased stress in broods where feather pecking occurs (11, 38).

It has been emphasized that the easiest method of assessing the welfare of laying hens is to assess the state of their feathers and injuries (9, 14, 29). In a study that included expert opinions for the purpose of creating a protocol to assess welfare, it was reported that the plumage condition in hens was the most significant indicator among 17 different parameters (32). It was stated that the main cause of plumage loss leading to reduced welfare is the behavior of feather picking and pecking (4). It is specified that this behavior cannot be eliminated even though the most suitable conditions are provided, and thus, to reduce the effect of the behavior of feather picking and feather pecking, it is needed to regularly observe the brood and visually assess the integument (3). Factors such as cage systems (23), cage density (20), and nutrition affect the formation of the behavior of feather picking and pecking (1, 32). Additionally, it was stated that the

formation of this behavior varies in different hybrids (5). This situation suggests a genetic background (8, 24).

In Türkiye, which is one of the most prominent countries in the world in terms of egg production, native laying hybrids constitute approximately 2.5% of the hens used in production (12). In the poultry farming program of the 2016-2020 Master Plan of the General Directorate of Agricultural Research and Policies of the Turkish Ministry of Agriculture and Forest Affairs, it has been planned to conduct efforts towards supplying breeding stock resources for laying and broiler hen production from domestic sources and to create feeding and breeding methods appropriate for this objective. For this reason, it was emphasized that it is needed to carefully investigate breeding and nutrition techniques in native hybrids and yields under private sector conditions with the effects of environmental factors (18).

This study aimed to investigate plumage conditions, injuries in the comb and cloaca, and feet in relation to bumblefoot syndrome at the end of the laying period (73 weeks of age) in native (Atak-S) and foreign (Isa Brown, Novogen White) genotypes reared at two different cage densities.

Materials and Methods

The study was carried out at the Food and Animal Farming Research and Application Center of Atatürk University. This study was approved by the Animal Ethics Committee of Animal Experiments of the Veterinary Medicine Faculty at Atatürk University (2020/07).

As the animal material, native Atak-S (A-S) and foreign Isa Brown (IB) and Novogen White (NW) hens, all at the same age (73 weeks old), were used. In the trial, 3 different genotypes (A-S, NW, and IB) and 2 different cage housing densities (8 hens/cage and 12 hens/cage) were utilized. A total of 480 hens, including 160 of each hybrid, were used, and each hybrid group was divided into subgroups containing 8 and 12 animals, each with 8 replications. Cage density-1 (CD-1) was defined as 468.75 cm^2 cage floor space per hen, while Cage Density-2 (CD-2) was defined as 312.50 cm^2 of cage floor space per hen. All cage units had equal dimensions to each other. The cage dimensions were as a depth of 60 cm, a width of 62.5 cm, the rear height of 46 cm, the front height of 51 cm, feeder length of 62.5 cm, and base slope of 7°. Each cage had 2 nipple waterers. The animals were grown in the same poultry house during both rearing and laying periods. The in-house temperature was kept at 16-24°C with sensors connected to the ventilation and heating systems. Lighting was adjusted as 17 hours of light per day with fluorescent bulbs giving white light. In the laying period, the animals were given egg starter feed (2750 ME 17.50 HP) in the 16th-20th weeks, 1-st period laying feed (2750 ME 16.26 HP) in the 21st-45th weeks, 2-nd period laying feed (2720 ME 15.83 HP) in the 46th-65th weeks, and 3-rd period laying feed (2720 ME 15.65 HP) after the 65th week in granule form as *ad libitum*.

Feather Scoring Method: At the end of the laying period (73 weeks of age), each hen was individually examined by visual examination for feathering score. Two methods are frequently used in scoring integuments. The first one of these is the assessment of the body as a whole, while the other is the assessment of body regions separately. While the former provides the opportunity for a faster and simpler assessment, it cannot explain the reasons for plumage loss occurring in different regions of the body (30). In the study, the feathering status in 6 different regions of the body (neck, breast, back, wing, tail, and cloaca) was assessed by scoring these body regions both separately and as a whole. The scoring was made in the range of 1-4 (Table 1) (8, 30). In total scoring, scores lower than 10 to 12 indicate a significant plumage loss in the entire body. Scores of 3 and higher locally and higher than 18-20 in total scoring show that the state of the plumage and integument is good (30).

Health (Integument) Scoring Method: To detect injuries in the body, the comb and cloaca regions were examined, and the feet were checked in relation to bumblefoot syndrome. The scoring was made in the range of 1-4 (Table 1) (8, 30). Scores of 2 and lower by body region show that the integument and plumage are significantly damaged, or they indicate the presence of heavy injury, abrasion, aggressive behavior in the brood, and bumblefoot syndrome (8, 30).

Table 1. Description of the scoring scheme used for the assessment of plumage and integument condition.

Parameter/Score	Feather Loss	Integument Damage
1	>75% of the feathers of the body region missing	Single or multiple injuries of >1.0 cm
2	>50% and <75% of the feathers of the body region missing	Multiple injuries of <0.5 cm or single injuries of >0.5 cm and <1.0 cm
3	>25% and <50% of the feathers of the body region missing	Single injury of <0.5 cm diameter or length
4	No feather loss or <25% of the feathers of the body region missing	No integument damage

DOI: 10.33988/auvfd.925177

Statistical analysis: The non-parametric Kruskal-Wallis H test was used for the genotypes (IB, A-S and NW) for plumage damage and injuries observed in different regions of the body on a Likert-type scale, whereas the non-parametric Mann-Whitney U test was utilized for the pairwise comparisons of density (CD-1 and CD-2) and the genotypes. By analyzing the normality of the distribution of the data with the Shapiro-Wilk test, it was determined that the data were non-normally distributed. The statistical analyses were carried out using the SPSS package software.

Results

The feather and health scores of the different genotypes are presented in Table 2. In the study, the effect of genotype on the feather score was found to be significant in all body regions except for the tail region ($P<0.05$). The mean total feather score was determined for IB, A-S, and NW as 11.53±0.250, 10.55±0.193 and 10.69±0.284, respectively. In terms of the feather score, the difference between the A-S and IB hybrids was found to be significant in all regions except for the tail region ($P<0.05$). Between the A-S and NW hybrids, the feather scores showed differences in the breast, cloaca and back regions ($P<0.05$). In all hybrids, the highest plumage loss was in the tail region, while the lowest was in the cloaca region in IB and the neck and wing regions in NW and A-S. Genotype had a significant effect on the health scores in all body regions except for the comb ($P<0.05$). The hybrid with the lowest health score in the cloaca region was IB. The NW hybrid showed higher values in terms of both foot scores than the other hybrids ($P<0.05$).

The feather and health scores of the hens at different cage densities are shown in Table 2. In terms of the feather score, the effect of cage density was determined to be significant in all body regions ($P<0.01$). It was observed that plumage loss increased as the cage density increased. While the total feather score was 12.94±0.211 for CD-1, it was 9.62±0.136 for CD-2. In the CD-1 conditions, the lowest plumage loss was in the cloaca region with a score of 2.40±0.056, while the highest one was in the tail region with a score of 1.93±0.050. In the CD-2 conditions, the lowest plumage loss was in the neck region with a score of 1.98±0.036, while the highest one was in the tail region with a score of 1.25±0.028. In terms of the health scores, both the comb and foot scores were found to be higher in the hens reared at the cage density-1 ($P<0.01$).

The feather and health scores of the hybrids in the cage density groups are presented in Table 3 and Figure 1. According to the findings of the study, in the IB and NW hybrids, as the cage density increased, the feather score showed a significant decrease in all body regions ($P<0.01$). In the A-S hybrid, in all body regions except for the breast region, as the cage density increased, the presence of plumage significantly decreased. In both density conditions, in terms of the total presence of plumage, the scores of the IB hybrid were higher than those of the others. In terms of the health score, it was observed that the cloaca region was not significantly affected by cage density in all hybrids. It was determined that the cage density showed a significant effect on the foot scores of the IB and A-S hybrids and the comb scores of the A-S and NW hybrids.

Table 2. The effects cage density on feather and health scores in laying hen hybrids.

	IB	A-S	NW	CD-1	CD-2	P				
	$\bar{x}$ ± SE	$\bar{x}$ ± SE	$\bar{x}$ ± SE	$\bar{x}$ ± SE	$\bar{x}$ ± SE	Cage Density	Hybrid	IB-AS	IB-NW	AS-NW
Feather Score										
Neck	2.20±0.047^{a}	2.00±0.044^{b}	2.06±0.065^{ab}	2.25±0.047^{x}	1.98±0.036^{y}	0.001	0.010	0.002	0.075	0.466
Breast	1.95±0.060^{a}	1.53±0.046^{b}	1.81±0.072^{a}	1.99±0.059^{x}	1.58±0.039^{y}	0.001	0.000	0.000	0.133	0.001
Cloaca	2.25±0.063^{a}	1.92±0.052^{b}	1.59±0.069^{c}	2.40±0.056^{x}	1.68±0.041^{y}	0.001	0.000	0.000	0.000	0.000
Back	1.77±0.059^{a}	1.58±0.046^{b}	1.73±0.065^{a}	2.09±0.054^{x}	1.42±0.033^{y}	0.001	0.025	0.015	0.850	0.037
Wing	1.81±0.044^{b}	2.00±0.038^{a}	2.04±0.051^{a}	2.30±0.034^{x}	1.71±0.029^{y}	0.001	0.000	0.001	0.001	0.457
Tail	1.54±0.050	1.53±0.047	1.46±0.059	1.93±0.050^{x}	1.25±0.028^{y}	0.001	0.518	0.715	0.253	0.395
Total	11.53±0.250^{a}	10.55±0.193^{b}	10.69±0.284^{b}	12.94±0.211^{x}	9.62±0.136^{y}	0.001	0.009	0.003	0.035	0.839
Health Score										
Comb	2.70±0.040	2.66±0.038	2.68±0.048	2.79±0.033^{x}	2.61±0.033^{y}	0.001	0.796	0.534	0.596	0.992
Cloaca	2.82±0.037^{a}	2.91±0.025^{b}	2.92±0.025^{b}	2.90±0.026	2.87±0.024	0.518	0.025	0.010	0.001	0.565
Right Foot	2.91±0.023^{b}	2.88±0.025^{b}	2.97±0.015^{a}	2.99±0.009^{x}	2.86±0.022^{y}	0.001	0.029	0.419	0.039	0.007
Left Foot	2.88±0.031^{b}	2.86±0.028^{b}	2.97±0.015^{a}	2.99±0.007^{x}	2.83±0.026^{y}	0.001	0.017	0.517	0.018	0.004

IB: Isa Brown, A-S: Atak-S, NW: Novogen White, CD-1: Cage density-1, CD-2: Cage Density-2.
^{a,b,c} Values within a row with different superscripts differ significantly at $P<0.05$.
^{x,y} Values within a row with different superscripts differ significantly at $P<0.01$.

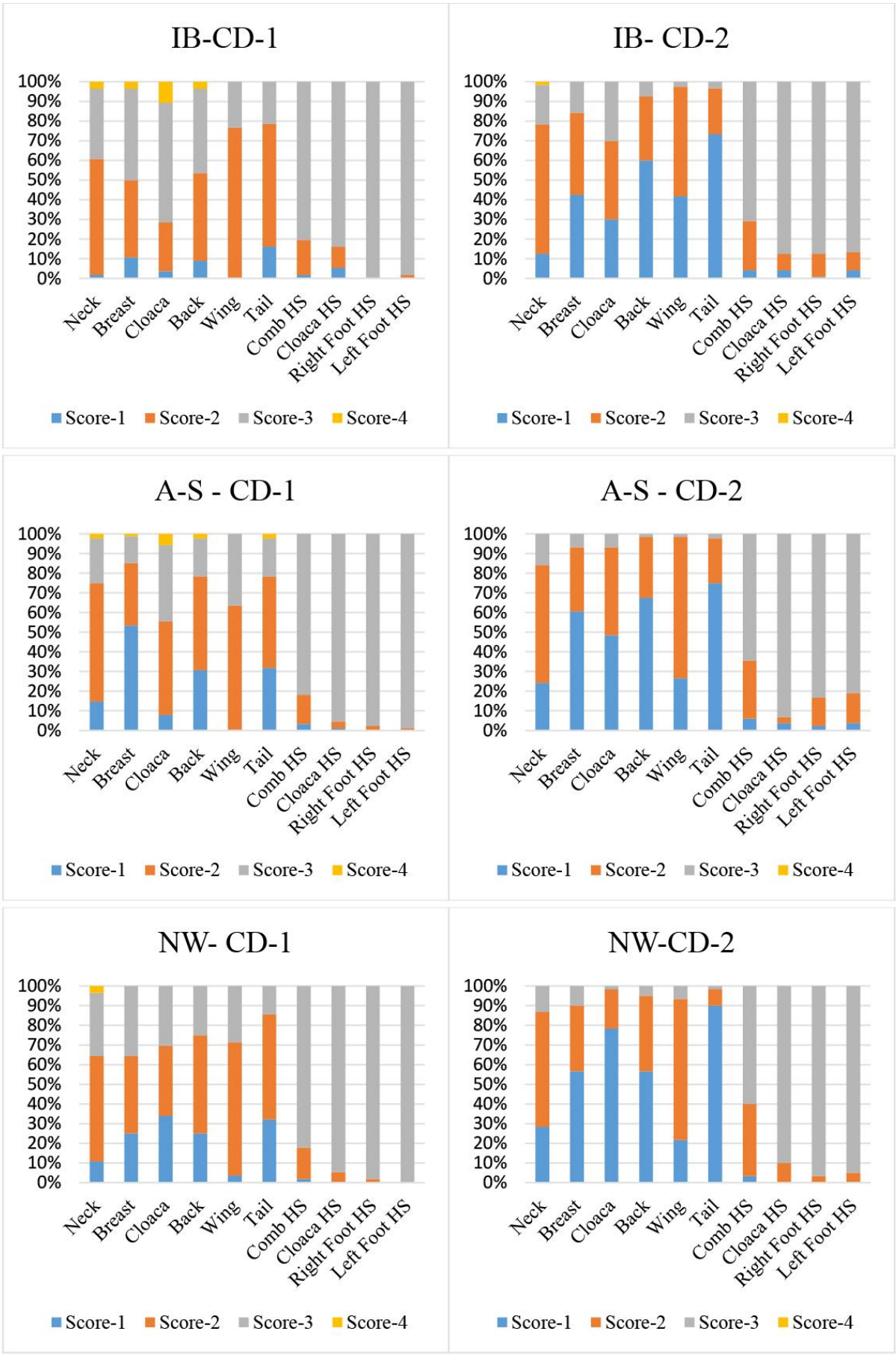

Figure 1. Feather and health scores of the hybrids in the cage density groups (%).

Table 3. The effects laying hen hybrids on the feather and health scores in the cage density groups.

	IB			A-S			NW		
	CD-1	CD-2		CD-1	CD-2		CD-1	CD-2	
Feather Score	**x̄ ± SE**	**x̄ ± SE**	**P**	**x̄ ± SE**	**x̄ ± SE**	**P**	**x̄ ± SE**	**x̄ ± SE**	**P**
Neck	2.41±0.080^{a}	2.11±0.057^{b}	0.003	2.13±0.072^{x}	1.92±0.055^{y}	0.029	2.29±0.094^{k}	1.85±0.082^{l}	0.001
Breast	2.43±0.098^{a}	1.73±0.066^{b}	0.000	1.63±0.081	1.46±0.054^{y}	0.157	2.11±0.104^{k}	1.53±0.087^{l}	0.000
Cloaca	2.79±0.091^{a}	2.00±0.071^{b}	0.000	2.42±0.077^{x}	1.58±0.054^{y}	0.000	1.96±0.108^{k}	1.23±0.060^{l}	0.000
Back	2.41±0.095^{a}	1.48±0.058^{b}	0.000	1.93±0.082^{x}	1.34±0.044^{y}	0.000	2.00±0.095^{k}	1.48±0.077^{l}	0.000
Wing	2.23±0.057^{a}	1.61±0.049^{b}	0.000	2.36±0.052^{x}	1.75±0.041^{y}	0.000	2.25±0.069^{k}	1.85±0.066^{l}	0.000
Tail	2.05±0.082^{a}	1.30±0.048^{b}	0.000	1.92±0.083^{x}	1.27±0.043^{y}	0.000	1.82±0.089^{k}	1.12±0.048^{l}	0.000
Total	14.32±0.342^{a}	10.23±0.254^{b}	0.000	12.39±0.316^{x}	9.33±0.177^{y}	0.000	12.43±0.400^{k}	9.07±0.268^{l}	0.000
Health Score	**x̄ ± SE**	**x̄ ± SE**	**P**	**x̄ ± SE**	**x̄ ± SE**	**P**	**x̄ ± SE**	**x̄ ± SE**	**P**
Comb	2.79±0.061	2.67±0.051	0.171	2.78±0.052^{x}	2.58±0.053^{y}	0.006	2.80±0.059^{k}	2.57±0.073^{l}	0.010
Cloaca	2.79±0.071	2.83±0.043	0.522	2.94±0.030	2.89±0.036	0.467	2.95±0.030	2.90±0.039	0.352
Right Foot	3.00^{a}	2.87±0.033^{b}	0.006	2.98±0.016^{x}	2.81±0.039^{y}	0.001	2.98±0.018	2.97±0,023	0.601
Left Foot	2.98±0.018^{a}	2.83±0.044^{b}	0.015	2.99±0.011^{x}	2.77±0.044^{y}	0.000	3.00	2.95±0.028	0.091

IB:Isa Brown, A-S: Atak-S, NW: Novogen White, CD-1: Cage density-1, CD-2: Cage Density-2.
^{a,b} Values within a row with different superscripts differ significantly at P<0.05.
^{x,y} Values within a row with different superscripts differ significantly at P<0.05.
^{k,l} Values within a row with different superscripts differ significantly at P<0.05.

Discussion and Conclusion

In this study, the integument status of native and foreign laying hybrids that were at the end of their laying period was assessed by the method of scoring by checking each animal one by one.

It was found in this study that the feather score in all body regions except for the tail region and the health score in the cloaca and feet showed a significant difference among the genotypes (P<0.05). It has been reported that feather pecking originates from behavioral disorders in hens, and this behavior shows genetic differences (8, 19, 26). When the plumage status in different body regions was examined in the study, it was observed that the highest plumage loss was in the NW hybrid in the cloaca region, in the A-S hybrid in the breast and back and in the IB hybrid in the wings. Studies have stated that, in animals with different feather colors, the genes that determine feather pigmentation may affect pecking behavior (2, 19). The IB, A-S, and NW hybrids that were used in this study had the respective feather colors of brown, black and white. Supporting this result, the effect of feather colors on the feather score was found significant in hens with white, black, and gray feathers (2). In some other studies, too, the changes in plumage conditions have been explained by the color of the feathers in brown, and white hens (4, 5, 8, 37).

It was explained that the feather and health scores in hens showed genetic differences between white- and brown layer hens (9, 27). Onbaşılar et al. (23) reported that feather scores differed in the neck, back, wings and tail regions of brown and white layer hens. In the study, while the NW hybrid had a white layer, the other two hybrids had brown-layers. White-layer hybrids are lightweight hybrids, while brown-layer hybrids have a medium-weight body structure (6, 23, 31). For this reason, their animal-specific area requirements should be kept in mind (32). Additionally, the different egg weights of the hybrids (22) may explain the differences in cloaca injuries as they lead to prolapse (25).

In the study, the highest amount of plumage loss occurred in the tail and back regions. It was reported that the reason for this is the behavior of pecking directed frequently towards these body regions (38). Giersberg et al. (8) also reported that, at the end of the laying period, the region's most affected in hens are the back and the tail. Studies where body regions were separately assessed and reported the highest plumage loss values in the cloaca and tail (3), and back, cloaca, and tail (10) regions have supported the results of this study.

In this study, the total feather score values for the IB, A, S and NW hybrids were 11.53, 11.00 and 10.55, respectively. Also, it was determined that the lowest loss of plumage was in the IB hybrid (P<0.05). However, in a study evaluating five different body regions, the total feather score was determined to be 14.7 in the LB hybrid and 14.8 in the LW hybrid. In the study, it was stated that there was no difference between hybrids in terms of total feather score (23). Tauson et al. (30) considered a total whole-body score of 10-12 and lower as a serious loss of plumage. It was reported that the plumage condition deteriorates in time throughout the laying period (23, 37), and loss of plumage reaches the highest level at the end of

the laying period (4, 14). These reports supported the finding in this study on the severe loss of plumage that was observed.

Assessment of the total feather score cannot explain the causes of plumage losses occurring in different regions of the body. Plumage and integument damage are affected by different causes in different genotypes (9). This situation is attributed to some behaviors that are genetically observed. The behavior of feather pecking in animals is expressed by animals non-aggressively pulling each other's feathers off. The basis of this behaviors is associated with the behaviors of searching for food and inadequate nutrition. This behaviors is frequently observed in the form of pecking the back, tail and cloacal regions (26, 32). Feather pecking is a significant problem in commercial breeding. Today, genetic selection and management programs that aim to reduce feather pecking are being applied at commercial coops (19). Aggressive pecking behaviors, on the other hand, is seen frequently in the form of pecking the head and neck region, which is associated with the formation of social hierarchy among the animals (26, 28). It is stated that this behavior becomes prevalent in the brood through social learning and that it leads to cannibalism and injuries involving blood through the pecking of the skin (8, 26). Besides these, the loss of plumage observed in the breast and abdomen regions is associated with the mobility of the animals within the cage and abrasion caused by the cage material (32, 34).

In this study, the effects of two different cage densities on the feather and integument health scores were examined. It was determined that, as the cage density increased, loss of plumage in all body regions and injuries in the comb and feet in the hens increased ($P<0.01$).

To increase their revenue, laying hen farmers have a tend to utilize their coops to the maximum extent (27). On the other hand, reducing the cage density has a significant effect on animal health and welfare (13, 25, 35). Providing hens with more area will affect their ability to move (36) and increase their welfare by allowing them to show their natural behaviors (i.e., stretching, turning around, walking, standing and wing flapping) (15).

Factors such as breeding, cage systems and cage density affect the formation of the behavior of feather picking and pecking (21). It was reported that reducing cage density affected pecking behavior in a positive direction (38). In the study by Weimer et al. (32) where 6 different housing densities (465-484, 581-606, 652-677, 754-780, 799-832, and 923-955 cm^2) were created, plumage conditions in 6 different body regions were investigated throughout the laying period. In their study, it was reported that, as the housing density increased, the presence of plumage significantly decreased in all body regions. Onbaşılar and Aksoy (20) examined the total feather scores (5 body regions) in their study, in which they formed a cage density of 1968 cm, 656 cm and 393.8 cm, and determined them as 16.56, 14.85, and 12.42, respectively. In the study, it was emphasized that the feather score was low in chickens that were raised intensively. Similarly, another study (35) stated that hens reared within 520 cm^2 had a poorer plumage condition than those reared within 748 cm^2. In support of the result of this study, different studies have reported that, by reducing cage density, plumage conditions (7, 13, 27, 35) and foot health (7, 29) were positively affected. It was reported that plumage loss is affected by an increase in cage density due to a reduction in feeder distance per animal and increased stress (7). The competition during feeding may increase the tendency of pecking by affecting social behaviors (32). In hens housed at high densities, as a result of the increased time of contact with the feeder area in the front of the cage, plumage loss and injuries may ocur, especially in the breast region (13). The poorer plumage score of densely populated cages can be caused by abrasion against cage wire or other hens (20). As opposed to the result of this study, Campe et al. (4) determined the effect of the factor of housing density on the feather score to be insignificant. In the housing density groups they created, Liebers et al. (17) examined plumage conditions (neck, back, wing), body injures (neck, breast, back, wing, leg, tail, cloaca), and head injuries, and they reported that housing density did not create a significant effect in any of the parameters. Onbaşılar and Aksoy (20) reported that cage density did not have a significant effect on foot health scores. The fact that the density groups in the aforementioned studies were close to each other and that the area per animal was broader in comparison to this study may explain the differences between the results. Also, some strains have a greater ability to adapt to high-density environments, and this may explain the differences between experiments (20).

Consequently, in all genotypes, a severe loss of plumage was observed at the end of the laying period. In the study, the best results were obtained from the IB hybrid in terms of the total plumage condition. Values observed in different body regions allow the assessment of animal welfare and poultry management. The highest plumage loss values were in the NW hybrid in the cloaca region, the A-S hybrid in the breast and back regions, and the IB hybrid in the wings. With the increase in cage density, the highest plumage loss occurred in the tail region in all hybrids. It was also concluded that, as the cage density increased, plumage loss and injuries in the comb and feet increased.

Financial Support

This research study was funded by Scientific Research Project Coordination Unit of Ataturk University, (Grant number: PRJ2014/25).

Conflict of Interest

The authors declared that there is no conflict of interest.

Author Contributions

UÖ, AY and MG conceived and planned the experiments. UÖ and MG carried out the experiments. UÖ, AY and MG contributed to the interpretation of the results. UÖ took the lead in writing the manuscript. All authors provided critical feedback and helped shape the research, analysis and manuscript.

Data Availability Statement

The data supporting this study's findings are available from the corresponding author upon reasonable request.

Ethical Statement

Approval was obtained specifying that conducting the study was appropriate in terms of ethical principles with the decision dated 25.06.2020 and numbered 2020/7 of the Ethics Committee of the School of Veterinary Medicine at Atatürk University.

Animal Welfare

The authors confirm that they have adhered to ARRIVE Guidelines to protect animals used for scientific purposes.

References

1. **Blatchford RA, Fulton RM, Mench JA** (2016): *The utilizationof the Welfare Quality R assessment for determining laying hen condition across three housing systems*. Poult Sci, **95**, 154–163.
2. **Bright A** (2007): *Plumage colour and feather pecking in laying hens, a chicken perspective?* Br Poult Sci, **48**, 253-263.
3. **Bright A, Jones TA, Dawkins MS** (2006): *A non-intrusive method of assessing plumage condition in commercial flocks of laying hens.* Anim Welf, **15**, 113-118.
4. **Campe A, Hoes C, Koesters S, et al** (2018): *Analysis of the influences on plumage condition in laying hens: How suitable is a whole body plumage score as an outcome?* Poult Sci, **97**, 358-367.
5. **De Haas EN, Bolhuis JE, De Jong IC, et al** (2014): *Predicting feather damage in laying hens during the laying period. Is it the past or is it the present?* Appl Anim Behav Sci, **160**, 75-85.
6. **Fatih Y, Uğur O, Hayrunnisa O, et al** (2018): *Effect of genotype on slaughtering performance, blood analyses and meat quality of laying hens reared in different conventional cage densities.* GSC Biological and Pharmaceutical Sciences, **5**, 54-65.
7. **Fidan ED, Nazlıgül A** (2013): *Cage position and density effect on some welfare criteria in Denizli chicken.* Indian J Anim Sci, **83**, 645-648.
8. **Giersberg MF, Spindler B, Kemper N** (2017): *Assessment of plumage and integument condition in dual-purpose breeds and conventional layers.* Animals, **7**, 97.
9. **Habig C, Distl O** (2014): *Evaluation of plumage condition and foot pad health in laying hens kept in a small group housing system.* Europ Poult Sci, **78**.
10. **Hartcher KM, Tran KTN, Wilkinson SJ, et al** (2015): *The effects of environmental enrichment and beak-trimming during the rearing period on subsequent feather damage due to feather-pecking in laying hens.* Poult Sci, **94**, 852-859.
11. **Janczak AM, Riber AB** (2015): *Review of rearing-related factors affecting the welfare of laying hens*. Poult Sci J, **94**, 1454-1469.
12. **Kamanlı S, Boga AG, Durmus İ** (2016): *Beyaz Yumurtacı Ebeveyn Hatlarında İkili Melez Kombinasyonların Bazı Verim ve Yumurta Kalite Özellikleri Bakımından Karşılaştırılması.* J Appl Poult Res, **13**, 1-4.
13. **Khumput S, Muangchum S, Yodprom S, et al** (2019): *Feather pecking of laying hens in different stocking density and type of cage.* Iran J Appl Anim Sci, **9**, 549-556.
14. **Labrash LF, Scheideler SE** (2005): *Farm feather condition score survey of commercial laying hens* J Appl Poult Res, **14**, 740-744.
15. **Lay DC, Fulton RM, Hester PY, et al** (2011): *Hen welfare in different housing systems*. Poult Sci, **90**, 278–294.
16. **Laywel** (2006): Welfare implications of changes in production systems for laying hens (DeliverablesD.3.1-D.3.3,WP3-Health). Available at http://www.laywel.eu/web/pdf/ deliverables%2031-33%20health.pdf. (Accessed Feb, 2017).
17. **Liebers CJ, Schwarzer A, Erhard M, et al** (2019): *The influence of environmental enrichment and stocking density on the plumage and health conditions of laying hen pullets.* Poult Sci J, **98**, 2474-2488.
18. **Master Plan** (2020): Ministry of Agriculture and Forestry. Agricultural Research Master Plan 2016- 2020. Ankara: Republic of Turkey Ministry of Agriculture and Forestry General Directorate of Agricultural Research And Policies; 2020 Available at https://www.tarimorman.gov.tr/TAGEM/Belgeler/yayin/MASTER%20PLAN_ 2016 - 2020.pdf. (Accessed May 15, 2020).
19. **Nicol CJ, Bestman M, Gilani AM, et al** (2013): *The prevention and control of feather pecking: application to commercial systems.* World Poultry Sci J, **69**, 775-788.
20. **Onbaşılar EE, Aksoy FT** (2005) : *Stress parameters and immune response of layers under different cage floor and density conditions.* Livest Prod Sci, **95,** 255-263.
21. **Onbaşılar EE, Kahraman M, Güngör ÖF, et al** (2020): *Effects of cage type on performance, welfare, and microbiological properties of laying hens during the molting period and the second production cycle*. Trop Anim Health Prod, **52**, 3713–3724.
22. **Onbaşılar EE, Ünal N, Erdem E** (2018): *Some egg quality traits of two laying hybrids kept in different cage systems.* Ankara Univ Vet Fak Derg, **65,** 51-55.
23. **Onbaşılar EE, Ünal N, Erdem E, et al** (2015): *Production performance, use of nest box, and external appearance of two strains of laying hens kept in conventional and enriched cages.* Poult Sci, **94,** 559-564.
24. **Ozdemir S, Arslan H, Ozenturk U, et al** (2018): *Atak-S ve Isa Brown tavukları arasındaki genetik çeşitliliğin SSR belirteçleri ile tahmini.* Kocatepe Veteriner Dergisi, **11**, 53-62.

25. **Özenturk U, Yıldız A** (2020): *Assessment of egg quality in native and foreign laying hybrids reared in different cage densities.* Braz J Poult Sci, **22**, 1-10.
26. **Rodenburg TB, Van Krimpen MM, De Jong IC, et al** (2019): *The prevention and control of feather pecking in laying hens: identifying the underlying principles.* World Poultry Sci J, **69**, 361-374.
27. **Sarıca M, Boğa S, Yamak US** (2008): *The effects of space allowance on egg yield, egg quality and plumage condition of laying hens in battery cages.* Czech J Anim Sci, **53**, 346-353.
28. **Savory C** (1995): *Feather pecking and cannibalism.* Worlds Poult Sci J, **51**, 215–219.
29. **Shepherd EM, Fairchild BD** (2010): *Footpad dermatitis in poultry*. Poult Sci J, **89**, 2043-2051.
30. **Tauson R, Kjaer J, Maria GA, et al** (2005): *Applied scoring of integument and health in laying hens.* Anim Sci Pap Rep, **23**, 153-159.
31. **Türkoğlu M, Sarıca M** (2018): Tavukçuluk Bilimi, Yetiştirme, Besleme, Hastalıklar. 5. Baskı. Ankara: Bey Ofset Matbaacılık.
32. **Weimer SL, Robison CI, Tempelman RJ, et al** (2019): *Laying hen production and welfare in enriched colony cages at different stocking densities.* Poult Sci J, **98**, 3578-3586.
33. **Welfare Quality R** (2009): Welfare Quality R assessment protocol for poultry (broilers, laying hens). Welfare Quality R Consortium, Lelystad, Netherlands.
34. **Widowski TM, Caston LJ, Casey-Trott TM, et al** (2017): *The effect of space allowance and cage size on laying hens housed in furnished cages, Part II: Behavior at the feeder.* Poult Sci, **96**, 3816–3823.
35. **Widowski TM, Caston LJ, Hunniford ME, et al** (2017): *Effect of space allowance and cage size on laying hens housed in furnished cages, Part I: performance and well-being.* Poult Sci, **96**, 3805–3815.
36. **Widowski TM, Classen H, Newberry RC, et al** (2013): Scientists Committee Report on Priority Welfare Issues for Laying Hens. National Farm Animal Care Council. Available at http://www.nfacc.ca/resources/codes-of-practice/poultrylayers/Layer SCReport.pdf. (Accessed Jan, 2019).
37. **Yamak US, Sarıca M** (2012): *Relationships between feather score and egg production and feed consumption of different layer hybrids kept in conventional cages.* Archiv Geflugelkd, **76**, 31-37.
38. **Zepp M, Louton H, Erhard M, et al** (2018): *The influence of stocking density and enrichment on the occurrence of feather pecking and aggressive pecking behavior in laying hen chicks.* J Vet Behav, **24**, 9-18.

Investigation of the neuroprotective effect of kefir in experimental spinal cord injury

Ziya YURTAL[1,a, ✉], Tuncer KUTLU[2,b], Muhammed Enes ALTUĞ[1,c], Bülent ÖZSOY[3,d], Halil ALAKUŞ[1,e]
Şule YURDAGÜL ÖZSOY[4,f]

[1]Hatay Mustafa Kemal University, Faculty of Veterinary Medicine, Department of Surgery, Hatay, Türkiye; [2]Hatay Mustafa Kemal University, Faculty of Veterinary Medicine, Department of Pathology, Hatay, Türkiye; [3]Aydın Adnan Menderes University, Faculty of Veterinary Medicine, Department of Animal Nutrition And Nutritional Diseases, Aydın, Türkiye; [4]Aydın Adnan Menderes University, Faculty of Veterinary Medicine, Department of Pathology, Aydın, Türkiye

[a]ORCID: 0000-0001-6080-1860; [b]ORCID: 0000-0002-8771-1256; [c]ORCID: 0000-0003-3896-9944; [d]ORCID: 0000-0003-0045-3790
[e]0000-0001-9265-2310; [f]0000-0002-0743-2063

ARTICLE INFO

Article History
Received : 02.02.2021
Accepted : 24.10.2021
DOI: 10.33988/auvfd.872947

Keywords
Kefir
Neuroprotective agents
Spinal cord injuries

✉Corresponding author
ziyayurtal@mku.edu.tr

How to cite this article: Yurtal Z, Kutlu T, Altuğ ME, Özsoy B, Alakuş H, Yurdagül Özsoy Ş (2023): Investigation of neuroprotective effect of kefir in experimental spinal cord injury. Ankara Univ Vet Fak Derg, 70 (1), 9-19. DOI: 10.33988/auvfd. 872947.

ABSTRACT

In this study, the antioxidant, anti-inflammatory, and neuroprotective effects of kefir were investigated in spinal cord injury that was experimentally created on rats with a compression trauma model. A total of 56 Wistar-Albino male rats were used in the study. Daily freshly prepared 18 ml/kg/day of kefir was given by oral gavage to animals 7 days before and during the trauma and during the trauma. Spinal cord injury was created according to the weight drop method. On the 1st and 7th days before euthanasia, intracardiac blood was collected for analysis, and then they were sacrificed. The damaged spinal cord segments were examined biochemically, immunohistochemically, and histopathologically. When compared to the sham groups, kefir had a positive effect in the preconditioning and treatment groups by decreasing spinal cord bleeding, edema, myelin sheath damage, liquefactive necrosis, neuronal necrosis, selectivity of canalis centralis, and gitter cell levels significantly. When compared to the sham groups, kefir was found to have a positive effect in the treatment groups by decreasing the neuron specific enolase (NSE), ionized calcium binding adapter molecule 1 (IBA-1), inducible nitric oxide synthase (INOS), cyclooxygenase 2 (COX-2) and myelin basic protein (MBP) levels significantly on the 1st and 7th days, and by increasing the glial fibrillary acidic protein (GFAP) level significantly. As a result, it was demonstrated that kefir had a protective and therapeutic effect on spinal cord injury.

Introduction

Acute spinal injuries have increased recently with the rapid growth of the industry, transportation, and construction industries (23). Spinal cord injury has two mechanisms, which are primary and secondary. Primary injury refers to mechanical damage, and secondary injury refers to the progressive cell damage that occurs after the trauma (25, 35). Spinal cord injuries (SCI) could lead to a complete and permanent loss of neurological function (38, 39). Despite the advancement of current drug and surgical techniques, there is no surgical technique or therapeutic agent that would provide a complete recovery in cases of spinal cord injury (16, 18). Therefore, researchers are still looking for new medical treatments for the treatment of spinal injuries (23). Guven et al. (17) emphasized that ultrastructural studies are needed to develop kefir as a promising therapeutic agent to be used in spinal cord injury. Kefir has a polysaccharide structure with a whitish yellowish color. It owes its strong antioxidant characteristic to the high amount of lactic acid bacteria it involves (5). In addition, kefir is reported to have anti-inflammatory (4, 30), antibacterial (29), antitumoral (26), immunological (11), cholesterol-lowering (27, 36), and antiapoptotic effects (10, 27, 29).

Brain-Derived Neurotrophic Factor (BDNF) is considered an important protein that affects brain function as well as the peripheral nervous system. In addition to preventing cell deaths, it demonstrates a neuroprotective effect under adverse conditions such as cerebral ischemia, hypoglycemia, neurotoxicity, and glutamatergic

stimulation by supporting neuronal differentiation, maturation, and survival in the nervous system (3, 21).

Spinal cord (medulla spinalis) damage causes important social and economic problems and there is no clear solution regarding its definitive treatment. There are drugs used today, but new searches continue because their efficacy cannot be fully demonstrated and they have serious side effects. With many studies, it is aimed that the individual, who has lost his active life as a result of the damage and lost his work force, can return to social life again. This study, which was planned based on previous experimental studies on the usability of this neuroprotective effect for treatment in cases with neural tissue damage such as trauma and ischemia, was planned to investigate the antioxidant, anti-inflammatory, and neuroprotective effects of kefir in spinal cord damage induced by an experimental trauma model in rats. The present study is a prerequisite study, and both the protective efficacy of kefir on the damaged spinal cord tissue and the therapeutic efficacy after trauma were evaluated.

Materials and Method

In this study, 56 healthy male Wistar-Albino rats that were 10-12 weeks old and weighed 300-400g were used. The animals were placed in individual cages and divided into seven equal groups with eight animals in each group. Experimental applications were carried out in accordance with the conditions for the care and use of laboratory animals (12 hours of light; 12 hours of darkness, and 24±3°C, in individual cages). During the experimental applications, rats were fed on commercial rat food (pellet food) including 22.5% HP, 2750 Kcal/kg, and tap water ad libitum.

The animals with spinal cord injury were given 18 ml/kg/day (13) oral gavage of freshly prepared kefir. Kefir grains were washed with distilled water and inoculated in UHT (Ultra High Temperature) whole milk. After each preparation of the beverage, the grains were filtered by sieving the fermented milk and washed again for later use. When the grains were not used, they were maintained in milk at 4°C. Kefir was prepared by adding 5% kefir grains sterile milk and fermenting at 25°C for 24 hours. The number of yeast cells was found to be $1.65x10^7$ (log10 cfu/g).

Animals: Group I; (Control group) The control group received no treatment and was used as a reference. Group II; (Sham-A group) trauma was created only and they were sacrificed on the 1st day. Group III; (Sham-B group) trauma was created only and they were sacrificed on the 7th day. Group IV; (Preconditioning A) were given 18ml/kg/day PO kefir for 7 days before the trauma, and they were sacrificed one day after the trauma was created. Group V; (Preconditioning B) It was the preconditioning group that was given 18ml/kg/day PO kefir for 7 days before the trauma, continued to be fed on 18ml/kg/day PO kefir for 7 days after the trauma, and were sacrificed on the 7th day. Group VI; (Treatment A) They were given 18ml/kg/day PO kefir after the trauma and were sacrificed on the 1st day. Group VII; (Treatment B) They were given 18ml/kg/day PO kefir for 7 days after the trauma and were sacrificed on the 7th day. The animals were determined to be healthy during the clinical examinations performed before the trauma. Their neurological examinations were evaluated through the Modified Tarlov Scale and finger opening tests. After the trauma, neurological examinations of the related groups were repeated on the 1st, 3rd, and 7th days.

Creation of spinal cord damage: In all surgical groups, 10 mg/kg Xylazine hydrochloride intraperitoneal (ip) (Alfazyne 2% injection 50 mL, EGE-VET, Türkiye) and 50 mg/kg ketamine hydrochloride (ip) (Alfamine 10% injection 50 mL EGE-VET, Türkiye) were given for general anesthesia. After the general anesthesia rats were identified in the sternal position, the back part was shaved and antisepsis was provided with povidone-iodine. Paravertebral muscles were reached after crossing the skin and subcutaneous tissues with a two-cm incision at the T5-T12 level with reference to the interscapular distance. The paravertebral muscles were dissected and the vertebral laminae were reached through the spinous process. The spinal cord was exposed at the T7-T10 level by total laminectomy preserving dura mater integrity.

Spinal cord injury was created using the weight drop method by dropping a 10g metal bar with a 3mm diameter from a height of 10 cm (100 g/cm). Rats were made paraplegic. Following hemostasis, paravertebral muscles and skin were sutured in accordance with their anatomical layers. While animals were under general anesthesia on the 1st and 7th days before euthanasia, intracardiac blood was collected for analysis, and then they were sacrificed. After sacrification, sections were taken from the proximal and distal of the trauma for tissue analysis. The samples were examined biochemically, immunohistochemically, and histopathologically.

Neurological examination: In the study, neurological examinations were performed before the sacrification in groups 2, 4, and 6, which underwent a surgical procedure and were sacrificed on the first day; and they were performed on the 1st, 3rd, and 7th days in groups 1, 3, 5 and 7, which underwent a control and surgical procedure and were sacrificed on the seventh day.

Modified Tarlov Scale was used for clinical motor examination and classified as follows; 0:complete

paralysis in the back extremities, no movements in the back extremities, no weight bearing; 1:noticeable back limb movements, no weight bearing; 2: frequent and / or strong back limb movements, pronounced posterior limb movements that do not result in weight overlay or locomotion; 3:back extremities support body weight, can take one or two steps; 4: there is a slight loss in walking; 5: normal walking (12).

Finger opening test used for a neurological examination. The rat was lifted from its back and its back extremities were suspended. Opening of the fingers was observed and the reflexes were classified as follows: 0: fingers not opened; 1: fingers slightly opened; 2: fingers fully opened (12).

Biochemical analyses: Plasma was extracted from the serous fluid and stored in the freezer (-24 °C). In the samples, BDNF (Brain Derived Neurotrophic Factor) levels were calculated by ELISA using commercial kits.

Histopathological and immunohistochemical assessments: Macroscopic changes that could occur in the spinal cord after the experimental trauma were noted and photographed. For histopathological examinations, the spinal cord extracted was placed in 10% buffered formalin stained with Hematoxylin Eosin (HE). For immunohistochemical examination Mouse specific HRP (ABC) (Abcam, ab128971) kit was used and the recommended procedure was applied in the kit. Endogenous peroxidase activity was eliminated by maintaining 3% H_2O_2 methanol for 30 minutes. Depending on the type of antibodies, either 10 minutes 45°C Proteinase K (Abcam, ab64220) (NSE, GFAP, IBA-1 antibodies) or temperature was applied as antigen retrieval (pH 6.0, % 0,1 Tween) (3x5 minutes) (INOS, MBP, COX-2 antibodies). Sections were incubated with the blocking serum of the kit at 37˚C for 10 minutes to prevent non-specific antigenic binding. Anti-Iba-1 antibody (Abcam, ab108539, 1/100, 15 minutes room temperature), Anti-iNOS antibody (Abcam, ab3523, 1/100, +4°C overnigth), Anti COX-2, C-Terminal antibody (Sigma, SAB4502491-100UG, 1/200, 2 hours 37˚C), Anti-GFAP antibody (Abcam, ab7260, 1/100, 1 hour 45˚C), Anti-NSE C Terminal antibody (Sigma, SAB4500768-100UG, 1/100, 1 hour 45˚C) and Anti-MBP antibody (Sigma, ab40390, 1/100, 1 hour 45˚C) were used in order to identify the lesions that could occur in the spinal cord. This was followed by treatment steps with biotinized serum (goat serum, at 37˚C for15 min) and streptavidin peroxidase (at 37˚C for 20 min). The AEC (RED) Substrate kit (Zymed Laboratories inc. Cat. No: 00-2007) (NSE, IBA1, INOS, COX-2) and DAP (3,3′-diaminobenzidine tetrahydrochloride, ScyTek Laboratories, Logan, UT) (GFAP, MBP) were used as the chromogene. The samples were counterstained with Harris hematoxylin. All steps were carried out in a moist camera environment, preventing the sections from drying out. Phosphat Buffer Saline (PBS, pH 7.4) was used in the washes. After all the microscopic results obtained were examined under a light microscope, their microphotographs were taken.

Statistical Analysis: Statistical analyses were performed using SPSS (version 17) software. Data were given as mean ± standard error (SE). The differences between the groups were analyzed with the One Way ANOVA Bonferroni Test. General Linear Model, Repeated Measures, multiple comparisons bonferroni test was used to evaluate time-dependent differences in neurological examination findings. Statistical significance was interpreted according to $P<0.05$ level.

Results

Neurological examination findings: MTS and the finger opening test were performed while evaluating the neurological examination (Day 1 was evaluated as acute; days 3 and 7 were evaluated as subacute).

In terms of MTS values, significant differences were found between the control groups and, the sham groups, preconditioning groups and treatment groups on the 1st day (P=0.000, Table 1). In the neurological examination performed on the first day, the MTS values in the preconditioning groups were higher compared to the sham and treatment groups. MTS values on the 3rd and 7th days in the preconditioning (group 5) and treatment (group 7) groups were higher compared to the sham (group 3) value. MTS values in the treatment group were higher compared to the preconditioning groups on the 3rd and 7th days. Looking at the MTS values, it can be argued that kefir provides clinical improvement (Table 1).

In terms of finger opening tests, significant differences were found between the control groups and, the sham, preconditioning and treatment groups on the 1st day (P=0.000). On the first day, finger opening test values in the preconditioning groups were higher compared to the sham and treatment groups. The fact that the finger-opening test values in the preconditioning group were higher compared to the sham and treatment groups on the 1st day showed that preconditioning played a protective role in preventing peracute injury. On the 7th day, finger opening test values in the preconditioning (group 5) and treatment (group 7) groups were found to be higher compared to the sham (group 3) value (Table 1). Looking at the finger opening test values, it can be argued that kefir provides a clinically moderate benefit in both the peracute and subacute periods.

DOI: 10.33988/auvfd.872947

Table 1. Effects of kefir on Modified Tarlov Test and Finger Opening Test in experimental spinal cord injury.

Groups	Modified Tarlov 1. day	Modified Tarlov 3. day	Modified Tarlov 7. day	Finger extension test 1. day	Finger extension test 3. day	Finger extension test 7. day
	Mean±SE	Mean±SE	Mean±SE	Mean±SE	Mean±SE	Mean±SE
Group 1: Control A	5.00±0.00	5.00±0.00	5.00±0.00	2.00±0.00	2.00±0.00	2.00±0.00
Group 2: Sham A	1.66±0.33*			0.16±0.16*		
Group 3: Sham B	1.71±0.47*	1.14±0.55**	1.42±0.57*	0.28±0.18*	0.28±0.28*	0.42±0.29*
Group 4: Preconditioning A	1.85±0.67*			0.57±0.29*		
Group 5: Preconditioning B	2.50±0.42**	1.87±0.54*	2.28±0.60*	0.87±0.22*	0.25±0.16*,β	0.85±0.34*,&
Group 6: Treatment A	1.25±0.55*			0.00±0.00*,≠		
Group 7: Treatment B	2.00±0.68*	2.00±0.75**	3.14±0.55	0.50±0.26*	0.62±0.26*	0.71±0.18*

A: Group sacrificed on day 1, B: Group sacrificed on day 7
*: When compared with the control group, the differences between the groups were found significant (P <0.005-0.000).
**:When Compared with the control group, the differences between the groups were found significant (P <0.05).
≠: Finger extension test, on the first day, the differences between the Peconditioning Group B and treatment A groups were found to be significant (P <0.05).
β: When compared to the first day, the differences in the finger extension test were found significant (P <0.05).
&: When compared to the third day, the differences in the finger extension test were found significant (P <0.05).

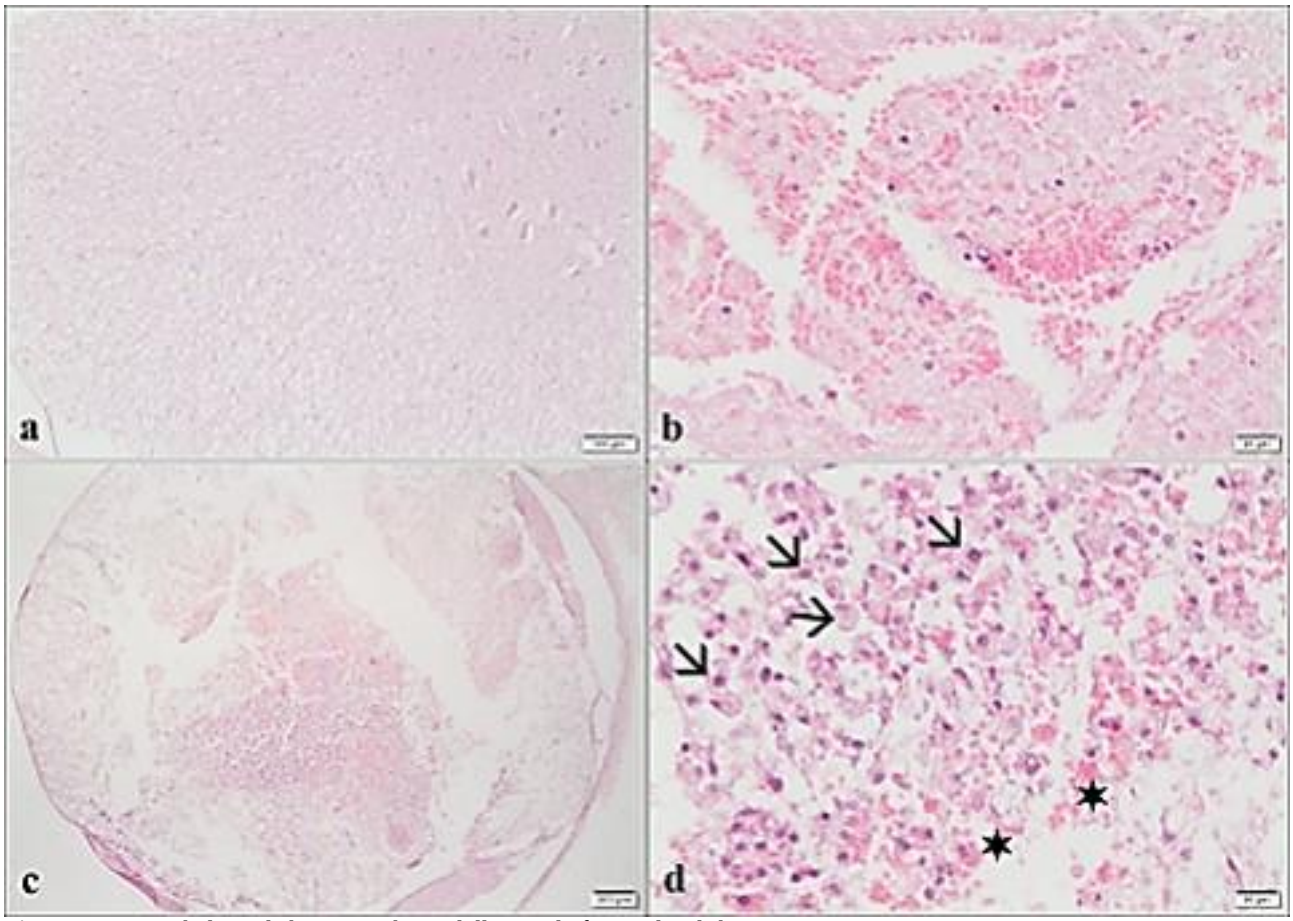

Figure 1. Histopathological changes in the medulla spinal of control and sham groups.
a. Medulla spinalis normal gray matter and white matter structure, Control group, HE, ×100 µm.
b. Hemorrhage and microglial cells in both gray and white matter, Sham A group, HE, ×20 µm.
c. Large necrosis sites in the transverse section, vacuolization in myelin sheaths and damaged canalis centralis, Sham B group, HE, ×200 µm.
d. Intensely gitter cells (arrows) and hemorrhage (stars), Sham B group, HE, ×20 µm.

Histopathological results: The cells in the anterior horn of the spinal cord were examined for damage. For this reason, the cells that have lost their eosinophilic cytoplasm and nucleus were considered dead neurons due to ischemic damage. Cells with cytoplasmic Nissl bodies, thin chromatin, and a prominent nucleolus were considered alive. Histopathological findings observed were classified as none (0), mild (1), moderate (2) and severe (3).

Group I; control group: The spinal cord had normal gray and white matter structure (Figure 1a). No

morphological changes were observed. Group II; (Sham-A): There was prevalent edema, hemorrhage in both gray and white matter, vacuolization in myelin sheaths and neuronal necrosis; and the structure of neurons lined with ependymal cells were observed to be damaged. A small number of microglia cells were noted (Figure 1b). Group III; (Sham-B): They were similar to Group 2, with more severe morphological changes in the damage zone (Figure 1c). In addition, intensive gitter cells were noted in this group (Figure 1d). Group IV (Preconditioning A): There was localized edema, hemorrhage, vacuolization in myelin sheaths and neuronal necrosis; and the structure of neurons lined with ependymal cells were observed to be damaged. Group V (Preconditioning B): There was no hemorrhage, liquefactive necrosis and gliosis; however, there was edema, hemorrhage, damage and vacuolization in myelin sheaths and neuronal necrosis; and the damage in the structure of neurons lined with ependymal cells were observed to decrease (Figure 2a and Figure 2b). Group VI (Treatment A): Moderate edema, hemorrhage, vacuolization in myelin sheaths and neuronal necrosis were also present in this group. It was observed that while the structure of the canal where ependymal cells were lined was preserved in some parts it was damaged in some other parts (Figure 2c). Group VII (Treatment B): The edema, hemorrhage, vacuolization in myelin sheaths and neuronal necrosis were milder compared to Group VI. It was observed that the structure of the canal lined with ependymal cells was preserved in part and deteriorated in another part (Figure 2d).

Histopathological changes shaped in the spinal cord are summarized in Table 2.

When compared to the sham groups, it was observed that kefir had positive effects in the preconditioning and treatment groups by significantly reducing spinal cord bleeding, edema, myelin sheath damage, liquefactive necrosis, neuronal necrosis, selectivity of the canalis centralis and gliosis/gitter cell levels (P=0.000, Table 2). On the other hand, kefir demonstrated a therapeutic effect on the 7th day by reducing liquefactive necrosis and gliosis/gitter cell levels more than the first day in the preconditioning and treatment groups (P=0.000, Table 2).

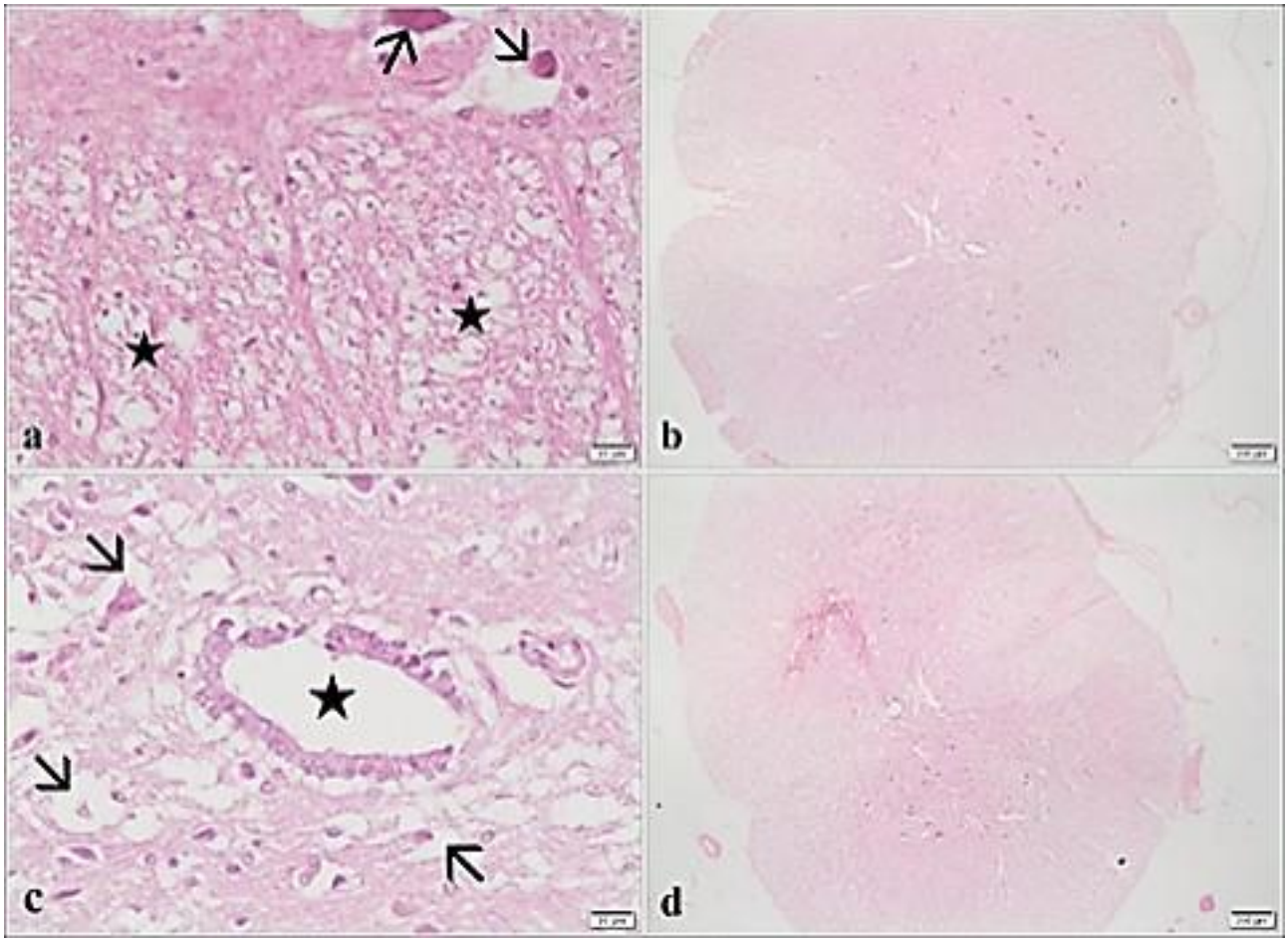

Figure 2. Histopathological changes in the medulla spinal of the preconditioning and treatment groups.
a. Basophilic necrotic neurons (arrows) with loss of nuclei, damage and vacuolization (stars) in myelinated sheaths, Preconditioning B group, HE, ×20 µm.
b. Canalis centralis structure is preserved, Preconditioning B group, HE, ×200 µm.
c. Pericellular edema (arrows) and condition of the canalis centralis (star), Treatment A group, HE, ×20 µm.
d. The appearance of the spinal cord, Treatment B group, HE. ×200 µm.

Table 2. Histopathological changes in the spinal cord.

Groups	Haemorrhage	Edema	Myelin Sheath Damage	Liquefaction Necrosis	Necrosis in Neurons	Canalis Sentralis Not Selected	Gliosis-Gitter Cells
	Mean±SE	Mean±SE	Mean±SE	Mean±SE	Mean±SE	Mean±SE	Mean±SE
1:Control	0.00±0.00	0.00±0.00	0.12±0.12	0.00±0.00	0.00±0.00	0.12±0.12	0.00±0.00
2:Sham A	2.00±0.18	1.75±0.16	1.87±0.22	2.00±0.18	1.62±0.18	2.25±0.16	0.62±0.18
3:Sham B	2.25±0.25	2.25±0.16	2.75±0.16	2.62±0.26	2.87±0.12	2.87±0.12	2.50±0.37
4:Preconditioning A	1.75±0.16	1.75±0.25	1.50±0.26 $^{\beta}$	1.75±0.31$^{\neq}$	0.87±0.22$^{*,\beta}$	2.25±0.16	0.25±0.16
5:Preconditioning B	0.25±0.16$^{€,\beta}$	1.00±0.00$^{*,\beta}$	1.00±0.00$^{*,\beta}$	0.37±0.18$^{€,\beta}$	1.00±0.00$^{\beta}$	1.00±0.00$^{€,\beta}$	0.00±0.00$^{\beta}$
6:Treatment A	1.50±0.26	2.00±0.18	2.25±0.16	1.87±0.12	1.75±0.16$^{\beta}$	1.12±0.35$^{€,\beta}$	0.25±0.16$^{\beta}$
7:Treatment B	1.12±0.22$^{\beta}$	1.00±0.00$^{*,\beta}$	1.00±0.00$^{*,\beta}$	0.00±0.00$^{€,\beta}$	0.75±0.16$^{€,\beta}$	0.50±0.26$^{€,\beta}$	0.12±0.12$^{\beta}$

A: First day, B: Seventh day.
Compared with the Sham A group: * : $P<0.05$; € : $P<0.005$.
Compared with the Sham B group: ≠ : $P<0.05$, β : $P<0.005$.
Compared with the Preconditioning A group: α : $P<0.05$, ¥ : $P<0.005$.
Compared with the Preconditioning B group: $: $P<0.05$, & : $P<0.005$.

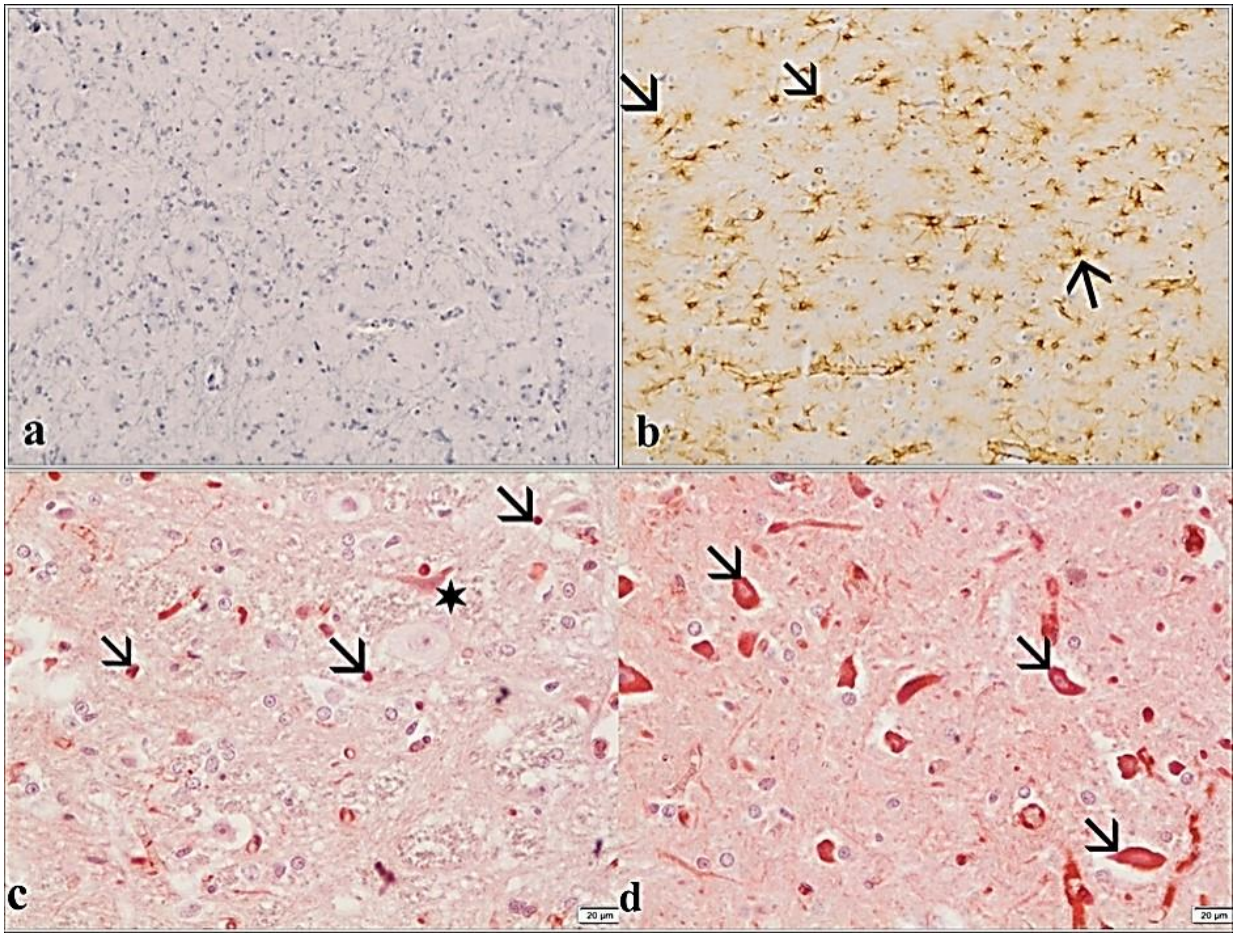

Figure 3. Immunohistochemical findings for GFAP, COX-2 and NSE antibodies.
a. Medulla spinalis GFAP negative, Control group DAB, ABC, ×100 µm.
b. Medulla spinalis GFAP positive astrocytes (arrows), Preconditioning B group, DAB, ABC, ×20 µm.
c. COX-2 positive microglia (arrows) and mild positive neuron cytoplasm in medulla spinalis, Sham A group, AEC, ABC, ×20 µm.
d. NSE positive neurons (arrows) in medulla spinalis, Sham A group, AEC, ABC, ×20 µm.

Immunohistochemical results: While immunoreactivity was not observed against GFAP, NSE, INOS and IBA-1 antibodies in the control group (Figure 3a); in the uninjured central nervous system, COX-2 positive staining in neurons and MBP positive staining in cords in myelin sheaths were observed.

GFAP positive fibrous astrocytes attracted attention most intensely in the 5th and 7th groups, as a result of the increase in the severity of the lesion and the repair in the astrocytes in parallel with the increase in the experimental period in the groups where experimental spinal cord injury was created (Figure 3b). Weaker immunoreactivity was

observed in Groups 3, 4, and 6, respectively, whereas immunosuppressive staining was not observed in Group 2.

The strongest immunoreactivity against the antibody used to demonstrate the COX-2 protein levels increasing after the spinal cord injury in astrocytes and microglia was observed in Groups 3, 2, 6, 4, 7 and 5, respectively. In addition, immunoreactivity was noted in non-damaged neuron cytoplasms (Figure 3c).

The strongest staining against the NSE antibody used to determine neuronal damage was observed in groups 3, 2, 6 and 4, respectively (Figure 3d). While there was moderate immune reactivity related to neuronal damage in group 7 compared to other groups and group 5, there was a significant decrease in the number of immune positive cells in group 5.

Immunohistochemical staining was performed for the presence of myelin basic protein (MBP) to determine the destruction of myelin sheaths. The strongest staining was observed particularly in the areas with severe damage. In the myelin sheaths with granular and irregular appearance among the healthy myelin sheaths in the form of cords, the strongest immunoreactivity was observed in the animals that belonged to the 3rd and 2nd groups, respectively (Figure 4a). Immunoreactivity in the form of wires and organized myelin sheaths as a result of more minimal myelin fragmentation due to reduced damage was also noticed in groups 5, 7, 4 and 6, respectively (Figure 4b).

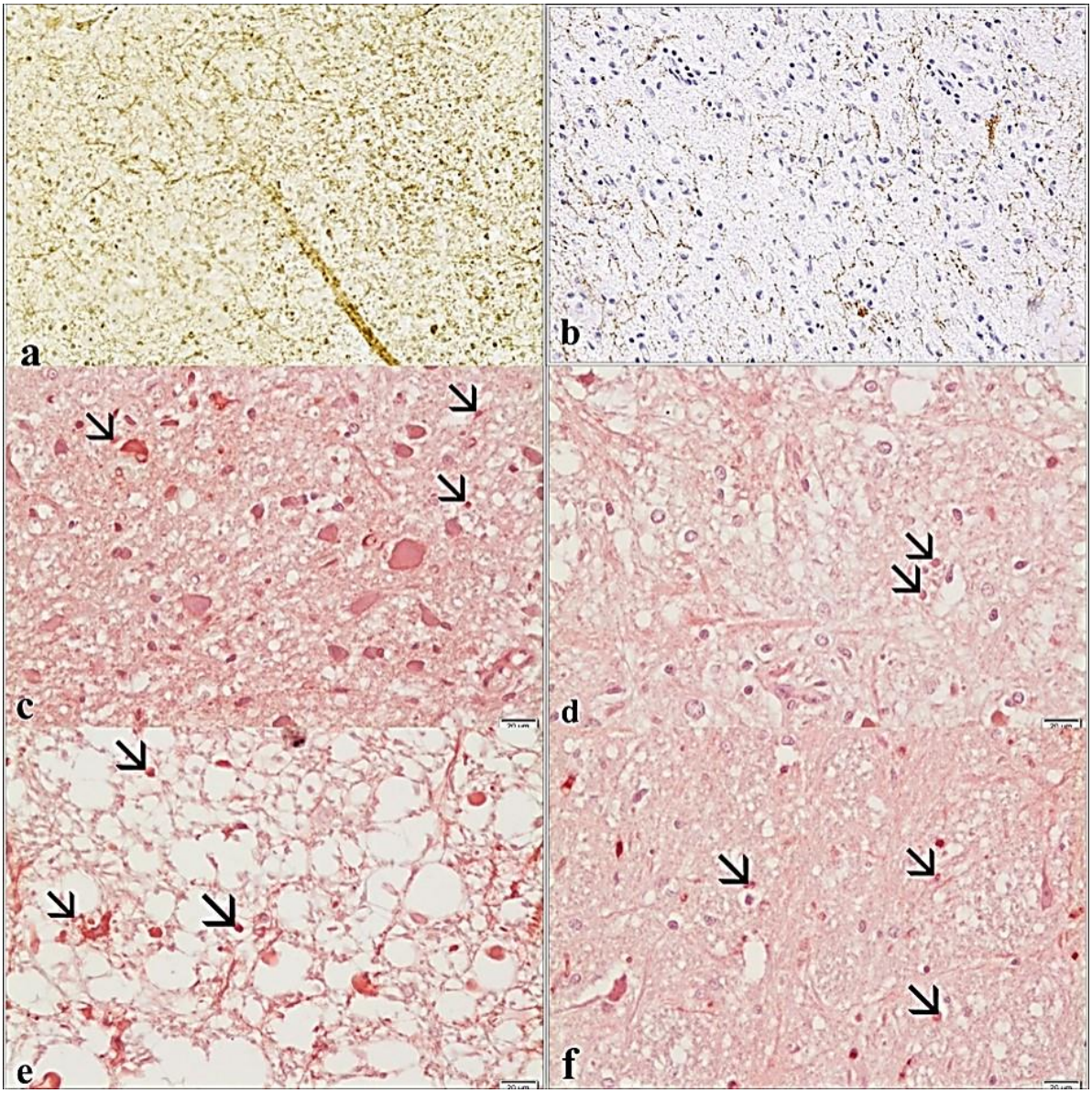

Figure 4. Immunohistochemical findings regarding MBP, IBA-1 and INOS antibodies.
a. Medulla spinalis MBP positive myelin sheaths, Sham B group, DAB, ABC, ×100 µm.
b. MBP weak positive myelin sheaths in medulla spinalis, Preconditioning A group, DAB, ABC, ×20 µm.
c. IBA-1 positive microglia (arrows) in medulla spinalis, Sham A group, AEC, ABC.
d. IBA-1 weak positive microglia (arrows) in medulla spinalis, Treatment A group, AEC, ABC, ×20 µm.
e. Medulla spinalis INOS moderate positive microglia (arrows), Sham B group, AEC, ABC, ×20 µm.
f. Medulla spinalis INOS weak positive microglia (arrows), Treatment B group, AEC, ABC, ×20 µm.

DOI: 10.33988/auvfd.872947

Table 3. Immunohistochemical changes in the spinal cord.

Groups	GFAP	NSE	IBA	iNOS	COX-2	MBP organized	MBP unorganized
	Mean±SE	Mean±SE	Mean±SE	Mean±SE	Mean±SE	Mean±SE	Mean±SE
1: Control	0.00±0.00	0.00±0.00	0.00±0.00	0.00±0.00	$3.00\pm0.00^{\alpha}$	3.00±0.00	0.00±0.00
2:Sham A	0.00±0.00	2.75±0.16	1.25±0.16	1.00±0.18	2.00±0.00	2.00±0.18	2.12±0.12
3:Sham B	0.62±0.18	3.00±0.00	1.75±0.16	$1.87\pm0.12^{*}$	$2.75\pm0.16^{€}$	$1.12\pm0.12^{€}$	1.87±0.12
4:Preconditioning A	$0.62\pm0.18^{*}$	$1.62\pm0.18^{€,\beta}$	$0.87\pm0.22^{\neq}$	$0.75\pm0.16^{\beta}$	1.62 ± 0.18^{B}	$0.75\pm0.16^{€}$	$1.12\pm0.12^{€,\beta}$
5: Preconditioning B	$2.00\pm0.00^{€,\beta}$	$0.50\pm0.18^{€,\beta}$	$0.37\pm0.18^{*,\beta}$	$0.37\pm0.18^{\beta}$	$0.87\pm0.12^{€,B}$	$2.00\pm0.00^{\beta}$	$0.50\pm0.18^{€,\beta}$
6:Treatment A	0.50±0.18	$2.00\pm0.00^{€,\beta}$	$0.62\pm0.26^{\beta}$	$0.62\pm0.26^{\beta}$	1.75 ± 0.16^{B}	$0.62\pm0.18^{€}$	$1.00\pm0.00^{€,\beta}$
7:Treatment B	$2.00\pm0.00^{€,\beta}$	$1.00\pm0.00^{€,\beta}$	$0.50\pm0.18^{\beta}$	$0.50\pm0.18^{\beta}$	$1.00\pm0.00^{€,B}$	$0.87\pm0.12^{€}$	$0.87\pm0.12^{€,\beta}$

A: First day, B: Seventh day, α : Immunoreactivity in neurons
Compared with the Sham A group: * : $P<0.05$; € : $P<0.005$
Compared with the Sham B group: ≠ : $P<0.05$, β : $P<0.005$.

Table 4. Effects of Kefir on Serum BDNF (ng / ml) in Experimental Spinal Cord Injury.

Groups	Group 1: Control	Group 2: Sham A (1.day)	Group 3: Sham B (7.day)	Group 4: Preconditioning A (1.day)	Group 5: Preconditioning B (7.day)	Group 6: Treatment A (1.day)	Group 7: Treatment B (7.day)
Mean	63.94	12.06	31.14	30.96	33.41	26.09	36.58
SE	±19.93	± 5.51	±14.32	±11.10	±16.57	±10.77	±13.84

IBA-1 and INOS positive cells were observed in the microglia cells around the vacuolizations in the damage area in groups 3, 2, 4, 6, 7 and 5, respectively, ranging from minimal to mild according to the severity of immunoreactivity (Figures 4c, 4d, 4e, 4f). INOS immunoreactivity was observed in some blood vessel endothelial cells among these microglial cells (Groups 3, 2, 4.6, respectively).

Immunohistochemical changes in the spinal cord were graded as none (0), mild (1), moderate (2) and severe (3).

When kefir was compared with the sham groups, it was found that the preconditioning groups showed a positive effect by significantly decreasing the NSE, IBA, INOS, COX-2, and unorganized-MBP levels and increasing the GFAP level on the 1st and 7th days and increasing spinal cord (P=0.000).

Compared to sham groups, it was found that kefir demonstrated a positive effect in treatment groups by decreasing the levels of NSE, IBA-1, INOS, COX-2 and MBP significantly on the 1st and 7th day and increasing the GFAP level (P=0.000, Table 3). On the other hand, kefir had a therapeutic effect by decreasing the levels of NSE, IBA-1, INOS, COX-2, and MBP more than day 1 on the 7th day in the preconditioning and treatment groups (P=0.005, Table 3).

Serum BDNF findings: When compared to the control group, Serum BDNF levels decreased significantly in the Sham A-B, Preconditioning A-B and Treatment A-B groups. When compared to Sham and B groups, kefir increased BDNF levels in preconditioning and treatment groups on the 1st and 7th days. Compared to the Sham A group, kefir increased BDNF levels on the 1st day more than the 7th day in the preconditioning and treatment groups (P=0.292, Table 4).

Discussion and Conclusion

Pathological injury mechanisms after SCI are mostly focused on primary and secondary injuries. Primary trauma of the spinal cord leads to irreversible primary injury (33, 37). In contrast, primary injury cascade reactions lead to reversible secondary injury with more serious levels of injury compared to primary injuries (24). Acute spinal cord injuries could result in severe central nervous system damage as well as motor and sensory dysfunction, and it has a high rate of disability (23). Despite the importance of motor dysfunction repair in SCI patients (34), the basic mechanisms have not been demonstrated yet and more basic research is required. In the study, the values in the preconditioning group were found to be higher compared to the sham and treatment groups in the neurological evaluation with the MTS. In terms of the finger opening test, the differences between the Preconditioning B and Treatment A groups were significant in the neurological evaluation on the 1st day (P=0.000). Many studies have reported that antioxidants

could delay the progression of neurodegeneration (1). Zhang et al. (40) applied compression from the T8 level to the spinal cord in rats and demonstrated locomotor healing in the MTS with combined anti-inflammatory therapy. In our study, it can be argued that the MTS values in the preconditioning group were higher than those in the other groups; and kefir contributed to the clinical improvement after trauma. Based on these findings, it can be argued that the preconditioned application of kefir provides clinical benefits. While there was a decrease in the finger opening test values after the trauma, an increase was observed in the groups that were fed kefir. Similar to the findings of our study, Şirin et al. (35) reported that there was a significant decrease in finger opening test values after spinal cord injury.

BDNF mainly promotes the survival and regeneration of neurons, and it has been defined in many brain regions including the bulbus olfactorius, cortex, hippocampus, basal forebrain, mesencephalon, hypothalamus, brainstem, and spinal cord (2). After SCI, the requirement for BDNF is increased (8, 15). Therefore, we believe that BDNF could be useful in identifying spinal cord injury and in monitoring the post-treatment process and prognosis. When compared to the control group, Serum BDNF levels decreased significantly in the Sham A-B, Preconditioning A-B, and Treatment A-B groups. When compared to Sham and B groups, kefir increased BDNF levels in preconditioning and treatment groups on the 1st and 7th days. When compared to the Sham A group, kefir demonstrated a therapeutic effect by increasing the BDNF levels in the preconditioning and treatment groups more on the 1st day compared to the 7th day (P=0.292).

Spinal cord injury always initiates an inflammatory response characterized by the infiltration of leukocytes and the synthesis of cytokines and chemokines. This excessive inflammation induced by a spinal cord injury induces degeneration of neurons and apoptosis of oligodendrocytes, causing a progressive injury. Astrocytes are one of the first cell populations to detect spinal cord injury. Astrocytes participate in repairing damaged parts of the brain; the presence of a significant increase in fibrous astrocytes during astrocytosis could be detected by strong GFAP expression in the brain tissue (6, 7). Intense astrocytosis does not occur within a short time following the spinal cord injury, and it is considered a chronic process. Similarly, myelin damage occurs immediately at the time of the injury; however, it does not start to appear morphologically within the few days following the trauma and it becomes visible with the sustained release of the metabolites applied to the damage (28). In the study, the GFAP and MBP expressions differed between the groups particularly in parallel with the increases in trauma and kefir application periods. However, it cannot be argued that kefir application provides full protection both in protecting myelin sheath structure and in sporrting astrocytosis. We attribute this to the short duration of both trauma and the kefir application in order to better observe morphological lesions. In the study, spinal cord damage lesions from kefir application that continued for 7 days before and after formation were observed less frequently compared to other groups, both in neurological examinations and at the histopathological level.

The rise of neuron-specific enolase (NSE), known to play a role in the pathogenesis of hypoxic-ischemic brain injury, has been blamed for neuronal damage following spinal cord injury. For this reason, NSE is believed to be an important marker that directly evaluates functional damage in neurons (19). While a large number of NSE positive neurons were observed in the group that did not receive kefir after the trauma, a significant reduction in immunoreactivity was also noted despite complete protection was not provided with the inclusion of kefir (P=0.000).

Traumatic spinal cord injury directly causes axonal and myelin damage as well as migration of inflammatory cells to the inflamed region (28). Miller et al. (28) reported that focal hemorrhage and necrosis were observed at the 1st hour following the trauma and stated that there was an increase in IBA-1 and INOS expression in macrophages and microglia in the area of damage. Monocytes and microglia begin to multiply around the primary lesion after 48 hours following the spinal cord injury. Neutrophils are no longer present after 3 days. They are replaced by a large number of monocytes and microglia (40). Microglia activation is a common incidence in spinal cord trauma and is claimed to cause tissue damage during the elaboration of proinflammatory agents. INOS is an inducible enzyme found in macrophages and endothelial cells. INOS release is very low in the brain and often cannot be expressed. However, the production of cytokines causes INOS expression in microglia and astrocytes, resulting in continuous and high levels of nitric oxide production, which could lead to further tissue damage, especially with toxic byproducts such as peroxynitrite. Nitric oxide is also toxic to neurons and is responsible for neuronal death (28).

IBA-1, which plays a role in the rearrangement of the actin cytoskeleton,is a cell surface marker directly associated with microglia activation, migration, and phagocytosis (22). Following the spinal cord injury, INOS and IBA-1 positive staining is observed in the microglia cells and macrophages around the vacuolizations and disintegrated myelin sheaths; however, immunoreactivity was observed to decrease due to the anti-inflammatory effect of kefir.

There are two forms of the cyclooxygenase enzyme called COX-1 and COX-2. In experimental acute spinal cord injury, the production of COX-2, mRNA and proteins

is identified to increase between 2 and 48 hours, and it was determined that COX-2 inhibition would contribute to the results of spinal cord injury selectively. In the central nervous system without damage, the presence of COX-2 in the neurons was demonstrated immunohistochemically (31); however, it was reported that the increase in COX-2 related to the damage accelerated neuronal death and the neuroinflammatory response resulting from the production of prostaglandin E2 (PGE_2) (14, 32). It is reported that COX-2, which is normally observed in neurons, is released with the injury from astrocytes and microglia, respectively (9, 20). In this study, severe COX-2 immunoreactivity was observed in groups in which trauma was created but no kefir application was made. Despite the fact that the complete protective effect of kefir, which is reported to have an anti-inflammatory effect (4, 30), was not observed, it was able to provide a reduction in the COX-2 release even with the application for 7 days before and after the experiment.

As a result, histopathological examinations concluded that kefir had a positive effect in preconditioning and treatment groups by decreasing spinal cord bleeding, edema, myelin sheath damage, liquefactive necrosis, neuronal necrosis, the selectivity of canalis centralis and gitter cell levels significantly. Immunohistochemical examinations concluded that kefir had a positive effect in the treatment groups by decreasing the NSE, IBA-1, INOS, COX-2, and MBP levels on the 1st and 7th days and significantly increasing the GFAP level. This was supported by the increase that was observed in serum BDNF levels. In addition, no side effects or negative consequences have been reported for the consumption of kefir, which is a probiotic substance; on the contrary, it is reported to have antioxidant, anti-inflammatory, antiapoptotic, antitumoral, cholesterol-lowering, and neuroprotective effects. In the present study, it can be argued that kefir reduces the negativities formed at the cellular level against traumatic spinal cord damage; however, it cannot be argued that it provides complete protection. We believe that this may be related to the shortness of the period of kefir consumption. Therefore, there is a need for further studies, in which kefir would be applied for a longer time and in greater amounts. It is predicted that the consumption of this beverage, which is easily accessible and easy to prepare, would have protective effects on spinal cord injuries.

Acknowledgements

The authors would like to thank Assoc. Prof. Dr. Pınar PEKER AKALIN for their contribution in the evaluation phase of biochemistry parameters. X. National and I. International Veterinary Pathology Congress (online) is presented as an oral presentation (27-37 October 2020, Burdur-Türkiye).

Financial Support

This work was supported by the Coordinatorship of Scientific Research Projects of Hatay Mustafa Kemal University [grant numbers 18.M.021].

Conflict of Interest

The authors have no conflict of interest to declare.

Author Contributions

ZY, ŞYÖ, TK, BÖ, MEA and HA conceived and planned the experiments. ZY, MEA and HA carried out the experiments. ZY, ŞYÖ, TK and BÖ planned and carried out the simulations. ŞYÖ, TK and BÖ contributed to sample preparation. ZY, ŞYÖ, TK, BÖ, MEA and HA contributed to the interpretation of the results. ZY, ŞYÖ, TK and MEA took the lead in writing the manuscript. All authors provided critical feedback and helped shape the research, analysis and manuscript.

Data Availability Statement

The data supporting this study's findings are available from the corresponding author upon reasonable request.

Ethical Statement

This study was approved by the Hatay Mustafa Kemal University Animal Experiments Local Ethics Committee (2017/10-2).

Animal Welfare

The authors confirm that they have adhered to ARRIVE Guidelines to protect animals used for scientific purposes.

References

1. **Banji OJ, Banji D, Ch K** (2014): *Curcumin and hesperidin improve cognition by suppressing mitochondrial dysfunction and apoptosis induced by D-galactose in rat brain.* Food Chem Toxicol, **74**, 51-59.
2. **Bathina S, Das UN** (2015): *Brain-derived neurotrophic factor and its clinical implications.* Arch Med Sci, **11**, 1164.
3. **Binder DK, Scharfman HE** (2004): *Brain-derived neurotrophic factor.* Growth Factors, **22**, 123.
4. **Delen E, Durmaz R, Oglakci A, et al** (2015): *Efficacy of kefir on the release of lysosomal proteases after expremintal spinal cord trauma.* J Clin Anal Med, **6**, 21-25.
5. **Duitschaever C, Kemp N, Emmons D** (1987): *Pure culture formulation and procedure for the production of kefir.* Milchwiss, **42**, 80-82.
6. **Eddleston M, Mucke L** (1993): *Molecular profile of reactive astrocytes—implications for their role in neurologic disease.* Neurosci, **54**, 15-36.
7. **Eng LF, Ghirnikar RS** (1994): *GFAP and astrogliosis.* Brain Pathol, **4**, 229-237.
8. **Erdem H, Oktay M, Yildirim U, et al** (2013): *Expression of AEG-1 and p53 and their clinicopathological significance in malignant lesions of renal cell carcinomas: a microarray study.* Pol J Pathol, **64**, 28-32.

9. **Font-Nieves M, Sans-Fons MG, Gorina R, et al** (2012): *Induction of COX-2 enzyme and down-regulation of COX-1 expression by lipopolysaccharide (LPS) control prostaglandin E2 production in astrocytes.* J Biol Chem, **287**, 6454-6468.
10. **Friques AG, Santos FD, Angeli DB, et al** (2020): *Bisphenol A contamination in infant rats: molecular, structural, and physiological cardiovascular changes and the protective role of kefir.* J Nutr Biochem, **75,** 108254.
11. **Furukawa N, Matsuoka A, Yamanaka Y** (1990): *Effects of orally administered yogurt and kefir on tumor growth in mice.* J Jpn Soc Nutr Food Sci, **43**, 450-453.
12. **Gale K, Kerasidis H, Wrathall JR** (1985): *Spinal cord contusion in the rat: behavioral analysis of functional neurologic impairment.* Exp Neurol, **88**, 123-134.
13. **Gao J, Ding G, Li Q, et al** (2019): *Tibet kefir milk decreases fat deposition by regulating the gut microbiota and gene expression of Lpl and Angptl4 in high fat diet-fed rats.* Food Res Int, **121**, 278-287.
14. **Gopez JJ, Yue H, Vasudevan R, et al** (2005): *Cyclooxygenase-2-specific inhibitor improves functional outcomes, provides neuroprotection, and reduces inflammation in a rat model of traumatic brain injury.* Neurosurg, **56**, 590-604.
15. **Guo R, Overman M, Chatterjee D, et al** (2014): *Aberrant expression of p53, p21, cyclin D1, and Bcl2 and their clinicopathological correlation in ampullary adenocarcinoma.* Hum Pathol, **45**, 1015-1023.
16. **Gurcan O, Gurcay AG, Kazanci A, et al** (2017): *Effect of asiatic acid on the treatment of spinal cord injury: An Experimental study in rats.* Turk Neurosurg, **27**, 259-264.
17. **Guven M, Akman T, Yener AU, et al** (2015): *The neuroprotective effect of kefir on spinal cord ischemia/reperfusion injury in rats.* J Korean Neurosurg Soc, **57**, 335.
18. **Hanci V, Kerimoğlu A, Koca K, et al** (2010): *The biochemical effectiveness of N-acetylcysteine in experimental spinal cord injury in rats.* Turk J Trauma Emerg Surg, **16**, 15-21.
19. **Haque A, Ray SK, Cox A, et al** (2016): *Neuron specific enolase: a promising therapeutic target in acute spinal cord injury.* Metab Brain Dis, **31**, 487-495.
20. **Hewett SJ, Bell SC, Hewett JA** (2006): *Contributions of cyclooxygenase-2 to neuroplasticity and neuropathology of the central nervous system.* Pharmacol Ther, **112**, 335-357.
21. **Huang EJ, Reichardt LF** (2001): *Neurotrophins: roles in neuronal development and function.* Annu Rev Neurosci, **24**, 677-736.
22. **Imai Y, Kohsaka S** (2002): *Intracellular signaling in M-CSF-induced microglia activation: role of Iba1.* Glia, **40**, 164-174.
23. **Jia Y, Lu T, Yao S, et al** (2019): *The effects of interferon-β on neuronal apoptosis and the expressions of BDNF and TrkB in rats with spinal cord injuries.* Int J Clin Exp Med, **12**,12693-12701.
24. **Kato K** (2012): *Stem cells in human normal endometrium and endometrial cancer cells: characterization of side population cells.* Kaohsiung J Med Sci, **28**, 63-71.
25. **Kavakli HS, Koca C, Alici O** (2011): *Antioxidant effects of curcumin in spinal cord injury in rats.* Turk J Trauma Emerg Surg, **17**, 14-18.
26. **Kubo M, Odani T, Nakamura S, et al** (1992): *Pharmacological study on kefir--a fermented milk product in Caucasus. I. On antitumor activity (1).* Yakugaku Zasshi, **112**, 489-495.
27. **Matsuu M, Shichijo K, Okaichi K, et al** (2003): *The protective effect of fermented milk kefir on radiation-induced apoptosis in colonic crypt cells of rats.* J Radiat Res, **44**, 111-115.
28. **Miller AD, Westmoreland SV, Evangelous NR, et al** (2012): *Acute traumatic spinal cord injury induces glial activation in the cynomolgus macaque (Macaca fascicularis).* J Med Primatol, **41**, 202-209.
29. **Mumford A** (2007): *An Investigation into the spatial organization of kefir grains.* Microb Divers, 1-11.
30. **Özsoy S** (2016): *The Protective Effect of Kefir on Carbon Tetrachloride-induced Histopathological Changes in the Livers of Rats.* Kafkas Univ Vet Fak Derg, **22**, 403-408.
31. **Resnick DK, Graham SH, Dixon CE, et al** (1998): *Role of cyclooxygenase 2 in acute spinal cord injury.* J Neurotrauma, **15**, 1005-1013.
32. **Rollason V, Flora Samer C, Daali Y, et al** (2014): *Prediction by pharmacogenetics of safety and efficacy of non-steroidal anti-inflammatory drugs: a review.* Curr Drug Metab, **15**, 326-343.
33. **Serarslan Y, Yönden Z, Özgiray E, et al** (2010): Protective effects of tadalafil on experimental spinal cord injury in rats. J Clin Neurosci, **17**, 349-352.
34. **Siebels á, Rohrmann K, Oberneder R, et al** (2011): *A clinical phase I/II trial with the monoclonal antibody cG250 (RENCAREX®) and interferon-alpha-2a in metastatic renal cell carcinoma patients.* World J Urol, **29**, 121-126.
35. **Sirin Y, Keles H, Besalti O, et al** (2012): *Comparison of ATP-MgCl2 and methylprednisolone in experimentally induced spinal cord trauma.* J Clin Anal Med, **3**, 442-447.
36. **St-Onge M-P, Farnworth ER, Jones PJ** (2000): *Consumption of fermented and nonfermented dairy products: effects on cholesterol concentrations and metabolism.* Am J Clin Nutr, **71**, 674-681.
37. **Toklu HZ, Hakan T, Celik H, et al** (2010): *Neuroprotective effects of alpha-lipoic acid in experimental spinal cord injury in rats.* J Spinal Cord Med, **33**, 401-409.
38. **Yu S, Yao S, Wen Y, et al** (2016): *Angiogenic microspheres promote neural regeneration and motor function recovery after spinal cord injury in rats.* Sci Rep, **6**, 1-13.
39. **Zhang D, Ma G, Hou M, et al** (2016): *The neuroprotective effect of puerarin in acute spinal cord injury rats.* Cell Physiol Biochem, **39**, 1152-1164.
40. **Zhang Z, Krebs CJ, Guth L** (1997): *Experimental analysis of progressive necrosis after spinal cord trauma in the rat: etiological role of the inflammatory response.* Exp Neurol, **143**, 141-152.

Evaluation of the effect of albendazole and *Nigella sativa* combination on Visceral Larvae Migrans (*Toxocara canis*) in mice

Ceren AŞTI[1,a, ✉], Hatice ÖGE[1,b]

[1]Ankara University, Faculty of Veterinary Medicine, Department of Parasitology, Ankara, Türkiye

[a]ORCID: 0000-0002-8424-2343; [b]ORCID: 0000-0002-4799-3455

ARTICLE INFO

Article History
Received : 09.02.2021
Accepted : 24.10.2021
DOI: 10.33988/auvfd.877478

Keywords
Albendazole
Mice
Nigella sativa
Toxocara canis
Visceral Larvae Migrans

✉Corresponding author
casti@ankara.edu.tr

How to cite this article: Aştı C, Öge H (2023): Evaluation of the effect of albendazole and *Nigella sativa* combination on Visceral Larvae Migrans (*Toxocara canis*) in mice. Ankara Univ Vet Fak Derg, 70 (1), 21-28. DOI: 10.33988/auvfd.877478.

ABSTRACT

Visceral Larvae Migrans (VLM) is a syndrome in humans, caused by *Toxocara canis* larvae. A current and completely successful treatment protocol against such a common infection has yet to be established. In this study, the effect of combination of albendazole and *N. sativa* oil for the treatment of VLM was investigated. Five experimental groups were constituted and a total of 125 *Swiss albino* (male, 6-8 weeks old) mice were used. All mice in each group were infected with 750 *T. canis* eggs with infective larvae, except the negative control group. 100 mg/kg albendazole and 0.15 ml *Nigella sativa* oil were applied orally to groups ALB and NSO separately and given orally to group COM in combination. The efficacy of the treatment was investigated parasitologically, histo-pathologically, and hematologically on the 7th, 14th, 28th, 45th, and 60th days post-infection with necropsies. The larval recovery analyses revealed that, the highest treatment efficacy was obtained in group of combination. The treatment efficacy was 72.46%, 48.81%, 36.25% in the groups of COM, ALB, and NSO, respectively. The most severe pathological changes were developed in Group ALB, and the inflammatory reactions and pathological changes in Groups of COM and NSO were mild. We conclude that *N. sativa* oil enhances the larvicidal effect of albendazole by having an anti-inflammatory effect and increasing tissue defense and immunity.

Introduction

Toxocara canis is a parasite frequently encountered in both puppies and adult dogs. In addition to being a common parasite in carnivore animals, *T. canis* is also an important parasite in humans, especially in play-age children, causing a zoonotic infection known as Visceral Larvae Migrans Syndrome (11).

Visceral Larvae Migrans (VLM) is characterized by hypereosinophilia (about 10.000 cells/mm3), hepatomegaly, fever, intermittent pulmonary infiltration, and hypergammaglobunemia, all caused by nematode larvae that have a non-human definitive host (5, 9).

The main purpose of the treatment of infection is to reduce the number of larvae migrating to tissues and also alleviate or eliminate clinical symptoms (23). It is recommended that patients be treated with long-term anthelmintic as well as an anti-inflammatory agent (29). Currently, albendazole can be used for VLM treatment in humans (31, 38). Since a fully effective anthelmintic has not been established yet, the researchers were encouraged to use microparticles, immunomodulatory agents, probiotics, immune system supporters and stimulants, tissue defense strengthening, mucosal integrity strengthening, and anti-inflammatory agents as alternative treatments to increase the treatment efficiency (3, 4, 14, 19, 32). There have also been several applications using molecules of plant origin for increasing the effectiveness of the treatments of VLM (34, 35). *Nigella sativa* has been considered as one of the medically important plants due to its immunomodulator effect on cellular and humoral immunity (13, 15, 27, 28) and anti-inflammatory effect on inflammation areas (6, 12, 24, 26). The main active agent showing this medicinal effect is thymoquinone (TQ) as a phytochemical agent (2-isopropyl-5-methyl-1,4-benzoquinone, $C_{10}H_{12}O_2$) (1, 36). Thymoquinone is found in 30-48% of the seeds (2, 16).

There have been a few studies investigating the effect of *N. sativa* on helminth infections (8, 25, 30). The aim of this study was to determine the effectiveness of a combination of albendazole and N. sativa oil against VLM in an experimentally infected mouse model. Albendazole is less absorbed from the digestive system, and it has been stated that this absorption increases in oily medium (16). Therefore, we hypothesized that whether a new drug formulation could be developed by enhancing the effect of albendazole with *N. sativa* oil.

Materials and Methods

Active substances and experimental groups: A total of 125 male *Swiss albino mice* (mean weight 30g and 6-8 weeks old) were used in this study, with 25 mice in experimental [albendazole (Vermiprazole oral suspension 10%), *N. sativa* oil, and combination] and control groups. The amount of albendazole active substance in the preparation was analyzed by a spectrophotometric method (37). The anthelmintic was administered orally to mice at a dose of 100 mg/kg in group of albendazole (ALB) and combination (COM) (39).

The oil obtained from the seeds of *N. sativa* was directly administered by oral gavage at a dose of 0.15 ml to mice in group of *N. sativa* oil (NSO) and COM (30). The modified method was used to determine the amount of TQ as the active ingredient in *N. sativa* oil, by High Performance Liquid Chromatography (HPLC) (10).

Infecting mice and treatment procedure: Infected dogs were treated with Pyrantel Pamoate (Kontil®, oral suspension, 250 mg/5ml) at a dose of 0.1 cc/kg to collect mature *T. canis*. Eggs were collected from mature females and incubated in 0.5% formalin at 26-28°C in humidity for 21-23 days until infective larvae developed. Mice were infected with 750 eggs containing infective larvae by oral gavage. The day infected mice were determined as day 0 of the experiment. A physiological salt solution was given to the group of negative control by oral gavage to provide the same stress and ambient conditions. Albendazole (100 mg/kg p.o), *N. sativa* oil (0.15 ml p.o), and a combination of albendazole and *N. sativa* oil (100 mg/kg p.o albendazole + 0.15 ml p.o *N. sativa* oil) were applied to mice in treatment groups for 5 days post-infection. 0.2 ml dose of physiological salt solution was given orally to Groups of positive (PC) and negative control (NC).

Necropsies of mice: Necropsies were performed on 5 mice from each experimental group on the 7th, 14th, 28th, 45th, and 60th days post-infection. Three of 5 mice were examined parasitologically and two of them were examined pathologically.

Brain, eye, internal organs, muscle tissue, and mesenterial lymphatic nodules were examined for larvae (Figure 1). Also, the organs with lumen like stomach, intestine, urinary bladder, etc., and body cavities (abdominal and thoracic cavities) were examined parasitologically on stereo-microscope. The brain and eye were examined immediately after removal. The heart, lungs, diaphragm muscles, gastric mucosa, liver, spleen, kidneys, testes, mesenterial lymphatic nodules, forelimb, and hindlimb muscles, intestinal and urinary bladder mucosa were incubated in pepsin-HCl digestion solution (5 g pepsin + 7 ml HCl + 988 ml 0.9% isotonic solution) at 37°C for 24 hours. At the end of the period, the molten organs and tissue fragments were filtered and centrifuged in 15 ml conical falcon tubes at 2000 rpm for 10 minutes. After centrifugation, the supernatant was removed and the samples were kept at +4°C with 10% formalin until the larvae were counting.

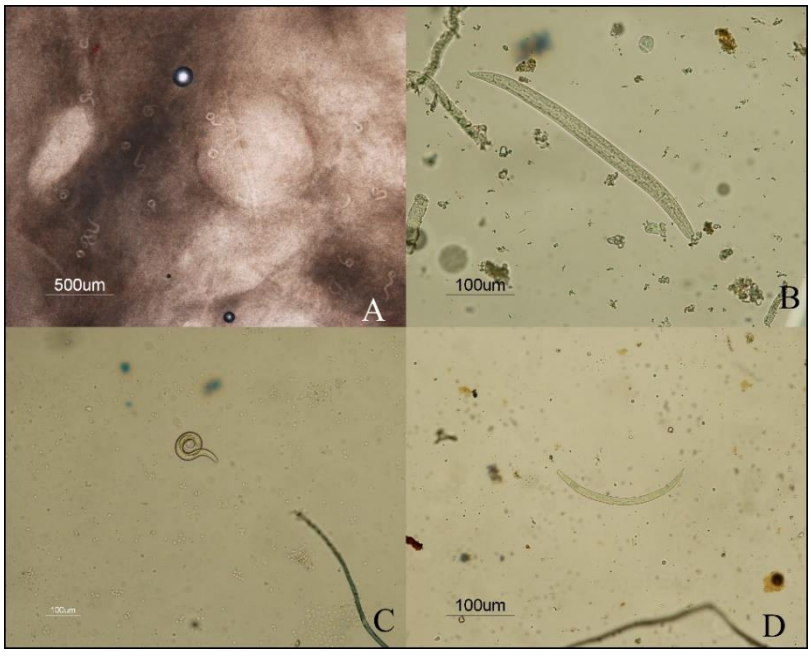

Figure 1. *Toxocara canis* larvae in different tissues. **A.** Brain, **B.** Hindlimb muscles, **C.** Eye, **D.** Diaphragm muscles.

DOI: 10.33988/auvfd.877478

Haematological and histo-pathological examination: Blood taken during euthanasia was used to prepare smears for hematological analysis. Three preparations were made from each mouse to determine the effect of treatment on blood cells, especially eosinophil leukocytes. The May-Grünwald Giemsa staining technique was used to stain the smears (21). The type and rate of the first 100 blood cells encountered in the microscopic area were calculated with the formula-leucocitaria method (18).

In order to examine the histopathological changes, 5µm thick sections were taken from tissue samples after 10% formalin fixation and paraffin blocking. The preparations were stained with Hematoxylin & Eosin (21). All treatment groups were compared to Groups PC and NC.

Statistical analysis: IBM SPSS Statistics Version 23 was used to evaluate the data. The statistical difference between the groups was analyzed by the Kruskal Wallis Test and the statistical difference was taken as P<0.10.

Results

Pharmacological results: In spectrophotometric analysis, the amount of albendazole in the oral suspension was 98%. Thymoquinone in *N. sativa* oil was found to be 1.39% using High Performance Liquid Chromatography method. According to the TQ percentage taken, 0.17% TQ was detected in 0.15 ml (0.13 g) *N. sativa* oil dosed to each mouse.

Parasitological results: On the 7th day, the total number of migrated larvae were 343.65. The number of migrating larvae decreased in each treatment group. The fewest larvae was found in the Group COM. Larvae were 31.00 in Group COM, and 36.33; 61.66 and 214.66 in Group ALB, NSO, and Group PC, respectively. They were especially concentrated in the liver and lungs, especially in Group PC. Numbers of larvae in liver and lungs were statistically different compared to the other necropsy days (P<0.05). It was also observed that the larvae began to migrate to brain on 7th day in all experimental groups. The decrease in the number of larvae in the extremity muscles of Group ALB was statistically different compared to Group PC (P<0.10). The decrease in the number of larvae of brain and diaphragm muscles in Group COM were statistically different compared to the Group PC and Group ALB (P<0.10) (Table 1).

Table 1. Average number of larvae on 7th, and 14th days.

	7th day					14th day				
	PC n=3 $\bar{x} \mp S_{\bar{x}}$	ALB n=3 $\bar{x} \mp S_{\bar{x}}$	NSO n=3 $\bar{x} \mp S_{\bar{x}}$	COM n=3 $\bar{x} \mp S_{\bar{x}}$	P	PC n=3 $\bar{x} \mp S_{\bar{x}}$	ALB n=3 $\bar{x} \mp S_{\bar{x}}$	NSO n=3 $\bar{x} \mp S_{\bar{x}}$	COM n=3 $\bar{x} \mp S_{\bar{x}}$	P
Brain	22.00∓1.528[3]	10.67∓1.667	22.00∓2.517	6.33∓3.1803[3]	0.033**	40.33∓2.603[3]	24.67∓6.173	32.33∓5.207	13.00∓3.786[3]	0.063*
Eye	-	-	0.33∓0.333	-	-	0.67∓0.333	-	-	-	-
Heart	1.33∓1.333	1.00∓1.000	0.33∓0.333	0.33∓0.333	0.983	1.67∓0.667	0.67∓0.333	1.33∓0.882	-	0.139
Lungs	36.33∓15.857	8.67∓3.180	6.00∓1.732	4.33∓1.667	0.107	2.00∓0.577	1.67∓1.202	0.33∓0.333	1.33∓0.882	0.391
Diaphragm Muscles	1.67∓0.333	0.67∓0.333[5]	1.33∓0.667	4.00∓1.000[5]	0.083*	1.67∓0.667	1.00∓1.000	0.67∓0.333	0.67∓0.667	0.585
Stomach	-	-	-	-	-	-	-	-	-	-
Liver	122.33∓65.804	10.33∓4.978	8.67∓5.175	6.67∓4.702	0.281	26.67∓5.925[3]	8.00∓4.041	11.33∓1.333	5.00∓0.577[3]	0.051*
Spleen	-	-	-	0.67∓0.667	-	1.00∓0.577	0.67∓0.667	0.67∓0.333	-	0.415
Kidneys	8.67∓1.667	2.00∓2.00	11.67∓3.667	4.67∓2.186	0.101	2.00∓0.000	2.00∓0.577	0.67∓0.333	0.67∓0.333	0.249
Testes	-	-	0.33∓0.333	-	-	0.33∓0.333	-	-	0.33∓0.333	0.532
M.Lymph Nodes	1.33∓0.333[3]	0.33∓0.333	1.00∓0.000	0.00∓0.000[3]	0.040**	1.00∓0.000	0.33∓0.333	0.33∓0.333	0.67∓0.333	0.326
Forelimb Muscles	11.67∓2.848[1]	1.33∓0.882[1]	7.67∓3.667	2.33∓1.202	0.043**	5.67∓3.667	4.33∓0.333	4.67∓1.764	1.33∓0.333	0.137
Hindlimb Muscles	9.00∓1.155[1]	1.00∓1.000[1]	2.33∓0.882	1.67∓0.882	0.072*	10.00∓3.464[3]	3.33∓0.333	7.00∓2.309	1.00∓0.577[3]	0.041**
Intestines	0.33∓0.333	0.33∓0.333	-	-	0.532	-	-	-	-	-
Urinary Bladder	-	-	-	-	-	-	-	-	-	-

*: P<0.10; **: P<0.05; There are statistically differences between groups [1]: PC and ALB; [2]: PC and NSO; [3]: PC and COM; [4]: ALB and NSO; [5]: ALB and COM; [6]: NSO and COM.

On the 14th day, the total number of migrated larvae was 222.99. The number of migrated larvae decreased, especially in Group COM compared with Group PC. The prevalences of larvae were 24.00; 46.00; 59.33; 93.00 in Groups COM, ALB, NSO, and Group PC, respectively. The number of larvae that passed into the neurotropic-myotropic phase from 14th day was determined more intensively. In all experimental groups, the count of larvae in the internal organs such as the liver, lungs, and kidneys decreased and increased in the brain. The larvae in brain were found to be closer in Group NSO than in Group PC. The liver was the second most common larvae in all groups. The extremity and diaphragm muscles were the most common tissues in this period after brain and liver. Compared to all groups, the minimum number of larvae in the brain extremity muscles, and liver were determined in Group COM. The number of larvae in the brain, liver ($P<0.10$), and hindlimb muscles were statistically different compared to Group PC ($P<0.05$) (Table 1).

The total number of migrated larvae on day 28th was 587.65. The numbers of larvae were 91.00 in Group COM; 102.66 in Group ALB; 179.66 in Group NSO; and 214.33 in Group PC. In all groups, the maximum number of larvae was detected in the brain and decreased in the liver and lungs. The decrease in the number of larvae in hindlimb muscle in Group COM was statistically different compared to Group PC ($P<0.05$) (Table 2).

The total number of migrated larvae on the 45th day was 603.99. The numbers of larvae were 42.00 in Group COM; 164.33 in Group NSO; 196.33 in Group ALB and 201.33 in Group PC. On 60th day, a total of 319.65 larvae migrated. Numbers of larvae were 48.00 in Group COM; 56.66 in Group ALB, 81.33 in Group NSO and 133.66 in Group PC. On the 28th, 45th, and 60th days, larvae in the brain were found to be increasing compared to the 7th and 14th days and this increase was statistically different ($P<0.05$) (Table 2).

Histopathological results: All histopathological results were evaluated by comparison with Groups NC and PC on each necropsy day. On the 7th day, Group ALB showed severe inflammatory cell infiltration in the lungs, liver, and diaphragm muscles. Severe neutrophil leukocyte cell infiltration around alveoli in the lungs, emphysema, edema, and eosinophil leukocytes were noted (Figure 2). Neutrophil leukocytes, mononuclear cell infiltration, and perivasculitis were detected with numerous Kupffer cells in the liver between the remark cords and around the *Vena centralis*. In Group NSO, severe inflammation replaced by mild cellular infiltration, and changed from polymorphonuclear to mononuclear (Figure 2). Also, it was found that the level of inflammation decreased and changed from polymorphonuclear to mononuclear in Group COM as Group NSO.

On the 14th day, it was observed that the inflammation in Group ALB was severe and that many organs and tissues (lungs, liver, kidneys, etc.) were affected. There was mononuclear cell infiltration around the alveoli in the lungs and *V. centralis* and trias hepatis in the liver, as well as emphysema and focal granulomas. Mononuclear cell infiltrations and eosinophil leukocytes were noted in extremity muscles. There were no serious pathological observations in Group NSO, unlike in Group ALB. In Group COM, mild mononuclear cell infiltration in the lungs, liver, heart, extremity and diaphragm muscles, and kidneys, emphysema, edema, and eosinophil leukocytes and granuloma structures, were observed in part of the mice (Figure 3).

On the 28th, 45th, and 60th days, similar organs were affected by infection. The inflammation became chronic, and the mononuclear cells dominated the lesions. Tissue repair was started on the 28th day. Also, granuloma formation was observed in the liver, heart, and lungs on the 45th and 60th days (Figure 4).

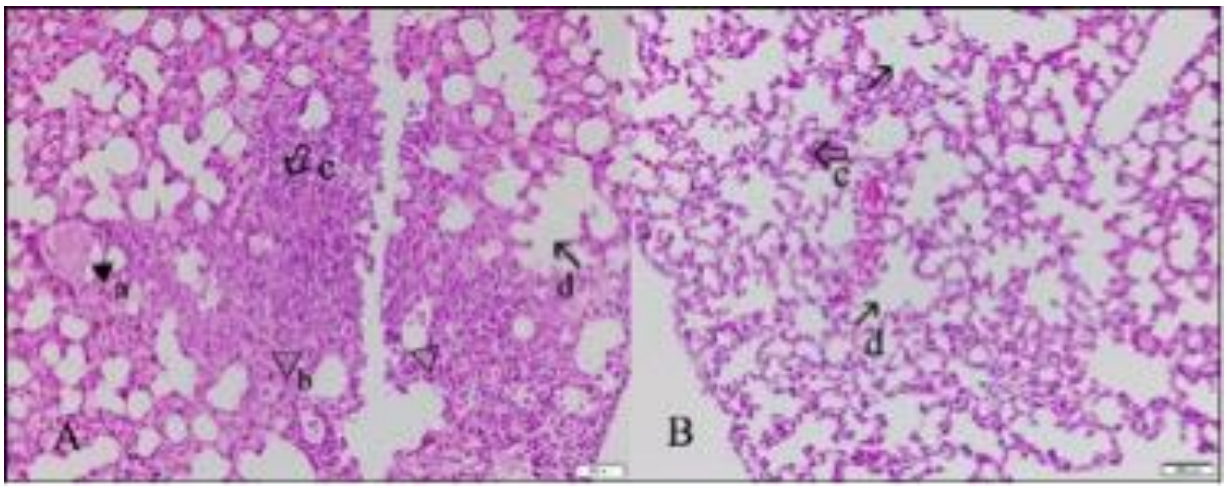

Figure 2. A. 7th day, Group ALB; edema in lung tissue (a), eosinophil leukocytes (b), multiple neutrophil leukocyte cell infiltration around alveoli (c) and emphysema (d). (H&E, scale bar: 50 µm). **B.** 7th day, Group NSO; mild cell infiltration around the alveoli in lung tissue (c) and areas of emphysema (d) (H&E, scale bar: 100µm).

DOI: 10.33988/auvfd.877478

Table 2. Average number of larvae on 28th, 45th, and 60th days.

	28th day					45th day					60th day				
	PC n=3 $\bar{x} \mp S_{\bar{x}}$	ALB n=3 $\bar{x} \mp S_{\bar{x}}$	NSO n=3 $\bar{x} \mp S_{\bar{x}}$	COM n=3 $\bar{x} \mp S_{\bar{x}}$	P	PC n=3 $\bar{x} \mp S_{\bar{x}}$	ALB n=3 $\bar{x} \mp S_{\bar{x}}$	NSO n=3 $\bar{x} \mp S_{\bar{x}}$	COM n=3 $\bar{x} \mp S_{\bar{x}}$	P	PC n=3 $\bar{x} \mp S_{\bar{x}}$	ALB n=3 $\bar{x} \mp S_{\bar{x}}$	NSO n=3 $\bar{x} \mp S_{\bar{x}}$	COM n=3 $\bar{x} \mp S_{\bar{x}}$	P
Brain	163.33∓50.466	70.67∓11.096	140.00∓43.405	69.00∓21.733	0.270	162.00∓90.279	140.67∓39.074	124.67∓17.072	36.67∓11.260	0.282	70.67∓6.009	30.33∓4.055	48.67∓10.975	30.67∓7.126	0.189
Eye	0.33∓0.333	0.33∓0.333	0.33∓0.333	0.33∓0.333	1.000	0.67∓0.667	-	-	-	-	0.67∓0.333	-	-	-	-
Heart	3.67∓0.882	1.33∓0.333	1.00∓0.00	1.00∓0.577	0.145	-	1.00∓0.577	0.33∓0.333	0.33∓0.333	0.367	2.33∓0.882	1.00∓1.000	1.67∓1.202	0.33∓0.333	0.328
Lungs	4.67∓0.882	2.67∓1.202	4.67∓1.202	1.67∓0.882	0.169	1.00∓1.000	-	0.33∓0.333	0.33∓0.333	0.737	2.67∓0.882	0.33∓0.333	0.33∓0.333	0.33∓0.333	0.120
Diaphragm Muscles	1.33∓0.882	1.00∓0.000	1.67∓0.882	1.33∓1.333	0.951	1.00∓0.577	0.67∓0.667	0.33∓0.333	-	0.438	1.33∓0.33[3]	0.33∓0.333	0.33∓0.333	0.00∓0.000[3]	0.088*
Stomach	-	0.67∓0.333	-	-	-	0.00∓0.000[1]	1.33∓0.333[1, 5]	0.33∓0.333	0.00∓0.000[5]	0.037**	-	-	-	-	-
Liver	11.00∓1.528	8.00∓2.517	8.33∓2.333	8.33∓5.364	0.852	4.00∓2.517	12.00∓5.196[5]	5.00∓1.732	0.33∓0.333[5]	0.058*	17.67∓6.692	9.33∓6.360	10.00∓3.786	7.33∓1.856	0.532
Spleen	-	-	-	-	-	0.33∓0.333	-	-	-	-	-	-	-	-	-
Kidneys	8.00∓3.055	10.33∓2.963	10.33∓4.333	4.67∓1.453	0.410	4.00∓1.732[3]	1.67∓0.333	2.67∓1.202	0.00∓0.000[3]	0.072*	3.67∓1.764	1.67∓1.202	1.00∓0.577	0.67∓0.667	0.377
Testes	-	-	0.33∓0.333	0.33∓0.333	0.532	-	-	0.33∓0.333	-	-	0.67∓0.667	0.33∓0.333	0.33∓0.333	-	0.737
M.Lymph Nodes	-	-	0.67∓0.667	0.33∓0.333	0.530	-	-	-	-	-	-	-	-	-	-
Forelimb Muscles	3.00∓1.000	3.67∓0.333	7.00∓1.528	2.67∓1.333	0.104	14.00∓8.327	20.33∓4.055	22.00∓7.550	3.00∓2.082	0.115	14.67∓2.028	6.00∓5.000	10.33∓1.764	2.33∓1.333	0.137
Hindlimb Muscles	19.00∓4.933[3]	4.00∓1.000	5.33∓0.882	1.33∓0.333[3]	0.025**	13.67∓7.265	18.67∓2.603[5]	8.33∓0.882	1.33∓0.882[5]	0.066*	19.33∓4.910	7.33∓0.882	8.67∓2.848	6.33∓2.906	0.138
Intestines	-	-	-	-	-	-	-	-	-	-	-	-	-	-	-
Urinary Bladder	-	-	-	-	-	-	-	-	-	-	-	-	-	-	-

*: P<0.10; **: P<0.05; There are statistically differences between groups [1]: PC and ALB, [2]: PC and NSO, [3]: PC and COM, [4]: ALB and NSO, [5]: ALB and COM; [6]: NSO and COM.

Table 3. Average of blood cell rates on 7th, and 45th days.

	7th day					45th day				
	PC n=3 $\bar{x} \mp S_{\bar{x}}$	ALB n=3 $\bar{x} \mp S_{\bar{x}}$	NSO n=3 $\bar{x} \mp S_{\bar{x}}$	COM n=3 $\bar{x} \mp S_{\bar{x}}$	P	PC n=3 $\bar{x} \mp S_{\bar{x}}$	ALB n=3 $\bar{x} \mp S_{\bar{x}}$	NSO n=3 $\bar{x} \mp S_{\bar{x}}$	COM n=3 $\bar{x} \mp S_{\bar{x}}$	P
Lymphocyte	60.3100∓4.06955	37.7867∓10.02937	52.9400∓3.34936	52.1333∓23.19438	0.468	68.8867∓4.94431	70.6667∓4.16356	73.3700∓8.41900	89.5533∓3.25677	0.144
Neutrophil Leukocyte	24.9733∓5.70535	9.1567∓3.54941	33.4567∓7.06373	24.7900∓15.39505	0.282	26.9967∓4.87826	23.5233∓1.91068	23.7733∓7.22509	9.5533∓2.80586	0.141
Monocyte	13.0400∓3.44730	52.6000∓13.35886[1]	5.3733∓2.52171[1]	23.0700∓9.71321	0.075*	2.5533∓0.29356	5.6833∓4.51934	2.7233∓1.42995	0.8867∓0.48254	0.354
Eosinophil Leukocyte	1.6600∓1.49323	0.4433∓0.44333	-	-	0.224	1.4400∓0.67486[2]	0.1133∓0.11333	0.1200∓0.12000	0.0000∓0.00000[2]	0.099*
Basophil Leukocyte	-	-	-	-	-	0.1100∓0.110000	-	-	-	-

*: P<0.10; **: P<0.05; There are differences between groups [1]: ALB and NSO; [2]: PC and COM.

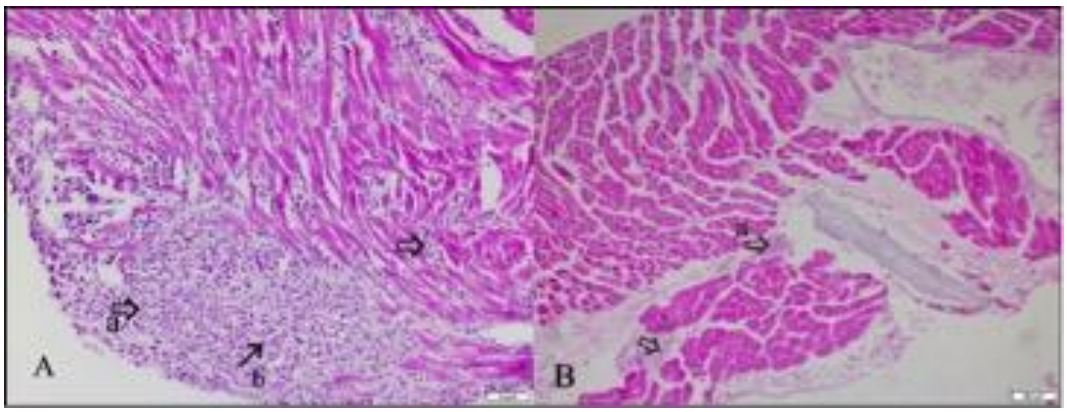

Figure 3. A. 14th day, Group ALB; heart muscle tissue severe mononuclear cell infiltration between muscles (a) and eosinophil leukocytes (b) (H&E, scale bar: 50 µm). **B.** 14th day, Group COM; mild mononuclear cell infiltration between muscles (a) (H&E, scale bar: 100µm).

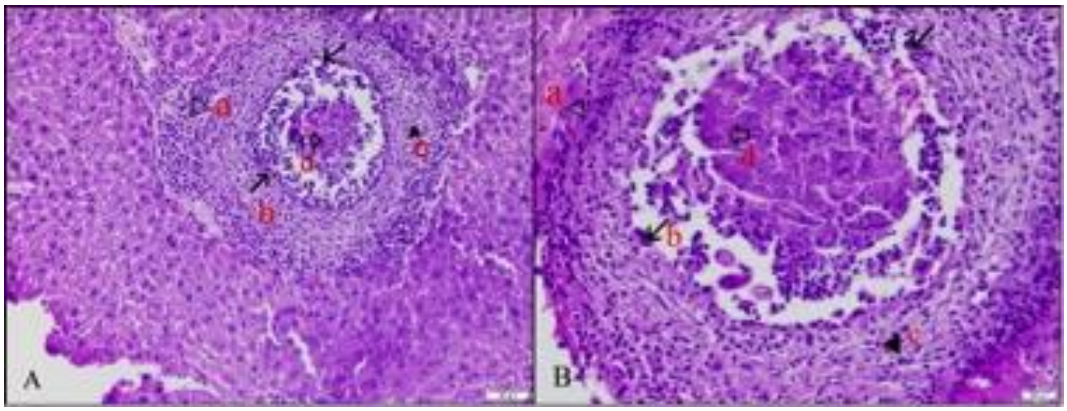

Figure 4. 60th day, Group NSO; coagulation necrosis in the center of liver tissue (d), around multinucleated giant cells (b), mononuclear cell infiltration (c) and granuloma structure surrounded by connective tissue (a) (**A.** H&E, scale bar: 50 µm), (**B.** H&E, scale bar: 20 µm).

Hematologic results: Blood cell ratios for all necropsies are given in Table 3. On the 7th day, the treatment groups were compared with Group PC; the ratio was decreased in all groups, and the values were similar in Groups NSO and COM. There was a statistical difference (P<0.10) between Group ALB and NSO. No statistical difference was found between the groups in terms of cell availability on the 14th and 28th day (P>0.10).

On the 45th day, when the ratios of all the experimental groups were compared with Group PC, it was observed that the lymphocyte ratio increased and the neutrophil leukocyte ratio decreased. Monocytes were increased in Group ALB, decreased in Group COM, and were similar in Group NSO. The absence of eosinophil leukocytes in Group COM showed statistical difference (P<0.10) with Group PC. No statistical difference was found between groups on 60th day (P>0.10).

Discussion and Conclusion

Numbers of migrated larvae were found at 856.98 in Group PC; 236.00 and 436.64 in Group COM and ALB respectively. It was found at 546.31 in Group NSO. The maximum reduction in the number of larvae was seen in Group COM compared to Group PC. The second group was ALB, followed by Group NSO. The most effective group was Group COM (72.46%), the second group was ALB (48.81%), and Group NSO was found to be minimal (36.25%) in terms of parasitological effect level.

Parasitological effect of treatment was 85.55% on the 7th day, and found to be 74.19%; 57.69%; 79.13%, and 64.08% on the 14th, 28th, 45th, and 60th, respectively. Musa et al. (30) reported that the effect in the combination group was 87.00% on the 7th day, showing a similarity with this study (85.55%) and *Nigella sativa* oil in two different doses for 7 days was given to mice, and the effect level was determined as 31.0% and 39.3% on the 7th day. But, in this study, the effect level of Group NSO 71.27% were found on the 7th day and a much higher effect level was obtained. It was thought that using the oil extract obtained directly from seed, the difference in the amount of *N. sativa* and TQ in the extract used and the geographic differences in plant structure/components could be effective on an effect level. The geography of the plant, the way it is obtained, the döşe, and the application time can affect the percentage of activity (20). It is reported that most of the TQ found in the composition of *Nigella sativa* is found in the seeds (30-48%) (2). In addition, it is reported that the fatty extract of the plant is more easily

absorbed from intestinal cells than alcohol and aqueous extract (33). In the current study, the oil extract obtained from the seeds of *N. sativa* was applied directly, and it's considered that a higher level of effect was achieved, unlike in the previous study (30).

The partial decrease in the number of larvae in Group NSO arises from the immunomodulatory and anti-inflammatory effect of the oil by increasing the host's tissue defense and regulating the immune response to affect the reduction of parasite settlement and tissue damage as noted by some researchers (7, 13, 15, 28). The changes in the tissues of mice in Group NSO and COM were milder than Group ALB and PC. Musa et al. (30) reported that the destruction of lungs, liver, and brain was decreased in *N. sativa* oil and albendazole group compared to the positive control group, whereas in the combination group. In this study, no antiparasitic effect was observed in Group NSO, as in some studies (17, 22, 25). In both Group NSO and COM, inflammation severity and degree of inflammatory changes were less than Group ALB. It has been observed that the application of oil with albendazole both regulates the body and tissue defense mechanisms of the host and prevents the localization of the parasite as well as mitigating the damage caused by the parasite.

It was determined that the blood values during the first two weeks of migration of the infection were consistent with the pathological findings. When evaluated together with pathological findings, the predominance of lymphocytes and macrophages in the inflammatory cells supports the decrease in the amount of blood as a result of migration to the tissue. Some researchers reported that *N. sativa* oil can increase and decrease the neutrophil leukocytes and interleukins in the blood and regulate the severity of the immune response (13, 15, 28).

In conclusion, the larvicidal-migration inhibitory effect of albendazole and the immunomodulatory, anti-inflammatory effect of *N. sativa* oil were found in Group COM with the highest parasitological and pathological effects. It's thought that *N. sativa* oil enhanced the effect of albendazole with its immunomodulatory and anti-inflammatory properties, so that infection was observed to be milder both parasitologically and pathologically in Group COM. The effect of *Nigella sativa* oil, when used alone, is lower than the other two treatment groups and being close to the Group PC. It's showed that plant oil does not directly affect larvae when applied alone. Pathological findings supported that the oil exhibits an anti-inflammatory effect in tissues and blood preparations. It is thought that such studies will open a new perspective on the development of the phytotherapy field in parasitic diseases. With this study, *Nigella sativa* oil has no direct lethal effect on the larvae, but may help in the development of supportive/complementary treatment procedures to reduce the side effects of immune system supplementation and/or host infection.

Acknowledgements

This study belongs to first author's PhD thesis titled "Evaluation of Effect of Albendazol and *Nigella Sativa* Combination in Visceral Larvae Migrans (*Toxocara canis*) in Mice" that it has been done in Ankara University Faculty of Veterinary Medicine, Department of Parasitology. It was also presented as an oral presentation at III. International Ankara Conference on Scientific Research, 02-04.10.2020, Ankara, Türkiye. For their contribution in obtaining and interpreting the pathology findings of this study, we thank to Prof. Dr. Osman Kutsal and Assist. Prof. A. Selin Tunç.

Financial Support

This research received no grant from any funding agency/sector.

Conflict of Interest

The authors declared that there is no conflict of interest.

Author Contributions

CA, and HÖ conceived and planned the experiments. CA prepared all samples, carried out all experiments and interpreted the results. HÖ contributed to interpretation of the results. CA took the lead in writing the manuscript.

Data Availability Statement

The data supporting this study's findings are available from the corresponding author upon reasonable request.

Ethical Statement

This study was approved by the Gazi University Animal Experiments Local Ethics Committee (207-22055/ G.U.ET-11-104).

Animal Welfare

The authors confirm that they have adhered to ARRIVE Guidelines to protect animals used for scientific purposes.

References

1. **Abukhader MM** (2013): *Thymoquinone in the clinical treatment of cancer: fact or fiction?* Pharmacogn Revn, **7**, 117-120.
2. **Ahmad A, Husain A, Mujeeb M, et al** (2013): *A review on therapeutic potential of Nigella sativa: a miracle herb.* Asian Pac J Trop Biomed, **3**, 337-352.
3. **Avila LFC, Conceicao FR, Telmo PL, et al** (2012): *Saccharomyces boulardii* reduces infection intensisty of mice with toxocariasis. Vet Parasitol, **187**, 337-340.
4. **Barrera MG, Leonardi D, Balmaro RE, et al** (2010): *In vivo evaluation of albendazole microspheres for the treatment of Toxocara canis larva migrans.* Eur J Pharm Biopharm, **75**, 451-454.

5. **Cypess RH** (1982): Visceral larvae migrans. 205-212. In: JH Steele (Ed), Handbook Series in Zoonoses, Section C: Parasitic Zoonoses. CRC Press, Florida.
6. **El-Dakhakhny M, Madi NJ, Lembert N, et al** (2002): *Nigella sativa oil, nigellone and derived thymoquinone inhibit synthesis of 5-lipoxygenase products in polymorphonuclear leukocytes from rats.* J Ethnopharmacol, **81**, 161-164.
7. **El Gazzar MA** (2007): *Thymoquinone suppresses in vitro production of IL-5 and IL-13 by mast cells in reponse to lipopolysaccharide stimulation.* Inflamm Res, **56,** 345-351.
8. **El-Shenawy NS, Soliman MFM, Eyad SI** (2008): *The effect of antioxidant properties of aqueous garlic extract and Nigella sativa as anti-schiostomiasis agents in mice.* Rev Inst Med Trop S Paulo, **50**, 29-36.
9. **Fillaux J, Magnaval JF** (2013): *Laboratory diagnosis of human toxocariasis.* Vet Parasitol, **193**, 327-336.
10. **Ghosheh OA, Houdi AA, Crooks PA** (1999): *High performance liquid chromatographic analysis pharmacologically active quinones and related compounds in the oil of the black seed (Nigella sativa L.).* J Pharmaceut Biomed, **19**, 757-762.
11. **Gillespie SH** (1988): *The epidemiology of Toxocara canis.* Parasitology Today, **4**, 180-182.
12. **Hajhashemi V, Ghannadi A, Jafarabadi H** (2004): *Black cumin seed essential oil, as a potent analgesic and antiinflammatory drug.* Phytother Res, **18**, 195-199.
13. **Haq A, Abdullatif M, Lobo PI, et al** (1995): *Nigella sativa: effect on human lymphocytes and polymorphonuclear leukocyte phagocytic activity.* Int Immunopharmacol, **30**, 147-155.
14. **Horiuchi A, Satou T, Akao N, et al** (2005): *The effect of free and polyethylene glycol-liposome-entrapped albendazole on larval mobility and number in Toxocara canis infected mice.* Vet Parasitol, **129**, 83-87.
15. **Islam SKN, Begum P, Ahsan T, et al** (2004): *Immunosuppressive and cytotoxic properties of Nigella sativa.* Phytother Res, **18**, 395-398.
16. **Kaya S** (2007): Antelmentikler, homeopati ve tıbbi bitkiler. 489-545. In: S Kaya (Ed), Veteriner Farmakoloji. Medisan Yayınevi, Ankara.
17. **Khan A, Khan MS, Avais M, et al** (2007): *Prevalence, hematology, and treatment of balantidiasis among donkeys in and around Lahore, Pakistan.* Vet Parasitol, **196**, 203-205.
18. **Konuk T** (1975): Pratik Fizyoloji I, Ankara Üniversitesi Yayınları, Ankara.
19. **Leonardi D, Echenique C, Lamas C, et al** (2009): *High efficacy of albendazole -PEG 6000 in the treatment of Toxocara canis larva migrans infection.* J Antimicrob Chemoth, **64**, 375-378.
20. **Liu W, Liu J, Yin D, et al** (2015): *Influence of ecological factors on the production of active substances in the anti-cancer plant Sinopodophyllum hexandrum (Royle) T.S. Ying.* Plos One, 1-22.
21. **Luna LE** (1968): Manual of Histological Staining Methods of the Armed Forces Institue of Pathology. McGraw-Hill Book Company, New York.
22. **Mady RF, El-Hadidy W, Elachy S** (2016): *Effect of Nigella sativa oil on experimental toxoplasmosis.* Parasitol Res, **115**, 379-390.
23. **Magnaval JF, Glickman LT** (2006): Management and treatment options for human toxocariasis. 113-126. In: CV Hollan, HV Smith (Eds), Toxocara Enigmatic Parasite. CABI Publishing, Oxfordshire.
24. **Mahmood MS, Gilani AH, Khwaja A, et al** (2003): *The in vitro effect of aqueous extract of Nigella sativa seeds on nitric oxide production.* Phytother Res, **17**, 921-924.
25. **Mahmoud MR, Al-Abnar HS, Saleh S** (2002): *The effect of Nigella sativa oil against the liver demage induced by Schistosoma mansoni infection in mice.* J Ethnopharmacol, **79**, 1-11.
26. **Majdalawieh AF, Fayyad MW** (2015): *Immunomodulatory and anti-inflammatory action of Nigella sativa and thymoquinone: a comprehensive review.* Int Immunopharmaco, **28**, 295-304.
27. **Majdalawieh AF, Hmaidan R, Carr RI** (2010): *Nigella sativa modulates splenocyte proliferation, Th1/Th2 cytokine profile, macrophage function and NK anti-tumor activity.* J Ethnopharmacol, **131**, 268-275.
28. **Mohany M, El-Feki M, Refaat I, et al** (2012): *Thymoquinone ameliorantes the immunological and histological changes induced by exposure to imidacloprid insecticed.* J Toxicol Sci, **37**, 1-11.
29. **Moreira GMSG, Telmo PL, Mendonça M, et al** (2014): *Human toxocariasis: current advances in diagnostics, treatment and interventions.* Trends Parasitol, **30**, 456-464.
30. **Musa D, Senocak G, Borazan G, et al** (2011): *Effects of Nigella sativa and albendazole alone and in combination in Toxocara canis infected mice.* J Pak Med Assoc, **61**, 866-870.
31. **Othman AA** (2012): *Therapeutic battle against larval toxocariasis: are we still far behind?*Acta Trop, **124**,171-178.
32. **Reis M, Trinca A, Ferreira MJU, et al** (2010): *Toxocara canis: potential activity of natural products against second-stage larvae in vitro and in vivo.* Exp Parasitol, **126**, 191-197.
33. **Riviere JE** (2009): Absorption, distribution, metabolism, and elimination. In: JE Riviere, MG Papich, HR Adams (Eds), Veterinary Pharmacology And Therapeutics. Wiley Blackwell, USA.
34. **Rogerio AP, Sa-Nunes A, Albuquerque DA, et al** (2003): *Lafoensia pacari extract inhibitis IL-5 production in toxocariasis.* Parasite Immunol, **25**, 393-400.
35. **Satou T, Horiuchi A, Akao N, et al** (2005): *Toxocara canis: search for a potential drug amongst ß-carboline alkolids- in vitro and mouse studies.* Exp Parasitol, **110**, 134-139.
36. **Schnieder-Stock R, Fakhoury IH, Zaki AM, et al** (2014): *Thymoquinone: fifty years of success in the battle against cancer models.* Drug Discov Today, **19**, 18-30.
37. **Tutun H, Sevin S, Yurdakök B, et al** (2013): Bazı albendazol preparatlarının etken madde miktarının belirlenmesi. 174. In: IV. Ulusal Veteriner Farmakoloji Ve Toksikoloji Kongresi. Elazığ, Türkiye.
38. **Woodhall DM, Fiore AR** (2013): *Toxocariasis: a review for pediatricians.* J Ped Infect Dis, **3**, 154-159.
39. **Yarsan E, Altınsaat Ç, Aycicek H, et al** (2003): *Effects of albendazole treatment on haematological and biochemical parameters in healthy and Toxocara canis infected mice.* Turk J Vet Anim Sci, **27**, 1057-1063.

Effect of nano-selenium and different stocking densities on performance, carcass yield, meat quality, and feathering score of broilers

Ömer SEVİM[1,a,✉], Umair AHSAN[2,b], Onur TATLI[1,c], Eren KUTER[3,d], Ehsan Karimiyan KHAMSEH[1,e]
Artun REMAN TEMİZ[1,f], Özge SAYIN ÖZDEMİR[1,g], Aybala Kübra AYDIN[1,h], Bekir Hakan KÖKSAL[1,i]
Özcan CENGİZ[1,j], Ahmet Gökhan ÖNOL[1,k]

[1]Aydın Adnan Menderes University, Faculty of Veterinary Medicine, Department of Animal Nutrition and Nutritional Diseases, Aydın, Türkiye; [2]Burdur Mehmet Akif Ersoy University, Department of Plant and Animal Production, Burdur Vocational School of Food, Agriculture and Livestock, Burdur, Türkiye; [3]Burdur Mehmet Akif Ersoy University, Faculty of Veterinary Medicine, Department of Animal Nutrition and Nutritional Diseases, Burdur, Türkiye

[a]ORCID: 0000-0001-6123-4159; [b]ORCID: 0000-0003-4741-3745; [c]ORCID: 0000-0003-2733-1937; [d]ORCID: 0000-0003-4536-9058
[e]ORCID: 0000-0003-3324-1364; [f]ORCID: 0000-0003-3974-6312; [g]ORCID: 0000-0002-3952-6769; [h]ORCID: 0000-0001-7420-7117
[i]ORCID: 0000-0002-5676-446X; [j]ORCID: 0000-0001-9526-8656; [k]ORCID: 0000-0002-7520-7423

ARTICLE INFO

Article History
Received : 09.12.2020
Accepted : 24.10.2021
DOI: 10.33988/auvfd.838120

Keywords
Broiler
Feathering
High stocking density
Nano-selenium
Performance

✉Corresponding author
osevim@adu.edu.tr

How to cite this article: Sevim Ö, Ahsan U, Tatlı O, Kuter E, Khamseh EK, Reman Temiz A, Sayın Özdemir Ö, Aydın AK, Köksal BH, Cengiz Ö, Önol AG (2023): Effect of nano-selenium and different stocking densities on performance, carcass yield, meat quality, and feathering score of broilers. Ankara Univ Vet Fak Derg, 70 (1), 29-36. DOI: 10.33988/auvfd.838120.

ABSTRACT

Effects of nano-selenium (nano-Se) and stocking density (SD) on growth performance, carcass yield, meat quality, and feathering score of broilers were investigated in this study. One-day-old 480 broiler chickens (45.3±2.4 g body weight) (Ross 308) were randomly divided into 4 treatments each comprising of 8 replicates. In the experiment, treatments consisted of a 2 × 2 factorial arrangement of dietary Se form (inorganic or nano) and SD (low = 12 birds/m^2; LSD, and high = 18 birds/m^2; HSD). No interaction was noted between Se form and SD for any trait. Nano-Se had no effect on growth performance, however, HSD decreased the body weight gain (BWG) ($P<0.05$) and feed intake (FI) ($P<0.001$) while feed conversion ratio (FCR) was unaffected. Neither nano-Se nor HSD had any effect on the relative carcass, breast, and thigh yields. Nano-Se improved the water-holding capacity (WHC) of breast meat 72-hpost-mortem ($P<0.05$). However, pH, colour, and cooking loss of meat remained unaffected by Se form or SD. There were no differences between nano- or inorganic Se and LSD or HSD regarding feathering scores for back and wing. In conclusion, dietary nano-Se improved the WHC and had no significant effect on other parameters. In addition, HSD may negatively affect the growth performance.

Introduction

Selenium (Se) belongs to the class of essential elements required for a wide range of functions such as sustaining of life, growth, meat quality, and feathering. The major factors that determine the effectiveness of Se are its dietary level and form. Today Se is still one of the most discussed elements in poultry nutrition (39). In a living organism, Se is present in the form of selenocysteine as part of selenoproteins (17, 38).

The bioavailability of Se is related to its physical form and is found in diets in two basic forms, inorganic and organic. Mostly inorganic Se sources (e.g. sodium selenite and sodium selenate) used in broiler diets (39). However, there has been an increasing interest in using organic selenium sources (e.g. selenocysteine and selenomethionine) in poultry diets. Se in plants occurs only in organic form and mainly selenomethionine (10). Recently, another form of Se that has been of particular

interest is nano-selenium (nano-Se). Nanotechnology is used in animal feeding as well as many other areas and the most important application of nanotechnology in this area are nanominerals. Nanominerals are characterized by a particle size of 1 to 100 nm. (40). Nano minerals have a larger surface area, higher surface activity and are absorbed more easily and effectively than other forms of the same mineral (21).

Optimal housing and nutrition are essential to keep the performance at the highest level in broiler production. One of these environmental conditions is stocking density (SD). High stocking density (HSD) can reduce fixed production costs (such as labor and maintenance) and increase the kilogram of chicken weight produced per unit of area, thus increasing the profitability (19). However, HSD creates stress among the animals, increasing the amount of ammonia in the environment, decreasing the litter quality, and adversely affecting animal health, performance, and product quality (13, 36). Some minerals, such as Se, may be used in broiler diets in order to decrease the adverse effects of HSD (38).

Some studies have reported the use of supplemental nano-Se on growth performance, carcass yield, and meat quality of broiler (10, 29). Moreover, dietary nano-Se has been used to alleviate the negative effect of heat and oxidative stress in broilers (9, 18). However, no study has reported the effect of supplemental nano-Se in broilers under the stressful condition of HSD. Therefore, this study aimed to examine the effect of dietary nano-Se on growth performance, carcass yield, meat quality, and feathering score of broiler chicks under HSD.

Materials and Methods

Experimental design and diets: The experiment comprised of 480 one-day-old Ross 308 male broiler chickens (45.3±2.4 g body weight) randomly allotted to 4 experimental groups with 8 replicates/group as a completely randomized design with 2×2 factorial arrangement of dietary Se form (inorganic or nano) and the SD (low = 12 birds/m^2(LSD) or high = 18 birds/m^2). At the end of experiment, an average 34.3 kg and 50.2 kg body weight/m^2 were determined in groups subjected to LSD and HSD, respectively. Birds were housed in floor pens occupying 1 m^2 floor space (feeders and drinker space excluded) with wood shavings as litter material. A 23L:1D lighting program was implemented up to 7 days and 18L:6D thereafter until day 42. The temperature of 32 °C was maintained during the first week followed by a reduction of 3°C per week until d 21 and a temperature of 24-26°C was maintained afterwards. Free access of birds to feed and water was ensured throughout the experiment. The duration of the experiment was 42 days.

Starter (d 1 to 10), grower (d 11 to 24), and finisher (d 25 to 42) diets based on corn-soybean meal were formulated according to Aviagen (5) in mash form (Table 1). Sodium selenite with 99.0% purity (Sigma-Aldrich Co., USA) was used as inorganic Se source. Nano-Se was prepared at the Department of Nanotechnology Engineering, Cumhuriyet University, Sivas, Türkiye. The nano-Se had 99.95% purity, ranging in size between 30 and 60 nm. Sodium selenite and nano-Se were supplemented at 0.66 and 0.30 mg/kg, respectively, in order to provide 0.3 mg/kg Se in diets. First, the feed additives (vitamins and minerals) were mixed among themselves, then this mixture added to the feed mixture and mixed again.

Table 1. Ingredient and nutrient composition of diets.

Ingredients (%)	Starter (1-10 d)	Grower (11-24 d)	Finisher (25-42 d)
Corn	55.52	56.01	58.95
Soybean meal (48% crude protein)	37.51	36.05	33.44
Vegetable oil	2.51	4.16	4.24
Limestone	0.88	0.84	0.81
Dicalcium phosphate	2.31	2.01	1.72
Salt	0.36	0.34	0.36
Methionine	0.36	0.24	0.13
Lysine	0.20	-	-
Vitamin premix*	0.25	0.25	0.25
Mineral premix**	0.10	0.10	0.10
Nutrient composition (calculated)			
Metabolizable energy (ME), kcal/kg	3033	3151	3191
Crude protein (CP)	22.96	22.00	21.00
Calcium	1.00	0.91	0.82
Available phosphorus	0.50	0.45	0.40
Methionine-cystine	1.09	0.95	0.80
Lysine	1.42	1.21	0.15
Selenium, mg/kg	0.35	0.35	0.35
Nutrient composition (analyzed)			
Dry matter	91.2	90.8	90.5
CP	23.16	22.18	21.24
Ether extract	6.32	8.04	8.23
Neutral detergent fiber	9.25	8.74	8.38
Crude ash	5.51	5.45	5.39
Selenium, mg/kg	0.34	0.34	0.34

*Vitamin premix (per kilogram diet): vitamin A 12 000 IU, vitamin D_3 3 000 IU, vitamin E 50 mg, vitamin K_3 5 mg, vitamin B_1 3 mg, vitamin B_2 6 mg, niacin 30 mg, calcium-d-pantothenate 10 mg, vitamin B_6 5 mg, vitamin B_{12} 0.03 mg, d-biotin0.1 mg, folic acid 1 mg, choline chloride 400 mg.
**Mineral premix (per kilogram diet): manganese 100 mg, iron 60 mg, copper 5 mg, cobalt 0.2 mg, iodine 1 mg, zinc 80 mg.

Chemical analysis of feed: The proximate composition of experimental diets was determined according to AOAC (3). Van Soest (42) method was used to measure the neutral detergent fiber (NDF) values of the feeds. The Zn content of feeds was determined by inductively coupled plasma optical emission spectrometry (ICP-OES). Feed sample (0.3 g) was subjected to wet digestion with 8 mL 65% nitric acid and 2 mL 37% hydrochloric acid in a sealing vessel at 180 °C in a microwave (MARS 6, CEM Corporation, Matthews, NC) for 20 min. The digested samples filtered in flask and diluted to 25 mL by adding deionized water for analysis in ICP-OES.

Performance parameters and carcass yield: The data for feed intake (FI) and body weight (BW) on per pen basis were recorded. Body weight gain (BWG) and feed conversion ratio (FCR) of broilers were calculated with these data for growth phases and overall growth period. Mortality was recorded daily. At d 42, three chickens from each replicate were slaughtered by decapitation. Carcasses, breasts, and thighs were weighed individually, and relative weights were calculated as a percent of live weight.

Meat quality parameters: After weighing the breast, samples from the left part of breast meat were taken immediately and placed in a refrigerator at 4 °C for storage. Breast muscle pH was measured at a depth of 2 cm using a pH meter (Orion Model 720, Thermo Electron Corporation, Beverly, MA, US) from three different sites and the average value was used. A chromameter (CR-400, Minolta Camera Co., Osaka, Japan) was employed to determine the meat colorfor L* (lightness), a* (redness), and b* (yellowness). Water-holding capacity (WHC) of breast meat samples were determined according to Joo (24). For this purpose, five pieces of breast meat (approximately 5 g) were weighed and placed between the weighed two filter papers with 100 cm^2 (10×10 cm) area. Then the meat samples and filter papers were placed between two 15×15 cm (225 cm^2) glass plates. Loads of 2250 g were applied on the glass plates to create a pressure of 10 g/cm^2 for 5 min followed by weighing the filter paper and calculation of percent WHC as follows:

$$\frac{\text{Final weight of filter paper} - \text{Initial weight of filter paper}}{\text{Initial weight of meat sample}} \times 100$$

The breast meat samples were weighed, put in a polyethylene bag, heated at 75°C internal temperature in a water bath for 45 minutes, and weighed again after cooling and drying between the layers of filter paper to determine the cooking loss (CL). CL was calculated by ascertaining the weight loss after cooking (22).

Feathering score: At d 42 of the experiment, 10 chickens from each pen were subjected to feather scoring according to Lai et al. (25). The back feathering was evaluated by using 5-point scoring method (1 to 5) with 1 indicating minimal coverage and 5 for complete coverage. A 3-point scoring method (0 to 2) was used for wing feathering. Wings without any defect were scored as 0, wings with lesions and torn feathers as 1, and wings with broken feathers and retarded feathering were scored as 2.

Statistical analysis: The effect of dietary Se form and SD was assessed using the GLM procedures of SPSS (version 22.0; IBM Corp., Armonk, NY, US). Feathering scores between groups were tested with Kruskal-Wallis and scores between main effects (Se form and SD) were compared with the help of the Mann-Whitney U test. The Duncan's Multiple Range Test was used for the comparison of means. The difference at 95% confidence interval ($P<0.05$) was assumed as significant.

Results

In the current study, no interaction was found between SD and dietary Se form for performance, carcass yield, meat quality, and feathering scores of broilers (Tables 2 and 5).

Table 2 shows the effect of dietary Se form on BWG, FI, and FCR of broilers under low or high stocking densities. Growth performance of broilers was not different regardless of dietary Se form. However, HSD significantly decreased the BWG ($P<0.05$) and FI ($P<0.001$) on d 25 to 42 and 0 to 42 whereas; there was no significant effect on FCR at any phase.

Neither dietary Se form nor SD had any significant effect on carcass, breast, and thigh yields (Table 3).

Dietary nano-Se significantly decreased the WHC of breast meat 72-h post-mortem ($P<0.05$) but did not affect other meat quality parameters (Table 4). HSD had no effect on pH, meat colour, WHC, and CL of breast meat at 15 min, 24-h and 72-h after slaughter.

Both dietary Se form and SD did not affect the feathering score of back and wing of broilers (Table 5).

Discussion and Conclusion

Owing to the varying reports, growth performance of broilers remains inconclusive in response to dietary Se. The current study showed that growth performance was similar in broiler chickens fed nano- or inorganic Se in conformity with the results of Boostani et al. (9), Liu et al. (27), and El Deep et al. (18). On the contrary, Selim et al. (34) and Mohammadi et al. (29) stated that 0.3 mg/kg dietary nano-Se improved the growth performance of broilers compared with inorganic Se. The incoherent results may depend on the differences in preparation of nano-Se, the strain of birds, the composition of diets, and housing conditions.

Table 2. Effects of stocking density and dietary selenium form on growth performance of broilers.

Item	Body weight gain, g				Feed intake, g				Feed conversion ratio			
	0-10 d	11-24 d	25-42 d	0-42 d	0-10 d	11-24 d	25-42 d	0-42 d	0-10 d	11-24 d	25-42 d	0-42 d
LSD												
Inorganic Se	209.29	690.17	1964.08	2818.21	204.37	1008.55	3595.91	4808.82	0.98	1.46	1.83	1.71
Nano-Se	203.92	686.18	1969.28	2814.05	204.88	987.77	3573.92	4766.57	1.01	1.44	1.82	1.70
HSD												
Inorganic Se	203.07	688.74	1892.14	2738.60	200.22	1000.62	3440.26	4641.10	0.99	1.45	1.82	1.70
Nano-Se	205.72	688.94	1900.13	2749.45	195.33	1003.94	3415.17	4614.44	0.95	1.46	1.80	1.68
SEM	4.36	15.32	26.74	27.95	7.07	25.13	38.36	39.34	0.03	0.01	0.02	0.02
SD												
Low	206.60	688.17	1966.68[a]	2816.13[a]	204.62	998.16	3584.91[a]	4787.70[a]	0.99	1.45	1.83	1.70
High	204.40	688.83	1896.14[b]	2744.02[b]	197.77	1002.28	3427.72[b]	4627.77[b]	0.97	1.45	1.81	1.69
Se form												
Inorganic	206.18	689.45	1928.11	2778.40	202.29	1004.58	3518.08	4724.96	0.98	1.46	1.83	1.70
Nano	204.82	687.56	1934.71	2781.75	200.11	995.85	3494.54	4690.51	0.97	1.45	1.81	1.69
SEM	3.08	10.83	18.91	19.76	5.00	17.77	27.12	27.81	0.02	0.01	0.02	0.01
P-values												
SD	0.616	0.966	0.013	0.015	0.340	0.871	0.000	0.000	0.467	0.754	0.444	0.354
Se form	0.757	0.902	0.807	0.906	0.759	0.731	0.544	0.389	0.884	0.531	0.412	0.354
SD × Se form	0.365	0.892	0.959	0.790	0.705	0.635	0.968	0.844	0.328	0.255	0.977	0.839

[a,b]: Means bearing different superscript within the same column are significantly different (P<0.05), SD: Stocking density, Se: Selenium, LSD: Low stocking density, HSD: High stocking density, SEM: Standard error of the mean.

Table 3. Effects of stocking density and dietary selenium form on relative carcass, breast, and thigh yields of broiler, % of body weight.

Item	Carcass	Breast	Thigh
LSD			
Inorganic Se	73.56	21.94	15.30
Nano-Se	73.34	21.28	15.34
HSD			
Inorganic Se	73.85	21.59	15.41
Nano-Se	73.51	21.63	15.28
SEM	0.324	0.221	0.078
SD			
Low	73.46	21.61	15.32
High	73.68	21.61	15.34
Se form			
Inorganic	73.71	21.76	15.35
Nano	73.43	21.45	15.31
SEM	0.214	0.312	0.111
P-values			
SD	0.466	0.998	0.843
Se form	0.371	0.323	0.680
SD × Se form	0.849	0.261	0.447

SD: Stocking density, Se: Selenium, LSD: Low stocking density, HSD: High stocking density, SEM: Standard error of the mean.

DOI: 10.33988/auvfd.838120

Table 4. Effects of stocking density and dietary selenium form on pH, meat colour, water holding capacity (%), and cooking loss (%) of broiler breast meat at different times after slaughtering.

Item	15 minutes				24 hours						72 hours				
	pH	L	a	b	pH	L	a	b	WHC	CL	pH	L	a	b	WHC
LSD															
Inorganic Se	6.45	52.13	2.67	5.20	5.87	59.31	3.17	7.69	12.63	32.22	5.87	59.00	3.36	6.83	12.99
Nano-Se	6.49	52.04	2.31	4.59	5.86	58.67	3.05	7.51	12.26	32.13	5.86	58.76	3.10	6.81	12.43
HSD															
Inorganic Se	6.45	52.33	2.56	4.81	5.90	59.21	3.10	7.70	13.03	32.01	5.88	58.52	3.32	6.87	13.13
Nano-Se	6.52	52.12	2.24	4.44	5.84	59.70	2.61	7.74	12.21	32.27	5.90	59.63	2.88	6.54	12.26
SEM	0.04	0.57	0.18	0.36	0.02	0.56	0.22	0.44	0.40	0.53	0.02	0.59	0.22	0.33	0.33
SD															
Low	6.47	52.09	2.49	4.89	5.87	58.99	3.11	7.60	12.44	32.18	5.86	58.88	3.23	6.82	12.71
High	6.49	52.23	2.40	4.63	5.87	59.46	2.86	7.74	12.62	32.21	5.89	59.08	3.10	6.70	12.72
Se form															
Inorganic	6.45	52.23	2.61	5.00	5.89	59.26	3.14	7.18	12.83	32.12	5.87	58.76	3.34	6.85	13.06[a]
Nano	6.51	52.08	2.28	4.52	5.85	59.19	2.83	7.63	12.23	32.27	5.88	59.20	2.99	6.68	12.35[b]
SEM	0.03	0.41	0.12	0.26	0.02	0.40	0.16	0.31	0.28	0.38	0.01	0.42	0.15	0.23	0.23
P-values															
SD	0.725	0.807	0.598	0.463	0.853	0.409	0.258	0.747	0.659	0.947	0.161	0.736	0.541	0.721	0.964
Se form	0.144	0.798	0.058	0.185	0.125	0.893	0.171	0.837	0.137	0.770	0.710	0.461	0.108	0.594	0.033
SD × Se form	0.742	0.918	0.910	0.740	0.287	0.316	0.411	0.856	0.579	0.650	0.521	0.254	0.670	0.625	0.635

[a,b]: Means bearing different superscript within the same column are significantly different (P<0.05), L: Lightness, a: Redness, b: Yellowness, WHC: Water holding capacity, CL: Cooking loss, SD: Stocking density, Se: Selenium, LSD: Low stocking density, HSD: High stocking density.

Table 5. Effects of stocking density and dietary selenium form on back and wing feathering score of broiler (x±Sx).

Item	Back	Wing
LSD and inorganic Se	4.45±0.08	0.43±0.06
HSD and inorganic Se	4.50±0.08	0.39±0.06
LSD and nano-Se	4.48±0.09	0.34±0.06
HSD and nano-Se	4.56±0.08	0.29±0.05
P-values	0.708	0.348
SD		
Low	4.46±0.06	0.38±0.04
High	4.53±0.06	0.34±0.04
P-values	0.564	0.463
Se form		
Inorganic	4.48±0.06	0.41±0.04
Nano	4.52±0.06	0.31±0.04
P-values	0.305	0.097

SD: Stocking density, Se: Selenium, LSD: Low stocking density, HSD: High stocking density.

The SD is generally recommended as 13-15 birds/m^2 or 30-35 kg BW/m^2 in environmentally controlled broiler houses (15, 16). Many researchers reported that increasing SD beyond these ranges exerts adverse effects on the growth performance of broilers (4, 6, 12). In our study, 34.3 and 50.2 kg/m^2 were found at d 42 in LSD and HSD groups, respectively. In line with these results, BWG and FI were significantly higher in LSD groups than HSD groups during 25 to 42 and 0 to 42 days. Particularly during the finishing phase, birds might have been difficulty accessing feed and water under HSD. This might have caused a decrease in FI and BWG. Additionally, Feddes et al. (20) stated that low FI and BWG may be due to a decrease in gaseous and heat exchange within the microclimate of the birds. However, disturbance in the digestive microbiota which affects the digestion and absorption of nutrients may decrease the performance of broilers at HSD (12). Increased dust and airborne pathogens may also affect performance negatively at HSD (33). Therefore, the FI might have decreased at HSD resulting in lowered BWG. However, FCR remained unaffected in response to SD in this study. Similar results were reported by Feddes et al. (20) and Madilindi et al. (28). In contrast, Astaneh et al. (4) found that HSD affected FCR negatively. In most of the studies involving SD revealed that HSD decreases both BWG and FI. However, in some studies including the present study, the decrease of FI and BWG might be so similar. In such a case, the FCR may not be affected.

Dietary nano-Se was unable to affect the carcass, breast, and thigh yields of broilers. Similarly, Bakhshalinejad et al. (7) reported that dietary Se source (inorganic, organic, and nano) or level (0.1 and 0.3 mg/kg) did not influence the carcass, breast, and thigh yields in broiler. And also Ahmadi et al. (2) stated that different dietary nano-Se levels (between 0.1 to 0.5 mg/kg) had no significant effect on breast and thigh yields of broiler. Se deficiency causes muscular dystrophy as well as exudative diathesis in chicks (39). However, sufficient or excess (up to 1 mg/kg) dietary Se provides proper muscle growth but does not increase muscle growth (2, 11). In this study, since the Se level in the diet (0.34 mg/kg) was sufficient, either inorganic or nano Se could not affect the carcass, breast, and thigh yields.

Carcass, breast, and thigh yields of broilers were similar irrespective of the SD. Likewise, other studies have suggested that SD does not affect carcass, breast, and thigh yields of broiler chickens (1, 41). However, Cengiz et al. (12) reported that HSD decreased the breast yield, increased the thigh yield, and had no effect on the carcass yield in broilers. The contrasting results may be associated with the differences in housing conditions and stocking densities.

In this study, dietary nano-Se did not affect pH, colour, and CL of breast meat of broiler chickens but decreased WHC 72-h post-mortem. Most of the researchers have revealed that nano-Se improved drip loss (DL) or WHC and had no effect on pH. Cai et al. (10) reported that dietary nano-Se reduced DL but did not affect the meat colour of broiler. Mohammadi et al. (28) reported that nano-Se had no significant effect on pH and WHC of broiler breast meat. However, Bakhshalinejad et al. (7) found that dietary nano-Se had no significant effect on pH but increased redness and yellowness, decreased DL and CL of breast meat. It is well documented that Se is essential for the antioxidant systems of the organism (38, 39). According to Huff-Lonergan and Lonergan (23), oxidation of meat could decrease the sensitivity to hydrolysis, increase protein degradation, and reduce the WHC of myofibrils, which would increase the water loss of the meat. Therefore, the decrease of WHC can be explained by an augmented bioavailability of nano-Se in comparison with its inorganic counterpart.

HSD did not affect the meat quality parameters of broilers in the present study. Similar results were reported by Tong et al. (41) and Patria et al. (31). In fact, it may be thought that the decrease in litter quality due to HSD would negatively affect breast meat quality. However, the broiler's breast skin and feathers probably prevented the meat quality from being adversely affected by the HSD. In the current study, it was determined that HSD has no significant effect on feathering.

Dietary nano-Se had no significant effect on feathering score of broiler chickens. These results are in agreement with those of Ravindran and Elliot (32) who noted that Se supplementation (0.4 mg/kg organic Se) was ineffective on the feathering score of broiler chickens. In contrast, Choct et al. (14) stated that organic Se supplementation (0.25 mg/kg) improved the feathering score in broilers as compared to inorganic Se. The inconsistencies in the results may depend on the differences in the feather scoring method, housing conditions of birds, dietary Se level, and form.

According to the results of the current study, HSD had no significant effect on the rate of feathering in broiler. Similarly, Skrbic et al. (35, 37) revealed that HSD (16 birds/m^2) did not affect the feathering score of broilers. In addition, Moreire et al. (30) described that feathering remained unaffected by SD of 16 birds/m^2. However, Beaulac and Schwean-Lardner (8) reported that HSD (50 kg/m^2) has negative effect on feathering in turkeys. According to these studies, it may be concluded that the number of birds in HSD groups was not enough to impose a negative effect on the feathering score. Moreover, it is well known that the process of feather forming is not only determined by environmental conditions but also by

genetics, the hormonal status of the organism, and nutrition (26). Differences between the results of the studies can be explained by these reasons.

The present study demonstrated that dietary nano-Se had no effect on growth performance, carcass yield, and feathering but may affect meat colour in broiler. However, growth performance is negatively affected by HSD.

Financial Support

The authors are thankful to the Scientific and Technological Research Council of Türkiye (TÜBİTAK) to finance the project (No. 117O848).

Conflict of Interest

The authors declare that they have no conflict of interest.

Author Contributions

ÖS designed the experiment and took the lead in writing the manuscript. OT, EK, EKK, ÖSÖ, AKA, and ART carried out the experiment and contributed to sample preparation. UA, BHK, ÖC, and AGÖ contributed to the interpretation of the results and edited the manuscript. All authors provided critical feedback and helped shape the research, analysis, and manuscript.

Data Availability Statement

The data supporting this study's findings are available from the corresponding author upon reasonable request.

Ethical Statement

The study was ethically approved by the committee for ethical use of animals of Aydın Adnan Menderes University, Türkiye (No: 64583101/2017/042).

Animal Welfare

The authors confirm that they have adhered to ARRIVE Guidelines to protect animals used for scientific purposes.

References

1. **Adeyemo GO, Fashola OO, Ademulegun TI** (2016): *Effect of stocking density on the performance, carcass yield and meat composition of broiler chickens.* Br Biotechnol J, **14**, 1-7.
2. **Ahmadi M, Ahmadian A, Seidavi AR** (2018): *Effect of different levels of nano-selenium on performance, blood parameters, immunity and carcass characteristics of broiler chickens.* Poult Sci J, **6**, 99-108.
3. **AOAC** (2000): Official Method of Analysis of the Association of Official Analytical Chemist. 17th Ed., AOAC International, Maryland, USA.
4. **Astaneh IY, Chamani M, Mousavi SN, et al** (2018): *Effects of stocking density on performance and immunity in Ross 308 broiler chickens.* Kafkas Univ Vet Fak, **24**, 483-489.
5. **Aviagen** (2014): Ross 308 Broiler: Nutrition Specifications. Ross 308 broiler nutrition specifications. Aviagen Huntsville, Alabama, USA.
6. **Azzam MMM, El-Gogary MR** (2015): *Effects of dietary threonine levels and stocking density on the performance, metabolic status and immunity of broiler chickens.* AJAVA, **10**, 215-225.
7. **Bakhshalinejad R, Hassanabadi A, Swick RA** (2019): *Dietary sources and levels of selenium supplements affect growth performance, carcass yield, meat quality and tissue selenium deposition in broilers.* Anim Nutr, **5**, 256-263.
8. **Beaulac K, Schwean-Lardner K** (2018): *Assessing the effects of stocking density on turkey tom health and welfare to 16 weeks of age.* Front Vet Sci, **5**, 213.
9. **Boostani A, Sadeghi AA, Mousavi SN, et al** (2015): *Effects of organic, inorganic, and nano-Se on growth performance, antioxidant capacity, cellular and humoral immune responses in broiler chickens exposed to oxidative stres.* Livest Sci, **178**, 330-336.
10. **Cai SJ, Wu CX, Gong LM, et al** (2012): *Effects of nano-selenium on performance, meat quality, immune function, oxidation resistance, and tissue selenium content in broilers.* Poult Sci, **91**, 2532–2539.
11. **Cemin HS, Vieira SL, Stefanello C, et al** (2018): *Broiler responses to increasing selenium supplementation using Zn-L-selenomethionine with special attention to breast myopathies.* Poult Sci, **97**, 1832-1840.
12. **Cengiz Ö, Köksal BH, Tatlı O, et al** (2015): *Effect of dietary probiotic and high stocking density on the performance, carcass yield, gut microflora, and stress indicators of broilers.* Poult Sci, **94**, 2395-2403.
13. **Cengiz Ö, Köksal BH, Tatlı O, et al** (2018): *Supplemental boric acid does not prevent the development of footpad dermatitis in broilers subjected to high stocking density*. Poult Sci, **97**, 4342-4350.
14. **Choct M, Naylor AJ, Reinke N** (2004): *Selenium supplementation affects broiler growth performance, meat yield and feather coverage.* Br Poult Sci, **45**, 677-683.
15. **Dozier WA, Thaxton JP, Branton SL, et al** (2005): *Stocking density effects on growth performance and processing yields of heavy broilers.* Poult Sci, **84**, 1332-1338.
16. **Dozier WA, Thaxton JP, Purswell JL, et al** (2006): *Stocking density effects on male broilers grown to 1.8 kilograms of body weight.* Poult Sci, **85**, 344–351.
17. **Edens EW, Parkhurst CR, Havenstein GB** (2000): *Housing and selenium influences on feathering in broilers.* J Appl Poult Res, **10**, 128-134.
18. **El-Deep MH, Ijiri D, Ebeid TA, et al** (2016): *Effects of dietary nano-selenium supplementation on growth performance, antioxidative status, and immunity in broiler chickens under thermoneutral and high ambient temperature conditions.* J Poult Sci, **53**, 274-283.
19. **Estevez I** (2007): *Density allowances for broilers: where to set the limits?* Poult Sci, **86**, 1265-1272.
20. **Feddes JJ, Emmanuel EJ, Zuidhoft MJ** (2002): *Broiler performance, body weight variance, feed and water intake, and carcass quality at different stocking densities.* Poult Sci, **81**, 774–779.
21. **Gangadoo S, Stanley D, Hughes RJ, et al** (2016): *Nanoparticles in feed: progress and prospects in poultry research.* Trends Food Sci Tech, **58**, 115-126.

22. **Honikel KO** (1998): *Reference methods for the assessment of physical characteristics of meat.* Meat Sci, **49**, 447-457.
23. **Huff-Lonergan E, Lonergan SM** (2005): *Mechanism of water-holding capacity of meat: the role of postmortem biochemical and structural changes.* Meat Sci, **71**, 194-204.
24. **Joo ST** (2018): *Determination of water-holding capacity of porcine musculature based on released water method using optimal load*. Korean J Food Sci Anim Resour, **38**, 823-828.
25. **Lai PW, Liang JB, Hsia LC, et al** (2010): *Effects of varying dietary zinc levels and environmental temperatures on the growth performance, feathering score and feather mineral concentrations of broiler chicks.* Asian-Australas J Anim Sci, **23**, 937-945.
26. **Leeson S, Walsh T** (2004): *Feathering in commercial poultry II Factors influencing feather growth and feather loss*. Worlds Poult Sci J, **60**, 52-63.
27. **Liu S, Tan H, Wei S, et al** (2015): *Effect of selenium sources on growth performance and tissue selenium retention in yellow broiler chicks.* J Appl Anim Res, **43**, 487-490.
28. **Madilindi MA, Mokobane A, Letwaba PB, et al** (2018): *Effects of sex and stocking density on the performance of broiler chickens in a sub-tropical environment.* S Afr J Anim Sci, **48**, 459-468.
29. **Mohammadi A, Ghazanfari S, Sharifi SD** (2019): *Comparative effects of dietary organic, inorganic, and nano-selenium complexes and rosemary essential oil on performance, meat quality and selenium deposition in muscles of broiler chickens.* Livest Sci, **226**, 21-30.
30. **Moreira J, Mendes AA, Garcia RG, et al** (2006): *Effect of strain, dietary energy level and stocking density on broiler performance.* Rev Bras Cienc Avic, **8**, 15-22.
31. **Patria CA, Afnan R, Arief II** (2016): *Physical and microbiological qualities of kampong-broiler crossbred chickens meat raised in different stocking densities.* Media Peternakan, **39**, 141-147.
32. **Ravindran V, Elliot S** (2017): *Influence of slenium source on the performnace, feathering and meat quality of broilers.* JAAN, **5**, 1-8.
33. **Sauter EA, Petersen CF, Steele EE, et al** (1981): *The airborne microflora of poultry houses.* Poult Sci, **60**, 569-574.
34. **Selim NA, Radwan NL, Youssef SF, et al** (2015): *Effect of inclusion inorganic, organic or nano selenium forms in broiler diets on: 1-growth performance, carcass and meat characteristics.*Int J Poult Sci, **14**, 135-143.
35. **Skrbic Z, Pavlovski Z, Lukic M** (2009): *Stocking density-factor of production performance, quality and broiler welfare.* Biotechnol Anim Husb, **25**, 359-372.
36. **Skrbic Z, Pavlovski Z, Lukic M, et al** (2009): *The effect of stocking density on certain broiler welfare parameters.* Biotechnol Anim Husb, **25**, 11-21.
37. **Skrbic Z, Pavlovski Z, Lukic M, et al** (2011): *The effect of stocking density on individual broiler welfare parameters: 2. Different broiler stocking densities.* Biotechnol Anim Husb, **27**, 17-24.
38. **Suchy P, Strakova E, Herzig I** (2014): *Selenium in poultry nutrition: a review*. Czech J Anim Sci, **59**, 495-503.
39. **Surai PF** (2018): Selenium in Poultry Nutrition and Health. Wageningen Academic Publishers, Netherlands.
40. **Swain PS, Rajendran D, Rao SBN, et al** (2015): *Preparation and effects of nano mineral particle feeding in livestock: a review.* Vet World, **8**, 888-891.
41. **Tong HB, Lu J, Zou JM, et al** (2012): *Effects of stocking density on growth performance, carcass yield, and immune status of a local chicken breed.* Poult Sci, **91**, 667–673.
42. **Van Soest PJ, Robertson JB, Lewis BA** (1991): *Methods for dietary fiber, neutral detergent fiber, and nonstarch polysaccharides in relation to animal nutrition*. J Dairy Sci, **74**, 3583-3597.

Serum ANGPTL4 and FGF2, energy-related blood biochemicals, cytokine responses and oxidative stress in dairy cows with subclinical ketosis

Efe KURTDEDE[1,a,✉], Arif KURTDEDE[2,b], Naci ÖCAL[3,c], Erdal KARA[3,d]

[1]Ankara University, Veterinary Faculty, Biochemistry Department, Ankara, Türkiye; [2]Ankara University, Veterinary Faculty, Internal Medicine Department, Ankara, Türkiye; [3]Kırıkkale University, Veterinary Faculty, Internal Medicine Department, Kırıkkale, Türkiye

[a]ORCID: 0000-0001-8436-3332; [b]ORCID: 0000-0003-0537-7256; [c]ORCID: 0000-0002-8679-2111; [d]ORCID: 0000-0001-7047-9502

ARTICLE INFO

Article History
Received : 31.03.2021
Accepted : 04.11.2021
DOI: 10.33988/auvfd.907076

Keywords
Cytokines
Dairy cows
Energy-related biochemical
Hepatokines
Subclinical ketosis

✉Corresponding author
efekurtdede@gmail.com

How to cite this article: Kurtdede E, Kurtdede A, Öcal N, Kara E (2023): Serum ANGPTL4 and FGF2, energy-related blood biochemicals, cytokine responses and oxidative stress in dairy cows with subclinical ketosis. Ankara Univ Vet Fak Derg, 70 (1), 37-42. DOI: 10.33988/auvfd.907076.

ABSTRACT

In this study, it was aimed to investigate the serum levels of ANGPTL4, FGF21, IL-1β, IL-6, SOD, MDA, and serum biochemical and hematological parameters in cows with subclinical ketosis. The mean serum β-hydroxybutyric acid (BHB) level was 1.37 ± 0.04 mmol/L in 10 dairy cows aged 3-5 years that were <21 days postpartum and diagnosed with subclinical ketosis. The mean serum BHB level was 0.40 ± 0.08 mmol/L in 10 healthy dairy cows in the same period and in the same age range. An increase in serum AST (P<0.001) and a decrease in serum albumin levels (P<0.05) indicated altered liver functions. An increase in serum non-esterified fatty acid (P<0.001) and decreases in serum HDL, triglyceride, and total cholesterol levels (P<0.05) were interpreted as indicators of increased metabolic pathology risk due to negative energy balance. Increases in serum ANGPTL4, FGF2, IL-1β, IL-6, and MDA (P<0.001) and SOD levels (P<0.05) were evaluated as indicators of the development of effective metabolic, inflammatory, and oxidative stress. It was concluded that significant increases in serum ANGPTL4, FGF2, IL-1β, IL-6, and MDA and SOD levels in dairy cows with subclinical ketosis were associated with negative energy balance, effective cytokine responses, and oxidative stress.

Introduction

In cows with high milk production, increased energy requirement and inadequate food intake result in negative energy balance (NEB) and subclinical ketosis at 7-28 days postpartum (6, 7).

Subclinical ketosis is characterized by a decrease in blood glucose and depletion of liver glycogen and other glucose reserves and gluconeogenesis activity, and lipid degradation in the liver, and an increase in ketone bodies in the blood (24, 38).

In NEB cows, changes in body lipid reserves result in increased circulating body levels of non-esterified fatty acids (NEFAs) and ketones. This adversely affects all tissues, but especially the liver (7, 12, 32).

Serum HDL, triglyceride, and total cholesterol are the main indicators of postpartum lipid metabolism changes (12, 23).

Angiopoietin-like 4 (ANGPTL4) is a glycoprotein that stimulates lipolysis by inhibiting lipoprotein lipase (LPL) activity, and thus regulates systemic energy and lipid metabolism. Fibroblast growth factor 21 (FGF21) is a hormonal factor that takes part in the regulation of metabolic response, such as hepatic lipid oxidation and ketogenesis, during energy deprivation (28). In dairy cows, circulating FGF21 and ANGPTL4 are predominantly expressed in the liver and adipose tissue metabolism due to negative energy balance (3, 20, 29).

It is important to determine serum total protein, albumin, glucose, and aspartate amino transaminase

(AST) levels in dairy cows in NEB (22, 25). Previous researchers (15, 18) indicate the utility of blood urea and creatinine levels and urine creatinine/total protein ratio in the assessment of renal functions in cows with subclinical ketosis.

Halliwell (13) reported that increased cellular respiration by-products in mitochondria during the postpartum period caused a marked increase in blood free radical levels, which is an indicator of oxidative stress. Oxidative stress, which increases due to lipid mobilization and activation of phagocytic cells and cytokines, is a part of the complex metabolic response process in cows in NEB (5, 35). One parameter used in determining oxidative stress is SOD, which is involved in the natural elimination of O2-. Another parameter is MDA, which is a by-product of lipid peroxidation, and is used to evaluate the oxidative degradation of lipids (1).

In high milk yielding cows, hematological values can prove useful in determining the metabolic status and the presence, severity, and prognosis of clinical and subclinical diseases (11, 21). Lacetera et al. (17) reported a possible relationship between the lymphocyte count and serum BHB and NEFA levels.

During the development of postnatal NEB, proinflammatory cytokines such as IL-1 and IL-6 actively participate in increases in serum NEFA and BHB, along with the acceleration of metabolic activation. IL-6 is involved in the development of metabolic inflammation and immunological response in cows with subclinical ketosis. In addition, IL-6 plays an important role in lipoprotein metabolism, fatty acid oxidation, urea cycle, oxidative stress, and proteasome activation (19, 37).

In the present study, we aimed to investigate the serum levels of ANGPTL4, FGF21, IL-1β, IL-6, SOD, MDA, and serum biochemical and hematological parameters in cows with subclinical ketosis.

Materials and Methods

Sampling: Twenty dairy cows on the same dairy farm, <21 days postpartum, 3-5 years old, and having given birth to two or more calves were included in the study. Calving took place in the autumn–winter sessions. Cows with a BCS of 3.5 were selected from cows with a BCS <0.5 from the dry period to calving. Animals with a previous lactation period and a longer drying period and with a previous history of metabolic disease were excluded from the study. Blood samples were taken approximately 4 hours after feeding.

The subclinical ketosis group consisted of 10 dairy cows with atypical symptoms of subclinical ketosis (lethargy, weight loss, decreased appetite, decreased milk production, and change in milk consistency). In this group mean blood serum BHB (mean 1.37 ± 0.04 mmol/L) was >1.20 and ketone bodies were absent in their urine samples. The control group included 10 healthy dairy cows that did not have clinical symptoms of any diseases and whose blood serum BHB (mean 0.40 ± 0.08 mmol/L) was <1.20.

Urinalysis: Samples were collected from urine during manual perineal massage. Urine samples were analyzed for ketone bodies within 1 hour with strip method, and the remainder aliquoted into 5 × 1.5 mL plastic tubes and stored at -80 °C until creatinine/protein ratio measurement.

Blood analysis: A total of 7 mL of blood was collected from the tail vein of cows; 5 mL was placed into coagulation tubes for serum samples and 2 mL into tubes containing anticoagulant (EDTA). Serum samples separated from blood samples immediately after collection were placed in Dappen dishes and stored at -80 °C.

Hematological parameters were studied in EDTA blood samples using a Mindray BC-5000 device.

In serum and urine samples thawed at room temperature before test applications, serum albumin, glucose, urea, uric acid, creatinine, total protein, aspartate amino transaminase (AST), and total bilirubin were measured using an automated biochemistry analyzer (Mindray BS-120). Quantitative analysis of protein and creatinine in urine samples was performed using a Mindray BS-300 device.

A portable measuring device (VET-TD-4235 Beta Keton Monitoring System, TalDoc Technology Corporation, Taiwan, ROC) was used to determine the level of BHB.

ANGPTL4, FGF21, and serum NEFA, IL-1β, and IL-6 levels were measured using respective ELISA test kits (Sun Red Biotechnology Company, Cat No: 201-04-291, Cat No: 201-04-3155, Cat No: 201-04-0186, Cat No: 201-04-0157, and Cat No: 201-04-0008). Serum superoxide dismutase (SOD) level was measured using a Cayman 706002 commercial test kit. Serum malondialdehyde (MDA) level was measured using a commercial ELISA test kit (Sun Red Biotechnology Company, Cat No: 2.01-04-0255).

Statistical analysis: For statistical assessment, prior to testing for statistical significance, all data were tested for parametric test assumptions, namely normality with the Shapiro–Wilk test and homogeneity with Levene's test. The differences between the two groups were analyzed using Student's t-test when parametric assumptions were met and the Mann–Whitney U test otherwise. All statistical analyses were examined with a 5% margin of error. The data were analyzed using SPSS v.14.01.

Results

Mean serum BHB level was 1.37 ± 0.04 mmol/L in the cows diagnosed with subclinical ketosis and 0.40 ± 0.08 mmol/L in the control group. The significantly elevated BHB levels (P<0.001) in the cows with subclinical ketosis were ascribed to developing NEB.

DOI: 10.33988/auvfd.907076

The glucose, albumin, total protein, AST, total cholesterol, triglycerides, HDL, and AST levels of the cows with subclinical ketosis and the controls are presented in Table 1. In the cows with subclinical ketosis, increase in serum AST ($P<0.001$), decrease in serum albumin ($P<0.05$), and decrease in serum HDL, triglyceride, and total cholesterol ($P<0.05$) were determined compared to the values in the control group.

The NEFA, BHB, ANGPTL4, FGF21, IL-1β, and IL-6 levels of the cows with subclinical ketosis and the controls are presented in Table 2. Significantly increases were found in serum BHB, NEFA, ANGPTL4, FGF21, IL-1β, and IL-6 values in the dairy cows with subclinical ketosis compared to the values determined in the healthy cows ($P<0.001$).

The urea, creatinine, urine protein/creatinine, SOD, and MDA levels of the cows with subclinical ketosis and the controls are presented in Table 3. The urea and SOD levels of the subclinical ketosis and control groups were significantly different ($P<0.05$). Statistically significant changes were determined in serum urea, SOD, and MDA values in the cows with subclinical ketosis compared to the values determined in the control cows. There was no statistical difference in serum creatinine and urine protein/creatinine values ($P<0.001$).

The WBC, lymphocyte, monocyte, neutrophil, and eosinophil counts of the cows with subclinical ketosis and the controls are presented in Table 4. No statistically significant difference was found in blood parameters.

Table 1. Glucose, albumin, total protein, AST, total cholesterol, triglycerides, HDL, and levels of the cows with subclinical ketosis and the controls.

Groups	Biochemical Parameters						
	Glucose (mg/dL)	Albumin (g/dL)	Total Protein (g/dL)	Total Cholesterol (mg/dL)	Triglyceride (mg/dL)	HDL (mg/dL)	AST (U/L)
Control	55.5 ± 11.81	2.96 ± 0.66	6.95 ± 1.72	159.6 ± 3.82	8.3 ± 3.16	155.2 ± 10.35	57.2 ± 10.45
Subclinical Ketosis	49.4 ± 12.24	2.35 ± 0.61*	5.90 ± 1.92	122.6 ± 34.21*	6.0 ± 2.62*	103.8 ± 21.65**	78.2 ± 10.32**

The results are presented as arithmetic mean ± standard deviation.
*The AST and HDL levels ($P<0.001$).
**The albumin, total cholesterol, and triglyceride measurements ($P<0.05$) of the two groups were significantly different (albumin $P=0.044$, total cholesterol $P=0.025$, triglyceride $P=0.094$).

Table 2. The NEFA, BHB, ANGPTL4, FGF21, IL-1β, and IL-6 levels of the cows with subclinical ketosis and the controls.

Groups	Biochemical Parameters					
	NEFA (µmol/mL)	ANGPTL4 (ng/mL)	FGF 21 (ng/L)	IL-1β (ng/mL)	IL-6 (ng/mL)	BHB (mmol/L)
Control	0.33 ± 0.07	5.81 ± 1.12	509.68 ± 26.36	113.20 ± 13.87	4.97 ± 0.45	0.40 ± 0.08
Subclinical Ketosis	0.70 ± 0.05*	15.16 ± 2.5*	1323.58 ± 70.82*	148.85 ± 17.22*	13.38 ± 1.37*	1.37 ± 0.04*

The results are presented as arithmetic mean ± standard deviation.
* The NEFA, ANGPTL4, FGF 21, IL-1β, IL-6, and BHB levels of the two groups were significantly different ($P<0.001$).

Table 3. Urea, creatinine, urine protein/creatinine, SOD, and MDA levels of the cows with subclinical ketosis and the controls.

Groups	Biochemical Parameters				
	Urea (mg/dL)	Creatinine (mg/L)	Urine protein / creatinine	SOD U/g protein	MDA nmol/g protein
Control	15.93 ± 3.69	0.96 ± 0.26	0.08 ± 0.02	67.60 ± 8.43	3.75 ± 0.23
Subclinical Ketosis	18.94 ± 4.4*	1.22 ± 0.13	0.07 ± 0.02	80.14 ± 6.59*	4.68 ± 0.19**

The results are presented as arithmetic mean ± standard deviation.
* The urea and SOD levels of the subclinical ketosis and control groups were significantly different ($P<0.05$) (urea $P=0.033$, SOD $P=0.002$).
** The MDA levels of the subclinical ketosis and control groups were significantly different ($P<0.001$).

Table 4. WBC, lymphocyte, monocyte, neutrophil, and eosinophil counts of the cows with subclinical ketosis and the controls.

Groups	Hematological Parameters				
	WBC (10^9/L)	Lymphocyte (10^9/L)	Monocyte (10^9/L)	Neutrophil (10^9/L)	Eosinophil (10^9/L)
Control (n = 10)	8.83 ± 4.16	5.35 ± 2.48	0.24 ± 0.16	2.88 ± 2.81	0.30 ± 0.14
Subclinical ketosis (n = 10)	9.84 ± 1.67	6.53 ± 2.48	0.30 ± 0.27	2.56 ± 1.03	0.33 ± 0.17

No statistically significant difference was found in blood parameters. But there is a numerical increase in the lymphocyte count in the cows with subclinical ketosis, although it was not statistically significant.

Discussion and Conclusion

The development and progression of NEB in dairy cows during the first 21 days postpartum and the subsequent mobilization of fat to the liver for utilization elevate serum BHB and NEFA levels, the most important laboratory indicators of subclinical ketosis (10). In the present study, subclinical ketosis was diagnosed in dairy cows at < 21 days postpartum through significantly elevated serum BHB as well as serum NEFA levels and the absence of ketone bodies in the urine. In defining subclinical ketosis, Folnozic et al. (10) ann Basbug et al. (4) considered both serum BHB and NEFA levels was found decisive,

In cows with subclinical ketosis, when the serum BHB value rises above 1.2 mmol/L, serum ANGPTL4 and FGF21 values also start to increase, indicating a response of lipid metabolism. If this metabolic response is prolonged, laboratory and clinical findings associated with subclinical ketosis become more prominent (9). Findings including clear clinical signs of ketosis and the presence of ketone bodies in urine suggest that ketosis has developed in cows (14). We thought that the cows in the present study were in the early stages of subclinical ketosis development, since the mean serum BHB level (1.37 ± 0.04 mmol/L) measured in 10 cows with subclinical ketosis was slightly above the threshold value (1.2 mmol/L). Issi et al. (15) stated that serum total protein, albumin, glucose, and aspartate amino transaminase levels provide important information about the functional status of the liver in cows with subclinical ketosis. In the present study, low total protein, albumin, and glucose levels and high aspartate amino transaminase levels measured in 10 cows with subclinical ketosis were attributed to liver degradation, which was thought to be caused by changes in lipid metabolism. Chen et al. (8) reported low serum glucose, triglyceride, and creatinine levels and elevated serum NEFA and AST levels in cows with subclinical ketosis with BHB levels of 1.2-1.6 mmol/L.

Many studies have shown that serum NEFA levels increase and HDL, triglyceride, and total cholesterol levels decrease as a result of NEB and lipid mobilization in the postpartum period (4, 10, 15, 27). In our study, a statistically significant increase in serum NEFA level in cows with subclinical ketosis showed that significant lipid mobilization had developed in the patients. In addition, statistically significant decreases in serum albumin, total protein, HDL, triglyceride, and total cholesterol levels indicated that the liver was mildly/moderately affected by the increased activity in lipid metabolism.

Similar to our results, Marutsova et al. (22) reported reduced serum total protein and albumin levels in dairy cows with subclinical ketosis, whereas Antanaitis et al. (2) reported increased total protein level and reduced albumin level and Issi et al. (15) demonstrated that total protein had increased.

Some researchers (15, 18) have suggested that serum urea, creatinine, and urine creatinine/total protein ratios are important indicators for evaluating renal functions in subclinical ketosis. In the present study, statistically significant changes were determined in serum urea, SOD, and MDA values in the cows with subclinical ketosis compared to the values determined in the control cows. However, there was no significant difference in serum creatinine or urine protein/creatinine values. The increase in serum urea level was found to be consistent with the findings reported by Issi et al. (15). Issi et al. (15) highlighted that serum urea and creatinine levels are increased in cows with subclinical ketosis and argue that glomerular filtration rate should be investigated to assess kidney functions. We recommend further studies that investigate renal functions using more sensitive and invasive methods.

Consistent with the findings published by Senoh et al. (31) and Karimi et al. (16), in the present study significant increases in serum MDA ($P<0.001$) and SOD ($P<0.05$) values and changes in energy-related metabolic parameters in cows with subclinical ketosis suggested that the cause of oxidative stress occurring in animals with subclinical ketosis was "ketosis-related acceleration in lipid mobilization". Some researchers (5, 26, 35) claimed that oxidative stress in postnatal dairy cows developed as a result of lipid mobilization in cows in NEB.

Zhang et al. (39) stated that an increase in serum NEFA level in the postpartum period in cows with NEB causes excessive production of polymorphic cells and proinflammatory cytokines, and, therefore, systemic inflammation and neutrophil counts may increase in cows with ketosis. The lack of statistically significant changes in hematological parameters in cows with NEB in our study may have been related to the severity of the disease and the length of the disease process, or it may have been due to the fact that serum NEFA values were not sufficiently elevated to affect hematological parameters. Schulz et al. (30) and Marutsova et al. (21) pointed out that the lymphocyte count is high in cows in the postnatal period in NEB. Similarly, in the present study, a numerical increase in lymphocyte count was noted in cows with subclinical ketosis, although it was not statistically significant.

Serum levels of ANGPTL4 and FGF21, which are synthesized by the liver and adipose tissue, are important in evaluating the stimulation of lipolysis, inhibition of lipogenesis and hepatic lipid oxidation, fatty acid oxidation, and the stimulation of ketogenesis in the liver (8). Wang et al. (36) reported increased serum NEFA, ANGPTL4, and FGF21 levels in postpartum cows with ketosis and fatty liver. Chen et al. (8) reported that serum FGF21 is a significant biomarker in cows with subclinical ketosis, which FGF21 continues to increase until serum BHB reaches 1.6 mmol/L, and that FGF21 starts to

DOI: 10.33988/auvfd.907076

decrease after BHB exceeds 1.6 mmol/L. In the present study, serum BHB, ANGPTL4, and FGF21 levels were elevated in cows with subclinical ketosis ($P<0.001$). A concomitant significant increase in serum NEFA levels supports the stimulation of lipolysis, inhibition of lipogenesis, hepatic lipid oxidation, fatty acid oxidation, and the stimulation of ketogenesis in the liver.

According to Trevisi et al. (33), high prenatal serum IL-1β and IL-6 levels were associated with increased oxidative stress parameters and this effect decreased, but postpartum 7-21. They stated that it continued. Trevisi et al. (34) recently reported a positive correlation between decreased liver function due to inflammation, metabolic stress, and increased serum IL-6 levels in lactating cows. Similarly, significant increases in serum BHB, NEFA, ANGPTL4, FGF21, IL-1β, IL-6, SOD, and MDA levels in dairy cows with subclinical ketosis showed effective metabolic, inflammatory, and oxidative stress in our study.

As a result of the present study, it is thought that there is no renal dysfunction that will significantly change serum creatinine and urinary creatinine/protein levels in cows with subclinical ketosis, and the level of kidney function loss can be evaluated with more sensitive methods. The increase in serum AST level and decrease in serum albumin level showed some deterioration in liver functions in these patients. In response to the NEB that developed in the patients, serum NEFA levels increased, while serum HDL, triglyceride, and total cholesterol levels decreased. Significant increases in serum SOD and MDA levels showed that patients developed significant oxidative stress. Elevated serum ANGPTL4 and FGF21 levels in the patient indicated that the liver and adipose tissue still had the ability to respond to negative energy-induced metabolic stress in cows with subclinical ketosis in NEB.

In conclusion, significant increases in serum IL-1β, IL-6, SOD, and MDA levels in dairy cows with subclinical ketosis were evaluated as indicators of effective metabolic, inflammatory, and oxidative stress development. The increase in oxidative stress markers along with the increase in FGF21 level was considered a remarkable finding. Considering that serum FGF21 has the function of supporting lipid oxidation and ketogenesis as an energy source in a low glucose environment, it was evaluated that significant increases in serum ANGPTL4 and FGF2 levels were associated with NEB, cytokine responses, and metabolic disorders due to oxidative stress.

Acknowledgements

This study is not produced from a doctoral-PhD or master's thesis or presented at scientific meetings.

Financial Support

This study was supported by Ankara University Scientific Research Grant (Grant No: 20B0239002).

Conflict of Interest

The authors declared that there is no conflict of interest.

Author Contributions

EK, AK, NÖ and EK conceived and planned the experiments. EK, AK, NÖ and EK carried out the experiments. EK, AK, NÖ and EK planned and carried out the simulations. EK, AK, NÖ and EK contributed to sample preparation. EK, AK, NÖ and EK contributed to the interpretation of the results. EK, AK, NÖ and EK took the lead in writing the manuscript. All authors provided critical feedback and helped shape the research, analysis and manuscript.

Data Availability Statement

The data supporting this study's findings are available from the corresponding author upon reasonable request.

Ethical Statement

This study was approved by the Kırıkkale University Animal Experiments Local Ethics Committee (Decision No: 2019/10/48).

Animal Welfare

The authors confirm that they have adhered to ARRIVE Guidelines to protect animals used for scientific purposes.

References

1. **Agalakova NI, Gusev GP** (2012): *Molecular mechanisms of cytotoxicity and apoptosis induced by inorganic fluoride.* ISRN Cell Biol, Article ID 403835.
2. **Antanaitis R, Juozaitiene V, Malasauskiene D, et al** (2019): *Can rumination time and some blood biochemical parameters be used as biomarkers for the diagnosis of subclinical acidosis and subclinical ketosis.* Vet Anim Sci, **8,** 100077.
3. **Badman MK, Pissios P, Kennedy AR, et al** (2007): *Hepatic fibroblast growth factor 21 is regulated by PPAR alpha and is a key mediator of hepatic lipid metabolism in ketotic states*. Cell Metab, **5**, 426-437.
4. **Basbug O, Akar Y, Ercan N** (2014): *The investigation of the prevalence of subclinical ketosis in Sivas region dairy cows*. Eurasian J Vet Sci, **30**, 123-128.
5. **Bernabucci U, Ronchi B, Lacetera N, et al** (2005): *Influence of body condition score on relationships between metabolic status and oxidative stress in periparturient dairy cows.* J Dairy Sci, **88**, 2017-2026.
6. **Bruckmaier RM, Gross JJ** (2017): *Lactational challenges in transition dairy cows.* Anim Prod Sci, **57**, 1471-1481.
7. **Brunner N, Groeger S, Raposo JC, et al** (2018): *Prevalence of subclinical ketosis and production diseases in dairy cows in Central and South America, Africa, Asia, Australia, New Zealand, and Eastern Europe*. Transl Anim Sci, **3**, 84-92.
8. **Chen Y, Dong Z, Li R, et al** (2018*): Changes in selected biochemical parameters (including FGF21) during*

subclinical and clinical ketosis in dairy cows. Med Weteryn, **74**, 727-730.

9. **Fiore E, Piccione G, Rizzo M, et al** (2018): *Adaptation of some energetic parameters during transition period in dairy cows*, J Appl Anim Res, **46**, 402-405.
10. **Folnozic I, Turk R, Duricic D, et al** (2015): *Influence of Body Condition on Serum Metabolic Indicators of Lipid Mobilization and Oxidative Stress in Dairy Cows During the Transition Period*. Rep Domestic Anim, **50**, 910-917.
11. **Gavan C, Retea C, Motorga V** (2010): *Changes in the hematological profile of Holstein primiparous in periparturient period and in early to mid-lactation*. Anim Sci Biotec, **43**, 244-246.
12. **Grummer RR** (1993): *Etiology of lipid-related metabolic disorders in periparturient dairy cows*. J Dairy Sci, **76**, 3882-3896.
13. **Halliwell B** (2007): *Biochemistry of oxidative stress*. Biochem Soci Trans, **35**, 1147-1150.
14. **Ingvartsen KL** (2006): *Feeding-and management-related diseases in the transition cow: Physiological adaptations around calving and strategies to reduce feeding-related diseases*. Anim Feed Sci, Technol, **126**, 175–213.
15. **Issi M, Gül Y, Basbug O** (2016): *Evaluation of renal and hepatic functions in cattle with subclinical and clinical ketosis.* Turk J Vet Anim Sci, **40**, 47-52.
16. **Karimi N, Mohri M, Azizzadeh M, et al** (2015): *Relationships between trace elements, oxidative stress and subclinical ketosis during transition period in dairy cows*. Iran J Vet Sci Techn, **7**, 46-56.
17. **Lacetera N, Scalia D, Franci O, et al** (2004): *Short communication: effects of nonesterified fatty acids on lymphocyte function in dairy heifers*. J Dairy Sci, **87**, 1012–1014.
18. **Li XB, Zhang ZG, Liu GW, et al** (2011): *Renal function of dairy cows with subclinical ketosis*. Vet Rec, **168**, 643.
19. **Loor JJ, Everts RE, Bionaz M, et al** (2007): *Nutrition-induced ketosis alters metabolic and signaling gene networks in liver of periparturient dairy cows*. Physiol Genomics, **32**, 105-116.
20. **Mamedova LK, Robbins K, Johnson BJ, et al** (2010): *Tissue expression of angiopoietin-like protein 4 in cattle.* J Anim Sci, **88**, 124-130.
21. **Marutsova V, Binev R, Marutsov P** (2015): *Comparative clinical and haematological investigations in lactating cows with subclinical and clinıcal ketosis*. Mac Vet Rev, **38**, 159-166.
22. **Marutsova VJ, Marutsov PD, Binev RG** (2019): *Evaluation of some blood liver parameters in cows with subclinical and clinical ketosis. Bulgarian* J Vet Med, **22**, 314-321.
23. **Mazur A, Rayssiquier Y** (1988): *Lipoprotein profile of the lactating co*w. Ann Rech Vet, **19**, 53-58.
24. **Opsomer G** (2015): *Interaction between metabolic challenges and productivity in high yielding dairy cows.* Jap J Vet Res, **63**, 1-14.
25. **Rodriguez-Jimenez S, Haerr KJ, Trevisi E, et al** (2018): *Prepartal standing behavior as a parameter for early detection of postpartal subclinical ketosis associated with inflammation and liver function biomarkers in peripartal dairy cows*. Journal of Dairy Science, **101**, 8224-8235.
26. **Sahoo SS, Patra RC, Behera PC, et al** (2009): *Oxidative stress indices in the erythrocytes from lactating cows after treatment for subclinical ketosis with antioxidant incorporated in the therapeutic regime*. Vet Res Commun, **33**, 281-290.
27. **Sato S, Kohno M, Ono H** (2005): *Relation between blood ß-hydroxybutyric acid and glucose, non-esterified fatty acid and aspartate aminotransferase in dairy cows with subclinical ketosis.* Jap J Vet Clin, **28**, 7-13.
28. **Schlegel G, Ringseis R, Keller J, et al** (2013): *Expression of fibroblast growth factor 21 in the liver of dairy cows in the transition period and during lactation*. J Anim Physiol Anim Nutr, **97**, 820–829.
29. **Schoenberg KM, Giesy SL, Harvatine KJ, et al** (2011): *Plasma FGF21 is elevated by the intense lipid mobilization of lactation*. Endocrinol, **152**, 4652-4661.
30. **Schulz K, Frahm J, Kersten S, et al** (2014): *Effects of elevated parameters of subclinical ketosis on the immune system of dairy cows: in vivo and in vitro results*. Arch Anim Nutr, **69**, 113-127.
31. **Senoh T, Oikawa S, Nakada K, et al** (2019): *Increased serum malondialdehyde concentration in cows with subclinical ketosis.* J Vet Med Sci, **81,** 817-820.
32. **Sun Y, Wang B, Shu S, et al** (2015): *Critical thresholds of liver function parameters for ketosis prediction in dairy cows using receiver operating characteristic (ROC) analysis*. Vet Quarterly, **35**, 159-164.
33. **Trevisi E, Amadori M, Cogrossi S, et al** (2012): *Metabolic stress and inflammatory response in high-yielding, periparturient dairy cows.* Res Vet Sci, **93**, 695-704.
34. **Trevisi E, Jahan N, Bertoni G, et al** (2015): *Pro-Inflammatory Cytokine Profile in Dairy Cows: Consequences for New Lactation.* Italian J Anim Sci, **14**, 3862.
35. **Turk R, PodpeCan O, Mrkun J, et al** (2013): *Lipid mobilisation and oxidative stress as metabolic adaptation processes in dairy heifers during transition period*. Anim Repr Sci, **141**, 109-115.
36. **Wang J, Zhu X, She G, et al** (2018): *Serum hepatokines in dairy cows: periparturient variation and changes in energy-related metabolic disorders*. BMC Veterinary Research, **14**, 236.
37. **Wankhade PR, Manimaran A, Kumaresan A, et al** (2017): *Metabolic and immunological changes in transition dairy cows: A review*. Vet World, **10**, 1367–1377.
38. **Yang W, Zhang B, Xu C, et al** (2019): *Effects of ketosis in dairy cows on blood biochemical parameters, milk yield and composition, and digestive capacity*. J Vet Res, **63**, 555-560.
39. **Zhang Y, Li X, Zhang H, et al** (2018): *Non-Esterified Fatty Acids Over-Activate the TLR2/4-NF-Kb Signaling Pathway to Increase Inflammatory Cytokine Synthesis in Neutrophils from Ketotic Cows*. Cell Physiol Biochem, **48**, 827-837.

DOI: 10.33988/auvfd.907076

Vertebral heart score and cardiothoracic ratio in Wistar rats

Elif DOĞAN[1,a,✉], Sıtkıcan OKUR[2,b], Armağan HAYIRLI[3,c], Zafer OKUMUŞ[2,d]

[1]Kastamonu University, Faculty of Veterinary Medicine, Department of Surgery, Kastamonu, Türkiye; [2]Atatürk University, Faculty of Veterinary Medicine, Department of Surgery, Erzurum, Türkiye, [3]Atatürk University, Faculty of Veterinary Medicine, Department of Animal Nutrition and Nutritional Diseases, Erzurum, Türkiye

[a]ORCID: 0000-0002-3321-8116; [b]ORCID: 0000-0003-2620-897X; [c]ORCID: 0000-0001-5880-1415; [d]ORCID: 0000-0002-4446-0848

ARTICLE INFO

Article History
Received : 29.03.2021
Accepted : 04.11.2021
DOI: 10.33988/auvfd.905135

Keywords
Cardio-Thoracic Rate
Vertebral Heart Size
Wistar Rat

✉Corresponding author
elifdogan@kastamonu.edu.tr

How to cite this article: Doğan E, Okur S, Hayırlı A, Okumuş Z (2023): Vertebral heart score and cardiothoracic ratio in Wistar rats. Ankara Univ Vet Fak Derg, 70 (1), 43-47. DOI: 10.33988/auvfd.905135.

ABSTRACT

The purpose of this study was to determine and compare the Vertebral Heart Size (VHS) and Cardio-Thoracic Rate (CTR) in normal Wistar Rats. The size of the organs in the chest cavity and the size of the heart can be measured by taking thorax radiographs. Thorax radiographs of 85 male Wistar rats were taken under anesthesia, and VHS and CTR were calculated in the digital environment. The mean VHS was 7.22 mm in the right lateral position and 7.34 mm in the left lateral position. In the radiography taken in the ventrodorsal position (P = 0.3530), the mean CTR was calculated as 0.89 mm. Also, no significant correlation was measured between VHS and CTR. In conclusion, our study results can be reference values, as no previous study has been found for Wistar rats.

Introduction

Radiographic examination of heart tissue is one of the routines in veterinary medicine (22). Chest radiography has an important place in the diagnosis of heart diseases, especially in terms of changes in the size of the heart, edema, and the shape of pulmonary vessels (27). Radiographic evaluations are equivalent to other cardiac diagnostic methods (3). Besides, vertebral heart size (VHS) measurement, one of these methods, has advantages such as monitoring the heart with continuous images, and the method being accessible and applicable (13). In this method, which Buchanan and Bucheler defined as VHS in 1995 the long and short axis lengths of the heart are summed and compared with the thoracic vertebrae (7). Studies have been published about the wider range of VHS reference values since the study of Buchanan and Bucheler (4, 6, 15). One of the most important aspects of these methods is to mark the method of measuring heart size by comparing the length of the fourth thoracic vertebra to the heart size on chest radiography, as described by Ljubica (18). These methods give the same results as echocardiographic and electrocardiographic measurements. There is no race variation and there is no difference between right and left lateral recumbency while radiography is taken (23, 32). However, since normal heart size and shape are different in each race, these differences should be taken into account when considering VHS (2). The breed recumbency, gender, and body weight affect VHS (6, 36). Therefore, reported reference values do not apply to all breeds, and breed-specific values must be established (14). Although the VHS measurement system has been described in cats, dogs (19), sheep (31), monkeys (28), ferrets, and rabbits (12, 24, 35), little information is available on rodents (10, 35). Literature on the VHS values of Wistar rats is lacking.

Thorax radiographs are widely used as a non-invasive method in Veterinary Medicine to investigate the chest cavity (25). In addition to VHS measurements, it is also important to determine the cardiothoracic ratio

(CTR), which is widely used in human medicine. The main goal of CTR is to relate systolic dysfunction with the left ventricle (30). Besides, this method plays an important role in the diagnosis of heart diseases by revealing the difference between normal heart rate and enlarged heart size (5). To our knowledge, no studies are stating VHS and CTR values or comparing these measurement methods for rats. Therefore, the purpose of this study was to determine the VHS and CTR values for use in cardiac studies using Wistar rats as experimental animals, and to correlate the VHS and CTR values measured on radiographs taken in the right and left lateral position.

Materials and Methods

Animals: This study was conducted on healthy, male, 10 months old Wistar rats (n=85), and free from cardiothoracic diseases upon the approval by Atatürk University Animal Experiments Local Ethics Committee (HADYEK) (2018/226). After clinical examinations of the rats including respiratory system (respiratory rate and type), cardiovascular system (heart rate, oxygen saturation), and body temperature, no heart disease was confirmed by monitoring via monitor (Cardell, 9404, Sharn Veterinary Inc., FL, USA), and right and left lateral thorax radiographs (Meditronics 3L 103, Japan) of all rats were obtained under xylazine-ketamine anesthesia (10 mg/kg IP xylazine HCl, 75 mg/kg IP ketamine HCl).

Measuring the Vertebral Heart Size: The VHS was measured according to the protocol established by Ljubica (18). The long heart axis (LA) was measured from the ventral border of the main stem bronchi (carina cranioventral border) to the apex of the heart (the farthest point in the ventral contour of the cardiac radiographic image) on the radiographs. The short axis (SA) was measured at the widest cardiac image point on a line perpendicular to the long axis at the level of the clavicle vena cava. Both measurements (long and short axes) were compared with the distance from the cranial edge of the 4th thoracic vertebra (T4) to the cranial edge of the 5th thoracic vertebra (Figure 1). The VHS was calculated according to the formula given below:

$$VHS = (LA / T4) + (SA / T4)$$

Measuring the Cardio-Thoracic Ratio: The CTR was calculated as described by Schillaci et al (29). In the dorso-ventral position, the distance between the thoracic walls and the width of the heart was measured at the T8 level. The thoracic diameter was measured as the longest thoracic distance (MTD) at the T8 level, and the longest distance (ML and MR) from the line passing through the middle of the heart to the right and left sides between the heart width organ boundaries. (Figure 2). The CTR was calculated according to the formula given below:

$$CTR = (MR + ML) / MTD$$

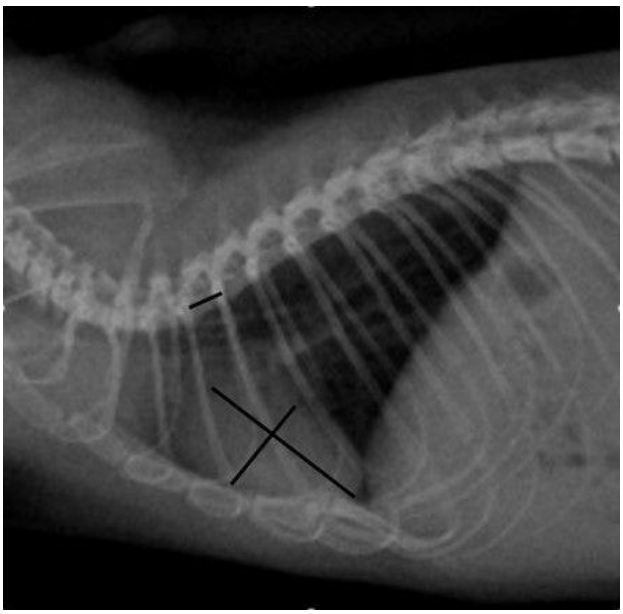

Figure 1. The vertebral heart size (VHS) measurement in lateral radiography.

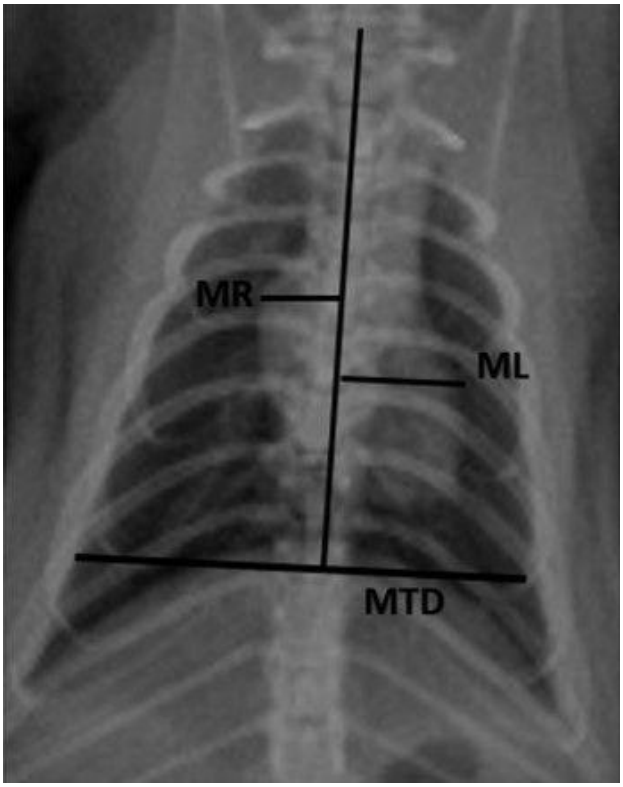

Figure 2. The cardiothoracic ratio (CTR) measurement on ventrodorsal radiography.

Statistical analysis: The data were subjected to the Student t-test and regression (PROC. REG) and correlation (PROC. CORR) analyses after testing for normality (Version 9.1; SAS Institute Inc., Cary, NC, USA). Statistical significance was declared at $P < 0.05$.

DOI: 10.33988/auvfd.905135

Results

Thorax radiographs were performed on all rats. The VHS measurements were made on thorax radiographs of the rats taken at right (R-VHS) and left lateral (L-VHS). The mean R-VHS and L-VHS was not different (P = 0.3530) and was 7.22±0.78 mm and 7.34±0.78 mm, respectively (Figure 3). The mean CTR was 0.89 mm. There was no correlation between VHS and CTR (Figure 4).

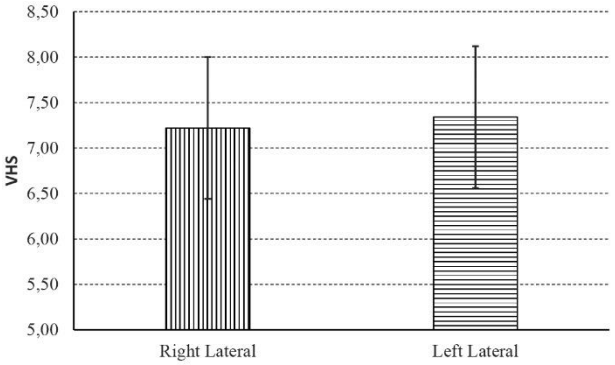

Figure 3. The vertebral heart size (VHS) measured in right and left lateral positions.

Discussion and Conclusion

This study determined and described the VHS and CTR in health Wistar Rats (18). It is important to determine the VHS for the diagnosis of heart diseases in veterinary medicine (21). The VHS is an effective method for objectively determining heart size on chest radiographs, and especially for detecting cardiomegaly caused by eccentric hypertrophy (27). In addition to method by Ljubica (18) suggesting calculation of the ratio of the long and short axis lengths of the heart to the width of the 4th thoracic vertebra, Buchanan and Bucheler (7) suggests transposing the long and short axes of the heart into the vertebral column. This method was preferred because it is a measurement that can be calculated automatically in the x-ray machine used in our study. The closest study of our study, has been newly published by Dias et al (9). Dias et al. measured the right lateral, ventrodorsal and dorsoventral VHS in Sprague-Dawley Rats (both male and female) and reported a mean of 7.70. In the present study the VHS was 7.22- 7.34 mm and the CTR was 0.89 for Wistar rats with no evidence of cardiac disease.

Abdolvahed Moarabi et al. (21) reported that the techniques used for VHS measurement are easy and the measurements taken are relatively independent of the patient (*e.g.*, gender, right, or left lateral). However, there are studies in the literature suggesting that the VHS measurements vary depending on the side of lying down. For example, Onuma M et al. (24) reported that the VHS values were significantly different in rabbits whose thorax radiographs were taken during right and left lateral. Also, Bavegems et al. (2) suggested that the heart silhouette would always be larger on the left lateral radiographs, as the heart is located on the left side of the chest cavity. Kraetschmer et al. (16) reported that the heart was significantly larger on the right lateral radiography in beagle dogs. In our study, we considered having chest radiographs in both the right lateral and left lateral positions, as different opinions were found in the literature reviews. There was no difference between the VHS measurements taken in both positions. De Moura et al. (8) and Marin et al. (20) reported the same results in right and left lateral radiographs on ferrets and greyhounds. Many studies have been conducted on VHS measurements, but since there is no study on rats, we cannot compare our results with other studies. Lamb et al. (17) reported different VHS values in male and female dogs. Since the use of generic references determined for other species and breeds may cause misdiagnosis (33), detailed studies on rats should be performed and breed-specific reference ranges should be determined.

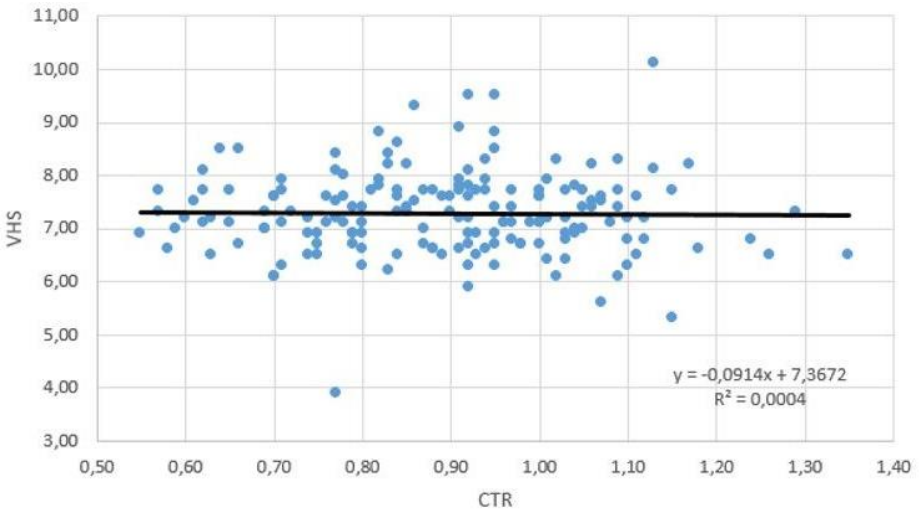

Figure 4. Relationship between the vertebral heart size (VHS) and cardiothoracic ratio (CTR) values.

The CTR is a method in which heart size is determined by measuring the heart and thorax cavity on radiographs (34). The main purpose of CTR measurement in humans is to compare the abnormalities of the left ventricle and systolic dysfunction (29). Studies reporting many types of CTR measurements have previously been published (1, 5, 26). However, as in the VHS, there is no study in which CTR measurements were made in Wistar rats in the literature review. The probability of getting the myocardial disease is higher with a high CTR value (30). Likewise, it is suggested that the CTR may be useful in the early diagnosis of heart diseases by detecting latent variations in the heart silhouette (26). In our study, the mean CTR was 0.89. These measurements should be evaluated by working together with different factors as in the VHS.

In disagreement with the current study, Oana Bîrsan et al. (5) found a significant correlation between VHS and CTR in healthy cats. They also reported that the CTR measurement can be used to evaluate VHS in cats. When heart width is examined within the scope of previously determined reference values, it appears as an important parameter in the diagnosis of heart diseases. The best measurement of this parameter can be made on thoracic radiographs (11). Therefore, as a result of our study, we think that previously undetermined VHS and CTR values should be evaluated as the first findings in rats. Simultaneous determination of the CTR and VHS may have merit for cardiology patients. The limitations of this study include not taking gender and body weight into consideration and using only healthy animals.

In conclusion, species, and breed-specific reference values should be determined to provide an accurate reference for clinical practitioners, to avoid misdiagnosis of heart diseases, and to be used in experimental cardiology studies.

Financial Support

This research received no grant from any funding agency/sector.

Conflict of Interest

The authors declared that there is no conflict of interest.

Author Contributions

ED, SO, AH and ZO conceived and planned the experiments. ED and SO carried out the experiments. ED, SO and ZO planned and carried out the simulations. ED, SO, AH and ZO contributed to sample preparation. AH, and ZO contributed to the interpretation of the results. ED took the lead in writing the manuscript. All authors provided critical feedback and helped shape the research, analysis and manuscript.

Data Availability Statement

The data supporting this study's findings are available from the corresponding author upon reasonable request.

Ethical Statement

This study was approved by the Atatürk University Animal Experiments Local Ethics Committee (2018/226).

Animal Welfare

The authors confirm that they have adhered to ARRIVE Guidelines to protect animals used for scientific purposes.

References

1. **Abdelgalil AI, Hassan EA, Torad FA** (2019): *Objective radiographic evaluation of cardiac size in clinically normal Zaraibi goats*. Indian J Anim Res, B-1097.
2. **Bavegems V, Van Caelenberg A, Duchateau L, et al** (2005): *Vertebral heart size ranges specific for whippets*. Vet Radiol Ultrasound, **46**, 400-403.
3. **Bhargavi S, Kannan TA, Ramesh G, et al** (2019): *Radiographic Evaluation of Heart Using VHS method in Rajapalayam Dog- Indigenous Breed of Tamil Nadu*. Int J Curr Microbiol App Sci, **8,** 1216-1220.
4. **Birks R, Fine DM, Leach SB, et al** (2017): *Breed-specific vertebral heart scale for the dachshund*. J Am Anim Hosp Assoc, **53**, 73-79.
5. **Bîrsan O, Baısan A, Mocanu D, et al** (2016): *Cardio-Thoracic Ratio Evaluation of Cardiac Sihlouette Compared with the Vertebral Heart Scale in Cats*. Bulletin UASVM Veterinary Medicine, **73**, 36-39.
6. **Bodh D, Hoque M, Saxena AC, et al** (2016): *Vertebral scale system to measure heart size in thoracic radiographs of Indian Spitz, Labrador retriever and Mongrel dogs*. VetWorld, **9**, 371-376.
7. **Buchanan JW, Bücheler JB** (1995): *Vertebral scale system to measure canine heart size in radiographs.* J Am Vet Med Assoc, **206,** 194–199.
8. **De Moura CR, Das Neves Diniz A, Da Silva Moura L, et al** (2015): *Cardiothoracic ratio and vertebral heart scale in clinically normal black-rumped agoutis (Dasyprocta prymnolopha, Wagler 1831).* J Zoo Wildl Med, **46**, 314-319.
9. **Dias S, Anselmi C, Espada Y, et al** (2021): *Vertebral heart score to evaluate cardiac size in thoracic radiographs of 124 healthy rats (Rattus norvegicus).* Vet Radiol Ultrasound, **62**, 394-401.
10. **Garcia EB, Eshar D, Thomason JD, et al** (2016): *Cardiac assessment of zoo-kept, black-tailed prairie dogs (Cynomys ludovicianus) anesthetized with isoflurane*. J Zoo Wildl Med, **47**, 955-962.
11. **Gardner A, Thompson MS, Heard DJ, et al** (2007): *Radiographic evaluation of cardiac size in flying fox species (Pteropus rodricensus, P. hypomelanus, and P. vampyrus)*. J Zoo Wildl Med, **38**, 192-200.
12. **Giannico AT, Garcia DAA, Lima L, et al** (2015): *Determination of normal echocardiographic, electrocardiographic, and radiographic cardiac parameters in the conscious New Zealand white rabbit*. J Exot Pet Med, **24**, 223-234.

13. **Gugjoo MB, Hoque M, Saxena AC, et al** (2013): *Vertebral scale system to measure heart size in dogs in thoracic radiographs.* Adv Anim Vet Sci, **1,** 1-4.
14. **Jacobson JH, Boon JA, Bright JM** (2013): *An echocardiographic study of healthy Border Collies with normal reference ranges for the breed*. J Vet Cardiol, **15**, 123-130.
15. **Jepsen-Grant K, Pollard RE, Johnson LR** (2013): *Vertebral heart scores in eight dog breeds*. Vet Radiol Ultrasound, **54,** 3-8.
16. **Kraetschmer S, Ludwig K, Meneses F, et al** (2008): *Vertebral heart scale in the beagle dog*. J Small Anim Pract, **49**, 240-243.
17. **Lamb CR, Boswood A** (2002): *Role of survey radiography in diagnosing canine cardiac disease*. Comp Cont Ed Prac Vet, **24**, 316-326.
18. **Ljubica SK, Krstic N, Trailovic RD** (2007): *Comparison of three methods of measuring vertebral heart size in German shepherd dogs.* Acta Veterinaria (Beogard), **57**, 133-141.
19. **Luciani MG, Withoeft JA, Pissetti HMC, et al** (2019): *Vertebral heart size in healthy Australian cattle dog*. Anat Histol Embryol, **48**, 264-267.
20. **Marin LM, Brown J, McBrien C, et al** (2007): *Vertebral heart size in retired racing greyhounds*. Vet Radiol Ultrasound, **48**, 332-334.
21. **Moarabi A, Mosallanejad B, Ghadiri A, et al** (2015): *Radiographic Measurement of Vertebral Heart Scale (VHS) in New Zealand White Rabbits*. IJVS, **10**, Serial No: 22.
22. **Nabi SU, Wani AR, Dey S** (2014): *Radiographıc measurements (vertebral heart scale) of popular breeds of dogs in India*. Appl Biol Res, **16,** 242-246.
23. **Nakayama H, Nakayama T, Hamlin RL** (2001): *Correlation of cardiac enlargement as assessed by vertebral heart size and echocardiographic and electrocardiographic findings in dogs with evolving cardiomegaly due to rapid ventricular pacing*. J Vet Intern Med, **15**, 217-221.
24. **Onuma M, Ono S, Ishida T, et al** (2010): *Radiographic measurement of cardiac size in 27 rabbits*. J Vet Med Sci, **72**, 529-531.
25. **Reichle JK, Wisner ER** (2000): *Non-cardiac thoracic ultrasound in 75 feline and canine patients*. Vet Radiol Ultrasound, **41,** 154-162.
26. **Rocha-Neto HJ, Moura LS, Pessoa GT, et al** (2015): *Cardiothoracic ratio and vertebral heart size (VHS) to standardize the heart size of the tufted capuchin (Cebus apella Linnaeus, 1758) in computerized radiographic images*. Pesq Vet Bras, **35**, 853-858.
27. **Root CR, Bahr RJ** (2002): The heart and great vessels. 402-419. In: DE Thrall (Ed), Textbook of Diagnostic Veterinary Radiology. 4th ed. WB Saunders Company, Philadelphia.
28. **Saunders RA, Kubiak M, Dobbs P** (2018): *Determination of vertebral heart score in three species of Spider monkey (Ateles fusciceps, A. hybridus and A. Paniscus)*. J Med Primatol, **47**, 51-54.
29. **Schillaci MA, Parish S, Jones-Engel L** (2009): *Radiographic measurement of the cardiothoracic ratio in pet macaques from Sulawesi Indonesia*. Radiography, **15**, 29-33.
30. **Schillaci MA, Lischka AR, Karamitsos AA, et al** (2010): *Radiographic measurement of the cardiothoracic ratio in a feral population of long tailed macaques (Macaca fascicularis)*. Radiography, **16**, 163-166.
31. **Singh A, Pandey RP, Purohit S, et al** (2020): *Measurement and comparison of vertebral heart size (VHS) in Muzaffarnagari sheep using two different methods*. J Entomol Zool, **8**, 834-837.
32. **Sleeper MM, Buchanan JW** (2001): *Vertebral scale system to measure heart size in growing puppies*. J Am Vet Med, **219**, 57-59.
33. **Taylor CJ, Simon BT, Stanley BJ, et al** (2020): *Norwich terriers possess a greater vertebral heart scale than the canine reference value*. Vet Radiol Ultrasound, **61**, 10-15.
34. **Torad FA, Hassan EA** (2014): *Two-dimensional cardiothoracic ratio for evaluation of cardiac size in German shepherd dogs*. JV Cardiology, **16**, 237-244.
35. **Ukaha Rock O, Iloh JI** (2018): *Measurement of Heart Size in the Rabbit (Oryctolagus cuniculus) by Vertebral Scale System*. J Sci Res, **18**, 1-7.
36. **Williams AR, Ueda Y, Stern JA, et al** (2020): *Vertebral Heart Score in Rhesus Macaques (Macaca mulatta): Generating Normal Reference Intervals and Assessing its Validity for Identifying Cardiac Disease*. JAALAS, **59**, 347-355.

Rapid molecular detection and isolation of canine distemper virus in naturally infected dogs

Hasbi Sait SALTIK[1,a,✉], Mehmet KALE[1,b]

[1]Burdur Mehmet Akif Ersoy University, Faculty of Veterinary Medicine, Department of Virology, Burdur, Türkiye

[a]ORCID: 0000-0002-3283-7062, [b]ORCID: 0000-0003-4156-1077

ARTICLE INFO

Article History
Received : 24.12.2020
Accepted : 08.11.2021
DOI: 10.33988/auvfd.846475

Keywords
Canine
Cell culture
Distemper
Fluorescent antibody
TaqMan

✉Corresponding author
hasbi.saltik@gmail.com

How to cite this article: Saltık HS, Kale M (2023): Rapid molecular detection and isolation of canine distemper virus in naturally infected dogs. Ankara Univ Vet Fak Derg, 70 (1), 49-56. DOI: 10.33988/auvfd.846475.

ABSTRACT

The canine distemper virus (CDV), which infects dogs and a broad range of animal species, remains a serious concern in Türkiye and across the world. The current study shows that CDV can be detected and isolated rapidly and specifically in naturally infected dogs. Whole blood, nasal swab, ocular swab, rectal swab, and urine samples from 50 stray dogs were used in the study (n = 250). The presence of the CDV genome was confirmed in 105 (42%) samples using one-Step real-time RT-PCR. In total, 39 dogs were diagnosed with CDV infection based on the detection of cytopathic effects in MDCK, which was verified by the fluorescent antibody technique. A total of 12 one-Step real-time RT-PCR negative samples, consisting of 4 rectal swabs and 8 urine samples, were found to be positive by virus isolation. Blood, nasal swab, ocular swab ($P<0.01$, $r = 1$), rectal swab ($P<0.01$, $r = 0.844$), and urine samples ($P<0.01$, $r = 0.697$) all showed positive correlations in the tests for viral genome detection and virus isolation. CPE levels of high 37 (31.62%), medium 26 (22.23%) and low 54 (46.15%) were detected in a total of 117 (46.8%) samples with viral growth in cell culture. The highest CPE levels detected by FAT were for rectal swab and urine samples. In conclusion, the one-step real-time RT-PCR method on rectal swab samples proved to be a very sensitive method for the rapid and reliable CDV detection. Besides, non-modified MDCK can be used to isolate CDV from naturally infected dogs.

Introduction

The canine distemper virus (CDV) causes an extremely contagious and fatal infection in domestic dogs and some other carnivores (3, 4, 33, 37). CDV belongs to the *Morbillivirus* genus of the *Paramyxoviridae* family of viruses. Morbilliviruses are negative-sense single-stranded RNA viruses with genomes approximately 16 kb in size. Although they are known to infect a large variety of susceptible wild species, the main reservoir for CDV has largely been dogs (21, 39). The virus is a continuous threat to dogs, especially young dogs with inadequate immunity (7, 11, 20, 49). Some studies have shown that unvaccinated and stray carnivorous species can contract a CDV infection and threaten the vaccinated population of dogs (8, 11, 15). The prevalence of CDV is higher in urban and rural areas where there is no practice in place for regular vaccinations and where a higher number of stray dogs exist (13, 18, 42). Regular vaccination has proven to help reduce the incidence of disease in domestic dogs (12, 24, 30).

CDV infections can cause multi-systemic symptoms, involving the respiratory, gastrointestinal, and central nervous systems (6, 32). The most common clinical symptoms are fever, cough, oculo-nasal discharge, diarrhea, lymphopenia, skin hyperplasia, and tremors (27, 43). The disease is primarily transmitted through aerosols or respiratory droplets since the infectious viral particles are abundant in the respiratory tract of infected dogs (1, 21). Since there may also be viral scattering with secretions of clinical and subclinical sick animals, contact transmission becomes another important transmission route.

The high mortality rates of CDV infections make it necessary to speed up the diagnostic procedure so that the infected dogs can be effectively quarantined and treated promptly. Hence there is a need for a sensitive and rapid

method to detect even small amounts of virus present in the early infection stages (17). Serological methods are useful in cases of CDV infection only when the results are evaluated together with clinical symptoms (42). However, it is difficult to follow the clinical symptoms in stray dogs. Moreover, subclinical cases often complicate the situation. A definitive diagnosis of CDV infection by virus isolation is fastidious as well as time-consuming. Therefore, researchers have developed modified cell cultures that are highly sensitive for characteristic CPEs of CDV when applied to clinical samples (44). Unfortunately, it is difficult to access such modified cells for routine diagnostic procedures. This study aimed to explore a rapid diagnostic method involving molecular and cell culture techniques to detect CDV in clinical samples of naturally infected dogs. Such an efficient and cost-effective method can make the control of CDV infection much easier. Our results also showed that CDV field strains could be replicated in non-modified MDCK without adaptation.

Materials and Methods

***Samples*:** The samples for this study were collected from unvaccinated stray dogs under 1 year of age with clinical symptoms compatible with CDV from the Western Mediterranean Region of Türkiye during 2016–17. A total of 250 samples were obtained from 50 dogs and stored at –80°C (Haier, China). These included whole blood (BS), nasal swab (NaS), ocular swab (OcS), rectal swab (ReS), and urine (UrS) samples (50 each). The swab samples were processed by homogenization (10% w/v) in phosphate-buffered saline (PBS) supplemented with 1% antibiotic-antimycotic agents. The homogenates and urine samples were centrifuged at 2000xg for 10 min at 4°C. Then 250 µL of the supernatants were collected for molecular testing. The remaining parts were stored at –80°C for virus isolation. All samples were quickly thawed in a 37°C water bath and passed through Millipore filters (Sartorius, Germany) of 0.22 µm pore size before inoculation. Blood samples were collected into EDTA-treated tubes and centrifuged at 4°C and 1500xg for 10 min until a buffy coat got separated. This buffy coat was diluted with 1 mL PBS after washing. The samples were divided into 4 groups according to the age of dogs as follows: 0–3, 4–6, 7–9, and 10–12 months of age. This study was approved by the Animal Ethics Committee (AEC) Burdur Mehmet Akif Ersoy University, Türkiye (No: 28-174-2016). The following assays were applied for all samples.

Molecular Detection: Viral RNA was extracted from 250 µL of supernatant, using a commercial kit (RiboEx™, GeneAll®, Korea) according to the manufacturer's instructions. One-step real-time RT-PCR assay was performed on a StepOne™ (48-well) instrument (Applied Biosystems™, USA), using TaqMan probes and the one-step real-time RT-PCR kit (GeneAll® 2xHyperScript™, Korea). Primer sets and probes targeting the N protein-encoding gene and cycling conditions used were the same as those previously described by Elia et al. (17), with only slight modifications (Table 1). The reactions were performed according to the manufacturer's instructions. Positive and negative control reactions were included for each reaction. Nuclease-free water and CDV RNA (strain Onderstepoort) were used as the negative and positive control, respectively. The protocol for the RT step involved incubation for 5 min at 58°C and 50°C. The cycling conditions included a pre-denaturation for 30 s at 95 °C, followed by 50 cycles each of 95°C for 5 s, 60°C for 30 s, and 72°C for 1 s. After the final cycle, the tubes were incubated for an additional 30 s at 40°C.

Cell culture and virus isolation: For the virus isolation, 400 µl of supernatants were transferred to 24-well plates with a confluent monolayer of MDCK cells. A well containing only cells but no virus or serum was used as the control for each 24-well plate. The plates were then incubated at 37°C for 1 h. After the adsorption step, 2 mL of Dulbecco's modified Eagle medium (DMEM) and high glucose (4.5 g/L) supplemented with L-Glutamine (Capricorn, Germany) were added along with antibiotics (10%) and antimycotics (7%). The plates were then incubated at 37°C and 5% CO2 for six days. After two serial passages, the plates were examined using a cell culture microscope (Life Technologies™ Floid®Cell Imaging Station, USA) for the presence of cytopathic effects (CPE). All supernatants gathered from the last passage were used for the Fluorescent Antibody Test (FAT).

Table 1. Primer pairs and probe set for the amplification of CDV N gene.

Primer/Prob*	Position	Sequence (5'-3')	Size (bp)
CDV-F	905-931	AGCTAGTTTCATCTTAACTATCAAATT	
CDV-R	966-987	TTAACTCTCCAGAAAACTCATGC	87
CDV-Pb	934-963	FAM-ACCCAAGAGCCGGATACATAGTTTCAATGC-TAMRA**	

*Flourogenic RT-PCR.
**6-carboxyfluorescein (FAM), 6-carboxytetramethylrhodamine (TAMRA).

Fluorescent Antibody Test: 250 µL of each supernatant was transferred to 6-well plates containing coverslip and seeded with MDCK cells. The control used for each 6-well plate was a well with cells only. The plates were incubated at 37°C for 1 h. After the adsorption step, 4 mL DMEM (with high glucose L-Glutamine) was added along with antibiotics (10%) and antimycotics (7%). All plates were incubated at 37°C and 5% CO_2 for five days, after which the plate coverslips were studied for FAT. The coverslips were rinsed in PBS. The staining procedure followed involved commercially available CDV polyclonal antiserum conjugated to fluorescein isothiocyanate (FITC) (catalog no: CJ-F-CDV-10ML; VMRD, USA) for direct FAT. The results were evaluated in a Floid®Cell Imaging system. The CDV-FAT substrate slide (containing two wells: one positive and one negative, catalog no: SLD-FAC-CDV; VMRD, USA) was used as a reference. The coverslips were examined for the presence of CDV antigen-positivity using a cell culture microscope Floid®Cell Imaging system. The positivity was calculated based on a previously described method, as the number of CDV antigen-positive cells divided by the total cells (25). CPEs were identified for each sample, at different levels (high, medium, and low) using FAT.

Statistical analysis: Data were analyzed using the IBM SPSS® Statistics 23.0 software. The statistical evaluation was performed using the Chi-squared and Spearman's correlation tests.

Results

One-Step real-time RT-PCR: 31 out of all the 50 dogs tested positive for CDV infection. The 87-bp fragment was amplified from extracts, and it was used to identify the virus by targeting the N protein. Specific signal amplification was obtained for the positive samples with cycle threshold (Ct) values ranging from 18 to 36. In total, 105 (42%) samples were positive for the presence of the CDV genome. BS, NaS, OcS, ReS, and UrS were positive in 20 (40%), 23 (46%), 22 (44%), 27 (54%) and 13 (26%) samples, respectively (Table 2).

Cell culture and virus isolation: In total, 39 out of 50 dogs were found to be positive by virus isolation. In MDCK cells, the presence of CPE was detected in a total of 117 (46.8%) samples, their distribution based on sample type being the following: 20 (40%) BS, 23 (46%) NaS, 22 (44%) OcS, 31 (62%) ReS, and 21 (42%) UrS (Figure 1 and Table 2). A total of 12 one-Step real-time RT-PCR negative samples were positive by virus isolation, of which 4 were ReS, and 8 were UrS.

Fluorescent Antibody Test: A strong bright green fluorescence was detected in the cytoplasm of the infected cells, whereas no green fluorescence was observed in the control coverslips. Characteristic inclusion bodies of CDV were also counted as antigen positivity. However, non-specific yellow stainings were not included in the interpretation. The interpretation of results was based on the intensity of fluorescence/staining reaction and accordingly categorized as high (>60%), middle (30–60%), and low (<30%) levels of CPE (Figure 2). CPE levels for the different sample types are shown in Table 3.

Statistical analysis: In viral genome detection, the relationship between real-time RT-PCR and virus isolation, demonstrated positive correlations for BS, NaS, and OcS ($P<0.01$, $r = 1$), ReS ($P<0.01$, $r = 0.844$), and UrS ($P<0.01$, $r = 0.697$). The highest positivity rate was detected in the age group of 0–3 months (68.1%) for viral genome detection and in the age group of 4–6 months (90.9%) for virus isolation. The distribution of CDV isolation and genome positivity rates in different age groups are shown in Table 4.

Table 2. Comparison of the results of real-time RT-PCR and virus isolation.

Real-time RT-PCR	CPE in MDCK	Sample numbers*				
		BS	NaS	OcS	ReS	UrS
+	+	20 (40%)	23 (46%)	22 (44%)	27 (54%)	13 (26%)
-	+	0	0	0	4 (8%)	8 (16%)
+	-	0	0	0	0	0
-	-	30 (60%)	27 (54%)	28 (56%)	19 (38%)	29 (58%)

*BS: Blood, NaS: Nasal swab, OcS: Ocular swab, ReS: Rectal swab, UrS: Urine.

Table 3. Cytopathic effect (CPE) results according to the samples.

Samples*	Levels of CPE			
	High	Middle	Low	Total
BS	1	2	17	20 (17.1%)
NaS	1	10	12	23 (19.6%)
OcS	3	5	14	22 (18.8%)
ReS	21	6	4	31 (26.5%)
UrS	11	3	7	21 (17.9%)
Total	37 (31.62%)	26 (22.23%)	54 (46.15%)	117 (%100)

*BS: Blood, NaS: Nasal swab, OcS: Ocular swab, ReS: Rectal swab, UrS: Urine.

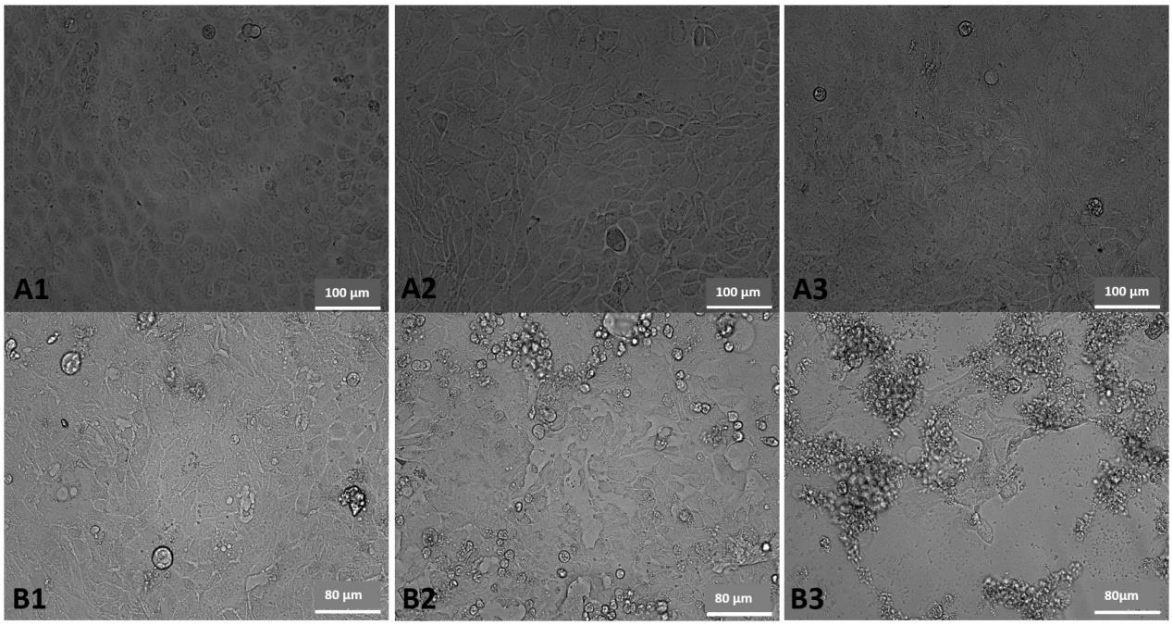

Figure 1. Cytopathic effect (CPE) of CDV in MDCK cells infected with rectal swab samples belongings to dog no 24.
A1-3: Untreated control cells. A1: 48h, A2: 96h, A3: 144h later. B1-B3: Sample inoculated cells. B1: 48h, B2: 96h, B3: 144h later. Pictures were taken with a Sony 1.3MP 1/3" ICX445 EXview HAD CCD camera, 20x objective with 460x optical magnification under an inverted microscope (Life Technologies™ Floid® Cell Imaging Station, USA).

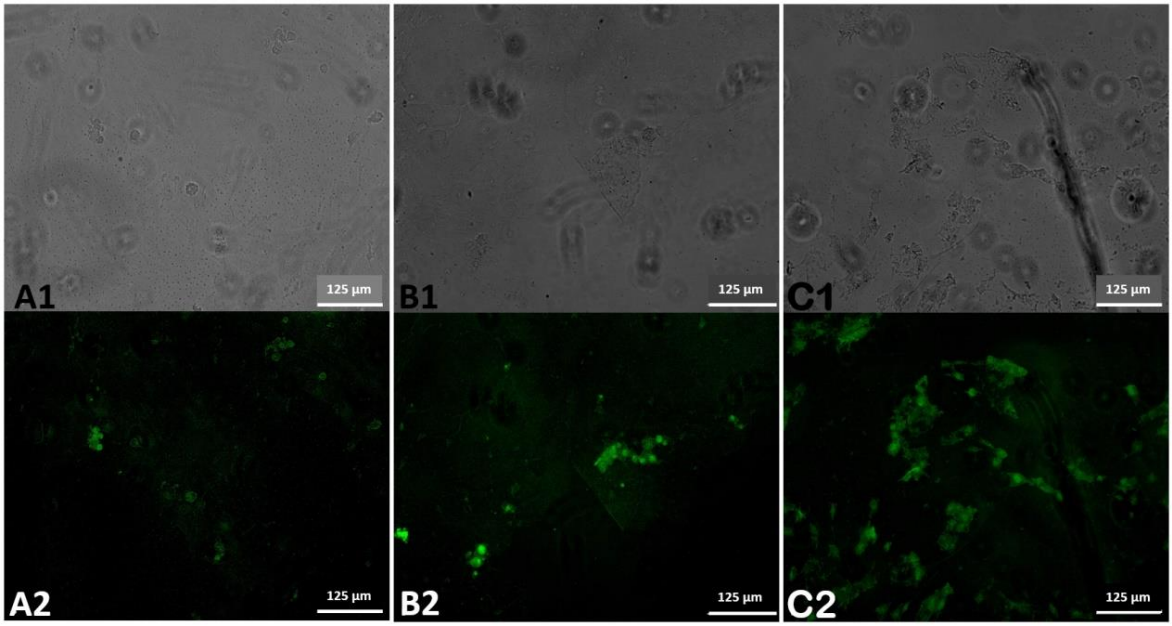

Figure 2. CPE of MDCK cells before FAT.
(A1: dog no 40, urine-low; B1: dog no 37, ocular swab-medium; C1: dog no 10, rectal swab-high). FAT was done on CDV-infected MDCK cells at 6 days post-inoculation (A2, B2, C2).
(A typical apple-green fluorescence indicating positive CDV antigens in infected cells).

Table 4. Distribution of viral genome and virus isolation results by age groups. Real-time RT-PCR and virus isolation-FAT results according to age.

Age group Months	Real-time RT-PCR		CPE		Total
	(+)	(-)	(+)	(-)	
0-3	15 (68.1%)	7	17 (77.2%)	5	22
4-6	6 (54.5%)	5	10 (90.9%)	1	11
7-9	6 (66.6%)	3	6 (66.6%)	3	9
10-12	4 (50%)	4	6 (75%)	2	8
Total	31 (62%)	19	39 (78%)	11	50

Discussion and Conclusion

CDV infection causes high morbidity and mortality in domestic and wild canids across the world (35). The progress of the disease can differ from strain to strain and also depends on the amount of virus as well as the age, immunity level, and environmental factors of the sensitive host (32). The disease is easily transmitted to young and unvaccinated dogs, which come into direct or indirect contact with infected dogs (2). Dogs that have not received the necessary antibodies through either colostrum or vaccination during the first 12 months of their life are more susceptible to infection (16, 21, 23). Several molecular assays are widely used to detect CDV infections. It has been reported that CDV infection has a higher chance of detection using the RT-PCR method as compared to immunohistochemistry methods, especially in cases of subacute and chronically infected dogs (26, 41). Some studies conducted using the conventional PCR techniques in Türkiye have reported the presence of CDV genomes in various samples collected from dogs (36, 40). In cases where intercalating dyes were used to measure real-time PCR products, there is the disadvantage of detecting the sum of all specific and non-specific PCR products (5). Recently, the real-time RT-PCR technique based on the TaqMan Probe system has enabled rapid, accurate, and highly specific diagnosis of CDV (16). The TaqMan Probe is used to avoid the disadvantages met while using other probes in detecting both specific and non-specific PCR amplification. The real-time RT-PCR method is preferred due to its higher sensitivity and specificity as compared to other diagnostic methods (14, 17). Diagnosis of CDV is especially challenging due to the diverse and non-specific clinical manifestations and due to the high seroprevalence rate in sub-clinical dogs. Veterinarians are routinely confronted with cases where the clinical picture is compatible with the disease, but the diagnostic tests yield contradictory results. This study is unique in being the first in the detection of the CDV genome in Türkiye using the one-Step TaqMan real-time RT-PCR assay.

The advantages of the one-Step TaqMan real-time RT-PCR method have been reported in several previous studies as well (5, 14, 16, 17, 45). The highly conserved nucleocapsid gene region of CDV was targeted in this study (17). This study aimed to obtain more specific and reliable positive results using fluorogenic probes that identify only specific PCR products. Based on our results (Table 2), we can confidently state that fluorogenic probes are highly useful reagents for the detection of CDV in naturally infected dogs. The detection was performed in a sensitive, specific, rapid, and reliable manner using the specific primer/probes designed for the reaction. Real-time RT-PCR yielded a high rate of positivity for CDV infection in the 0–3 months of age category, as indicated in Table 4.

As a result, we have successfully shown that a rapid and reliable diagnosis can be made for CDV infection in very young dogs using the real-time system with the TaqMan probe. Disadvantages of PCR methods in viral genome detection have already been widely reported (19, 34, 38). Some of these disadvantages are that the viral load may be too low in samples taken from naturally infected animals and that even smaller volumes of these samples are used in the PCR test. Moreover, the fragile nature of the RNA genome and the contamination with RNases from the environment may adversely affect the results of a PCR test. As a result, the potential negative effects of PCR inhibitors hamper viral genome detection. These disadvantages may lead to false-negative results. In our study, virus isolation and FAT techniques were used to eliminate these disadvantages particularly. Moreover, it is always important to confirm test results with other reliable methods to eliminate the false-negative results.

CDV polyclonal antiserum is known to be highly suitable for specific detection of CDV infection in cell cultures, as it does not stain for other non-specific viral agents. It is thus a specific tool used for the diagnosis of acute and primary infections in dogs and will continue to be the most popular critical reagent used in routine diagnosis via FAT. The only limitation of FAT is that it requires fluorescent imaging microscopy and the presence of skilled lab staff. Despite limitations, the FAT is one of the best methods of diagnosis as it is rapid, flexible, and accurate (31).

Viral growth has been reported to successfully occur in MDCK cells and Vero but not in MV1 cells. Based on this study, wild-type CDV isolation in MDCK cells proved to be the most effective, though CPEs are the most evident in Vero (28). In our study, the characteristic CPEs observed in the MDCK cells were also identified by the CDV-specific antiserum. Similar findings have also been reported in other studies that were based on the isolation of the CDV in non-modified MDCK cells without adaptation (46, 47). It was reported that the Vero-expressing signaling lymphocyte activation molecule (SLAM) was highly useful for the isolation of CDV from clinical samples. The major advantage of this cell type for CDV isolation is that CDV propagation can be detected as early as 1-day post-infection (44). In our study, the notable CPEs could be observed in MDCK cells 6-days post-inoculation.

Our findings show that some CDV strains can infect MDCK cells without the need for adaptation. The viral load in samples from naturally infected animals could be quite low and, the isolation of CDV in cell cultures tends to be prolonged, requiring blind-passages before the occurrence of CPEs (28). Blind passages play a crucial

role in virus isolation in natural infections. Therefore, at least two blind passages were made in the cell cultures of high-volume cultivated samples.

In our study, ReS, and UrS were the most prominent samples with a high level of CPE identification (Table 3). The lowest level of CPEs was in the BS. A study by Pawar et al. (37) supports these findings of our study. CDV can be detected at high titers from several body fluids, including urine (17, 41). High levels of CPE were detected in ReS and UrS, which may be due to the high reproducibility of viral load in these samples (17). Here we report the first isolation of CDV in MDCK cell culture from naturally infected dogs in Türkiye and the successful isolation from urine samples. Likely, our careful sampling at the right time in the post-infection period increased the efficiency of CDV isolation. According to the findings of this study, notable CPEs were observed in infected MDCK cells, and the optimal harvest time was 6 days after inoculation, with UrS reaching the highest CPE level. Although there are previous studies related to CDV isolation from different sample types, they provide limited information about isolation from urine samples in particular (44, 47). In the CDV infection, the sample type used for molecular diagnosis and virus isolation may depend on the clinical symptoms (36). Based on our data, we recommend the use of ReS for CDV diagnosis and isolation. The data we obtained are coherent with several previous studies (17, 22, 40).

The highest amount of positivity was found to be in the 0–3 months age group for viral genome determination and in the 4–6-months age group for virus isolation (Table 4). According to these results, it was concluded that dogs under 6 months of age were at higher risk of CDV infection. The results of Gray et al. (20) support our findings. In stray dogs using the same habitats as infected animals, such high rates of CDV infection would likely be caused by continuous exposure to secretions/excretions of infected animals. Moreover, these dogs are periodically collected and kept in shelters for ear tagging, spaying, vaccination, etc. The potential for exposure and CDV transmission to susceptible dogs only increases during this period. Additionally, the fact that CDV persists in infected animals (21) and that they can spread the virus again after immunosuppression is a permanent threat to susceptible animal species. However, CDV prevalence was reported to be lower in places where vaccination programs are applied regularly (10, 30, 48). Mostly, domestic dogs that are taken out twice a day should be prevented from interacting with stray dogs. However, it may be difficult to prevent the dogs from exposure to infected materials in the area that is contaminated with secretion and excretion of infected dogs. Such material threatens the vaccinated dogs as well (9). Since there is no vaccination program intended for stray dogs, all carnivores are at risk of contracting the disease (29).

It is important to have a vaccination program for stray dogs to decrease the constant presence of the virus in the environment in general. It has been shown in our study that field strains can be isolated by methods that are not difficult to apply in practice. In this way, using field strains in the vaccines will result in a more effective campaign against CDV. Stray dogs that roam for food, water, shelter, mating, etc., are the key reservoirs that allow the virus to circulate and persist in rural and urban areas. Moreover, it is necessary to follow wildlife animal movements as well. Since there is no control program in place for CDV in the wildlife, it increases the risk of transmission between wild and domestic carnivores. The one-step real-time RT-PCR and virus isolation methods used in this study are the preferred methods for the detection of CDV in clinical samples. These methods are sensitive, provide highly specific results, and are useful for rapid detection in naturally infected dogs. Besides, according to the findings of this study, non-modified MDCK cells should be preferred for the isolation of CDV from naturally infected dogs. CDV is likely to remain an important threat to dogs, particularly those that are 0–6 months of age, if there is no program in place to control the increasing population of stray dogs in urban areas (42).

We concluded that ocular swabs and blood samples are the preferred alternative samples, although rectal and nasal swabs were found to be the best clinical samples for the detection of CDV. Based on our findings in the urine samples, we can also suggest that there is a need for more detailed studies on urinary system symptoms in infected dogs.

Acknowledgement

This article was summarized from the PhD thesis by Hasbi Sait SALTIK (Burdur Mehmet Akif Ersoy University, Institute of Health Sciences).

Financial Support

Financial support of this study by the University of Burdur Mehmet Akif Ersoy BAP grant number 0403-DR-16 is highly appreciated.

Conflict of Interest

The authors declared that there is no conflict of interest.

Author Contributions

HSS conceived and planned the experiments. HSS carried out the experiments. HSS planned and carried out the simulations. HSS contributed to sample preparation. HSS and MK contributed to the interpretation of the results. HSS took the lead in writing the manuscript. All authors

provided critical feedback and helped shape the research, analysis and manuscript.

Data Availability Statement

The data supporting this study's findings are available from the corresponding author upon reasonable request.

Ethical Statement

This experiment was approved and performed under the guidelines of the Animal Ethics Committee (AEC) Burdur Mehmet Akif Ersoy University, Türkiye (No:28-174-2016).

Animal Welfare

The authors confirm that they have adhered to ARRIVE Guidelines to protect animals used for scientific purposes.

References

1. **Anderson DE, Wang LF** (2011): New and emerging paramyxoviruses. 435-459. In: SK Samal (Ed), The Biology of Paramyxoviruses. Caister Academic Press, Maryland, USA
2. **Appel MJ, Gillespie JH** (1972): Canine distemper virus. 1-96. In: SGC Hallauer and K Meyer (Ed), Virology Monographs. Springer, Vienna.
3. **Appel MJG, Summers B** (1999): Canine distemper: current status. 68-72. In: L Carmichael (Ed), Recent Advances in Canine Infectious Diseases. International Veterinary Information Service (IVIS).
4. **Appel MJG, Summers BA** (1995): *Pathogenicity of morbilliviruses for terrestrial carnivores.* Vet Microbiol, **44**, 187-191.
5. **Arya M, Shergill IS, Williamson M, et al** (2005): *Basic principles of real-time quantitative PCR. Expert* Rev Mol Diagn, **5**, 209-219.
6. **Beineke A, Puff C, Seehusen F, et al** (2009): *Pathogenesis and immunopathology of systemic and nervous canine distemper*. Vet Immunol Immunopathol, **127**, 1-18.
7. **Blancou J** (2004): *Dog distemper: imported into Europe from South America.* Hist Med Vet, **29**, 35-41.
8. **Blixenkrone-Moeller M, Svansson V, Have P, et al** (1993): *Studies on manifestations of canine distemper virus infection in an urban dog population.* Vet Microbiol, **37**, 163-173.
9. **Calderon MG, Remorini P, Periolo O, et al** (2007): *Detection by RT-PCR and genetic characterization of canine distemper virus from vaccinated and non-vaccinated dogs in Argentina.* Vet Microbiol, **125**, 341-349.
10. **Chappuis G** (1995): *Control of canine distemper*. Vet Microbiol, **44**, 351-358.
11. **Demeter Z, Palade EA, Rusvai M** (2009): *Canine distemper: Still a major concern in Central Europe.* Lucr Stiint Univ Stiint Agric Banat Timis Med Vet, **42**, 136-150.
12. **Di Sabatino D, Savini G, Lorusso A** (2015): *Canine distemper and endangered wildlife: Is it time for mandatory vaccination of dogs.* Vaccine, **33**, 6519.
13. **Diaz NM, Mendez GS, Grijalva CJ, et al** (2016): *Dog overpopulation and burden of exposure to canine distemper virus and other pathogens on Santa Cruz Island, Galapagos*. Prev Vet Med, **123**, 128-137.
14. **Dorak MT** (2007): Real-time PCR. Taylor & Francis. New York.
15. **Ek-Kommonen C, Sihvonen L, Pekkanen K, et al** (1997): *Outbreak of canine distemper in vaccinated dogs in Finland.* Vet Rec, **141**, 380-383.
16. **Elia G, Camero M, Losurdo M, et al** (2015): *Virological and serological findings in dogs with naturally occurring distemper*. J Virol Methods, **213**, 127-130.
17. **Elia G, Decaro N, Martella V, et al** (2006): *Detection of canine distemper virus in dogs by real-time RT-PCR.* J Virol Methods, **136**, 171-176.
18. **Esin E** (2013): Köpeklerde Canine Distemper Virus enfeksiyonunun araştırılması. Doktora Tezi. Selçuk Üniversitesi Sağlık Bilimleri Enstitüsü, Konya.
19. **Fong TT, Lipp EK** (2005): *Enteric viruses of humans and animals in aquatic environments: health risks, detection, and potential water quality assessment tools.* Microbiol Mol Biol Rev, **69**, 357-371.
20. **Gray LK, Crawford PC, Levy JK, et al** (2012): *Comparison of two assays for detection of antibodies against canine parvovirus and canine distemper virus in dogs admitted to a Florida animal shelter.* J Am Vet Med Assoc, **240**, 1084-1087.
21. **Greene CE** (2013): Infectious diseases of the dog and cat. Elsevier Health Sciences, London.
22. **Gustavsson L, Westin J, Andersson LM, et al** (2011): *Rectal swabs can be used for diagnosis of viral gastroenteritis with a multiple real-time PCR assay.* J Clin Virol, **51**, 279-282.
23. **Headley SA, Sukura A** (2009): *Naturally occurring systemic canine distemper virus infection in a pup*. Braz J Vet Pathol, **2**, 95-101.
24. **Jóźwik A, Frymus T** (2002)*: Natural distemper in vaccinated and unvaccinated dogs in Warsaw.* J Vet Med, **49**, 413-414.
25. **Kapil S, Neel T** (2015): *Canine distemper virus antigen detection in external epithelia of recently vaccinated, sick dogs by fluorescence microscopy is a valuable prognostic indicator.* J Clin Microbiol, **53**, 687-691.
26. **Keawcharoen J, Theamboonlers A, Jantaradsamee P, et al** (2005): *Nucleotide sequence analysis of nucleocapsid protein gene of canine distemper virus isolates in Thailand.* Vet Microbiol, **105**, 137-142.
27. **Lan N, Yamaguchi R, Inomata A, et al** (2006): *Comparative analyses of canine distemper viral isolates from clinical cases of canine distemper in vaccinated dogs.* Vet Microbiol, **115**, 32-42.
28. **Lednicky JA, Meehan TP, Kinsel MJ, et al (2004):** *Effective primary isolation of wild-type Canine distemper virus in MDCK, MV1 Lu and Vero cells without nucleotide sequence changes within the entire haemagglutinin protein gene and in subgenomic sections of the fusion and phospho protein genes.* J Virol Methods, **118**, 147–157.
29. **Lorusso A, Savini G** (2014): *Old diseases for new nightmares: distemper strikes back in Italy.* Vet Ital, **50**, 151-154.

30. **MacLachlan NJ, Dubovi EJ** (2016): Paramyxoviridae and pneumoviridae. In: MacLachlan NJ, Dubovi EJ, editors. Fenner's veterinary virology. 5th ed. London, UK: Academic press, 327-56.
31. **Madeley CR, Peiris JSM** (2002): *Methods in virus diagnosis: immunofluorescence revisited.* J Clin Virol, **25**, 121–134.
32. **Martella V, Cirone, F, Elia G, et al** (2006): *Heterogeneity within the hemagglutinin genes of canine distemper virus (CDV) strains detected in Italy.* Vet Microbiol, **116**, 301-309.
33. **Martinez-Gutierrez M, Ruiz-Saenz J** (2016): *Diversity of susceptible hosts in canine distemper virus infection: a systematic review and data synthesis*. BMC Vet Res, **12**, 78.
34. **Nuanualsuwan S, Cliver DO** (2002): *Pretreatment to avoid positive RT-PCR results with inactivated viruses.* J Virol Methods, **104**, 217-225.
35. **Origgi F, Plattet P, Sattler U, et al** (2012): *Emergence of canine distemper virus strains with modified molecular signature and enhanced neuronal tropism leading to high mortality in wild carnivores.* Vet Pathol, **49**, 913-929.
36. **Özkul A, Sancak AA, Güngör E, et al** (2004): *Determination and phylogenetic analysis of canine distemper virus in dogs with nervous symptoms in Turkey.* Acta Vet Hung, **52**, 125-132.
37. **Pawar RM, Raj GD, Gopinath VP, et al** (2011): *Isolation and molecular characterization of canine distemper virus from India.* Trop Anim Health Prod, **43**, 1617-1622.
38. **Richards GP** (1999): *Limitations of molecular biological techniques for assessing the virological safety of foods.* J Food Prot, **62**, 691-697.
39. **Roelke-Parker ME, Munson L, Packer C, et al** (1996): *A canine distemper virus epidemic in Serengeti lions (Panthera leo).* Nature, **37,** 441–445.
40. **Sahna K, Gencay A, Atalay O** (2008): *Viral aetiology of diarrhoea in puppies from a same shelter in Turkey: presence of mixed infections.* Rev Med Vet, **159**, 345-346.
41. **Saito T, Alfieri A, Wosiacki S, et al** (2006): *Detection of canine distemper virus by reverse transcriptase-polymerase chain reaction in the urine of dogs with clinical signs of distemper encephalitis*. Res Vet Sci, **80**, 116-119.
42. **Saltık HS, Kale M** (2020): *Evaluation of infection with N protein-specific Immunoglobulin M and G in naturally occurring distemper in dogs.* Vet Med-Czech, **65**, 168–173.
43. **Schobesberger M, Summerfield A, Doherr MG, et al** (2005): *Canine distemper virus-induced depletion of uninfected lymphocytes is associated with apoptosis.* Vet Immunol Immunopathol, **104**, 33-44.
44. **Seki F, Ono N, Yamaguchi R** (2003): *Efficient isolation of wild strains of canine distemper virus in Vero cells expressing canine SLAM (CD150) and their adaptability to marmoset B95a cells.* J Virol, **77**, 9943-9950.
45. **Shin YJ, Cho KO, Cho HS, et al** (2004): *Comparison of one-step RT-PCR and a nested PCR for the detection of canine distemper virus in clinical samples.* Aust Vet J, **82**, 83-86.
46. **Swati, Deka D, Uppal SK, et al** (2015): *Isolation and phylogenetic characterization of Canine distemper virus from India*. VirusDisease, **26**, 133-140.
47. **Tan B, Wen YJ, Wang FX, et al** (2011): *Pathogenesis and phylogenetic analyses of canine distemper virus strain ZJ7 isolate from domestic dogs in China.* Virol J, **8**, 1.
48. **Temilade BE, Solomon OOO, Omotayo OE, et al** (2015): *Seropositivity of Canine Distemper Virus (CDV) in Dogs Presenting at Abeokuta, Nigeria*. Public Health Research, **5**, 109-119.
49. **Wyllie SE, Kelman M, Ward MP** (2016): *Epidemiology and clinical presentation of canine distemper disease in dogs and ferrets in Australia, 2006–2014.* Aust Vet J, **94**, 215-222.

A morphological and stereological investigation on the tongue of the merlin

Mehmet Aydın AKALAN[1,a,✉], Aysun ÇEVİK DEMİRKAN[1,b], İsmail TÜRKMENOĞLU[1,c], İbrahim DEMİRKAN[2,d] Vural ÖZDEMİR[1,e], Murat Sırrı AKOSMAN[1,f]

[1]Afyon Kocatepe University, Faculty of Veterinary Medicine, Department of Anatomy, Afyonkarahisar, Türkiye; [2]Afyon Kocatepe University, Faculty of Veterinary Medicine, Department of Surgery, Afyonkarahisar, Türkiye

[a]ORCID: 0000-0001-9924-2920, [b]ORCID: 0000-0002-5824-5831; [c]ORCID: 0000-0001-6591-7774; [d]ORCID: 0000-0002-0908-8331
[e]ORCID: 0000-0001-6591-7774, [f]ORCID: 0000-0001-6675-8840

ARTICLE INFO

Article History
Received : 18.02.2021
Accepted : 15.11.2021
DOI: 10.33988/auvfd.882553

Keywords
Falco columbarius
Merlin
Morphology
Stereology
Tongue

✉Corresponding author
makalan@aku.edu.tr

How to cite this article: Akalan MA, Çevik Demirkan A, Türkmenoğlu İ, Demirkan İ, Özdemir V, Akosman MS (2023): A morphological and stereological investigation on the tongue of the merlin. Ankara Univ Vet Fak Derg, 70 (1), 57-64. DOI: 10.33988/auvfd.882553.

ABSTRACT

The study aimed to reveal the similarities and differences of the tongue of the merlin with other bird species. Merlin is the smallest bird of the *Falconidae* family and lives in America, the northern regions of Europe and Asia, the Middle East, and Central Asia. Since these species don't have teeth, lips, and cheeks, the tongue fulfills significant functions related to nutrition, and it differs morphologically as a result of differences in eating habits. In this study, the tongues obtained from five adult merlin (*falco columbarius*) were examined by morphological and stereological methods. It was determined that the tongue of the merlin was thin, long, and rectangular, the front part was oval, W-shaped *papilla linguales caudales* were found between the body and root of the tongue. The average length of the tongue was 26.32 ± 1.38 mm, the width was 7.26 ± 0.32 mm, and the thickness was 1.58 ± 0.14 mm. The histology of the tongue showed that the dorsal and ventral surfaces are covered with keratinized multilayered squamous epithelium; there are taste buds in the epithelial layer, the number of taste buds is higher especially on the root of the tongue; and the presence of *paraglossum*, which is in the hyaline cartilage structure. The volume of the tongue was on an average of 374.2 ± 14.08 mm^3.

Introduction

Merlin is the smallest bird of the family *Falconidae*. This raptor has 24-33 cm length and 53-69 cm wingspan. Facial features are weaker than hawks. They live in the northern regions of America, Europe, Asia, the Middle East, and Central Asia (19).

The tongue is located at the base of the mandible, containing various tissues such as cartilage and bone, glands, muscles, nerves, blood vessels, and connective tissue (3). The structure and function of the tongue are closely associated with the diet and adaptation of animals to nature (6). Teeth, lips, and cheeks are missing in avian species, so the tongue accomplishes significant functions such as capturing, separating, processing, and swallowing food (16). As a result of all these functions and different feeding habits in different birds, the tongue varies considerably in poultry morphologically (3, 27).

The tongue of the bird consists of three parts: the *apex lingua* (tip), the *corpus lingua* (body), and the *radix lingua* (root) (31). It has both mechanical and taste buds. The number and localization of these taste buds depend on the bird's diet or whether it is a flightless or water bird. These taste buds localization and number vary depending on the bird's diet and changes between water birds and flightless birds (33, 35). Morphology of tongues especially in bird species has been studied but most of these investigations are interested in the tongue of herbivores and omnivorous birds (26, 27). It appears that studies on the tongue of carnivorous birds are scarce (13, 25).

It was aimed to examine the morphological, histological, and stereological examination of the merlin tongue and reveal the similarities or differences with other bird species in this study.

Materials and Methods

Five adult Merlins (*Falco columbarius*) obtained from the Afyon Kocatepe University Veterinary Faculty Animal Hospital were used. This study was approved by the local ethical committee (Afyon Kocatepe University Animal Experiment Local Ethical Committee No: 49533702/41). Due to untreatable diseases apart from digestive tract diseases birds were euthanized by the department of surgery with a combination of ketamine (60 mg/kg) and xylazine (6 mg/kg). The cadavers were fixed in 10% formaldehyde solution.

For gross anatomical examination, five birds were decapitated and washed in running tap water. The tongues were examined in the oral cavity, and then they were cut and examined separately. Measurements were made with a digital caliper (Mitutoyo, Japan). Nomina Anatomica Avium was used for anatomic denomination (7).

The volume of the tongue was estimated by using The Cavalieri principle. Since the cadavers had already been fixed, the shrinkage ratio could not be calculated in the volume calculation. The slice thickness of the tongues was 2 mm, and a point-counting grid with 1 mm dot spacing was randomly left on the same face of each slice (Figure 1). The tongue volume was calculated by the following formula;

$$V = (t.\ a(p).\ \Sigma P)\ mm^3$$

V= volume; t: section thickness (2 mm); a(p): area associated with one test point (1 mm x 1 mm); and ΣP: Total number of points hitting the tongue section (20).

Slices corresponding to the *apex* (tip), *corpus* (body), and *radix* (root) parts of the tongue were subjected to histological tissue follow-up and embedded in paraffin blocks. The 5 µm thick histological sections were stained by the Hematoxylin-Eosin method. Histological examinations were carried out by a microscope camera (M-Shot brand, MDX4 model, Guangzhou, China) and M-Shot Digital Imaging System 9.3.3.1 software integrated into a light microscope (Olympus brand, MD2 model, Shinjuku-ku, Tokyo) with a motorized table (Lang brand, MS 316 model, Hüttenberg, Germany).

Results

It was found that the tongue was thin, long, and rectangular with an oval front (Figure 2). The tongue did not fill the floor of the oral cavity, there were gaps in the front and sides, and it was attached to the floor of the oral cavity via the *frenulum linguae* almost in the middle of the tongue.

Between the body (*corpus linguae*) (Figure 3a) and the root (Figure 3b) of the tongue, the *alae lingua* (Figure 3 black arrows) was observed being shaped by the *papilla linguales caudales* (Figure 3c) in a W-shaped direction towards the tongue body. Moreover, these *papillae linguae caudales* showed dark brownish-black pigmentation. The number of *papillae linguae caudales* was determined to be 14. These *papillae* were cone-shaped.

There were many salivary glands with draining ducts on the body and root of the tongue (Figure 2*). Larynx cranialis and glottis (Figure 2b, Figure 4*) were observed just behind the radix linguae. There were *papillae* (Figure 4 white arrows) located behind the *glottis* forming the *papillae pharyngis caudoventrales* and the number in each half was 17-18. Most of these *papillae* (except the medial one) possessed pigmentation close to black. Morphometric measurements of the tongues were shown in Table 1.

Figure 1. A point-counting grid with point spacing 1 mm used for the measurement of 2 mm tongue sections.

DOI: 10.33988/auvfd.882553

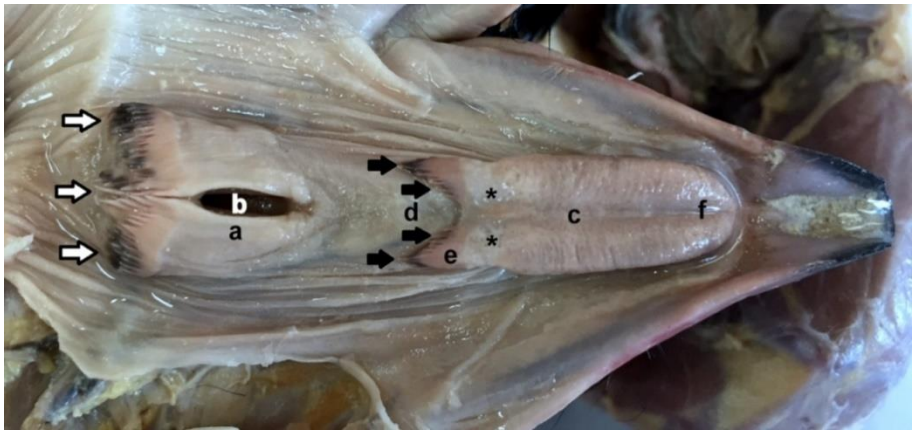

Figure 2. The merlin tongue view from inside the roof of the oral cavity (a: larynx cranialis, b: glottis, c: corpus lingua, d: radix lingua, e: alae lingua, f: apex lingua, *: orifices of gll. linguales, black arrows: papilla linguales caudales, white arrows: papilla pharyngis caudoventrales).

Figure 3. Dorsal view of alae linguae located between corpus and radix linguae (a: corpus lingua, b: radix lingua, c: alae lingua, black arrows: papilla linguales caudales).

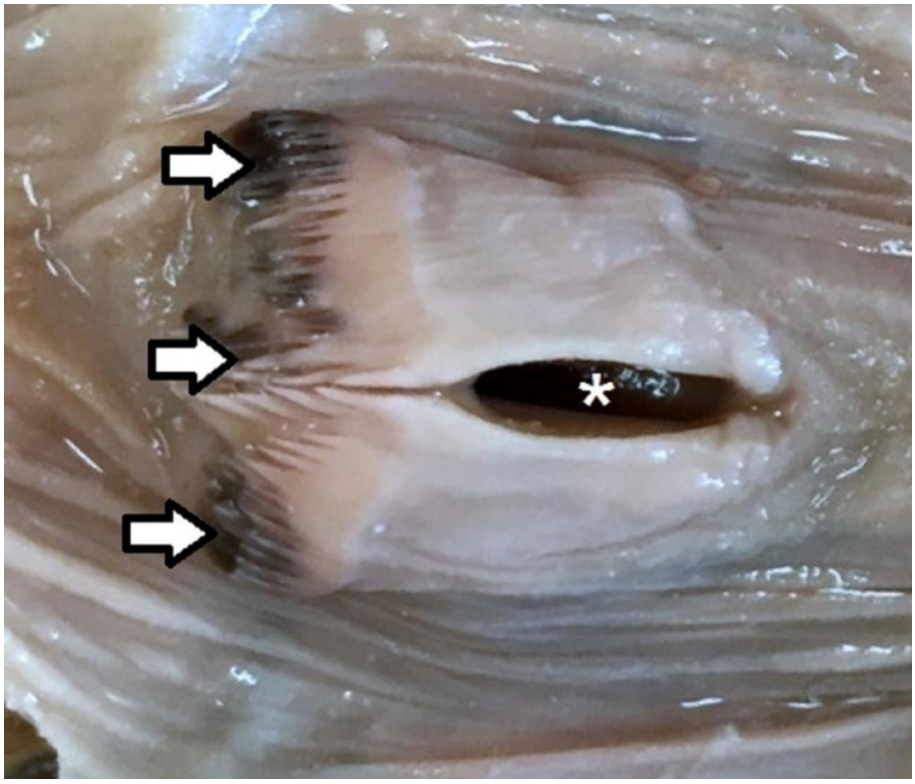

Figure 4. Dorsal view of papilla pharyngis caudoventrales (white arrows: papilla pharyngis caudoventrales, *: glottis).

Table 1. Morphometric measurement values of animals.

Measurements (mm)	Min	Max	A.M.	S.E.	S.D.
Frenilum linguae length	13.9	15.7	14.77	0.3077	0.6881
Larynx cranialis length	11.4	12.6	12.02	0.1885	0.4214
Glottis length	6.8	7.23	7.06	0.0628	0.1405
Sulcus medianus linguae length	12.3	15.2	13.46	0.5162	1.1542
Tongue length	24.5	28.2	26.32	0.6167	1.3789
Tongue Width	6.9	7.6	7.26	0.1423	0.3183
Tongue Thickness	1.42	1.78	1.58	0.0604	0.1351

A.M.: Arithmetic Mean.
S.E.: Standart Error.
S.D.: Standart Deviation.

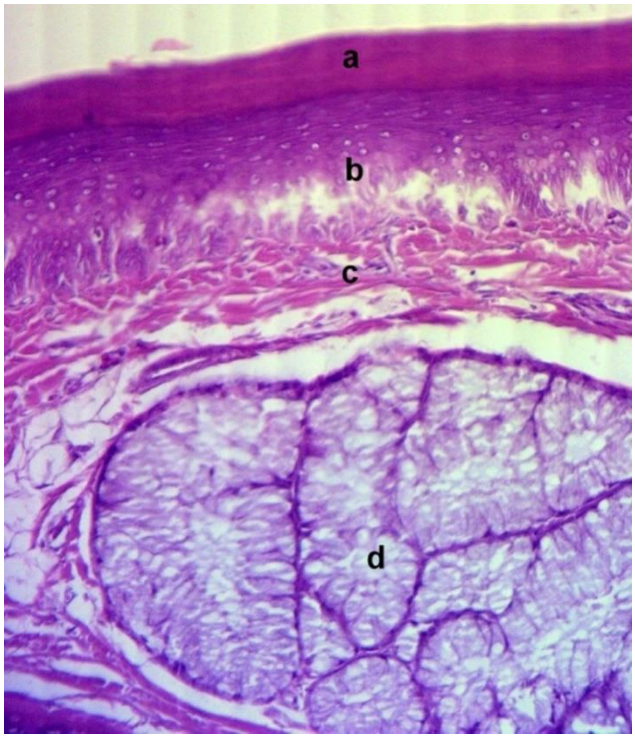

Figure 5. Dorsal surface of the merlin tongue (Hematoxylin-Eosin, 10X. a: keratinized layer, b: epithelial layer, c: connective tissue, d: gland).

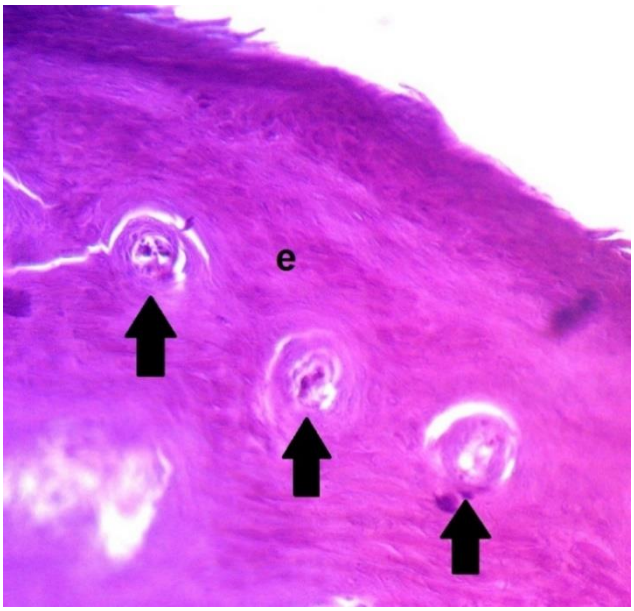

Figure 6. Taste buds (black arrows) within the epithelial layer (e) of the merlin tongue (Hematoxylin-Eosin, 100X).

Microscopic examinations revealed that the dorsal and ventral surfaces of the merlin tongue were covered with keratinized multilayered squamous epithelium (Figure 5a) and there were numerous taste buds in the epithelial layer. (Figure 6 black arrows) The number of taste buds was higher, especially on the root of the tongue. There was a richly vascularized connective tissue (Figure 7b) just below the multilayered squamous epithelial layer (Figure 7a). The *lamina propria* layer from the loose connective tissue (Figure 7b) made protrusions called *dermal papillae* (Figure 7 black arrows) towards the epithelial layer. There were many glands (Figure 5d) embedded in the submucosa layer and surrounded by connective tissue. These glands were found in the body (anterior salivary glands) and root of the tongue (posterior salivary glands). Skeletal muscle fibers seen in tongue tissue sections were seen in the transversal section. In other words, the orientation of the skeletal muscles were parallel to the long axis of the tongue. In addition to skeletal muscle and numerous vessels in the tongue tissue, the extension of the *paraglossum* (Figure 8c), in the hyaline cartilage structure was noted.

The average volume of the merlin tongue was calculated as 374.2 ± 14.08 mm^3 (Table 2).

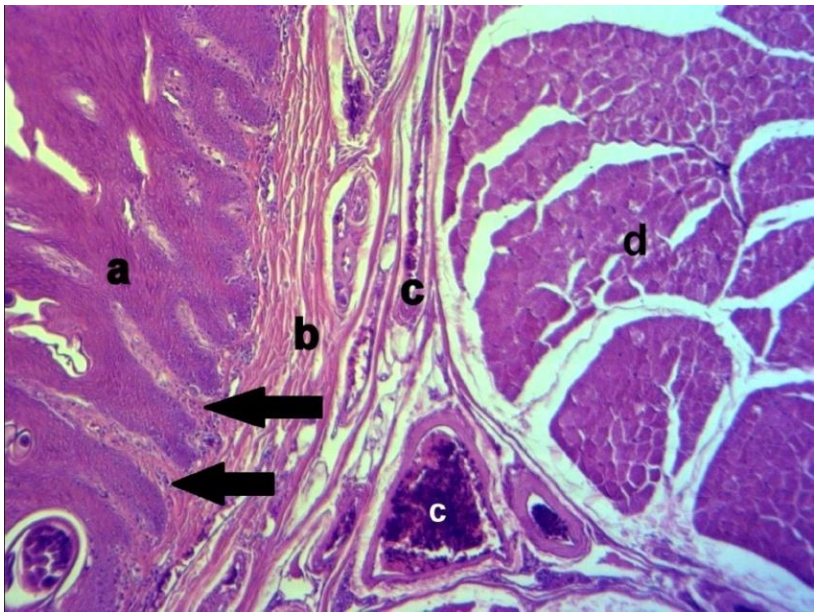

Figure 7. Cross-section of the merlin tongue (Hematoxylin-Eosin, 20X. a: epithelial layer, black arrows: dermal papilla, b: connective tissue, c: blood vessels, d: muscle layer).

Figure 8. Cross-section of the merlin tongue (Hematoxylin-Eosin, 4X. a: epithelial layer, b: connective tissue, c: paraglossum, d: muscle layer).

Table 2. Tongue volume values of animals.

	Animals					
	I	**II**	**III**	**IV**	**V**	**A.M.**
Volume (mm3)	365	391	385	352	378	374.2
Standart Error						6.2953
Standart Deviation						14.0769

A.M.: Arithmetic Mean.

Discussion and Conclusion

Avian tongues are mainly responsible for taking food and swallowing. For this reason, the tongue differs depending on the nutrition, type of food consumed and the shape of the lower beak (3, 16, 31). In the morphological studies, it has been reported that the tongue is in the form of a triangle in seagull (24), white-eared bulbul (32), black francolin (28); toothpick like in Japanese pygmy woodpecker (13); protruding arrow like in the African pied crow (21); arrow like in the hooded crow (11); needle like in the heron (12); mushroom in hummingbird (34); spearhead like in the jungle nightjar (14); lip like in the

scarlet macaw (15); and rasp like in penguins (29). The present study revealed that the merlin tongue was thin and elongated rectangular in shape and its tip was oval similar to the white-tailed eagle (25), golden eagle (33), and hawk (38) tongue. Some studies (3, 27) reported that the tongue fills the floor of the oral cavity, similar to our findings, the tongue did not fill the floor of the oral cavity in seagull (24), hawk (38), Euroasian coot (2). These differences in the shapes of tongues in poultry may be associated with the diet, lifestyle, and structure of the lower beak.

Studies on the tongue size of carnivorous birds are limited. The length of the hawk's tongue was 17 mm with 4 mm width, and 1.2 mm thickness on average (38). In this study, the average length, width, and thickness of the merlin tongue were 26.3 mm, 7.3 mm, and 1.58 mm, respectively. These differences between the tongue sizes of these birds, which have similar feeding habitats, could be related to the body size.

Erdogan and Iwasaki (16) stated that the presence or the number of papillae, or the shape of the papillar row were not associated with the feeding habit of birds. Moreover there was no *alae lingua* in the tongue of the omnivorous greater rhea (35), along with the carnivorous heron (12) and the stork (39). However, in herbivorous been goose (23) and long-legged buzzard (18), alae lingua with papilla linguales caudales exist in the form of the letter "V" and the same pattern can be seen in carnivorous white-tailed eagle (25). The alae lingua in the herbivorous zebra finch (9) and omnivorous Euroasian coot (2) show the letter "W" shape whereas the omnivorous hooded crow (30) and carnivorous cattle egret (4) possess the letter "U" shape pattern. It was determined that the *papilla linguales caudales* were in the form of the letter "U" in the Merlin tongue.

The number of *papilla linguales caudales* of the tongue was reported in long-legged buzzard (18), southern lapwing (17), hawk (38). In the present study, the number of *papillae linguales caudales* in the tongue of the merlin was found to be 14, similar to the Euroasian hobby (1). This similarity is not surprising since these birds are in the same genus (*Falco*).

In microscopic studies in various bird species, keratinization of the tongue epithelium was a common feature of birds (5, 27). Besides, tongue epithelial keratinization was lower in waterfowl (22). The tongues of common buzzard (10), cattle egret (5), and hawk (8) have keratinized epithelial tissue and that this keratinized tissue acts as a toothlike function in poultry, especially in helping to pluck plants. In our current study, it has been determined that multi-layered squamous epithelial tissue in the merlin tongue showed significant keratinization.

Kobayashi et al. (29) reported that there was no taste buds in the penguin tongue. On the other hand, the presence of taste buds in the epithelial tissue like the merlin tongue was mentioned in the African pied crow (22), common buzzard (10), and common kingfisher tongues (5). Loose connective tissue, skeletal muscle, blood vessels, and a large number of glands were found in the tongue tissue in various bird species (5, 8-10, 21). Microscopic findings in the merlin tongue were similar to these findings. The presence of *paraglossum* in the hyaline cartilage structure, which was located close to the ventral in the transversal sections of the merlin tongue, was reported in different bird species i.e. common kingfisher, long-legged buzzard, ostrich (5, 15, 26).

Volume calculations are generally determined by stereological methods on images obtained by imaging techniques such as Magnetic Resonance Imaging (MRI), Computed Tomography (CT), and Ultrasound (US) in the human tongue (37, 40). The tongue volume was determined as 2.1 mm^3 for the golden-winged sunbird, 1.1 mm^3 for the green-headed sunbird, and 0.6 mm^3 for the variable sunbird (36). In the current study, we determined the average volume of the merlin tongue as 374.2 ± 14.08 mm^3. These sunbirds consume the nectar from flowers and have a small size tube-like tongue. Also, it is thought that the body dimensions being smaller than Merlin may reveal this difference.

In conclusion, the morphological structure of the merlin tongue was revealed and its volume was calculated by the stereological method. We found that the multi-layered squamous epithelial tissue was keratinized, and there was a *paraglossum* in the hyaline cartilage structure in the body and root of the tongue. The data generated here could be useful for those who are interested in the morphology of the tongue of the carnivorous birds, particularly in the Merlin.

Acknowledgements

This paper was presented in International Congress on Biological and Health Sciences, 2021.

Financial Support

We declare that, this study was financially supported by the Scientific Research Projects Committee (Project number: 18.KARİYER.118), Afyon Kocatepe University, Afyonkarahisar, Türkiye.

Conflict of Interest

The authors declared that there is no conflict of interest.

Author Contributions

MAA, ACD, MAA, VÖ, İT and İD conceived and planned the experiments. MAA and ACD carried out the experiments. MAA, ACD and MSA contributed to the

interpretation of the results. MAA took the lead in writing the manuscript. ID contributed to the editing and spelling of the article. All authors provided critical feedback and helped shape the research, analysis and manuscript.

Data Availability Statement

The data supporting this study's findings are available from the corresponding author upon reasonable request.

Ethical Statement

This study was approved by the Afyon Kocatepe University Animal Experiment Local Ethical Committee (Ethics committee number: 49533702/41).

Animal Welfare

The authors confirm that they have adhered to ARRIVE Guidelines to protect animals used for scientific purposes.

References

1. **Abumandour MMA** (2014): *Gross anatomical studies of the oropharyngeal cavity in Eurasian hobby (Falconinae: Falco Subbuteo, Linnaeus 1758).* J Life Sci Res, **1,** 80-92.
2. **Abumandour MMA, El-Bakary NER** (2017): *Morphological Characteristics of the Oropharyngeal Cavity (Tongue, Palate and Laryngeal Entrance) in the Eurasian Coot (Fulica atra, Linnaeus, 1758).* Anat Histol Embryol, **46,** 347–358.
3. **Abumandour MMA, El-Bakary NER** (2017): *Morphological features of the tongue and laryngeal entrance in two predatory birds with similar feeding preferences: common kestrel (Falco tinnunculus) and Hume's tawny owl (Strix butleri).* Anat Sci Int, **92,** 352–363.
4. **Al-Ahmady Al-Zahaby S** (2016): *Light and scanning electron microscopic features of the tongue in cattle egret.* Microsc Res Tech, **79,** 595-603.
5. **Al-Ahmady Al-Zahaby S, Elsheikh EH** (2014): *Ultramorphological and histological studies on the tongue of the common kingfisher in relation to its feeding habit.* J Basic Appl Zool, **67,** 91-99.
6. **Başak F, Atalgin ŞH, Bozkurt EÜ** (2017): *Tongue and lingual salivary glands of the canary: SEM and histochemical study.* Folia Morphol, **76,** 348-354.
7. **Baumel JJ, King SA, Breazile JE, et al** (1993): Handbook of Avian Anatomy. Nomina Anatomica Avium, 2nd ed., Cambridge, Massachusetts, USA.
8. **Bozkurt EÜ, Gültiken ME, Yıldız D** (2018): *Ultrastructure of the tongue and histochemical features of the lingual salivary glands in buzzards.* Turkish J Vet Anim Sci, **42,** 161-167.
9. **Dehkordi RAF, Parchami A, Bahadoran S** (2010): *Light and scanning electron microscopic study of the tongue in the zebra finch Carduelis carduelis (Aves: Passeriformes: Fringillidae).* Slov Vet Res, **47,** 139-144.
10. **El-Beltagy AM** (2013): *Comparative studies on the tongue of whitethroated kingfisher (Halcyon smyrnensis) and common buzzard (Buteo buteo).* Egypt Acad J Biol Sci, **4,** 1–14.
11. **Elsheikh EH, Al-Ahmady Al-Zahaby S** (2014): *Light and scanning electron microscopical studies of the tongue in the hooded crow (Aves: Corvus corone cornix).* J Basic Appl Zool, **67,** 83-90.
12. **Emura S** (2009): *SEM studies on the lingual dorsal surfaces in three species of herons.* Med Biol, **153,** 423–430.
13. **Emura S, Okumura T, Chen H** (2009): *Scanning electron microscopic study of the tongue in the Japanese pygmy woodpecker (Dendrocopos kizuki).* Okajimas Folia Anat Jpn, **86,** 31-35.
14. **Emura S, Okumura T, Chen H** (2010): *Scanning electron microscopic study of the tongue in the jungle nightjar (Caprimulgus indicus).* Okajimas Folia Anat Jpn, **86,** 117-120.
15. **Emura S, Okumura T, Chen H** (2012): *Scanning electron microscopic study on the tongue in the scarlet macaw (Ara macao).* Okajimas Folia Anat Jpn, **89,** 57–60.
16. **Erdogan S, Iwasaki S** (2014): *Function-related morphological characteristics and specialized structures of the avian tongue.* Ann Anat, **196,** 75–87.
17. **Erdoğan S, Perez W** (2015): *Anatomical and scanning electron microscopic characteristics o f the oropharyngeal cavity (tongue, palate and laryngeal entrance) in the southern lapwing (Charadriidae: Vanellus chilensis, Molina 1782).* Acta Zool Stockh, **96,** 264-272.
18. **Erdogan S, Pérez W, Alan A** (2012): *Anatomical and scanning electron microscopic investigations of the tongue and laryngeal entrance in the long-legged buzzard (Buteo rufinus, Cretzschmar, 1829).* Microsc Res Tech, **75,** 1245-1252.
19. **Gooders J** (1995): Field Guide to the Birds of Britain and Europe, HarperCollins Ltd, UK.
20. **Gundersen HJG, Bendtsen TF, Korbo L, et al** (1988): *Some new, simple, and efficient stereological methods and their use in pathological research and diagnosis.* APMIS, **96,** 379-394.
21. **Igwebuike UM, Eze UU** (2010): *Anatomy of the oropharynx and tongue of the African pied crow (Corvus albus).* Vet Arh, **80,** 523-531.
22. **Iwasaki S** (2002): *Evolution of the structure and function of the vertebrate tongue.* J Anat, **201,** 1–13.
23. **Iwasaki S, Asami T, Chiba A** (1997): *Ultrastructural study of the keratinization of the dorsal epithelium of the tongue of Middendorff's bean goose, Anser fabalis middendorffii (Anseres, Antidae).* Anat Rec, **247,** 149–163.
24. **İnce NG, Pazvant G, Kahvecioglu KO** (2010): *Macro Anatomic Investigations on Digestive System of Marmara Region Sea Gulls.* J Anim Vet Adv, **9,** 1757-1760.
25. **Jackowiak H, Godynicki S** (2005): *Light and scanning electron microscopic study of the tongue in the white tailed eagle (Haliaeetus albicilla, Accipitridae, Aves).* Ann Anat, **187,** 251-259.
26. **Jackowiak H, Ludwig M** (2008): *Light and scanning electron microscopic study of the structure of the ostrich (Strutio camelus) tongue.* Zool Sci, **25,** 188–194.
27. **Jackowiak H, Skieresz-Szewczyk K, Godynicki S, et al** (2011): *Functional Morphology of the Tongue in the Domestic Goose (Anser Anser f. Domestica).* Anat, **294,** 1574–1584.
28. **Kadhim KK, Atia MAK, Hameed Al-T** (2014): *Histomorphological and histochemical study on the tongue*

of the black francolin (Francolinus francolinus). Int J Anim Vet Adv, **6,** 156-161.

29. **Kobayashi K, Kumakura M, Yoshimura K, et al** (1998): *Fine structure of the tongue and lingual papillae of the penguin.* Arch Histol Cytol, **61,** 37-46.
30. **Moussa EA, Hassan SA** (2013): *Comparative gross and surface morphology of the oropharynx of the hooded crow (Corvus cornix) and the cattle egret (Bubulcus ibis).* J Vet Anat, **6,** 1-15.
31. **Onuk B, Tutuncu S, Kabak M, et al** (2013): *Macroanatomic, light microscopic, and scanning electron microscopic studies of the tongue in the seagull (Larus fuscus) and common buzzard (Buteo buteo).* Acta Zool Stockh, **96,** 60-66.
32. **Parchami A, Dehkordi RAF** (2013): *Light and electron microscopic study of the tongue in the White-eared bulbul (Pycnonotus leucotis).* Iran J Vet Res, **14,** 9-14.
33. **Parchami A, Dehkordi RAF, Bahadoran S** (2010): *Scanning electron microscopy of the tongue in the golden eagle Aquila chrysaetos (Aves: Falconiformes: Accipitridae).* World J Zool, **5,** 257-263.
34. **Rico-Guevara A, Rubega MA** (2011): *The hummingbird tongue is a fluid trap, not a capillary tube.* PNAS, **108,** 9356-9360.
35. **Santos TC, Fukuda KY, Guimarães JP, et al** (2011): *Light and scanning electron microscopy study of the tongue in Rhea americana.* Zool Sci, **28,** 41-46.
36. **Schlamowitz R, Hainsworth FR, Wolf LL** (1976): *On the Tongues of Sunbirds.* Condor, **78,** 104-107.
37. **Sharma K, Shrivastav S, Hotwani K** (2016): *Volumetric MRI Evaluation of Airway, Tongue, and Mandible in Different Skeletal Patterns: Does a Link to Obstructive Sleep Apnea Exist (OSA)?* Int J Orthod, **27,** 39-48.
38. **Toprak B, Balkaya H, Yılmaz S** (2016): *Atmacada (Accipiter nisus) Ağız–Yutak Boşluğunun Makroskobik Yapısı Üzerine İncelemeler.* FÜ Sağ Bil Vet Derg, **30,** 165-170.
39. **Tütüncü Ş, Onuk B, Kabak M** (2012): *Leylek (Ciconia ciconia) dili üzerindeki morfolojik bir çalışma.* Kafkas Univ Vet Fak Derg, **18,** 623-626.
40. **Uysal T, Yagci A, Ucar FI, et al** (2013): *Cone-beam computed tomography evaluation of relationship between tongue volume and lower incisor irregularity.* Eur J Orthod, **35,** 555-562.

DOI: 10.33988/auvfd.882553

First detection of carbapenem resistance in *Enterobacteriaceae* isolates isolated from dairy cows' mastitis infection in Türkiye

Orkun BABACAN

Department of Veterinary, Kepsut Vocational School, Balıkesir University, Kepsut, Balıkesir, Türkiye

ORCID: 000-0003-0258-1825

ARTICLE INFO

Article History
Received : 20.11.2020
Accepted : 18.11.2021
DOI: 10.33988/auvfd.828306

Keywords
Antimicrobial resistance
Carbapenem resistance
E. coli
Esbl
Mastitis

Corresponding author
orkun_babacan@hotmail.com

How to cite this article: Babacan O (2023): First detection of carbapenem resistance in *Enterobacteriaceae* isolates isolated from dairy cows' mastitis infection in Türkiye. Ankara Univ Vet Fak Derg, 70 (1), 65-74. DOI: 10.33988/auvfd.828306.

ABSTRACT

With this study, carbapenem resistance genes were declared for the first time in *Enterobacteriaceae* isolates isolated from dairy cows' mastitis infection in Türkiye. In the bacteriological examination of 212 milk samples, 14 (6.60%) *E. coli*, three (1.41%) *Klebsiella oxytoca,* and two (0.94%) *Klebsiella pneumonia* were isolated. At least two *E. coli* isolates were found to be resistant to all of the antibiotics used in the antibiogram test. The highest resistance was found against cefotaxime and amoxicillin in *K. oxytoca* isolates. According to the results of PCR targeting *bla*CTX-M, *bla*TEM, and *bla*SHV genes, the *bla*CTX-M gene was detected in one *K. oxytoca* and four *E. coli* isolates, which were found ESBL positive. According to the results of PCR targeting carbapenem and colistin resistance genes, the IMP gene was detected in four *E.coli*, one *K. oxytoca,* and one *K. pneumonia* isolates. OXA-48-like gene was detected in two *E. coli* isolates. This two *E. coli* isolates were also IMP gene positive. While NDM gene was detected in two *E. coli*, KPC gene was detected in one *E. coli* isolate. One of the colistin resistance genes, *mcr-1* was detected in two *E.coli* strains with PCR. This study showed that ESBL production and carbapenem resistance in *Enterobacteriaceae* family strains to become prevalent and increasing, especially among *E. coli* isolates. Furthermore, identification of multiple antibiotic resistance in the isolates indicated that antibiotic resistance also spread rapidly and increased.

Introduction

Multidrug resistance in *E. coli* has been known worldwide. Because mastitis is one of the most frequent infections that cause several economic losses particularly due to milk and milk quality loss and treatment expenses in dairies (30, 33, 54), antibiotics are the most common important treatment choice in mastitis infections of dairy cows (20, 34, 52, 54). However, as antibiotic use in animals produced to obtain human food, the presence of antibiotic residue in the milk and/or multiple antibiotic resistance (MDR) developing in bacteria may pass to drinking milk and dairy products, has great importance for food hygiene, safety, and public health (31, 34). In recent years, as a global problem in livestock and public health fields, it has been reported that the existence of *Enterobacteriaceae* strains, producing ESBL, especially *E. coli*, increases in the mastitis infections of dairy cows (35, 52). In agriculture and livestock breeding, the resistance developing against antibiotics which are also used in the treatment of humans has become a global problem for public health (34). It has been reported that the resistance developing rapidly against a new antibiotic active substance is one of the severe problems threatening public health (3, 57). A good antibiotic treatment is performed by administering an effective antibiotic active substance selected after determining the antibiotic susceptibility of the agents isolated from udder tissue and/or milk. However, as antibiotic treatment is started mostly without determining mastitis pathogens, it has been reported that the development of antibiotic resistance should be necessarily monitored. Although mastitis treatment is similar in all the countries across the world,

penicillin, aminopenicillins and their clavulanic acid combinations, and third and fourth-generation cephalosporins are mostly used in Europe (20, 54).

Antibiotic-resistant *E. coli* strains increase due to the spread of carbapenem-resistant *Enterobacteriaceae* (CRE) isolates, which have multiple drug resistance, these are causing treatment difficulties (50). Third and fourth-generation cephalosporins are stated as critical antimicrobials by the World Health Organization. In *Enterobacteriaceae*, resistance to cephalosporins is often associated with the production of extended-spectrum β-lactamases (ESBLs). Among others, ESBL producing *E. coli* strains spreads around the world in humans as well as livestock, and it's easily spread is associated with several factors such as high virulence gene content, transfer of plasmids carrying ESBL gene, or exchange of genes encoding ESBL on mobile elements (24).

Extended-spectrum beta-lactamase (ESBL) enzymes are responsible for the hydrolysis of oxyimino-beta-lactam antibiotics used in the treatment of human and animal infections. ESBL was first declared in *Enterobacteriaceae* (*Enterobacterales* in the new taxonomy) in 1983 and since then ESBL-producing *Enterobacteriaceae* (E-ESBLhas become a great risk to human health. These bacteria were responsible for 1700 deaths in the USA due to treatment errors in most infections in 2013 (49). ESBL is one of the most known resistance mechanisms frequently observed in *E. coli, Klebsiella, and Enterobacter* spp. species included in the *Enterobacteriaceae* family (22). The major ESBL types determined in the species included in the Enterobacteriaceae family are *TEM, SHV,* and *CTX-M*. *CTX-M, TEM,* and *SHV* type beta-lactamases are considered to be plasmid-related (7, 22).

Carbapenemases are beta-lactamases that hydrolyze penicillins, most often cephalosporins and varying degrees of carbapenems and monobactams. Monobactams are not degraded by metallo-beta-lactamases. Carbapenemases are a source of concern as they cause resistance to all beta-lactams and can easily spread. Detection of these isolates is very important for infection control and public health (26).

Carbapenem-resistant genes such as *blaKPC, blaNDM, blaIMP, blaOXA48,* and a plasmid-mediated *mcr-1* gene that conferred colistin resistance in *Enterobacteriaceae*, specialize in more information worldwide. The spread of *mcr-1* encoding plasmids among carbapenem-resistant *Enterobacteriaceae* raises concerns about the emergence of incurable bacterium and becomes a serious risk for public health worldwide. IMP carbapenemase is also common in some countries in the world. (26). In Türkiye, this is the first research study for these carbapenemase genes in animal bacterium isolates.

The aim of this study is to perform phenotypic and genotypic characterization of *Enterobacteriaceae* strains isolated from mastitis infections in dairy cows in terms of ESBL production, carbapenem, and colistin resistance.

Materials and Methods

Materials and Sampling: In the study, 212 cow milk samples collected from the 52 different private family type dairy farms, which have 10 and more Holstein and/or Simmental cows, in Balıkesir city during the period of June 2018 and June 2020 were examined. In these farms there were a total of 639 dairy cows. The milk samples were taken by veterinarians for microbiological examinations about 5 ml into the sterile sample containers, after teats were cleaned with antiseptic and first milk discarded. All samples were collected before administering antibiotic treatment. One hundred twenty milk samples were taken from the udder lobes from cows which with clinical mastitis symptoms such as inflammation, pain and reduced milk yield. Ninety two milk samples were collected from the udder lobe from dairy cows with subclinical mastitis, which were positive as a result of the California Mastitis Test. These samples were delivered to the laboratory under cold chain conditions (8, 42, 58). The samples not to be included in the analysis immediately were frozen at (-20) °C and stored.

Isolation and Identification of bacterial strains from milk samples: At first, milk samples were slowly shaken for homogenization and then were inoculated onto 5% sheep blood agar (Merck, Germany), MacConkey Agar (Merck, Germany), Tryptone Bile X-Glucuronide (TBX) agar, Bile Aesculin Azide Agar (Merck, Germany), and RPF-Baird Parker (RPF-BP) (Merck, Germany) agar. While 5% sheep blood agar, Bile Aesculin Azide agar, RPF-Baird Parker (RPF-BP), and MacConkey Agar were incubated at 37°C for 24 hours; TBX agar was incubated at 44°C for 18-24 hours as reccommended by the manufacturers. At the end of the incubation, the pink colonies in MacConkey agar and blue-green colonies in TBX agar were selected for the identification of *Klebsiella* spp. and *Escherichia coli* (*E. coli*). Firstly, Gram staining, microscopic and colony morphologies, hemolysis characteristics, coagulase activity on RPF-BP agar, black or colorless colonies on Bile Aesculine Azide agar were evaluated, and then biochemical tests (indole, oxidase, catalase, TSI agar, metil red Voges Proskauer, etc.) were performed to all different colonies (53). As a result of the biochemical tests, the isolates identified as *Klebsiella spp., K. pneumonia, K. oxytoca, E. coli, S. aureus, Staphylococcus spp., S. uberis, Streptococcus spp., Micrococcus spp., Pseudomonas spp., Mucor, Corynebacterium spp., Enterococcus spp.*. A few other colonies were arranged in the tubes with 3 ml sterile saline and adjusted to McFarland 0.5-0.63 turbidity and they were identified and verified in Vitek 2 Compact device (Biomerieux, France)

DOI: 10.33988/auvfd.828306

with Gram negative and Gram positive identification cards (Biomerieux, Vitek 2 GN Card, 2019; Biomerieux, Vitek 2 GP Card, 2019). All identified isolates were taken into cryotubes and kept at -20°C.

Determination of Antibiotic Susceptibilities of Enterobacteriaceae isolates: The antibiogram tests of *Klebsiella* spp. and *E. coli* isolates were performed based on disc diffusion method according to European Committee on Antimicrobial Susceptibility Testing (EUCAST) and Clinical and Laboratory Standards Institute (CLSI) standards (6, 12, 18, 19, 27). The antibiotic discs used in this study were selected not only for which they are used in the treatment of ruminants (21, 29, 38, 42) but also observe for ESBL production and carbapenem resistance. For this purpose, a member of penicillins, cephalosporins, carbapenems quinolones, sulphonamides, aminoglycosides, macrolides, tetracyclines were used in disc diffusion tests. Used antibiotic discs are shown in Table 2.

The isolates were thawed and inoculated onto Brain Heart Infusion Broth (Biomerieux, France) from cryotubes to review and incubated at 37 °C for 24 hours. At the end of the incubation, all isolates were confirmed with Gram staining then antibiogram tests were performed (27).

After susceptibility tests, inhibition zones were recorded as resistant (R), intermediate (I), and susceptible (S) based on the breakpoints recommended by EUCAST in terms of *Enterobacteriaceae* for ampicillin, amoxicillin, amoxicillin-clavulanic acid, ofloxacin, doxycycline, cephalexin, cefotaxime, ceftazidime, ertapenem, meropenem, gentamycin, chloramphenicol, ciprofloxacin, sulfamethoxazole-trimethoprim, erythromycin, and tetracycline (27). Cephoperazone, penicillin G, and streptomycin were interpreted based on the breakpoints suggested by CLSI for *Enterobacteriaceae* (16, 17, 18). The susceptibility of neomycin was interpreted by criteria reported by Fouad et al. (29). Marbofloxacin and enrofloxacin were evaluated based on the breakpoints suggested by CLSI VET08 ED4:2018 (19). ***Phenotypic Detection of ESBL and Carbapenemase in Enterobacteriaceae isolates:*** In order to investigate the extended-spectrum beta-lactamase (ESBL) activities of the isolates, the combination disc diffusion tests were performed and evaluated according to EUCAST criteria (16). Cefotaxime (Liofilchem, 5µg) and cefotaxime-clavulanic acid (Liofilchem, 30+10µg) combination discs were used in this test.

According to the EUCAST procedure (26), isolates, whose zone diameters were found to be <28 and <25 mm against meropenem and ertapenem in the screening test, respectively, were subjected to the confirmatory combination disc tests (KPC, AmpC, metallo-beta lactamase, OXA-48, ESBL/loss of porin). In this test, meropenem (Liofilchem, 10µg,), ertapenem (Liofilchem, 10µg,), merpenem+dipicolinic acid (Liofilchem, Italy), meropenem+EDTA (Liofilchem, Italy), meropenem+ phenylboronic acid (Liofilchem, Italy), meropenem+ cloxacillin (Liofilchem, Italy), temocillin (Liofilchem, Italy) combined and single discs were used. Tests were evaluated by the EUCAST procedure (26).

Detection of ESBL, carbapenemase, and colistin resistance by PCR: All *E. coli* and *Klebsiella* spp. isolates were subcultured into Nutrient Broth (NB, Oxoid, UK) to obtain pure cultures and incubated at 37°C for 18 hours. After incubation, 1 mL NB broth culture of the isolates was centrifuged at 5000 *g* for 10 min. After the centrifugation process, the supernatant was removed and DNA extraction was performed using the pellet through GeneJET Genomic DNA Purification kit (Thermo Scientific, US) and DNA Purification Protocol for Gram-negative bacteria.

PCR was performed to examine ESBL, carbapenemase, and colistin resistance gene regions. Specific primer pairs were used to amplify the sequences of these genes, which were synthesized commercially from the selected genes described previously by Bektaş et al. (7) and Hatrongjit et al. (32) (Table 1).

The PCR reaction mix for all ESBL genes was carried out in a total volume of 25 µl, containing 5 µl of DNA extract (template DNA) and 20 µl of PCR mix. PCR mix contained 12.5 µL DreamTaq PCR Master Mix (2X) Kit (Thermo Scientific, US), 7.3 µL DEPC water, 0.1 µL Primer F (100 pmol/µL), and 0.1 µL Primer R (100 pmol/µL). Amplification conditions were performed for these genes according to as described previously by Bektaş et al. (7).

Isolates were tested for the presence of carbapenemase and colistin resistance genes by multiplex PCR as described previously by Hatrongjit et al. (32). The PCR reaction mix was performed in a total volume of 15 µl, containing 2 µl of DNA extract (template DNA) and 13 µl of PCR mix. PCR mix consisted of 8.8 µL DreamTaq PCR Master Mix (2X) Kit (Thermo Scientific, US), 2.2 µL DEPC water, 0.2 µL each Primer F (100 pmol/µL), 0.2 µL each Primer R (100 pmol/µL). Amplification conditions were performed for these genes according to as described previously by Hatrongjit et al. (32).

All PCR amplicons (10 µl ampicon and 2 µl Bluejuice gel loading buffer 10X, Thermo Scientific, US) were electrophoresed on 1.5% agarose (Prona) gel prepared into 200 ml Tris-borate-EDTA (TBE) buffer (Thermo Scientific, US) and visualized on a bio-visualizing system (EBOX CX5 TS EDGE, Vilber). DNA molecular weight marker (Gene Ruler 100bp DNA Ladder plus, Thermo Scientific, US) was used.

Table 1. Primer sequences, target ESBL, and carbapenemase genes, base pairs and references.

Primers	Sequence	Target ESBL genes	Base pairs	References
CTX-M-F CTX-M-R	TCTTCCAGAATAAGGAATCCC CCGTTTCCGCTATTACAAAC	*bla*CTX-M	909 bp	Bektaş et al. (7)
TEM-F TEM-R	TCCGCTCATGAGACAATAACC TTGGTCTGACAGTTACCAATGC	*bla*TEM	931 bp	Bektaş et al. (7)
SHV-F SHV-R	TGGTTATGCGTTATATTCGCC GGTTAGCGTTGCCAGTGCT	*bla*SHV	868 bp	Bektaş et al. (7)
IMP-F IMP-R	GGAATAGAGTGGCTTAAYTCTC GGTTTAAYAAAACAACCACC	*IMP*	232 bp	Hatrongjit et al. (32)
OXA-48-like-F OXA-48-like-R	GCGTGGTTAAGGATGAACAC CATCAAGTTCAACCCAACCG	*OXA-48-like*	438 bp	Hatrongjit et al. (32)
NDM-F NDM-R	GGTTTGGCGATCTGGTTTTC CGGAATGGCTCATCACGATC	*NDM*	621 bp	Hatrongjit et al. (32)
KPC-F KPC-R	CGTCTAGTTCTGCTGTCTTG CTTGTCATCCTTGTTAGGCG	*KPC*	798 bp	Hatrongjit et al. (32)
MCR1-F MCR1-R	GGGTGTGCTACCAAGTTTGC CATTGGCGTGATGCCAGTTT	*mcr-1*	1126 bp	Hatrongjit et al. (32)

*E.coli (*ATCC ® 25922™), *K. pneumoniae* (ATCC ® 700603™), *E.coli* (CCUG 62975; CTX-M positive), *E.coli* (NCTC 13846; colistin resistant mcr-1 positive), *E.coli* (NCTC 13476; IMP positive), *K.pneumonia* (NCTC 13438; KPC positive) and *E.coli* (NCTC 14320; IMP, KPC and OXA-48-like positive) were used as control strains in the isolation, identification, disc diffusion and PCR tests.

Results

On bacteriological examination, 14 (6.60%) *E. coli*, three (1.41%) *Klebsiella oxytoca*, and two (0.94%) *Klebsiella pneumonia* were isolated from 212 milk samples. Two of 14 *E. coli* were isolated in the milk samples of the cows with clinical mastitis and 12 *E. coli* were isolated from milk samples of cows with subclinical mastitis. *Klebsiella oxytoca* (n:3) and *Klebsiella pneumonia* isolates (n:2) were isolated from subclinical mastitis cases. Table 2 shows the isolation data of all bacterium from milk samples.

Table 2. Isolates and milk sample numbers.

Isolates	Number of isolates	Number of milk samples
E. coli	14	14
K. oxytoca	3	3
K. pneumonia	2	2
Staphylococcus aureus	12	12
Staphylococcus spp.	7	7
Enterococcus spp.	3	3
Micrococcus spp.	1	1
Streptococcus spp.	2	2
Streptococcus uberis	7	7
Pseudomonas spp.	1	1
Corynebacterium spp.	7	7
Kocuria spp.	1	1
Mucor spp.	4	4
No bacterial growth	-	148
Total	64	212

Table 3 shows the results of disc diffusion tests. At least two *E. coli* isolates were found to be resistant to all of the antibiotics used in the antibiogram test. The highest resistance was found against cefotaxime and amoxicillin in *K. oxytoca* isolates, whereas, the highest resistance was found in *K. pneumonia* isolates against sulphamethoxazole/ trimethoprim.

According to the results of the disc diffusion test, ESBL was detected positive in four *E. coli* and one *K. oxytoca* isolates. *K. pneumonia* isolates were showed no ESBL production. In combined disc diffusion tests, these ESBL positive strains also were found positive, which were much more 5 mm broad zone diameter with cefotaxime+clavulanic acid compared with cefotaxime disc.

According to the PCR results of *bla*CTX-M, *bla*TEM, and *bla*SHV genes, the *bla*CTX-M gene was detected in one *K. oxytoca* and four *E. coli* isolates, which were found ESBL positive. (Figure 1A).

In antibiogram tests, seven *E. coli*, one *K. oxytoca*, and one *K. pneumonia* isolates were found resistant against meropenem and ertapenem. Also, these isolates were confirmed in terms of carbapenem resistance according to the EUCAST procedure (26). In phenotypic mechanism determination tests, the presence of the OXA-48-like gene was confirmed by the resistance of Temocillin. Two *E. coli* strains were shown Temocillin resistant. The presence of IMP and NDM gene to determine the mechanism of metallo-beta-lactamase (MBL), the presence of increased synergy with dipicolinic acid was detected in six *E. coli* (two of also have OXA-48 type), one *K. oxytoca*, and one *K. pneumonia* strains by combined disk diffusion tests. The presence of the KPC gene was confirmed by synergie with boronic acid and one *E. coli* was found positive.

Table 3. Disc diffusion test results of *Enterobacteriaceae* isolates.

	E. coli (n:14)			*K. oxytoca* (n:3)			*K. pneumonia* (n:2)		
Antibiotic discs	**S**	**I**	**R**	**S**	**I**	**R**	**S**	**I**	**R**
Amoxicillin (Oxoid, 10µg)	4	-	10	1	-	2	1	-	1
Amoxicillin-clavulanic acid (Oxoid, 30µg)	4	1	9	2	1	-	2	-	-
Ampicillin (Oxoid, 10µg)	6	1	7	2	1	-	1	-	1
Cephalexin (Oxoid, 30µg)	8	1	5	1	1	1	2	-	-
Cephoperazone (Oxoid, 75µg)	3	-	11	1	1	1	1	-	1
Cefotaxime (Liofilchem, 5µg)	7	1	6	1	-	2	1	-	1
Ceftazidime (Liofilchem, 30 µg)	8	1	5	1	1	1	1	-	1
Chloramphenicol (Oxoid, 30µg)	4	-	10	3	-	-	2	-	-
Ciprofloxacin (Oxoid, 5µg)	6	-	8	3	-	-	2	-	-
Doxycyline (Oxoid,	4	3	7	3	-	-	2	-	-
Enrofloxacin (Oxoid, 5µg)	2	1	11	3	-	-	1	-	1
Erithromycin (Oxoid, 15µg)	3	-	11	2	1	-	1	-	1
Gentamicin (Oxoid, 10µg)	9	-	5	3	-	-	2	-	-
Marbofloxacin (5µg)	2	1	11	3	-	-	1	-	1
Neomicin (Oxoid, 10µg)	3	-	11	2	-	1	1	-	1
Ofloxacine (Oxoid, 5µg)	12	-	2	3	-	-	2	-	-
Penicillin G (Oxoid, 10U)	4	-	10	2	-	1	2	-	-
Spiramycin (Oxoid, 100µg)	12	-	2	3	-	-	2	-	-
Streptomycin (Oxoid, 10µg)	12	-	2	3	-	-	2	-	-
Tetracyclin (Oxoid, 30µg)	10	-	4	3	-	-	2	-	-
Trimethoprim-Sulfahamethoxazole (Oxoid, 25µg)	-	-	14	2	-	1	-	-	2

S: Susceptable, I:Intermediate, R:Resistant.

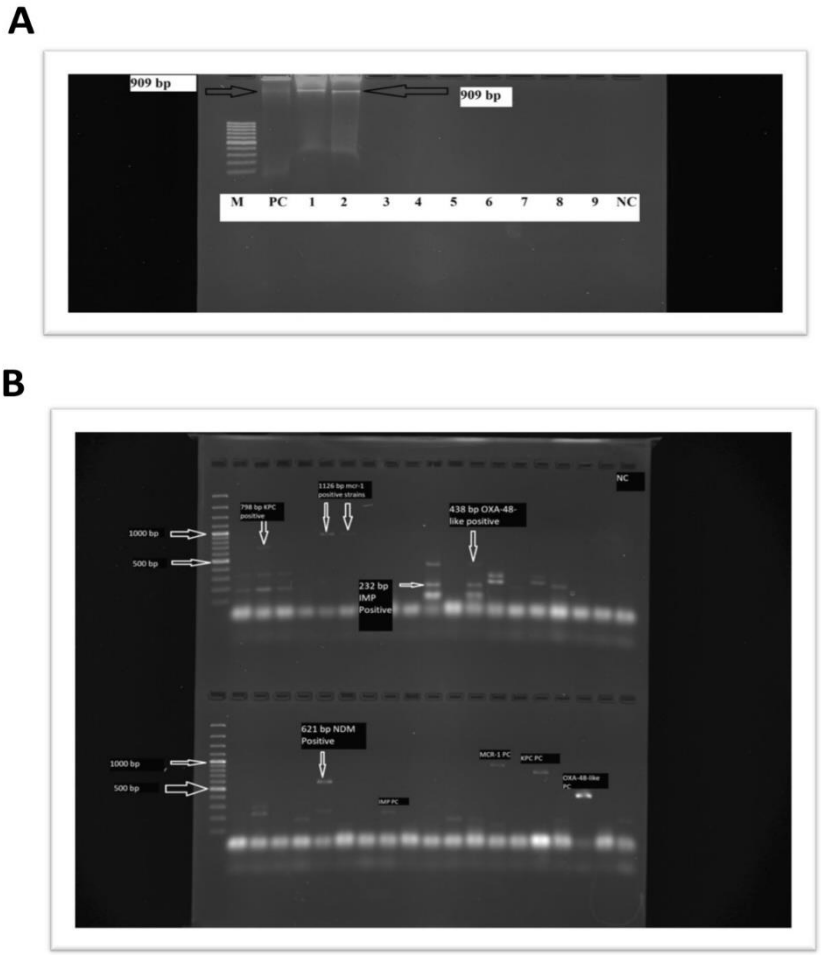

Figure 1. A) PCR results of CTX-M gene for Enterobacteriaceae isolates (M: Marker, PC: Positive control, NC: Negative control: Line 2-3: positive isolates Line 3-9: Negative isolates) B) Multiplex PCR results of carbapenemase and colistin resistance genes for *Enterocteriaceae* isolates with 100 bp plus ladder (PC: Positive control, NC: Negative control, Marked Lines: positive *Enterobacteriaceae* strains with marked gene).

According to the results of PCR targeting carbapenem and colistin resistance genes, the IMP gene was detected in four *E.coli*, one *K. oxytoca* and one *K. pneumonia* isolates, respectively. OXA-48-like genes were detected in two *E. coli* isolates. Also in these OXA-48-like positive two *E. coli* isolates have an IMP gene. While NDM gene was detected in two *E. coli*, KPC gene was detected in one *E. coli* isolate. One of the colistin resistance genes, *mcr-1* was detected in two *E.coli* strains with PCR (Figure 1B).

Discussion and Conclusions

In dairy cows, *E. coli* is a foodborne zoonosis with high importance for public health (48). In this study, the presence of *E. coli* was detected to be 6.60% in cow milk with mastitis. Messele et al. (44) have reported that the *E. coli* isolation rate was 7.1% from milk. Makolo et. al. (41) stated that they isolated six *E. coli* and seven *Klebsiella pneumonia* from 147 milk samples. Zhang et al. (58) reported that they isolated *E. coli* at the rate of 20.1% from 393 milk samples. Klibi et al. (35) stated that they isolated 79 *E. coli* and 30 *Klebsiella pneumonia* in 300 milk samples. Manasa et al. (42) reported that they isolated *E. coli* at the rate of 41%. Considering the mentioned studies, the presence rate of *E. coli* in this study was thought to be significant. In this study, two *K. pneumonia* and three *K. oxytoca* were isolated.

According to the disc diffusion test results, multiple drug resistance was determined in *E. coli* isolates. According to these results, it was considered that multiple drug resistance may spread among the isolates. In *K. oxytoca* isolates, the highest resistance was found against cefotaxime, cephalexin, cefoperazone, neomycin, penicillin G, and trimethoprim-sulfamethoxazole, respectively. Dinç et al. (22) were found the resistance rates in 92 *E. coli* strains isolated from mastitis infections of cattle against erythromycin (69.6%), ampicillin (39.1%), tetracycline (34.8%), nalidixic acid (25.0%), chloramphenicol (22.8%), trimethoprim-sulfamethoxazole (21.7%) and amoxicillin-clavulanic acid (21.7%) and also 25.0% of the 92 *E. coli* strains were susceptible to all tested antibiotics. They also reported that 54.3% of *E. coli* strains were resistant to two or more antibiotics, but they could not detect ESBLs in 92 *E.coli* strains. Makolo et al. (41) stated high multiple resistance to tetracycline, penicillin, and erythromycin. Bhat et al. (8) determined that the isolates were susceptible mostly to enrofloxacin and gentamicin but all the isolates were resistant to penicillin. Penicillin and gentamicin results in this study were found to be similar to the results of Bhat et al. (8) and they were found to be compatible with Dinç et al. (22) in terms of *E. coli* isolates with multiple resistance.

ESBL-producing strains have been widespread throughout the world since they were first described in 1983. This spread occurs as a result of clonal replication, transfer of ESBL genes to plasmids, and rarely, the emergence of new enzymes. The most important group among ESBLs is the CTX-M enzymes that emerged in the early 2000s. This group is followed by SHV and TEM-derived ESBLs (9, 11, 14, 26, 40). *Escherichia* species where ESBL production is most common are *E. coli* and *Klebsiella pneumoniae*, but other clinically important *Enterobacteriaceae* species are also ESBL producers (9, 15, 26, 39). According to EARS-Net data, rates of invasive *K. pneumoniae* non-sensitive to 3rd generation cephalosporins are more than 25% in most European countries and even more than 50% in many countries. KPC type, except Italy and Greece, where carbapenemase-producing isolates are high. Most local ESBL test results had been considered ESBL positive (25, 26).

Beta-lactam antibiotics are used frequently for treatment purposes in human and animal health. Extended-spectrum beta-lactamases are resistant to penicillin, 1st and 4th generation cephalosporins, and monobactams. Extended-spectrum beta-lactamases are generally associated with the plasmid. The most frequent beta-lactamases groups in *Enterobacteriaceae* isolates are TEM, SHV, and CTX-M. TEM and SHV groups are originated from TEM-1/TEM-2 and SHV-1 (*bla*TEM-1/*bla*TEM-2 and *bla*SHV-1) beta-lactamase genes; the CTX-M gene may be transferred by conjugation (51). Dinç et al. (22) stated that they were not determined ESBL in 92 *E. coli* strains isolated from cattle mastitis. In this study, in one *K. oxytoca* isolates, CTX-M genes were determined. In four *E. coli* isolates, the *bla*CTX-M gene was found. Among the studies conducted in Türkiye last seven years, ESBL increase has been observed in *E. coli* strains which have been the isolates of cattle mastitis infection.

Many researchers have reported that ESBL production among *Enterobacteriaceae* isolates has an increasing prevalence (51). This increase has been associated with the clonal transfer of the strains producing ESBL and the horizontal transfer of these genes carrying plasmids. Dinç et al. (22) conducted a study on milk samples taken from different cities, including Balıkesir in Türkiye and they reported that they could not detect ESBL in *E. coli* strains isolated from mastitis infection of cow's. In this study, ESBL were identified in one *K. oxytoca* isolates and four *E. coli* isolate in Balıkesir city, which indicated that ESBL genes spread among the strains and the resistance became widespread in seven years. Aslantaş et. al. (4) detected 12 (46.2%) harbored *bla*CTX-M-15, 11 (42.3%) *bla*CTX-M-1, two (7.7%) *bla*CTX-M-3 and one (3.8%) *bla*CMY-2. In addition to ESBL/AmpC genes, other β-lactamase genes were detected in 22 isolates (84.6%), of which 21 isolates harbored *bla*TEM-1b and

DOI: 10.33988/auvfd.828306

one isolate harbored *bla*OXA-1 in combination with ESBL/AmpC genes.

Today, carbapenem resistance in Gram-negative bacteria is a worldwide problem. (46). Most carbapenemases are encoded by transposable elements on enzymes derived from plasmids. In *Enterobacteriaceae* members, changes or loss of porin (or possibly PBP) and ESBL or AmpC enzyme production can also be seen with reduced susceptibility to carbapenems. Carbapenemases are particularly sensitive to one of the carbapenems (imipenem, meropenem, ertapenem, doripenem) (26).

In the 1990s, the problem of carbapenem resistance was reported in many Mediterranean countries in Europe, especially in *Pseudomonas aeruginosa* (13, 26). In the early 2000s, an outbreak of *Klebsiella pneumoniae* related to metallo-β-lactamase (VIM) encoded by Verona integron and *K. pneumoniae* carbapenemase (KPC) was reported in Greece (26, 56). Today, OXA-48 carbapenemases are the most common carbapenemase group in Europe (2, 26). Other particularly problematic carbapenemases are New Delhi metallo-β-lactamases (NDMs) (2, 26), which are quite common in the Indian subcontinent and the Middle East and have been reported on several occasions in Europe, as well as instances of regional spread in some countries (5, 27). IMP-carbapenemases are also common in some parts of the world (26, 47).

Nordmann et al. (46) reported that carbapenem nonsusceptibility or resistance rates by region, especially for *E. coli*, up to 3% in Asia-Pacific, up 34% in India, Nepal, Pakistan, Vietnam, up to 7% in Europe, between 0.2%–0.4% in North America, between 0.4%–9.0% in Latin America (46).

Countries in Africa, including Morocco, Kenya, and South Africa have reported NDM-1 as the most dominant carbapenemase gene. Latin America and China have reported KPC-2 as the most dominant carbapenemase gene (12). In Türkiye, authors reported only AmpC-producing *E. coli* strains (4).

In Türkiye, there is no study about findings of carbapenem resistance and IMP, OXA-48 like, NDM and KPC genes in animal bacterium isolates. Recently Al et al. (1) reported that no carbapenem resistance in *Enterocateriacae* strains isolated from raw milk. With this study, carbapenem resistance genes (IMP, OXA-48 like, NDM and KPC) were declared for the first time in *Enterobacteriaceae* isolates isolated from dairy cows' mastitis infection in Türkiye.

Köck et al. (36) reported that they isolated carbapenem-resistant *Enterobacteriaceae* from poultry meat, chicken, pig, cows or raw milk, cattle, and various types of seafood. Pamipuntu et al. (50) were reported that they isolated a total of 182 *E. coli* isolates in 64 water samples obtained from drinking water containers of dairy cattle in 32 dairy farms. Also, they found two isolates resistant to imipenem but showed positive results for only *blaNDM* gene detection by the PCR in these *E. coli* strains.

Carbapenemases are a source of concern because they may confer resistance to virtually all β-lactams, and are readily transferable. Because of this, resistance mechanisms to a wide range of antimicrobial agents and their infections with high mortality rates in epidemiologically (10, 26, 43, 55).

Colistin (also known as polymyxin E) and other polymyxins are used for the treatment of severe human infections with *Pseudomonas aeruginosa* and carbapenem-insensitive ESBL-producing *Enterobacteriaceae* and *Acinetobacter* spp. Such strains are also has been found in foods of animal origin and there are signs of *mcr-1* gene flow from animals to humans (28). In this study, the *mcr-1* gene was found in two *E. coli* isolates. However, colistin resistance is not very important for cow mastitis cases and colistin has not commonly used for the treatment of cow mastitis infection (28). But this result is important for public health.

Until recently, in Türkiye has not been reported any IMP, OXA-48 like, NDM and KPC carbapenem resistance genes in *E. coli* and *Klebsiella* spp. from dairy cows' mastitis infection isolates. This study results showed that carbapenem resistance was detected for the first time in Türkiye and that occurred in *Enterobacteriaceae* strains in cow's mastitis agents in Türkiye. So, this is important for the epidemiology of carbapenem resistance in Türkiye; but more epidemiological studies are needed in animal isolates in Türkiye.

Consequently, determining ESBL and carbapenem resistance in the species especially included in the *Enterobacteriaceae* family revealed the presence of ESBL and carbapenem resistance, becoming prevalent and increasing, especially among *E. coli* isolates in Türkiye. Also, the fact that multiple antibiotic active substance resistance was determined in the isolates revealed that antibiotic resistance spread and increased rapidly. For these reasons, it has been considered that researching and monitoring the presence of ESBL and carbapenem resistance genes in the bacteria isolated in animal diseases are essential in terms of obtaining epidemiological data. Finally, this study is evaluated in terms of public health, it demonstrates the importance of control and prevention of antimicrobial resistance with the scope of the One Health concept.

Acknowledgements

The author would like to thank the Republic of Turkey Ministry of Health General Directorate of Public Health Microbiology Reference Laboratory for supplied the control strains used in this study and supportted to identification of a few colonies.

Financial Support

This research received no grant from any funding agency/sector.

Conflict of Interest

The author declared that there is no conflict of interest.

Data Availability Statement

The data supporting this study's findings are available from the corresponding author upon reasonable request.

Ethical Statement

This study does not present any ethical concerns.

Animal Welfare

Not applicable.

References

1. **Al S, Hızlısoy H, Ertaş Onmaz E, et al** (2020): *A molecular investigation of carbapenem resistant Enterobacteriaceae and blaKPC, blaNDM and blaOXA-48 genes in raw milk.* Kafkas Univ Vet Fak Derg, **26,** 391-396.
2. **Albiger B, Glasner C, Struelens MJ, et al** (2015): *Carbapenemase-producing Enterobacteriaceae in Europe: assessment by national experts from 38 countries, May 2015.* Euro Surveill, **20.**
3. **Alonso CA, Zarazaga M, Ben Sallem R, et al** (2017): *Antibiotic resistance in Escherichia coli in husbandry animals: the African perspective.* Lett App Microbiol, **64,** 318–334.
4. **Aslantaş Ö, Elmacıoğlu S, Yılmaz EŞ** (2017): *Prevalence and characterization of ESBL- and AmpC-producing Escherichia coli from cattle.* Kafkas Univ Vet Fak Derg, **23,** 63-67.
5. **Baraniak A, Izdebski R, Fiett J, et al** (2016): *NDM-producing Enterobacteriaceae in Poland, 2012-2014: interregional outbreak of Klebsiella pneumoniae ST11 and sporadic cases.* J Antimicrob Chemother, **71**, 85-91.
6. **Bauer AW, Kirby WM, Sherris JC, et al** (1966): *Antibiotic susceptibility testing by a standardized single disk method.* Am J Clin Pathol, **45,** 493- 496.
7. **Bektaş A, Güdücüoğlu H, Gürsoy NC, et al** (2018): *Investigation of extended spectrum beta-lactamase (esbl) genes in esbl-producing Escherichia coli and Klebsiella pneumoniae strains.* Flora, **23,** 116-123.
8. **Bhat AM, Soodan JS, Singh R, et al** (2017): *Incidence of bovine clinical mastitis in Jammu region and antibiogram of isolated pathogens.* Vet World, **10,** 984–989.
9. **Bradford PA** (2001): *Extended-spectrum β-lactamases in the 21st century: characterization, epidemiology, and detection of this important resistance threat.* Clin Microbiol Rev, **14,** 933-951.
10. **Bratu S, Landman D, Haag R, et al** (2005): *Rapid spread of carbapenem-resistant Klebsiella pneumoniae in New York City: a new threat to our antibiotic armamentarium.* Arch Intern Med, **165,** 1430-1435.
11. **Bush K, Jacoby GA, Medeiros AA** (1995): *A functional classification scheme for β -lactamases and its correlation with molecular structure.* Antimicrob Agents Chemother, **139,** 211-1233.
12. **Codjoe FS, Donkor ES** (2018): *Carbapenem resistance: A review.* Med Sci, **6**, 1-28.
13. **Cantón R, Akóva M, Carmeli Y, et al** (2012): *Rapid evolution and spread of carbapenemases among Enterobacteriaceae in Europe.* Clin Microbiol Infect, **18,** 413-431.
14. **Cantón R, Novais A, Valverde A, et al** (2008): *Prevalence and spread of extendedspectrum β-lactamase-producing Enterobacteriaceae in Europe.* Clin Microbiol Infect, **14,** 144-153.
15. **Carattoli A** (2008): *Animal reservoirs for extended-spectrum β-lactamase producers.* Clin Microbiol Infect, **14,** 117-123.
16. **Clinical and Laboratory Standards Institute (CLSI)** (2014): Performance standards for antimicrobial susceptibility testing; twenty forth informational supplement M100-S24. (Vol. 34, No. 1). Wayne, PA, USA.
17. **Clinical and Laboratory Standards Institute (CLSI)** (2017): Performance standards for antimicrobial susceptibility testing; 24th Informational Supplement M100-S26. Wayne, PA, USA.
18. **Clinical and Laboratory Standards Institute (CLSI)** (2018): Performance standards for antimicrobial disk and dilution susceptibility tests for bacteria isolated from animals. 5th ed. CLSI standard VET01. Wayne, PA, USA.
19. **Clinical and Laboratory Standards Institute (CLSI)** (2018): Performance standards for antimicrobial disk and dilution susceptibility tests for bacteria isolated from animals. 5th ed. CLSI standard VET08 ED4. Wayne, PA, USA.
20. **De Jong A, El Garch F, Simjee S, et al** (2018): Monitoring of antimicrobial susceptibility of udder pathogens recovered from cases of clinical mastitis in dairy cows across Europe: VetPath results. *Vet Microbiol*, **213,** 73–81, 2018.
21. **De Schmitt-van Leemput E, Zadoks RN** (2007): *Genotypic and phenotypic detection of macrolide and lincosamide resistance in Streptococcus uberis.* Dairy Sci, **90,** 5089–5096.
22. **Dinç G, Ata Z, Temelli S** (2012): *Investigation of extended-spectrum beta-laktamase activity and antibiotic resistance profile of Escherichia coli strains isolated from bovine mastitis.* Ank Univ Vet Fak Derg, **59,** 85-88.
23. **Effendi MH, Harijani N** (2019): *Prevalence of pathogenic Escherichia coli isolated from subclinical mastitis in east java province, Indonesia.* Indian Vet J, **96,** 22-25.
24. **Eisenberger D, Carl A, Balsliemke J, et al** (2018): *Molecular characterization of extended-spectrum b-lactamase-producing Escherichia coli isolates from milk samples of dairy cows with mastitis in Bavaria, Germany.* Microb Drug Resist, **24,** 505-510.
25. **European Centres for Disease Prevention and Control (ECDC)** (2014): Antimicrobial resistance surveillance in Europe 2014. Annual report of the European Antimicrobial Resistance Surveillance Network (EARS-Net).
26. **European Committee on Antimicrobial Susceptability Testing (EUCAST)** (2017): Breakpoint tables for interpretation of MICs and zone diameters. Version 9.0.

Available at http://www.eucast.org/fileadmin/src/media/PDFs/EUCAST_files/ Breakpoint_tables/v_9.0_Breakpoint_Tables.pdf. (Accessed September 29, 2020).

27. **European Committee on Antimicrobial Susceptibility Testing (EUCAST)** (2019): EUCAST guidelines for detection of resistance mechanisms and specific resistances of clinical and/or epidemiological importance. Version 2.0. Available at https://www.eucast.org/fileadmin/src/media/PDFs/EUCAST_files/Resistance_mechanisms/EUCAST_detection_of_resistance_mechanisms_170711.pdf. (Accessed September 29, 2020).
28. **Flioussis G, Kachrimanidou M, Christodoulopoulos G, et al** (2020): *Bovine mastitis caused by a multidrug-resistant, mcr-1-positive (colistin-resistant), extended-spectrum β-lactamase– producing Escherichia coli clone on a Greek dairy farm.* J Dairy Sci, **103,** 852-857.
29. **Fouad Z** (2011): Antimicrobial Disk Diffusion Zone Interpretation Guide. Available at https://doi.org/10.13140/RG.2.2.13801.70240. (Accessed September 29, 2020).
30. **Gao X, Fan C, Zhang Z, et al** (2019): *Enterococcal isolates from bovine subclinical and clinical mastitis: Antimicrobial resistance and integron-gene cassette distribution.* Microb Pathog, **129,** 82–87.
31. **Gemechu T, Yunus HA, Soma M, et al** (2019): *Bovine mastitis: prevalence, isolation and identification of major bacterial pathogens in selected areas of Bench Maji Zone Southwest Ethiopia.* J Vet Med Anim Health, **11,** 30-36.
32. **Hatrongjit R, Kerdsin A, Akeda Y, et al** (2018): *Detection of plasmid-mediated colistin-resistant and carbapenem-resistant genes by multiplex PCR.* MethodsX, **5,** 532- 536.
33. **Horpiencharoen W, Thongratsakul S, Poolkhet C** (2019): *Risk factors of clinical mastitis and antimicrobial susceptibility test results of mastitis milk from dairy cattle in western Thailand: Bayesian network analysis.* Prevent Vet Med, **164,** 49–55.
34. **Jayarao B, Almeida R, Oliver SP** (2019): *Antimicrobial resistance on dairy farms.* Foodborne Pathog Dis, **16,** 1–4.
35. **Klibi A, Jouini A, Boubaker El Andolsi R, et al** (2019): *Epidemiology of β-lactamase-producing staphylococci and gram negative bacteria as cause of clinical bovine mastitis in Tunisia.* Biomed Res Int, **2019,** 1–9.
36. **Köck R, Daniels-Haardt I, Becker K, et al** (2018): *Carbapenem-resistant Enterobacteriaceae in wildlife, food-producing, and companion animals: a systematic review.* Clin Microbiol Infect, **24,** 1241-1250.
37. **Krömker V, Leimbach S** (2017): *Mastitis treatment-reduction in antibiotic usage in dairy cows.* Reprod Domest Anim, **52,** 21–29.
38. **Laven R** (2013): *Treatment of E. coli mastitis: are antibiotics needed?* Livestock, **18,** 59-61.
39. **Livermore DM, Cantón R, Gniadkowski M, et al** (2007): *CTX-M: changing the face of ESBLs in Europe.* J Antimicrob Chemother, **59,** 165-174.
40. **Livermore DM** (1995): *β-Lactamases in laboratory and clinical resistance.* Clin Microbiol Rev, **8,** 557-584.
41. **Makolo D, Suleiman AB, Olonitola OS, et al** (2019): *Antimicrobial Susceptibility Profile of Coliforms from Bovine Mastitis Cases among Pastoral Herds in Parts of Kaduna State , Nigeria : Curbing the Environmental Health Risk.* Asian J Adv Res Rep, **3,** 1–12.
42. **Manasa V, Venkata Sai Kumar T, Prasada Rao T, et al** (2019): *Incidence of bovine clinical mastitis caused by Escherichia coli.* Int J Curr Microbiol Appl Sci, **8,** 1249–1256.
43. **Marchaim D, Navon-Venezia S, Schwaber MJ, et al** (2008): *Isolation of imipenem-resistant Enterobacter species: emergence of KPC-2 carbapenemase, molecular characterization, epidemiology, and outcomes.* Antimicrob Agents Chemother, **52,** 1413-1418.
44. **Messele YE, Abdi RD, Tegegne DT, et al** (2019): *Analysis of milk-derived isolates of E. coli indicating drug resistance in central Ethiopia.* Trop Anim Health Pro, **51,** 661–667.
45. **Naas T, Poirel L, Nordmann P** (2008): *Minor extended-spectrum β-lactamases.* Clin Microbiol Infect, **14,** 42-52.
46. **Nordmann P, Poirel L** (2019): *Epidemiology and diagnostics of carbapenem resistance in Gram- negative bacteria*. Clin Infect Dis, **69,** 521-528.
47. **Nordmann P, Naas T, Poirel L** (2011): *Global spread of Carbapenemase-producing Enterobacteriaceae.* Emerg Infect Dis, **17,** 1791-1798.
48. **Nüesch-Inderbinen M, Kappeli N, Morach M, et al** (2019): *Molecular types, virulence profiles and antimicrobial resistance of Escherichia coli causing bovine mastitis.* Vet Rec Open, **6,** 1-9.
49. **Palmeria JD, Ferreira NDM** (2020): *Extended-spectrum beta-lactamase (ESBL)-producing Enterobacteriaceae in cattle production – a threat around the world.* Heliyon, **6,** e03206.
50. **Pamipuntu N, Pamipuntu S** (2020): *Detection of antimicrobial resistance genes of carbapenem-resistant Enterobacteriaceae in Escherichia coli isolated from the water supply of smallholder dairy farms in Saraburi and Maha Sarakham, Thailand.* Int J of One Health, **6,** 1-5.
51. **Pehlivanoğlu F, Türütoğlu H, Öztürk D, et al** (2017): *Characterization of extended- spectrum beta-lactamase-producing fecal Escherichia coli isolates in laying hens.* Ank Univ Vet Fak Derg, **64,** 301–306.
52. **Pillar CM, Stoneburner A, Shinabarger DL, et al** (2014): *In vitro susceptibility of bovine mastitis pathogens to a combination of penicillin and framycetin: development of interpretive criteria for testing by broth microdilution and disk diffusion.* Dairy Sci, **97,** 6594–6607.
53. **Quinn PJ, Markey BK, Leonard FC, et al** (2004): Veterinary Microbiology and Microbial Disease. Second Edition, Blackwell Science Ltd, Oxford.
54. **Šlosárková S, Nedbalcová K, Bzdil J, et al** (2019): *Antimicrobial susceptibility of streptococci most frequently isolated from Czech dairy cows with mastitis.* Ann Anim Sci, **19,** 679–694.
55. **Souli M, Galani I, Antoniadou A, et al** (2010): *An outbreak of infection due to βlactamase Klebsiella pneumoniae carbapenemase 2-producing K. pneumoniae in a Greek University Hospital: molecular characterization, epidemiology, and outcomes.* Clin Infect Dis, **50,** 364–373.
56. **Vatopoulos A** (2008): *High rates of metallo-β-lactamase-producing Klebsiella pneumoniae in Greece – a review of the current evidence.* Euro Surveill, **13,** 8023.
57. **World Health Organisation** (2017): Available at http://www.who.int/drugresistance/documents/surveillance report/en./. (Accessed October 29, 2019).

58. **Zhang D, Zhang Z, Huang C, et al** (2018): *The phylogenetic group, antimicrobial susceptibility, and virulence genes of Escherichia coli from clinical bovine mastitis.* Dairy Sci, **101,** 572–580.

Presence of SARS-CoV-2 on surfaces and materials in supermarket social areas in Türkiye

Muammer GÖNCÜOĞLU[1,a] ✉, Naim Deniz AYAZ[2,b], Sabri HACIOĞLU[3,c], Samiye Öznur YEŞİL[3,d] Özcan YILDIRIM[3,e], Cevdet YARALI[3,f], Harun SEÇKİN[4,g], Bekir PAKDEMİRLİ[5,h]

[1]Ankara University, Faculty of Veterinary Medicine, Department of Food Hygiene and Technology, Ankara, Türkiye; [2]Kırıkkkale University, Faculty of Veterinary Medicine, Department of Food Hygiene and Technology, Kırıkkale, Türkiye; [3]Republic of Türkiye, Ministry of Agriculture and Forestry, Veterinary Control Central Research Institute, Ankara, Türkiye; [4]Republic of Türkiye, Ministry of Agriculture and Forestry, General Directorate of Food and Control, Ankara, Türkiye; [5]Republic of Türkiye, Ministry of Agriculture and Forestry, Ankara, Türkiye

[a]ORCID: 0000-0001-7245-1941; [b]ORCID: 0000-0003-2219-2368; [c]ORCID: 0000-0002-5493-0807; [d]ORCID: 0000-0002-8776-3822
[e]ORCID: 0000-0002-1113-6136; [f]ORCID: 0000-0002-0391-9456; [g]ORCID: 0000-0003-1115-6708; [h]ORCID: 0000-0002-0336-0613

ARTICLE INFO

Article History
Received : 19.04.2021
Accepted : 27.11.2021
DOI: 10.33988/auvfd.915360

Keywords
Contact surfaces
Foods
Real-time RT-PCR
SARS-CoV-2
Supermarket

✉**Corresponding author**
goncu@veterinary.ankara.edu.tr

How to cite this article: Göncüoğlu M, Ayaz ND, Hacıoğlu S, Yeşil SÖ, Yıldırım Ö, Yaralı C, Seçkin H, Pakdemirli B (2023): Presence of SARS-CoV-2 on surfaces and materials in supermarket social areas in Türkiye. Ankara Univ Vet Fak Derg, 70 (1), 75-80. DOI: 10.33988/auvfd.915360.

ABSTRACT

The aim of this study was to monitor the presence of SARS-CoV-2, the virus that cause the coronavirus disease 2019 (COVID-19), particularly on certain foods and surfaces that come in contact with food in district supermarkets in Ankara, Türkiye, where the highest number of COVID-19 cases was reported based on data from the Ministry of Health. For this purpose, a total of 172 samples were taken from 5 supermarkets in 4 districts in Ankara. RNA was extracted from the samples and RdRp gene-targeting reverse transcription quantitative polymerase chain reaction (RT-qPCR) assays were used to determine the presence of SARS-CoV-2. The results showed that all the supermarket samples collected during the period when there was a high number of COVID-19 cases in the district did not have SARS-CoV-2 except for one sample that was taken from a supermarket where COVID-19 had been detected among the staff. In this supermarket, COVID-19 RNA was detected with a high number of copies of 5 000, using Real-Time RT-PCR assay in pooled swab samples taken from salt shakers, pepper shakers, red pepper shakers, and vinegar and oil bottles in the social area that the staff used for lunchbreaks and other breaks. This finding shows that it is of great importance for public health agencies to monitor COVID-19 cases in food businesses in regions with a high number of cases and to take samples from these businesses at certain intervals, as a form of "early warning system."

Introduction

Coronoviruses (CoVs) were first known as viral agents related to the *Coronaviridae* family, which caused significant health problems mainly in mammals, birds, and fish. Later, human CoVs were discovered, associated with mild respiratory disorders (9, 17). In 2003, the severe acute respiratory syndrome-associated coronavirus (SARS-CoV) broke out globally; followed 10 years later by the Middle East respiratory syndrome-related coronavirus (MERS-CoV), which affected a more limited geographic area (26). In December 2019, a new coronavirus emerged in Wuhan, China. The novel coronavirus (2019-nCoV) was identified from a patient's broncho-alveolar lavage fluid (28). Full genome sequencing and phylogenetic analysis revealed that it belongs to a distinct clade from the betacoronaviruses associated with the previous SARS-CoV and MERS-CoV (28). The International Virus Taxonomy Committee named the virus SARS-CoV-2 and classified it under the genus *Betacoronavirus*. Although the main source of the transmission of SARS-CoV-2 has not yet been clearly determined, it is presumed to have been transmitted to humans from wild animals sold in the Huanan Seafood Wholesale Market in Wuhan (5). The disease caused by

this virus was named coronavirus disease 2019 (COVID-19) by the World Health Organization (WHO).

A total of 124,218,483 cases of COVID-19, 2,734,668 of which resulted in death, have been reported worldwide from the start of the epidemic to March 28, 2021 (1). Official authorities, especially WHO, emphasize that the main route of transmission of SARS-CoV-2 is person to person through respiratory droplets released during coughing, sneezing, and/or speaking (25). Studies have reported that other potential routes of transmission are droplet-contaminated surfaces or aerosols (21). Therefore, people can indirectly come in contact with COVID-19 by touching a contaminated surface and then touching their mouth, nose, or eyes (27). Although no direct foodborne transmission has been reported, examination of clinical records has revealed high incidence rates of gastrointestinal symptoms, particularly diarrhea, nausea, vomiting, and abdominal discomfort (2, 11, 14, 29, 12).

Considering this information, this study was carried out to investigate if SARS-CoV-2 can be detected in foods offered for sale in supermarkets and on surfaces that come in contact with food in such supermarkets in the districts of Ankara province in Türkiye, where the number of COVID-19 cases was reported by the country's Ministry of Health as the highest in the country. In addition, samples taken from the materials and surfaces used by the supermarket staff while eating in the social areas of the supermarket were collected and included in the study.

Materials and Methods

A total of 172 samples were taken from 5 supermarkets in 4 districts in Ankara. First, samples were collected from a supermarket in district that was closed officially because COVID-19 had been detected in some staff. The samples were taken both from the staff's social area and from the sales areas. Next, after examining the data from the Ministry of Health on districts with high numbers of COVID-19 cases, the districts of were chosen for further sampling. All samples were collected from popular supermarkets in these districts.

Collection of samples: All staff who participated in the collection of the samples were trained on sample collection, labeling, documentation, and biosecurity measures, and were transported from the laboratory to the collection sites and back to the laboratory. During the sampling, the sample collectors wore high-level biosecurity clothing. All the samples were collected after the closing times of the supermarkets, when all customers and staff have left and before the routine cleaning procedures. The surface samples were collected using the swab method, but fresh vegetables and fruits that could be consumed unpeeled were collected as whole foods. The surfaces from which samples were taken were "high-touch surfaces" by customers and supermarket personnel, as identified in literature (24).

The samples were delivered to the Etlik Veterinary Control Central Research Institute Virology Laboratory under a cold chain within two hours, where they were subjected to PCR analyses.

Sampling model: In each supermarket, 3 swab samples from each of the surfaces in the list below (in nos. 1 and 2) and 3 whole food samples of the fruits and vegetables listed below (in no. 3) were taken.

1. Surfaces
   a. Handles of supermarket trolleys
   b. POS device
   c. Cupboard and refrigerator covers and holders
   d. Cashier counters (movable bands)
   e. Butcher counter and cutting boards
   f. Staff gloves from different sections
2. Food packaging surfaces
   a. PET bottles (water bottles, other drink bottles, etc.)
   b. Glass vials
   c. Paper packaging (of flour, chocolate, etc.)
   d. Plastic packaging (of chips, pasta, yoghurt/ cheese, etc.)
   e. Cardboard packaging products
3. Vegetables and fruits
   a. Green leafy vegetables (lettuce, roka, parsley, etc.)
   b. Fruits (plums, strawberries, etc.)

Apart from the above samples, a total of 33 samples were taken from plastic surfaces such as salt shakers, pepper shakers, red pepper shakers, and vinegar and oil bottles used only by the personnel in the staff social areas of the supermarket with confirmed COVID-19 cases among its personnel. The samples were taken 36 hours after the supermarket was closed down due to the COVID-19 cases. No one had entered the officially closed plant during this period, and the samples were collected before the supermarket was cleaned and disinfected.

The surface swab samples were taken using a swab with a synthetic tip and a plastic shaft. The swab specimen collection vials contained 1.5-2.0ml sterile water. The sampling was done from 3 to 4 different material surfaces. The swab surface area was planned to be approximately 25 cm^2 (24). To increase the positive predictive value of the sampling process, each sampling area was swabbed several times. All the swabs were transported to the laboratory under a cold chain within two hours.

Extraction and real-time RT-PCR protocol: The swab samples were vortexed and 200µl samples were separated for RNA extraction. The RNA was extracted with the

DOI: 10.33988/auvfd.915360

cador Pathogen 96 QIAcube HT Kit using the QIAcube automated extraction robot (Qiagen, Hilden, Germany).

Primers and probe sets that targeted the SARS-CoV-2 RdRp gene were used (7). A 20µl reaction was set up that contained 5 µl of RNA and 12.5 µl of the 5x reaction buffer provided in the QuantiNova Pathogen+IC Kit (Qiagen, Hilden, Germany) that contained 0.8 nM each of a forward primer and a reverse primer and a 0.25nM probe. Thermal cycling was performed at 50°C for 10 minutes for the reverse transcription, followed by 95°C for 3 minutes and then 45 cycles each of 95°C for 5 s and of 58°C for 30 s. The RT-qPCR assays were performed using a Bio-Rad CFX96 thermal cycler (Bio-Rad Laboratories, Montreal).

Positive and negative controls were used for accuracy. The ETLVET3 (MW306668) isolate was used as the positive control. The DNA amount of the SARS-CoV-2 RdRp gene region was also measured. The SARS-CoV-2 RdRp gene region base was serially diluted according to log10 and was used as a standard in the evaluation of the results.

Results

All the samples from the supermarkets that were selected based on the high number of COVID-19 cases in their district were SARS-CoV-2-negative. However, the COVID-19 RNA was detected by real-time RT-PCR in the samples from the supermarket that had positive cases among its personnel.

In that supermarket, the pooled swab samples taken from salt shakers, pepper shakers, red pepper shakers, and vinegar and oil bottles that the staff used at meal times in their social area were positive.

The raw data, standard curve results, and copy number quantification summary were exported from Biorad CFX Manager Version 3.1. The slope of the standards was determined as -3.25 with an R2 value of 0.99 and a reaction efficiency of 103%.

As a result of the quantitation, the virus copy numbers in these samples were determined as 5 000 with a Ct value of 32. On the other hand, the other samples from this supermarket were determined as negative. The real-time RT-PCR result diagram is shown in Figure1.

Discussion and Conclusion

This study was performed to investigate the presence of SARS-CoV-2 in some foods, different contact surfaces, and different food packages in supermarkets in regions where the number of COVID-19 cases is high. According to our results, all the samples were negative except for one supermarket that had positive cases among its staff, where SARS-CoV-2 RNA was detected with a very high copy number, due to which the supermarket was officially closed. The detection of SARS-CoV-2 in the swab samples taken from the salt shakers, pepper shakers, and vinegar and oil bottles that were used by the personnel and were pooled 36 hours after the official closure of the supermarket is of great importance.

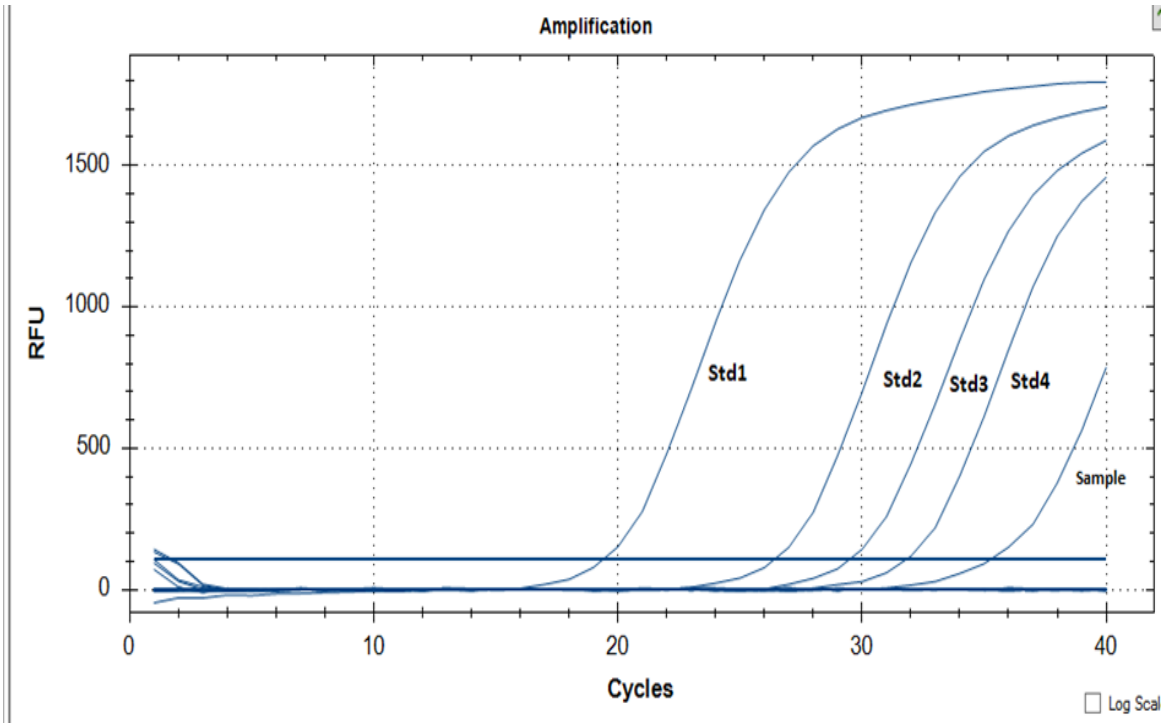

Figure 1. Real time RT-PCR result of a positive sample.

These results show that if personnel in food businesses are infected with SARS-CoV-2, they may infect the surfaces that food and customers come in contact with. Considering that the sampling was done 36 hours after the supermarket was closed, it showed that the virus RNA could be found on surfaces for more than 24 hours. Furthermore, the surfaces where the samples were found to be positive were used during eating and socializing, at which times people have a lot of contact with their mouths and noses. Although the customers were unlikely to have come in contact with infected droplets here, the results emphasize the negative impact of hygiene and attention deficit, considering the mouth-nose-eyes infection route. Cai et al. (2) reported that people may indirectly contract SARS-CoV-2 by touching their mouth, nose, or eyes after touching a contaminated surface. Considering our findings, it is thought that personnel working in food businesses, with or without symptoms, may pose significant public health hazards in cases where the necessary precautions are not taken, considering the potential droplet contamination.

It is general knowledge that viruses are obligate intracellular microorganisms. Thus, they cannot reproduce in environments other than living bodies, and they lose their vitality and infectivity doses over time. On the other hand, there have been studies on the viability of SARS-CoV-2 on different surfaces under approximate room temperature conditions. In one such study, cardboard, stainless steel, and plastic surfaces that were experimentally contaminated with 10^5 viruses were kept under room temperature conditions with 40% humidity. It was found that SARS- CoV-2 can survive on cardboard, stainless steel, and plastic surfaces for 24 hours, 48 hours, and 72 hours, respectively (21). Another experimental study with a similar number of viruses showed that the virus could survive for up to 21 days in biosafety equipment, especially in masks and gloves (13). Although this result was extreme, the findings from these two studies coincide with our findings from this study. We also detected SARS-CoV-2 RNA in the samples that we took 36 hours after the closure of the infected supermarket.

WHO and the United Nations Food and Agriculture Organization (FAO) stated in their guidelines published in April 2020 that the possibility of COVID-19 transmission through food or food packaging is low. This guide noted that COVID-19 is a respiratory disease, and the primary route of transmission is through person-to-person contact through direct contact with respiratory droplets from the infected person when the person coughs or sneezes. The guidelines also state that there is no evidence of SARS-CoV-2 transmission through food or food packaging (23). Since the publication of the guide, no other source of transmission of the disease has been reported besides the respiratory tract. However, this does not eliminate the possibility of fecal-oral contamination of food packaging or contact surfaces or their contamination with droplets from infected persons.

According to many studies conducted in different countries, sewage systems can be considered an important sources of transmission of coronavirus (14, 18). The similarity between the results obtained in the first SARS-CoV epidemic and the current findings is striking. In 2003, during the SARS-CoV outbreak, Lee (15) reported that the sewage system in Hong Kong served as a reservoir because the sewage system accommodated the feces of SARS-CoV patients. During the same period, SARS-CoV RNA was found in the sewage systems of two hospitals in Beijing (22). Chan et al. (4) also stated that the fecal excretion of SARS-CoV RNA may take more than 30 days.

The presence of SARS-CoV-2 in the feces of patients, in wastewater, on surfaces used in experimental studies, and finally, especially in frozen foods, is of great importance in terms of the characteristics of the agent, its spread, and its different potential transmission routes (3, 19, 20, 10, 12, 16).

Considering the homology between these three coronaviruses (SARS-CoV-2, SARS-CoV, and MERS-CoV), another confirmation of possible fecal-oral contamination emerges with a low-temperature tolerance of up to two weeks and a survival capacity of 20–30°C. The longer-term persistence of SARS-CoV-2 in the stool compared to respiratory swabs provides strong clinical evidence that fecal-oral transmission is likely (8, 11). Cheung et al. (6) reported that while 70.3% of the stool tests of the patients remained positive for SARS-CoV-2 RNA, their respiratory tract samples were negative. Additionally, Zhang et al. (27) confirmed the presence of live viruses in stool samples; and stool can contaminate food, water, hands, etc. and cause infection. Although these results strengthen the hypothesis that the virus may have a chance of spreading through the fecal-oral route, such hypothesis has not yet been proven.

To the best of our knowledge, this study is the first to detect SARS-CoV-2 from the salt shakers, pepper shakers, and vinegar and oil bottles used on tables during staff meals in the staff social area of a supermarket where some staff contracted COVID-19. The results show how important it is for public health agencies to monitor food businesses for COVID-19 cases and to take and test samples from these businesses. In our results, in addition to the detection of the SARS-CoV-2 RNA in the supermarket with active staff cases, the copy number there was found to be high. It is likewise important that the RNA of the agent was not detected in the supermarkets whose staff were not known to be positive for COVID-19. For these reasons, collection and testing of samples from supermarkets, restaurants, and other food-related

establishments in regions with high numbers of COVID-19 cases at certain intervals should continue as a form of "early warning system," as it has been determined that there is a possibility of transmission of the virus to surfaces that food and customers come in contact with, especially in food businesses, if the personnel carry the agent, whether symptomatically or asymptomatically. Considering that the sampling was done 36 hours after the establishment was closed, it was determined that the virus could be found on the surfaces of the materials used during eating for more than 36 hours. Thus, it is thought that the people who came in contact with the droplets there also had hygiene and attention deficit, since they acquired the agent through their mouth, nose, and eyes.

Acknowledgements

The authors are thankful to the staff of Republic of Türkiye, Ministry of Agriculture and Forestry for their support in sampling.

Financial Support

This work was financed by Republic of Türkiye, Ministry of Agriculture and Forestry.

Conflict of Interest

The authors declared that there is no conflict of interest.

Author Contributions

MG, NDA and HS conceived and planned the study. BP and HS approved the plan and publication of the study. MG, NDA, SH, SÖY, ÖY and CY contributed the sample collection procedures. SH carried out the experiments. MG, NDA, SH and CY contributed the interpretation of the results. MG took the lead in writing the manuscript. All authors provided critical feedback and helped the research, analysis and manuscript.

Data Availability Statement

The data supporting this study's findings are available from the corresponding author upon reasonable request.

Ethical Statement

This study does not present any ethical concerns.

Animal Welfare

Not applicable.

References

1. **Anon** (2020): *Johns Hopkins Coronavirus Resource Center-2020: COVID-19 case tracker*. Available at https://coronavirus.jhu.edu/. (Accessed 24 March 2021).
2. **Cai J, Sun W, Huang J, et al** (2020): *Indirect virus transmission in cluster of COVID-19 cases, Wenzhou, China, 2020.* Emerg Infect Dis, **26**, 1343-1345.
3. **Cha MH, Regueiro M, Sandhu DS** (2020): *Gastrointestinal and hepatic manifestations of COVID-19: A comprehensive review.* World J Gastroenterol, **26**, 2323-2332.
4. **Chan KH, Poon LL, Cheng VCC, et al** (2004): *Detection of SARS coronavirus in patients with suspected SARS.* Emerg Infect Dis, **10**, 294.
5. **Chen N, Zhou M, Dong X, et al** (2020): *Epidemiological and clinical characteristics of 99 cases of 2019 novel coronavirus pneumonia in Wuhan, China: A descriptive study.* Lancet, **395**, 507-513.
6. **Cheung KS, Hung IF, Chan PP, et al** (2020): *Gastrointestinal manifestations of SARS-CoV-2 infection and virus load in fecal samples from the Hong Kong cohort and systematic review and meta-analysis.* Gastroenterology, **159**, 81-95.
7. **Corman VM, Landt O, Kaiser M, et al** (2020): *Detection of 2019 novel coronavirus (2019-nCoV) by real-time RT-PCR.* Euro Surveil, **25**, 2000045.
8. **D'Amico F, Baumgart DC, Danese S, et al** (2020): *Diarrhea during COVID-19 infection: pathogenesis, epidemiology, prevention and management.* Clin Gastroenterol Hepatol, **18**, 1663-1672.
9. **Drosten C, Günther S, Preiser W, et al** (2003): *Identification of a novel coronavirus in patients with severe acute respiratory syndrome.* N Engl J Med, **348**, 1967-1976.
10. **Elsamadony M, Fujii M, Miurac T, et al** (2021): *Possible transmission of viruses from contaminated human feces and sewage: Implications for SARS-CoV-2.* Sci Total Environ, **755**, 142575.
11. **Gu J, Han B, Wang J** (2020): *COVID-19: Gastrointestinal manifestations and potential fecal–oral transmission.* Gastroenterology, **158**, 1518-1519.
12. **Han J, Zhang X, He S, et al** (2021): *Can the coronavirus disease be transmitted from food? A review of evidence, risks, policies and knowledge gaps.* Environ Chem Lett, **19**, 5-16.
13. **Kasloff SB, Strong JE, Funk D, et al** (2020): *Stability of SARS-CoV-2 on critical personal protective equipment.* Sci Rep, **11**, 1-7.
14. **Kocamemi BA, Kurt H, Sait A, et al** (2020): *Routine SARS-CoV-2 wastewater surveillance results in Turkey to follow Covid-19 outbreak.* MedRxiv, Available at https://www.medrxiv.org/content/medrxiv/early/2020/12/22/2020.12.21.20248586.full.pdf. (Accessed 24 March 2021).
15. **Lee SH** (2003): *The SARS epidemic in Hong Kong.* J Epidemiol Community Health, **57**, 652-654.
16. **Masotti F, Cattaneo S, Stuknytė M, et al** (2021): *Transmission routes, preventive measures and control strategies of SARS-CoV-2 in the food factory.* Crit Rev Food Sci Nutr, 1-12.
17. **Memish ZA, Assiri A, Alhakeem R, et al** (2014): *Middle East respiratory syndrome corona virus, MERS-CoV. conclusions from the 2nd scientific advisory board meeting of the WHO collaborating center for mass gathering medicine, Riyadh.* Int J Infect Dis, **24**, 51-53.
18. **Randazzo W, Truchado P, Cuevas-Ferrando E, et al** (2020): *SARS-CoV-2 RNA in wastewater anticipated COVID-19 occurrence in a low prevalence area.* Water Res, **181**, 115942.
19. **Rizoua M, Galanakisa IM, Aldawoudb TMS, et al** (2020): *Safety of foods, food supply chain and environment*

within the COVID-19 pandemic. Trends Food Sci Technol, **102**, 293-299.

20. **Thippareddi H, Balamurugan S, Patel J, et al** (2020): *Coronaviruses – Potential human threat from foodborne transmission?* LWT - Food Sci Technol, **134**, 110147.
21. **Van Doremalen N, Bushmaker T, Morris DH, et al** (2020). *Aerosol and surface stability of SARS-CoV-2 as compared with SARS-CoV-1.* N Engl J Med, **382**, 1564-1567.
22. **Wang XW, Li J, Guo T, et al** (2005): *Concentration and detection of SARS coronavirus in sewage from Xiao Tang Shan Hospital and the 309th Hospital of the Chinese People's Liberation Army.* Water Sci Technol, **52**, 213-221.
23. **World Health Organization** (2020): *COVID-19 and Food Safety: Guidance for Food Businesses.* Available at https://www.who.int/publications/i/item/covid-19-and-food-safety-guidance-for-food-businesses. (Accessed 24 March 2021).
24. **World Health Organization** (2020): *Surface sampling of coronavirus disease (COVID-19): A practical "how to" protocol for health care and public health professionals.* Available at https://www.who.int/publications/i/item/surface-sampling-of-coronavirus-disease-(-covid-19)-a-practical-how-to-protocol-for-health-care-and-public-health-professionals. (Accessed 24 March 2021).
25. **World Health Organization** (2021): *Coronavirus disease (COVID-19) pandemic.* Available at https://www.who.int/emergencies/diseases/novel-coronavirus-2019?gclid. (Accessed 24 March 2021).
26. **Zaki AM, Van Boheemen S, Bestebroer TM, et al** (2012): *Isolation of a novel coronavirus from a man with pneumonia in Saudi Arabia.* N Engl J Med, **367**, 1814-1820.
27. **Zhang W, Du RH, Li B, et al** (2020): *Molecular and serological investigation of 2019-nCoV infected patients: implication of multiple shedding routes*. Emerg Microbes Infect, **9**, 386-389.
28. **Zhu N, Zhang D, Wang W, et al** (2020): *China novel coronavirus investigating and research team. A novel coronavirus from patients with pneumonia in China, 2019.* N Engl J Med, **382**, 727-733.
29. **Zuber S, Brüssow H** (2020): *COVID 19: Challenges for virologists in the food industry.* Microb Biotechnol, **13**, 1689-1701.

DOI: 10.33988/auvfd.915360

Dynamic thiol-disulphide homeostasis and ischemia modified albumin levels in neonatal calf diarrhea

Osman Safa TERZİ[1,a], Erdal KARA[2,b,✉], Yasin ŞENEL[2,c], Ebubekir CEYLAN[1,d], Salim NEŞELİOĞLU[3,e], Özcan EREL[3,f]

[1]Ankara University, Faculty of Veterinary Medicine, Internal Medicine Department, Ankara, Türkiye; [2]Kırıkkale University, Faculty of Veterinary Medicine, Internal Medicine Department, Kırıkkale, Türkiye; [3]Yıldırım Beyazıt University, Faculty of Medicine, Clinical Biochemistry Department, Ankara, Türkiye

[a]ORCID: 0000-0002-7877-8897; [b]ORCID: 0000-0001-7047-9502; [c]ORCID: 0000-0003-0272-2712; [d]ORCID: 0000-0002-3993-3145
[e]ORCID: 0000-0002-0974-5717; [f]ORCID: 0000-0002-2996-3236

ARTICLE INFO

Article History
Received : 27.04.2021
Accepted : 11.12.2021
DOI: 10.33988/auvfd.928731

Keywords
Dynamic thiol-disulphide homeostasis
Ischemia modified albumin
Neonatal calf diarrhea
Oxidative stress

✉Corresponding author
erdalk185@hotmail.com

How to cite this article: Terzi OS, Kara E, Şenel Y, Ceylan E, Neşelioğlu S, Erel Ö (2023): Dynamic thiol-disulphide homeostasis and ischemia modified albumin levels in neonatal calf diarrhea. Ankara Univ Vet Fak Derg, 70 (1), 81-86. DOI: 10.33988/auvfd.928731.

ABSTRACT

The aim of this study was to determine dynamic thiol-disulphide homeostasis (TDH) parameters and ischemia modified albumin (IMA) levels in calves with neonatal diarrhea and compare with healthy controls. A total of 50 calves were included in the study. There were 25 calves in both diarrhea and healthy groups. Serum native thiol, total thiol, disulfide and IMA levels were measured using new methods. Native thiol (P=0.025) and total thiol (P=0.041) values decreased significantly in calves with neonatal diarrhea compared to the healthy control group. Disulphide (P= 0.133), disulphide/native thiol ratio (P=0.001) and IMA (P=0.0018) parameters were lower in healthy group, and the difference between the two groups was significant for the parameters other than disulphide. This study shows that TDH is impaired in neonatal calf diarrhea and IMA levels are increased due to oxidative stress.

Introduction

Calf diarrhea is one of the most important problems of cattle breeding in the neonatal period when the levels of maternal antibodies transferred by passive immunity decrease rapidly. Neonatal calf diarrhea cases characterized by excessive and watery defecation due to infectious and non-infectious causes (5, 15, 16). Calf losses are in the range of 10-15% in developed European countries. Even in farms with very good management conditions, this rate generally does not fall below 5%. It has been reported that in herds where these conditions are not well provided, mortality and morbidity rates can reach 50% and 100%, respectively. Diarrhea causes 60% of the deaths during the neonatal period (32, 34). Reasons such as calf death, costs for treatment and prophylaxis, growth retardation during the growth period, and the sale of animals below their value can be considered the most important economic problems in farms. The economic loss in the neonatal period depends on calf mortality in Türkiye is reported to be around 525 million euros annually (36).

Thiols are organic compounds that react with oxidants to form disulfide bonds. (6, 30). These bonds can turn back into thiols, resulting in dynamic thiol-disulfide homeostasis (TDH) (18). Dynamic TDH has important effects on detoxification, protection with antioxidants, apoptosis, regulation of enzymatic activity, and signaling mechanisms of cells (4). In recent years, many studies have been carried out in the field of human medicine, including gastrointestinal system diseases (20, 23, 30, 40) related to TDH (10). Oxidative stress, especially in farm animals, can be seen in many diseases, including calf diarrhea (24, 26, 40).

In acute ischemic cases, the metal binding capacity of albumin decreases, resulting in the formation of the metabolic substance known as ischemia modified albumin (IMA) (22). New evidence has been provided that the concentrations of IMA, one of the biomarkers associated with oxidative stress clinically, differ in the diagnosis of acute intestinal disease (28, 33).

The aim of the study was to analyse the TDH and serum IMA levels in calves with neonatal diarrhea. Considering the literature, it is the first study evaluating TDH and IMA levels in newborn calves with diarrhea.

Materials and Methods

Study population and location: A total of 50 calves were included in the study; 25 calves with diarrhea (15 males, 10 females) and 25 healthy calves (14 males, 11 females) between the ages of 3-28 days. Animals with diseases other than calf diarrhea in the patient group and animals that were subjected to non-standard care and feeding conditions in both groups were excluded. The study was carried out in Bala Tarım Dairy Farm, which has a capacity of approximately 1000 dairy cows in the Bala district of Ankara. This study was approved by Kırıkkale University Animal Experiments Local Ethics Committee (Date:24/12/2020).

Sample Collection and Analysis: Blood samples were taken from the jugular vein for TDH and IMA tests from diarrhea and healthy control groups. The samples were centrifuged at 3000 rpm for 10 minutes, after which the serum was separated and stored at -80 °C. Later, all parameters were studied in the same session and in the same serum sample. Serum native thiol, total thiol, disulphide and % disulfide/native thiol ratio were measured with the newly developed method by Erel and Neselioğlu (9). IMA levels were evaluated with the new method created by Bar-Or et al. (2).

Statistical Analysis: Statistical analyses were performed using GraphPad Prism version 8.4.2. (GraphPad Software, La Jolla California USA, www.graphpad.com). For all analyses, $P<0.05$ was considered significant. Normality assumption was evaluated using the Shapiro-Wilk Test. Descriptive analysis, mean and standard deviation data were presented. Due to the normal distribution of data, an independent sample t test was used to compare parameters between groups.

Results

Demographic characteristics, TDH and IMA values of healthy and diarrhea groups are given in Table 1. There was no statistical difference between the two groups in gender ($P>0.9999$) and age ($P=0.4222$) data.

In this study, neonatal diarrhea group was compared with healthy controls by measuring TDH and IMA parameters. Native thiol and total thiol values decreased significantly in calves with neonatal diarrhea compared to the healthy control group (Table 1, Figure 1a, Figure 1b). Disulphide, % disulphide/native thiol ratio and IMA parameters were lower in the healthy group, and the difference between the two groups was significant for the parameters other than disulphide (Table 1, Figure 1c, Figure 1d).

Table 1. Demographic characteristics, TDH parameters and IMA values of the control and diarrhea groups.

Variable	Healthy Control group mean±SD (n=25)	Diarrhea group mean±SD (n=25)	*P*
Native Thiol	386.40±32.74	360.3±45.33	**0.0251***
Total Thiol	437.8±37.19	409.4±56.60	**0.0416***
Disulphide	25.71±4.534	27.57±4.062	0.1331
% Disulphide/native thiol ratio	6.663±1.056	7.910±1.422	**0.001***
IMA	0.887±0.0597	0.940±0.0537	**0.0018***
Age	17.84±8.107	16.04±7.607	0.4222
Gender			>0.9999
Male (n/%)	14/56	15/60	
Female (n/%)	11/44	10/40	

*Indicates a significant statistical difference with $P<0.05$.

DOI: 10.33988/auvfd.928731

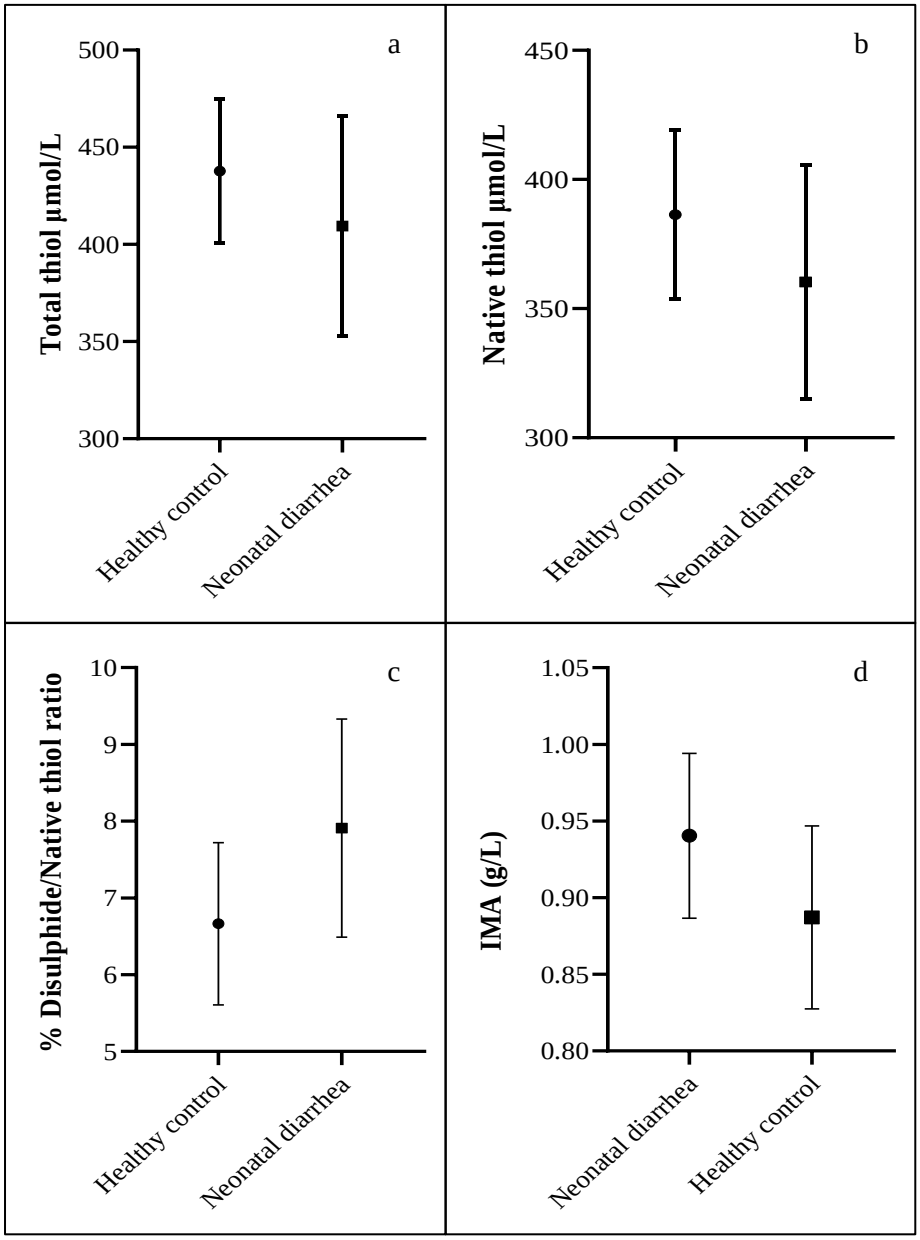

Figure 1. Thiol-disulphide homeostasis parameters and ischemia-modified albumin levels in healthy control and neonatal diarrhea groups. a)Total thiol (µmol/L) values b)Native thiol (µmol/L) values c)%Disulphide/native thiol ratio d) IMA (Ischemia-modified albümin) (g/L) values.

Discussion and Conclusion

High levels of free oxygen radicals in blood samples taken from healthy newborn calves indicate the occurrence of oxidative stress immediately after birth. Although the level of oxygen radicals in the blood decreases within the first week, it tends to increase again after change of care and feeding conditions (13). In the study conducted by Topaktaş (39), there are different opinions. In the studies in which the changes in the total oxidant level (TOS) and total antioxidant level (TAS) in newborn calves in the first month period were followed; Blood samples were taken from 20 calves (10 males and 10 females) at 0, 24, 72 hours and 14, 28 days in total 5 times after birth and analyzed in terms of TOS and TAS values (39). It was revealed that there was no significant change in TOS and TAS values in blood serum in the first 28-day period, which corresponds to the neonatal period in calves. Even though newborn calves can cope with oxidative stress, calf diarrhea, which is frequently encountered in the first 28 days of age, makes this struggle difficult. In diarrhea cases, intestinal permeability is impaired and oxidative stress increases, often the 2nd and 3rd weeks as a result of the acceleration of oxidative metabolism with the resulting in sepsis, by triggering many local or systemic

pathological units (25, 29, 31, 38). Physiologically native thiol, disulfide and total thiol are in a balance. This system, also known as TDH, is affected by various situations where oxidative stress occurs as a result of oxidation and reduction reactions (9). In order to evaluate the effects of oxidative stress on TDH in calf diarrhea, serum TDH parameters of 3-28 days old calves with diarrhea were compared with those of healthy ones.

Before the new method (Erel and Neselioglu 2014) was found, only the levels of some oxidant or antioxidant substances were determined in the studies (12, 14, 24). However, in our study, the levels of TDH parameters (native thiol, total thiol, disulfide and % disulfide/native thiol ratio) were measured with the aforementioned new method and TDH status was evaluated.

Reactive oxygen species (ROS) are highly toxic to cells, and the formation of oxygen radicals above the physiological level can initiate oxidative damage in the gut, damaging the intestinal antioxidant defense system (34, 35, 37). Thiol protein groups form an important antioxidant group and account for 52.9% of total serum antioxidant capacity in healthy people (9). Therefore, it can be expected that compounds containing thiol will decrease in plasma due to oxidation in the inflamed intestine (30). In the studies carried out; it was observed that oxidative stress occurred in calves with diarrhea, antioxidant values were significantly decreased and oxidant levels increased compared to healthy calves (1, 24, 34). Similar results are also seen in treatment studies (14, 19).

In the study of Neselioglu et al. (30) in people with ulcerative colitis; native thiol, total thiol and disulfide levels were significantly reduced when compared with healthy controls. According to our results, it is seen that native thiol and total thiol levels decrease in calves with diarrhea, and disulfide levels increase, although not statistically significant. In this ulcerative collitis study, it is stated that the reason for the reduction of disulfide bonds may be the conversion of thiol groups to disulfide bonds. Thus, it was observed that the TDH system did not shift to thiol group or disulfide bond formation and TDH system weakened. Similar to this study in humans, Çamkerten et al. (3) in their study in sheep with sarcoptic mange, it was revealed that the levels of native thiol, total thiol and disulfide were significantly lower in the patient group. According to the literature, it is known that while disulfide levels are higher in people with degenerative diseases, these values are lower in some immunological and oncological diseases (9). In our study, we see that disulfide levels in calves with diarrhea are higher than the healthy control group, although it is not statistically significant.

In the current literature, there is no study on the status of the TDH system in gastrointestinal system diseases in the veterinary field. In a study by Erdoğan et al. (11); the effects of dehorning with hot iron under the effect of generel or local anesthesia and painkillers on TDH were investigated. Native thiol and total thiol levels decreased without any significance in all groups throughout the study period. Disulfide levels did not show any significant changes in group, time, and group by time interactions. In this dehorning study (11), the decrease in thiol concentrations without an increase in disulfide levels was attributed to either insufficient uptake or increased degradation. Another reason for this situation is that changes in thiol and disulfide levels are thought to be caused by factors related to nutrition, not oxidative stress. In our study, low thiol and high disulfide (not statistically significant) levels were observed in the diarrhea group and it is thought that the reason might be directly oxidative stress.

Oxidative stress strongly affects albumin. Oxygen radicals bind to albumin and change its structure and IMA is formed. For this reason, IMA has been accepted as an indirect marker of increased oxidative stress. (27). In human medicine, studies conducted on people with inflammatory bowel disease, one of the gastrointestinal system diseases; It was concluded that IMA levels were higher than healthy controls (17) and positively correlated with disease activity levels (21). In a study conducted on children with irritable bowel disease; it was observed that TDH was impaired and IMA levels increased in the patient group (8). Although many parameters, indicate oxidative stress in gastrointestinal system diseases, have been evaluated in the field of veterinary medicine in the current literature, there is no study investigating IMA levels. In a study on dogs with Canine Distemper (7), IMA, disulfide, % disulfide/native thiol ratio and % disulfide/total thiol ratio levels were higher, while native thiol, total thiol, % native thiol/total thiol ratio and albumin levels were significantly lower than the control group, and this was interpreted as canine distemper increased oxidative stress in dogs. The results obtained in our study are parallel to the studies conducted in the field of human and veterinary medicine, both in terms of TDH parameters and IMA levels.

In conclusion, this study shows that TDH is impaired and IMA levels are increased due to oxidative stress in neonatal calf diarrhea. More studies should be conducted to detail our results in etiological terms and to evaluate the effectiveness of antioxidants in prevention or treatment options for neonatal calf diarrhea.

Financial Support

This research received no grant from any funding agency/sector.

Conflict of Interest

The authors declared that there is no conflict of interest.

Author Contributions

OST, EK, YŞ and EC undertook the planning of the study, forming the groups and collecting the samples. SN and EE performed biochemical analyzes. All authors contributed equally to the evaluation of the results and the creation of the article.

Data Availability Statement

The data supporting this study's findings are available from the corresponding author upon reasonable request.

Ethical Statement

This study was approved by the Kırıkkale University Animal Experiments Local Ethics Committee. (Date: 24/12/2020).

Animal Welfare

The authors confirm that they have adhered to ARRIVE Guidelines to protect animals used for scientific purposes.

References

1. **Ahmed W, Hassan SE** (2007): *Applied studies on coccidiosis in growing buffalo-calves with special reference to oxidant/antioxidant status.* World Journal of Zoology, **2**, 40-48.
2. **Bar-Or D, Lau E, Winkler JV** (2000): *A novel assay for cobalt-albumin binding and its potential as a marker for myocardial ischemia-a preliminary report.* J Emerg Med, **19**, 311-315.
3. **Çamkerten İ, Çamkerten G, Erdoğan H, et al** (2019): *Serum thiol disulphide levels among sheep with sarcoptic mange.* Kafkas Univ Vet Fak Derg, **25**, 865-868.
4. **Circu ML, Aw TY** (2010): *Reactive oxygen species, cellular redox systems, and apoptosis.* Free Radic Biol Med, **48**, 749-762.
5. **Constable PD, Hinchcliff KW, Done SH, et al** (2016): Veterinary Medicine - E-BOOK: A textbook of the diseases of cattle, horses, sheep, pigs and goats. Elsevier Health Sciences.
6. **Cremers CM, Jakob U** (2013): *Oxidant sensing by reversible disulfide bond formation.* J Biol Chem, **288**, 26489-26496.
7. **Değirmençay Ş, Çamkerten G, Çamkerten İ, et al** (2021): *An investigation of thiol/disulfide homeostasis and ischemia-modified albumin levels to assess the oxidative stress in dogs with canine distemper.* Veterinarski Arhiv, **91**, 39-49.
8. **Durankuş F, Şenkal E, Çam S, et al** (2021): *Altered thiol/disulfide homeostasis and ischemia-modified albumin levels in children with irritable bowel syndrome.* Pediatrics International, **63**, 300-305.
9. **Erel O, Neselioglu S** (2014): *A novel and automated assay for thiol/disulphide homeostasis.* Clin Biochem, **47**, 326-332.
10. **Erel Ö, Erdoğan S** (2020): Thiol-disulfide homeostasis: an integrated approach with biochemical and clinical aspects. Turk J Med Sci, **50**, 1728-1738.
11. **Erdogan H, Camkerten İ, Camkerten G, et al** (2019): *The Effect of hot-iron disbudding on thiol-disulphide homeostasis in calves.* Kafkas Univ Vet Fak Derg, **25**, 335-339.
12. **Erkilic EE, Erdogan HM, Ogun M, et al** (2016): *Relationship between hepcidin and oxidant/antioxidant status in calves with suspected neonatal septicemia.* Veterinary World, **9**, 1238-1241.
13. **Gaál T, Ribiczeyné-Szabó P, Stadler K, et al** (2006): *Free radicals, lipid peroxidation and the antioxidant system in the blood of cows and newborn calves around calving.* Comp Biochem Physiol - B Biochem Mol Biol, **143**, 391-396.
14. **Garkhal J, Chethan G, Gupta V, et al** (2017): *Antioxidant potential of coenzyme Q10 in Escherichia coli associated calf diarrhea.* Indian J Anim Sci, **87**, 694-700.
15. **Gomez DE, Weese JS** (2017): *Viral enteritis in calves.* The Canadian veterinary journal = La Revue Veterinaire Canadienne, **58**, 1267-1274.
16. **Gökçe E, Erdoğan H** (2013): *Neonatal buzağılarda kolostral immunoglobulinlerin pasif transferi.* Turkiye Klinikleri J Vet Sci, **4**, 18-46.
17. **Guntas G, Sahin A, Duran S, et al** (2017): *Evaluation of Ischemia-Modified Albumin in Patients with Inflammatory Bowel Disease.* Clin Lab, **63**, 341-347.
18. **Jones DP, Liang Y** (2009): *Measuring the poise of thiol/disulfide couples in vivo.* Free Radic Biol Med, **47**, 1329-38.
19. **Kabu M, Cigerci IH, Uyarlar C, et al** (2015): *Determination of pre and post treatment oxidative status and oxidative DNA damage in diarrheic calves.* Indian J Anim Res, **49**, 830-833.
20. **Kaplan M, Ates I, Yuksel M, et al** (2017): *Thiol/disulphide homeostasis in celiac disease.* World J Gastrointest Pharmacol Ther, **8**, 120-126.
21. **Kaplan M, Yuksel M, Ates I, et al** (2016): *Is ischemia modified albumin a disease activity marker for inflammatory bowel diseases?* J Gastroenterol Hepatol, **31**, 1120-1125.
22. **Keating L, Benger JR, Beetham R, et al** (2006): *The PRIMA study: presentation ischaemia-modified albumin in the emergency department.* Emergency Medicine Journal : EMJ, **23**, 764-768.
23. **Köseoğlu H, Alışık M, Başaran M, et al** (2018): *Dynamic thiol/disulphide homeostasis in acute pancreatitis.* Turk J Gastroenterol, **29**, 348-353.
24. **Kumar S, Jakhar K** (2020): *Haematological, biochemical and oxidative stress parameter as prognostic indicators in calf diarrhoea.* The Pharma Innovation Journal, **9**, 10-13.
25. **Lewis K, Caldwell J, Phan V, et al** (2008): *Decreased epithelial barrier function evoked by exposure to metabolic stress and nonpathogenic E. coli is enhanced by TNF-alpha.* Am J Physiol Gastrointest Liver Physiol, **294**, G669-678.
26. **Lykkesfeldt J, Svendsen O** (2007): *Oxidants and antioxidants in disease: oxidative stress in farm animals.* Vet J, **173**, 502-511.
27. **Ma S-g, Jin Y, Xu W, et al** (2012): *Increased serum levels of ischemia-modified albumin and C-reactive protein in type 1 diabetes patients with ketoacidosis.* Endocrine, **42**, 570-576.
28. **Montagnana M, Danese E, Lippi G** (2018): *Biochemical markers of acute intestinal ischemia: possibilities and limitations.* Ann Transl Med, **6**, 341-341.

29. **Moura FA, de Andrade KQ, Dos Santos JCF, et al** (2015): *Antioxidant therapy for treatment of inflammatory bowel disease: Does it work?* Redox Biol, **6**, 617-639.
30. **Neselioglu S, Keske PB, Senat AA, et al** (2018): *The relationship between severity of ulcerative colitis and thiol-disulphide homeostasis.* Bratisl Lek Listy, **119**, 498-502.
31. **Oldham KM, Wise SR, Chen L, et al** (2002): *A longitudinal evaluation of oxidative stress in trauma patients.* JPEN J Parenter Enteral Nutr, **26**, 189-197.
32. **Orro T, Nieminen M, Tamminen T, et al** (2006): *Temporal changes in concentrations of serum amyloid-A and haptoglobin and their associations with weight gain in neonatal reindeer calves.* Comp Immunol Microbiol Infect Dis, **29**, 79-88.
33. **Peoc'h K, Nuzzo A, Guedj K, et al** (2018): *Diagnosis biomarkers in acute intestinal ischemic injury: so close, yet so far*. Clin Chem Lab Med, **56**, 373-385.
34. **Ranjan R, Naresh R, Patra RC, et al** (2006): *Erythrocyte lipid peroxides and blood zinc and copper concentrations in acute undifferentiated diarrhoea in calves.* Vet Res Commun, **30**, 249-254.
35. **Sido B, Hack V, Hochlehnert A, et al** (1998): *Impairment of intestinal glutathione synthesis in patients with inflammatory bowel disease.* Gut, **42**, 485-492.
36. **Şahal M, Terzi OS, Ceylan E, et al** (2018): *Buzağı ishalleri ve korunma yöntemleri.* Lalahan Hayvancılık Araştırma Enstitüsü Dergisi, **58**, 41-49.
37. **Van der Vliet A, Bast A** (1992): *Role of reactive oxygen species in intestinal diseases.* Free Radic Biol Med, **12**, 499-513.
38. **Winterbourn CC, Buss IH, Chan TP, et al** (2000): *Protein carbonyl measurements show evidence of early oxidative stress in critically ill patients.* Crit Care Med, **28**, 143-149.
39. **Topaktaş B** (2019): Sağlıklı buzağılarda doğumu takip eden ilk bir ay içerisinde total oksidan seviye ve total antioksidan kapasitedeki değişimlerin araştırılması. Yüksek Lisans Tezi. Erciyes Üniversitesi Sağlık Bilimleri Enstitüsü, Kayseri.
40. **Yüksek N, Çatalkaya E, Başbuğan Y, et al** (2021): *Effect of Probiotic on Total Antioxidant (TAS) and Total Oxidant (TOS) in Treatment of Newborn Calf Diarrhea*. Turkish Journal of Veterinary Research, **5**, 11-15.

Investigation of the *in vitro* antibacterial, cytotoxic and *in vivo* analgesic effects of silver nanoparticles coated with *Centella asiatica* plant extract

Ogün BOZKAYA[1,4,a,✉], Hüsamettin EKİCİ[2,b], Zehra GÜN GÖK[3,c], Esra ARAT[4,d], Seda EKİCİ[5,e] Mustafa YİĞİTOĞLU[3,f], İbrahim VARGEL[5,g]

[1]Hacettepe University, Institute of Science, Department of Bioengineering, Ankara; [2]Kırıkkale University, Faculty of Veterinary Medicine, Department of Pharmacology and Toxicology, Kırıkkale; [3]Kırıkkale University, Faculty of Engineering and Architecture, Department of Bioengineering, Kırıkkale; [4]Kırıkkale University, Scientific and Technological Research Application and Research Center, Kırıkkale; [5]Veterinary Control Central Research Institute, Ankara; [6]Hacettepe University, Faculty of Medicine, Department of Plastic Reconstructive and Aesthetic Surgery, Ankara

[a]ORCID: 0000-0001-8381-8649; [b]ORCID: 0000-0001-6403-737X; [c]ORCID: 0000-0001-6426-0395; [d]ORCID: 0000-0002-9259-2538
[e]ORCID: 0000-0002-7982-5261; [f]ORCID: 0000-0002-6024-9129; [g]ORCID: 0000-0002-7657-8170

ARTICLE INFO

Article History
Received : 26.10.2021
Accepted : 04.01.2022
DOI: 10.33988/auvfd.1014802

Keywords
Analgesic effect
Antibacterial effect
Centella asiatica
Cytotoxicity
Silver nanoparticles

✉Corresponding author
ogunbozkaya@hacettepe.edu.tr

How to cite this article: Bozkaya O, Ekici H, Gün Gök Z, Arat E, Ekici S, Yiğitoğlu M, Vargel İ (2023): Investigation of the *in vitro* antibacterial, cytotoxic and *in vivo* analgesic effects of silver nanoparticles coated with *Centella asiatica* plant extract. Ankara Univ Vet Fak Derg, 70 (1), 87-96. DOI: 10.33988/auvfd.1014802.

ABSTRACT

In recent years, researchers have shown an increased interest in using medicinal plants for the synthesis of silver nanoparticles (AgNPs) having various therapeutic properties. *Centella asiatica* (CA), a medicinal plant, has been used to treat minor burn wounds, psoriasis, and hypertrophic wounds among many other pathological conditions. The current study aimed to synthesize CA coated AgNPs (CA-AgNPs) with appropriate biocompatibility and various therapeutic properties, including antimicrobial and analgesic activities. The synthesized CA-AgNPs were characterized by ultraviolet-visible (UV-Vis) spectroscopy, zeta potential measurements, and fourier transform infrared (FT-IR) spectroscopy. The formation of spherical CA-AgNPs was confirmed by a single surface plasmon resonance (SPR) peak emerging at 420 nm wavelength by UV-Vis. The average hydrodynamic diameter and zeta potential of the particles were found to be 29.5 nm and -24.5 mV, respectively. The FT-IR analyses showed that the AgNPs were coated and stabilized by bioactive compounds from the CA extract. MTT cytotoxicity assay revealed that CA-AgNPs at ≤1 mM concentrations exhibited biocompatibility for L929 fibroblast cells. The antimicrobial activity of CA-AgNPs was confirmed by significant inhibition of *Staphylococcus aureus* and *Escherichia coli*. In addition, the analgesic effect of CA-AgNPs was investigated for the first time in the literature by tail-flick and hot plate methods, and statistically significant results were obtained for both methods. Taken together, these results suggest that CA-AgNPs can be used as an effective antibacterial and analgesic agent in a variety of biomedical applications, including coating wound dressings.

Introduction

Plants have been used in the treatment of wounds, treatment of diseases, and protection against diseases since the earliest periods of human history. The ethnomedicinal use of plants (in the form of teas, syrups, oils, etc.) in the therapy of wounds and diseases is not only inexpensive and reachable, but also supplies a natural resource of medicinal materials. Studies on medicinal plants have approved that herbal drugs display fewer side effects in comparison to chemical (synthetic) matters, and are more cost-effective. While about 3% of the chemicals listed in the Western pharmacopoeia are effective for the treatment of wounds and skin diseases, herbal drugs are considered to be largely beneficial (23). With the development of science and scientific methods, the chemical structure of many bioactive components in the structure of plants has been clarified and many researches (*in vitro* and *in vivo*) have been made on these molecules (25). Many therapeutic effects of plants, such as antimicrobial, antitumor, antiviral, antiinflammatory,

antimalarial are known (45). In addition, the analgesic effects of some plants used in traditional medicine in recent years have been investigated by ethnobotanical studies. The analgesic effect of a plant is characterized by its activity to prevent, reduce, or relieve pain (44). *Centella asiatica* (CA) has critical importance among medicinal plants with therapeutic and analgesic effects.

In Asian countries, CA has been utilized as a traditional herbal medicine for hundreds of years. This medicinal plant has been reported to enhance wound healing and reduce scar formation (11, 28, 38, 51). CA extract shows wound healing, antioxidant, anticonvulsant, anti-inflammatory, antidiabetic, anti-psoriatic, anti-ulcer, sedative, immunostimulant, and cardioprotective properties (35). It has also been reported that CA improves memory and cognitive functions in rats (14, 43). Besides all these features, a methanolic extract of this plant demonstrated *in vitro* antiproliferative property in mouse fibrosarcoma cells, human gastric adenocarcinoma cells, human liver cancer cells, murine melanoma cells, MK-1, B16F10, SVK-14, keratinocytes, and *in vivo* tumor model test systems (3, 4, 6, 54). CA extract contains major triterpenoid components (madecassoside, asiatic acid, asiaticoside, and madecassic acid, etc.), and mixtures of them can stimulate collagen synthesis in *in vitro* human fibroblasts (5). Among the components of CA extract, asiaticoside has strong wound healing properties and reduces wound formation (27, 50). Asiaticoside increases fibroblast proliferation and extracellular matrix synthesis in wound healing (19). Madecassoside's effect on wound healing can include many mechanisms, including antioxidant activity, collagen synthesis, and angiogenesis (27, 50). Asiatic acid has antioxidant, anti-inflammatory, and neuroprotective properties (30, 52).

Nanoparticles research is an area of important scientific attention because of their large surface area to volume ratio and various physicochemical characteristics (33, 34). Many nanoparticles, such as copper, zinc, gold, and silver, have been synthesized by researchers. However, among these, silver nanoparticles (AgNPs) have proven to be highly effective against bacteria, viruses, and other eukaryotic microorganisms (31). AgNPs show the highest antimicrobial activity among all silver forms due to their large surface areas and sizes (42). AgNPs are synthesized by physical, chemical, and biological/green methods (21). The synthesis of AgNPs with plant extract (green synthesis) has attracted great interest in recent years because it is a low-cost and environmentally friendly method (46). The most important advantage of AgNPs synthesized from plant extracts is that they contain therapeutic molecules of plants used in traditional medicine (29).

The analgesic effects of extracts of *Centella asiatica* prepared with various solvents were investigated in the literature, but no such study was found with CA-coated AgNPs (CA-AgNPs). Therefore, the aim of this study is to investigate the analgesic activities of *Centella asiatica* coated AgNPs, which we produced by the green synthesis method, in rats. Additionally, the cytotoxic and antibacterial effects of the synthesized CA-AgNPs were also investigated. We will use the obtained CA-AgNPs as an active agent in wound dressing materials due to their antimicrobial, biocompatibility and analgesic properties.

Materials and Methods

Materials: The dried CA leaves were purchased from a local market (Şifa Market, Bursa, Türkiye). For high-performance liquid chromatography (HPLC) analyses, the analytical standards of asiatic acid, asiaticaside, madecassic acid and madecassoside were purchased from Sigma-Aldrich (Germany). For AgNPs synthesis, $AgNO_3$ was supplied from Sigma-Aldrich (Germany). For antibacterial analyses, the cultures of *E. coli* (ATCC 25922) and *S. aureus* (ATCC 25923) were taken from Kırıkkale University Scientific and Technological Research Laboratories (KÜBTUAM). The solid and liquid broth used in antibacterial tests and bacterial culture were obtained from Sigma-Aldrich (Germany). For cytotoxicity test, cell culture chemicals (DMEM, FBS, Trypsin/EDTA solution, Penicillin/Streptomycin) were obtained from Biochrom (Merck, Germany) and other cell culture materials were taken from Greiner (Austria).

Preparation of CA Plant Extract: Approximately 10 grams of dried CA samples were taken and extracted in a mixture of 100 mL methanol-water mixture (10:90% v/v) with an automatic extraction apparatus for 1 hour. After extraction, the solvent was removed with the aid of an evaporator. The resulting solid plant extract was dissolved in water and the solution was filtered with a 0.45 µm filter. The prepared solution was analyzed by HPLC (41).

Synthesis of CA-AgNPs: For CA-AgNPs synthesis, 1% solution of the plant extract obtained in the above-mentioned method in methanol:water was prepared and the pH of the solution was adjusted to 11 with 5 M NaOH to form negative charge groups (COO^- groups) in the plant extract. 5 mL of this solution was taken and added to the $AgNO_3$ solution (20 mL) which was prepared at different concentrations (0.1, 0.2, 0.3, 0.4, 0.5, 1, 2, 4, 6, 8 and 10 mM). With the addition of plant extract, the color of the $AgNO_3$ solutions immediately turned yellow-brown. The resulting mixtures were stirred at room temperature until this color change was constant (approximately 24 h). The synthesized CA-AgNPs were then purified by passing through 0.45 µL filter and stored at +4 ºC in falcon tubes.

Characterization of CA-AgNPs: The SPR peaks of the synthesized CA-AgNPs were measured by UV-Vis spectrophotometer between 350-600 nm to evaluate the

DOI: 10.33988/auvfd.1014802

production of AgNPs. The size and zeta potential of CA-AgNPs were found by a Zetasizer (Malvern Instruments, Malvern, UK). The chemical structure of the CA-AgNPs was investigated by a FTIR (Vertex 70V, Bruker) with ATR method after the CA-AgNPs powders obtained by drying the samples at room temperature.

Evaluation of Antibacterial Properties of the Synthesized CA-AgNPs: A minimal inhibition concentration (MIC) assay was performed to determine the antimicrobial activity of the synthesized CA-AgNPs. Fresh 24-hour cultures of *E. coli* and *S. aureus* strains were used for the experiment. Bacteria concentration equivalent to 0.5 McFarland turbidity solution (OD 0.08-0.13 at 600 nm) was prepared with sterile phosphate buffer solution from 24-hour fresh cultures and spectrophotometric measurements were made to check the turbidity. The microorganisms whose concentration was adjusted were diluted 1:10 before MIC test. Microdilution method was used in the experiment. For the microdilution method, 100 µL of Mueller Hinton broth and 100 µL of material were added to the 96-well plates to be tested. Then, 5 µL of the prepared microorganism was added to the suspension. For sterility control only wells with medium and antibiotic wells (Gentamicin-64 µg mL^{-1}) were assayed for experimental control. The plate was incubated at 37 °C for 16-20 hours. After incubation, the turbidity was checked with visually. The growth was observed only in wells containing microorganisms, while turbidity was not observed in wells containing antibiotic and materials. Sterility control was considered successful due to the absence of turbidity in the sterility wells. Since CA-AgNPs have a brown color, the turbidity of samples could not be properly checked. To evaluate if bacteria have grown in suspensions containing CA-AgNPs, 10 µL was taken from each well and inoculated on Mueller Hinton agar. The samples were incubated at 37 °C for 18-24 hours. The reproduction was checked after incubation.

Cytotoxicity Tests: The cytotoxicity effects of CA and CA-AgNPs samples were investigated by MTT test. MTT is a very sensitive test to determine cell viability using 3,[4,5-dimethylthiazol-2-yl]-2,5-diphenyltetrazolium bromide (MTT) salt. L929 fibroblast) cells were inoculated into 96-well plates at a concentration of $10x10^3$ per well. Cells were incubated at 37 ºC for 24 hours in a 5% CO_2 conditioned incubator. Then, CA and CA-AgNPs solutions at various concentrations (between 1 mM and 10 mM) were applied to L929 fibroblast cells and incubated for 24 hours. For the control group, just cell medium was used. CA and CA-AgNPs were studied in triplicate. At the end of the 24-hour incubation, the cell medium was discarded from the wells and 50 µl of MTT solution (1 mg/ml) was added each. After 2 hours of incubation, the MTT solution was removed from the wells and 100 µl of isopropanol was added to each well and read at 570 nm wavelength in the ELISA plate reader. Cell viability (%) was obtained by comparing the results from the ELISA reader with the control group (15, 32).

Analgesic Effect: In this study, 14 healthy male Wistar albino rats aged 4-12 weeks were used. The number of animals to be used in the experiments was determined by performing a t-test with the G-power program according to the number of groups, 80% power expectation, and the expected effect width between groups on the basis of previous studies (46, 53). The rats were kept in separate cages at specific ambient conditions (22±3 ºC, 55±2% humidity, 12 hours dark-12 hours light). Rats were fed ad-libitum with commercial feed and water without dietary restrictions. Before the study, all animals were weighed. The animals were divided into two groups, seven in each group. The tail flick method was used in one group and the hot plate method was used in the other group. Equal amounts (1 mL) of saline and 1 mM CA-AgNPs solutions were applied transdermally to both groups. All studies were carried out in Kırıkkale University Hüseyin Aytemiz Experimental Research and Application Laboratory. The study was approved by Kırıkkale University Animal Experiments Local Ethics Committee with the decision dated 26.05.2021, numbered 2021/05, meeting numbered 24.

The tail flick method, which is used to determine the analgesic effect, was first suggested by D'Amour and Smith (9). In this method, the analgesic effect is characterized by the time elapsed after thermal heat is applied to the tail of the animal until it withdraws its tail. In this study, the animals' tail pulling response was monitored by applying heat to approximately 2 cm proximal part of the tail. Then, the time (seconds) was determined when the animal pulled its tail from the point where the radiant heat was applied. Experiment time was limited to a maximum of 15 seconds in order to avoid injury to the animal tail.

The hot plate test was used to figure out analgesic effect by the method explained by Eddy and Leimbach (10). Rats were kept on a hot plate at 53±1 °C. The reactions of animals (such as pulling their hind legs, licking, kicking or jumping) placed on the hot surface were monitored from the first moment. The maximum experimental time was limited to 30 seconds to avoid injury to the animals (39). To measure of animals' response to temperature, basal measurement was made 30 minutes before serum and CA-AgNPs application.

Statistical analysis: The data was first analyzed for the parametric test assumption. The distribution of differences (normality test) between saline and CA-AgNPs application was tested by Shapiro Wilk test in both methods. Levene test was applied to inhibition percentage for homogeneity of variances in both methods. The test

results revealed that the data was normally distributed and variances are homogeneous. The paired t was applied to test the difference between saline and CA-AgNPs application in both methods. Student t test (independent t test) was applied to see if there is a difference between inhibition percentages in both methods. The $P < 0.05$ was accepted as statistical significance level. IBM SPSS Statistics for Windows, Version 25.0 (Armonk, NY: IBM Corp.) was used for analysis. All results were expressed as mean ± SE.

Results

Synthesis and characterization of CA-AgNPs: In this study, biosynthesis of AgNPs was performed by using green synthesis method using CA plant extract. According to HPLC analysis results, it was determined that CA extract contains four bioactive molecules that play a role in wound healing and analgesic effect (Figure 1). When silver ions were added to the plant extract, they were reduced to AgNPs through the functional groups in the structure of the plant. The color change of the solution from yellow to dark brown indicates the formation of AgNPs.

The formation and stability of AgNPs in colloidal solution were analyzed by UV-VIS (Perkin Elmer Lambda 35) spectrometer. It was observed that the solution showed maximum absorbance at 420 nm and the absorbance value increased with increasing $AgNO_3$ concentrations (Figure 2a). The sizes and zeta potentials of the synthesized CA-AgNPs were analyzed with Zeta sizer and the results are shown in Table 1. It was found that all of the synthesized AgNPs had negative zeta potential and these results showed that produced AgNPs were stable. The formation of a single peak in the zeta potential distribution graph (Figure 2b) proves that the solutions remained stable and were not subjected to sedimentation and aggregation. It was observed that the zeta diameters of the synthesized CA-AgNPs were different from each other, but all AgNPs had a hydrodynamic diameter below 100 nm. This is a desired result because in previous studies, it was showed that with the reduction of the diameter of AgNPs, their surface areas increased and thus their antimicrobial activity increased (42).

Table 1. The zeta potential (mV) and zeta diameters (nm) of the synthesized CA-AgNPs.

Concentration (mM)	Zeta Potential (mV)	Zeta Size (nm)
0.1	-16.4	26.64
0.2	-39.7	64.95
0.3	-23.0	40.15
0.4	-21.0	36.17
0.5	-19.7	19.33
1.0	-20.4	25.18
2.0	-26.9	26.82
4.0	-25.0	32.39
6.0	-24.4	26.46
8.0	-28.2	27.58
10.0	-27.2	28.42

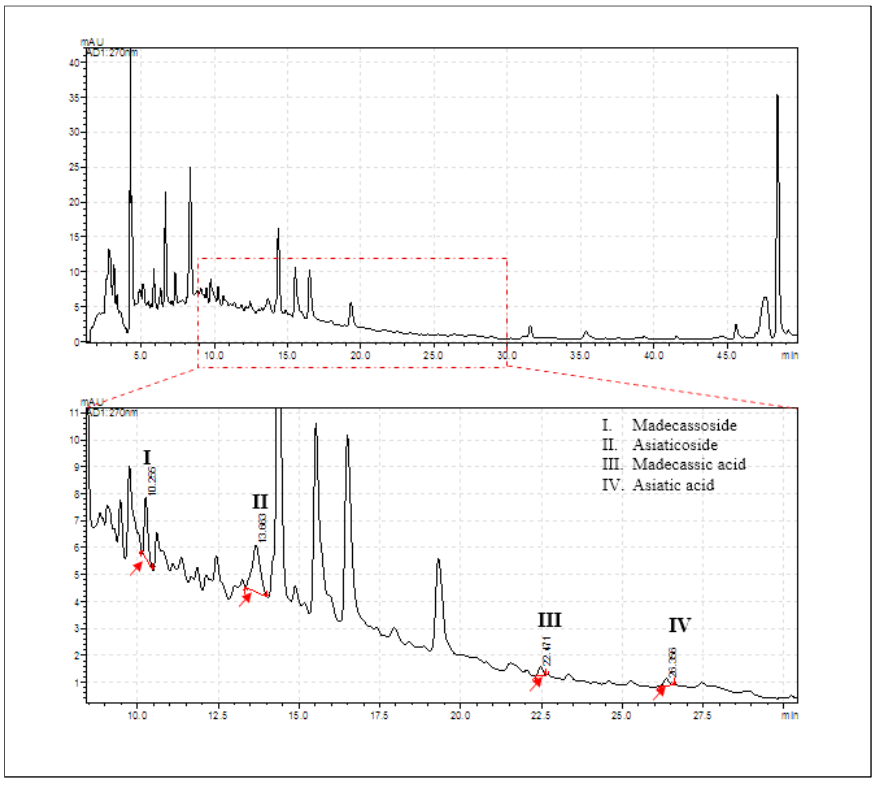

Figure 1. HPLC chromatogram of the CA extract.

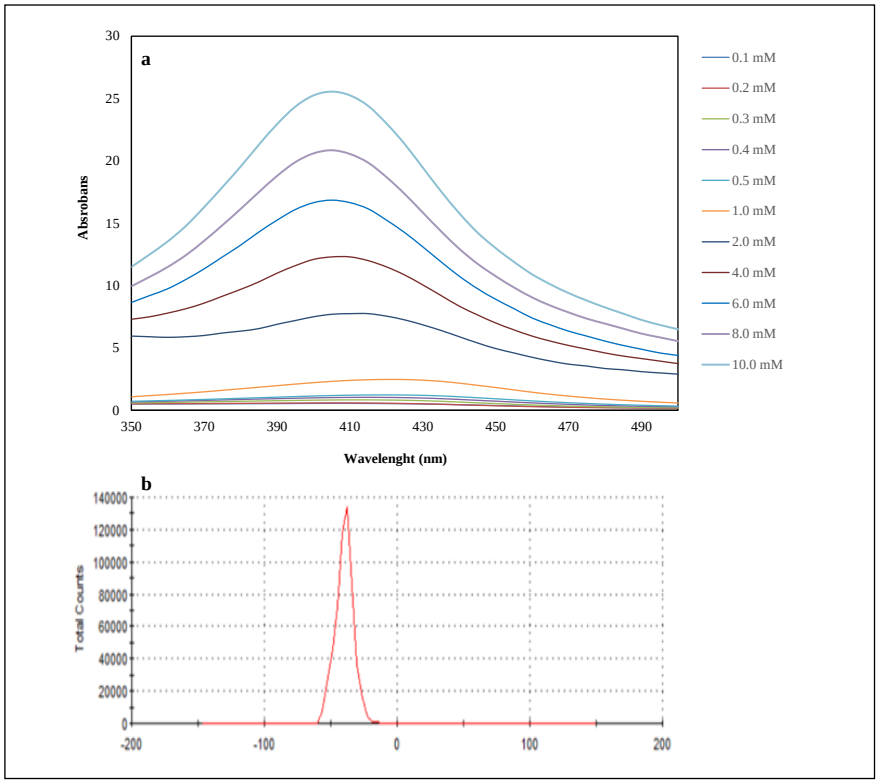

Figure 2. UV-VIS spectrums of CA-coated AgNPs at different Ag^{+} concentration between 350-600 nm wavelength (a) and zeta potential distributions of synthesized 1.0 mM CA-AgNPs group (b).

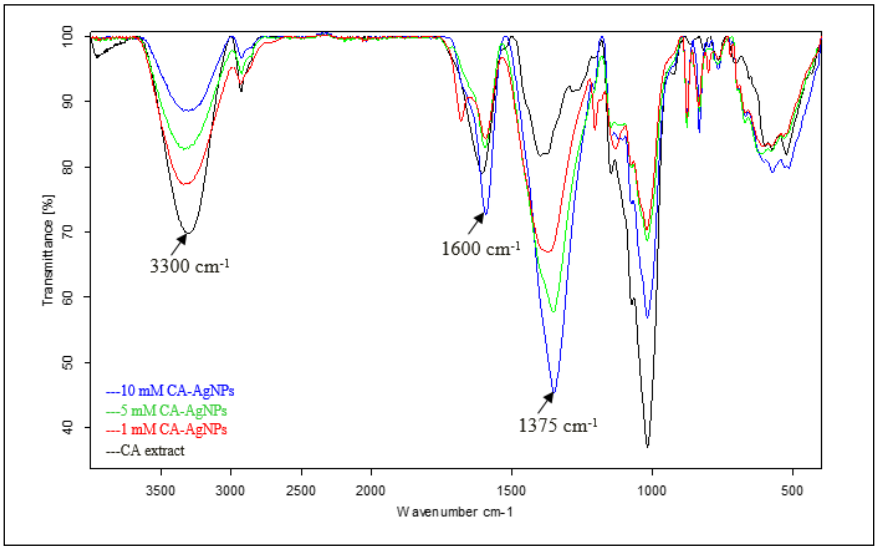

Figure 3. FTIR spectra of the CA extract and CA-AgNPs at different concentration.

Since *Centella asiatica* leaf has a rich content in terms of saponin and phenolic compounds, it contains quite a lot of hydroxyl, carbonyl and carboxyl groups in its structure. Therefore, FTIR analysis was performed to investigate the presence of plant functional groups in both the plant extract and CA-AgNPs synthesized at different $AgNO_3$ concentrations, and the results are shown in Figure 3. In FTIR spectrum of pure plant extract, vibrations were observed at 1375 cm^{-1} and 1600 cm^{-1} due to C=O groups of carboxylic acids and phenols. The stretching at 1375 cm^{-1} was assigned to C-O stretching and O-H deformation, possibly found in the acid groups found in CA leaf extract. Wide stretching at 3300 cm^{-1} was assigned free O-H groups in phenols. When FTIR spectra of the synthesized CA-AgNPs solutions of 1, 5 and 10 mM are examined, the change has emerged in the absorption bands in 1375 cm^{-1} and 3300 cm^{-1} depending on the silver concentration in the absorption bands with the formation of silver nanoparticle. In addition, a change in the frequency of 1600 cm^{-1} carbonyl stretching was observed in CA-AgNPs samples and the increase in the peak intensity of 1375 cm^{-1} may be caused by the occurrence of carbonyl groups during reduction in alkaline medium. The decrease in the intensity of the O-H stretching peaks at 3300 cm^{-1} indicates that OH groups of plant extract were involved in reduction and stabilization of AgNPs (2, 15).

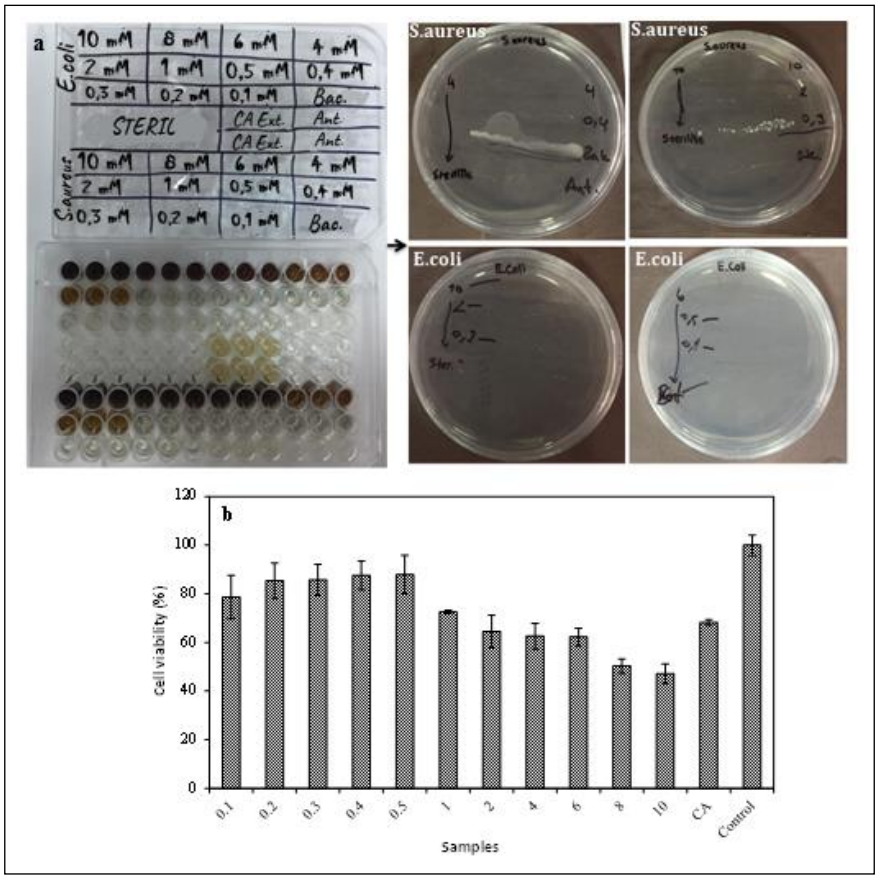

Figure 4. Antibacterial test results; colonies of *S. auresus* and *E. coli* bacteria at different concentrations after incubation with CA-AgNPs (a) and cell viability values of the synthesized CA-AgNPs groups and CA extract determined by MTT test (b).

Antibacterial and cytotoxicity testresults: For antibacterial test, microdilution method was used and the performed test image and results were given in Figure 4a. For *S. aureus* bacteria, 0.4 mM AgNPs was determined as the minimal inhibitory concentration and it was observed that bacteria incubated with concentrations lower than this concentration grew on agar. For *E. coli*, it was observed that bacteria did not grow at all AgNPs concentrations and all AgNPs groups were found to have a 100% lethal effect on this bacterium. In addition, there was no growth in the wells kept sterile and containing antibiotics. It was observed that bacteria that were incubated in sterile medium were grown on agar.

The cytotoxic effect of synthesized CA-AgNPs on L929 fibroblast cells was examined by MTT test. The viability of cells incubated with CA-AgNPs at different concentrations for 24 h was calculated according to the control groups and the results obtained are given in Figure 4b. According to the MTT test results, no significant toxicity was observed in L929 fibroblast cells, where CA-AgNPs having concentration between 0.1 and 1 mM. In L929 fibroblast cells, where CA-AgNPs having concentration between 2 and 10 mM were applied, cell viability fell below 70%. According to the ISO 10993-5 standard evaluation criteria, we can say that the synthesized CA-AgNPs with a concentration higher than 1 mM show cytotoxic properties.

Analgesic effects: In this study, the analgesic effects of CA-AgNPs prepared from the extract of *Centella asiatica* plant on rats were evaluated using tail flick test and hot plate test (Table 2). In these studies, the duration of pain sensation after the administration of CA-AgNPs to experimental animals was examined.

As shown in Table 2, while the average time for animals to feel pain after transdermal saline application in the tail flick test was 4.38±0.34 seconds, this time increased to an average of 6.81±0.45 seconds after the administration of CA-AgNPs. Accordingly, CA-AgNPs inhibited pain by an average of 35.71 ± 2.16%. Statistically, the difference within and between groups was found significant ($t=-11.20$, $df=6$, $P<0.001$).

In the hot plate method, the average time to feel pain after transdermal saline application to the right hind leg of the animals was 16.71±0.58 seconds, while this time increased to an average of 23.33±0.99 seconds after the application of CA-AgNPs. Accordingly, CA-AgNPs inhibited pain by an average of 27.80±3.04%. Statistically, the difference within and between groups was found to be significant ($t=-7.22$, $df=6$, $P<0.001$).

DOI: 10.33988/auvfd.1014802

Table 2. Analgesic effect of *Centella asiatica* coated AgNPs by tail flick and hot plate methods in rats.

	Tail flick				Hot plate			
Animal	**Animal weight (g)**	**After Saline (sec)**	**After CA-AgNPs (sec)**	**Inhibition (%)**	**Animal weight (g)**	**After Saline (sec)**	**After CA-AgNPs (sec)**	**Inhibition (%)**
1	161.9	3.5	5.2	32.7	150.8	15.3	19.1	19.9
2	149.4	3.4	5.7	40.4	156.7	14.6	25.1	41.8
3	158.4	4.7	7.1	33.8	159.1	17.5	21.3	17.8
4	152.5	5.4	8.6	37.2	161.2	18.8	25.1	25.1
5	159.1	4.1	7.3	43.8	154.5	16.7	23.7	29.5
6	153.7	3.9	6.1	36.1	153.7	18.2	26.8	32.1
7	153.1	5.7	7.7	26.0	160.8	15.9	22.2	28.4
Value	155.4±4.4	4.38 ±0.34	6.81±0.45[a]	35.71±2.16	156.7±3.9	16.71±0.58	23.33±0.99[a]	27.80±3.04[b]

Values are mean ± SEM (n=7). [a]P<0.001 represented significant compared to control (saline). [b]P>0.05 represented no significant difference compared to tail flick inhibition percentage (P=0.055).

Tail flick and hot plate methods measure the delay of analgesic response of animals to thermal stimulus. In principle, these two methods are similar to each other. However, while tail flick is a spinal response, the hot plate is predominantly supraspinal (44). In both methods, it was determined that CA-AgNPs prolong the time for animals to feel pain and thus have an analgesic effect. Even though there was no statistical difference between the two methods in terms of inhibition percentages according to P=0.055 value, the difference may be significant level (t=2.12, df=12, P=0.055).

Discussion and Conclusion

The present study clearly shows that CA extract can be utilized favorably to produce AgNPs with an easy green method. Increasing the Ag concentration (between 0.1-10 mM) in the synthesis procedure yielded more AgNPs in an aqueous environment. The obtained CA-AgNPs at different concentration were characterized with many different techniques and it was found that the synthesized CA-AgNPs were stable and in spherical shape, have a SPR peak at around 420 nm. In the literature, AgNPs were reported to be yellow-brown solutions and showed SPR in the range of 420-430 nm (16, 17). This SPR peak observed in the nanoparticle samples we obtained shows that the silver ions were reduced to AgNPs with the used plant extract. Also, negative zeta potentials of AgNPs shows the stabilizer effect of CA plant extract, because, the negatively charged CA-AgNPs repels each other in solutions (13, 48).

The fact that the spectrum of the synthesized CA-AgNPs according to the FTIR results is highly similar to the spectrum of the plant extract shows that the CA-AgNPs are stabilized by phenolics, saponins or carbohydrate-derived biomolecules containing high OH groups in the plant (12).

According to the antibacterial test results, the synthesized CA-AgNPs have been shown to have antibacterial effects on both Gram positive and Gram negative bacteria and certain groups of AgNPs can have potential to be used as antimicrobial agents in many applications. The antibacterial effects of AgNPs have been studied in many previous studies and AgNPs show the high antimicrobial activity compared to other silvers salts due their small size and large surface area (42). In an aqueous environment, AgNPs are oxidized in the presence of oxygen and protons, and released Ag^+ ions show antimicrobial effects (24, 26, 37). The release rate of these ions depends on the some parameters, such as shape, size, concentration and coating agents (26, 42, 47). AgNPs with a particle size of 1-100 nm have been showed to inhibit all bacterial strains at a concentration of 75 µg mL^{-1}. It has also been observed that nanoparticles with a particle size of 1-10 nm have a high affinity to adhere to the surface of the cell membrane compared to larger nanoparticles. Therefore, small sized AgNPs can interact more with the bacterial cell membrane thanks to their large surface area and can cause more damage to the bacteria (42, 47). Ivask et al. (22) investigated the toxic effects of AgNPs with sizes ranging from 10 to 80 nm on bacteria, yeast, algae, crustacean and mammalian cells. At the end of this research, it has been confirmed that small size nanoparticles show highly toxic effects. According to another study that was performed to research the antimicrobial effects of AgNPs at different shape, it was observed that triangular nanoparticles have more

antimicrobial effects compared to spherical and rod-shaped nanoparticles (36).

The cytotoxic effect of all produced CA-AgNPs on L929 fibroblast were investigated with MTT test and it was found that the CA-AgNPs have cytotoxic effect when the concentration of CA-AgNPs was higher than 1 mM. Due to their high antimicrobial properties, AgNPs are frequently used in medicine, medical devices, health products, hygiene products, food and cosmetics industry. However, the strong oxidative activity of silver ions released from AgNPs induces cytotoxicity, genotoxicity, immunological responses and even cell death, causing various adverse effects on biological systems (1, 7, 8). The cytotoxic effects of AgNPs on human cells depend on the concentration, shape, synthesis method and coating agent used (1). Therefore, in our study, we investigated the cytotoxic effects of CA-AgNPs that we synthesized at different Ag concentration.

Centella asiatica extract is a medicinal plant known to have analgesic effects as well as other therapeutic properties (46, 49). Inamdar et al. (20) stated that terpene acids (madecassic acid and asiatic acid), which are mainly responsible for the analgesic and anti-inflammatory activity of *Centella asiatica*, are effective in controlling inflammatory conditions or rheumatism. Somchit et al. (49) reported that CA extracts showed significant analgesic activity in hot plate and acetic acid-induced writhing tests. According to the study, intraperitoneal administration of CA significantly reduced PGE2-induced paw edema. The extract showed significant anti-inflammatory activity even at 2mg/kg compared to the control and the larger dose was found to be more effective than mefenamic acid. Saha et al. (46) reported that both chloroform and methanol extracts of CA showed significant analgesic effects in mice.

In this study, we also proved that CA-AgNPs, which we synthesized for use as a therapeutic and antimicrobial agent in a wound dressing material, have analgesic effects transdermally by thermal (tail flick and hot plate) methods. Pain is one of the symptoms that patients find particularly bothersome during the wound healing process (40). Therefore, the specific concentration of CA-AgNPs we synthesize is a biocompatible agent with properties that will increase the comfort of the patient during the wound healing process. Further studies are also recommended in *in vivo* infected and non-infected wound models.

Acknowledgment

This study constitutes a part of Ogün Bozkaya's doctoral dissertation studies entitled "*In Vitro* and *In Vivo* Investigation of Wound Healing Effect of Polymer Fibers Containing Silver Nanoparticles Coated with *Centella asiatica* Plant Extract" at Hacettepe University, Institute of Science, Bioengineering doctorate program.

Financial Support

This study was financially supported by Kırıkkale University Scientific Commite under the project no 2019/029. The authors are grateful to Kırıkkale University for their supporting.

Conflict of Interest

The authors declared that there is no conflict of interest.

Author Contributions

OB, HE, ZGG, EA, SE, MY and İV conceived and planned the experiments. OB, HE and EA carried out the experiments. OB, HE and EA planned and carried out the simulations. OB, HE, EA and SE contributed to sample preparation. OB, HE, ZGG, EA, SE, MY and İV contributed to the interpretation of the results. O.B. took the lead in writing the manuscript. All authors provided critical feedback and helped shape the research, analysis and manuscript.

Data Availability Statement

The data supporting this study's findings are available from the corresponding author upon reasonable request.

Ethical Statement

The study was approved by Kırıkkale University Animal Experiments Local Ethics Committee with the decision dated 26.05.2021, numbered 2021/05, meeting numbered 24.

Animal Welfare

The authors confirm that they have adhered to ARRIVE Guidelines to protect animals used for scientific purposes.

References

1. **Akter M, Sikder MT, Rahman MM, et al** (2018): *A systematic review on silver nanoparticles-induced cytotoxicity. Physicochemical properties and perspectives*. J Adv Res, **9**, 1–16.
2. **Akturk O, Gun Gok Z, Erdemli O, et al** (2019): *One-pot facile synthesis of silk sericin-capped gold nanoparticles by UVC radiation: Investigation of stability, biocompatibility, and antibacterial activity*. J Biomed Mater Res - Part A, **107**, 2667–2679.
3. **Babu TD, Kuttan G, Padikkala J** (1995): *Cytotoxic and anti-tumour properties of certain taxa of Umbelliferae with special reference to Centella asiatica (L.) Urban*. J Ethnopharmacol, **48**, 53–57.
4. **Babykutty S, Padikkala J, Sathiadevan P, et al** (2009): *Apoptosis induction of Centella asiatica on human breast*

cancer cells. African J Tradit Complement Altern Med, **6**, 9-16.

5. **Bonte F, Dumas M, Chaudagne C, et al** (1994): *Influence of asiatic acid, madecassic acid, and asiaticoside on human collagen I synthesis*. Planta Med, **60**, 133–135.
6. **Bunpo P, Kataoka K, Arimochi H, et al** (2004): *Inhibitory effects of Centella asiatica on azoxymethane-induced aberrant crypt focus formation and carcinogenesis in the intestines of F344 rats*. Food Chem Toxicol, **42**, 1987–1997.
7. **Chen X, Schluesener HJ** (2008): *Nanosilver: a nanoproduct in medical application*. Toxicol Lett, **176**, 1–12.
8. **Chernousova S, Epple M** (2013): *Silver as antibacterial agent: ion, nanoparticle, and metal*. Angew Chemie Int Ed, **52**, 1636–1653.
9. **D'amour FE, Smith DL** (1941): *A method for determining loss of pain sensation*. J Pharmacol Exp Ther, **72**, 74–79.
10. **Eddy NB, Leimbach D** (1953): *Synthetic analgesics. II. Dithienylbutenyl-and dithienylbutylamines*. J Pharmacol Exp Ther, **107**, 385–393.
11. **Ermertcan AT, Inan S, Ozturkcan S, et al** (2008): *Comparison of the effects of collagenase and extract of Centella asiatica in an experimental model of wound healing: an immunohistochemical and histopathological study*. Wound Repair Regen, **16**, 674–681.
12. **Eze FN, Tola AJ, Nwabor OF, et al** (2019): *Centella asiatica phenolic extract-mediated bio-fabrication of silver nanoparticles: Characterization, reduction of industrially relevant dyes in water and antimicrobial activities against foodborne pathogens*. RSC Adv, **9**, 37957–37970.
13. **Farhadi S, Ajerloo B, Mohammadi A** (2017): *Green biosynthesis of spherical silver nanoparticles by using date palm (Phoenix dactylifera) fruit extract and study of their antibacterial and catalytic activities*. Acta Chim Slov, **64**, 129–143.
14. **Gupta YK, Kumar MHV, Srivastava AK** (2003): *Effect of Centella asiatica on pentylenetetrazole-induced kindling, cognition and oxidative stress in rats*. Pharmacol Biochem Behav, **74**, 579–585.
15. **Gün Gök Z, Demiral A, Bozkaya O, et al** (2020): *In situ synthesis of silver nanoparticles on modified poly(ethylene terephthalate) fibers by grafting for obtaining versatile antimicrobial materials*. Polym Bull, **45**, 1-20.
16. **Gün Gök Z, Günay K, Arslan M, et al** (2020): *Coating of modified poly (ethylene terephthalate) fibers with sericin-capped silver nanoparticles for antimicrobial application*. Polym Bull, **77**, 1649–1665.
17. **Gün Gök Z, Karayel M, Yiğitoğlu M** (2021): *Synthesis of carrageenan coated silver nanoparticles by an easy green method and their characterization and antimicrobial activities*. Res Chem Intermed, **47**, 1843–1864.
18. **Gün Gök Z, Yiğitoğlu M, Vargel İ, et al** (2021): *Synthesis, characterization and wound healing ability of PET based nanofiber dressing material coated with silk sericin capped-silver nanoparticles*. Mater Chem Phys, **259**, 124043.
19. **Hashim P, Sidek H, Helan MHM, et al** (2011): *Triterpene composition and bioactivities of centella asiatica*. Molecules , **16**, 1310–1322.
20. **Inamdar PK, Yeole RD, Ghogare AB, et al** (1996): *Determination of biologically active constituents in Centella asiatica*. J Chromatogr A, **742**, 127–130.
21. **Iravani S, Korbekandi H, Mirmohammadi SV, et al** (2014): *Synthesis of silver nanoparticles: chemical, physical and biological methods*. Res Pharm Sci, **9**, 385.
22. **Ivask A, Kurvet I, Kasemets K, et al** (2014): *Size-dependent toxicity of silver nanoparticles to bacteria, yeast, algae, crustaceans and mammalian cells in vitro*. PLoS One, **9**, e102108.
23. **Jarić S, Kostić O, Mataruga Z, et al** (2018): *Traditional wound-healing plants used in the Balkan region (Southeast Europe)*. J Ethnopharmacol, **211**, 311–328.
24. **Kharat SN, Mendhulkar VD** (2016): *Synthesis, characterization and studies on antioxidant activity of silver nanoparticles using Elephantopus scaber leaf extract*. Mater Sci Eng C, **62**, 719–724.
25. **Kumar B, Vijayakumar M, Govindarajan R, et al** (2007): *Ethnopharmacological approaches to wound healing-Exploring medicinal plants of India*. J Ethnopharmacol, **114**, 103–113.
26. **Lee SH, Jun B-H** (2019): *Silver nanoparticles: synthesis and application for nanomedicine*. Int J Mol Sci, **20**, 865.
27. **Lee J, Jung E, Kim Y, et al** (2006): *Asiaticoside induces human collagen I synthesis through TGFβ receptor I kinase (TβRI kinase)-independent Smad signaling*. Planta Med, **72**, 324–328.
28. **Lee J-H, Kim H-L, Lee MH, et al** (2012): *Asiaticoside enhances normal human skin cell migration, attachment and growth in vitro wound healing model*. Phytomedicine, **19**, 1223–1227.
29. **Li F-S, Weng J-K** (2017): *Demystifying traditional herbal medicine with modern approach*. Nat Plants, **3**, 1–7.
30. **Liu M, Dai Y, Li Y, et al** (2008): *Madecassoside isolated from Centella asiatica herbs facilitates burn wound healing in mice*. Planta Med, **74**, 809–815.
31. **Logeswari P, Silambarasan S, Abraham J** (2015): *Synthesis of silver nanoparticles using plants extract and analysis of their antimicrobial property*. J Saudi Chem Soc, **19**, 311–317.
32. **Melekoğlu A, Ekici H, Arat E, et al** (2020): *Evaluation of melamine and cyanuric acid cytotoxicity: an in vitro study on L929 fibroblasts and CHO cell line*. Ankara Univ Vet Fak Derg, **67**, 399–406.
33. **Mukundan D, Mohankumar R, Vasanthakumari R** (2017): *Comparative study of synthesized silver and gold nanoparticles using leaves extract of Bauhinia tomentosa Linn and their anticancer efficacy*. Bull Mater Sci, **40**, 335–344.
34. **Netala VR, Kotakadi VS, Nagam V, et al** (2015): *First report of biomimetic synthesis of silver nanoparticles using aqueous callus extract of Centella asiatica and their antimicrobial activity*. Appl Nanosci, **5**, 801–807.
35. **Orhan IE** (2012): *Centella asiatica (L.) Urban: from traditional medicine to modern medicine with neuroprotective potential*. Evidence-based Complement Altern Med, **2012**.
36. **Pal S, Tak YK, Song JM** (2007): *Does the antibacterial activity of silver nanoparticles depend on the shape of the nanoparticle? A study of the gram-negative bacterium Escherichia coli*. Appl Environ Microbiol, **73**, 1712–1720.
37. **Patil AH, Jadhav SA, More VB, et al** (2019): *Novel one step sonosynthesis and deposition technique to prepare*

silver nanoparticles coated cotton textile with antibacterial properties. Colloid J, **81**, 720–727.

38. **Paocharoen V** (2010): *The efficacy and side effects of oral Centella asiatica extract for wound healing promotion in diabetic wound patients*. J Med Assoc Thai, **93**, S166–S170.
39. **Pozsgai G, Payrits M, Sághy É, et al** (2017): *Analgesic effect of dimethyl trisulfide in mice is mediated by TRPA1 and sst4 receptors*. Nitric Oxide, **65**, 10–21.
40. **Price P, Fogh K, Glynn C, et al** (2007): *Managing painful chronic wounds: the wound pain Management Model*. Int Wound J, **4**, 4–15.
41. **Rafamantanana MH, Rozet E, Raoelison GE, et al** (2009): *An improved HPLC-UV method for the simultaneous quantification of triterpenic glycosides and aglycones in leaves of Centella asiatica (L.) Urb (APIACEAE)*. J Chromatogr B Anal Technol Biomed Life Sci, **877**, 2396–2402.
42. **Rai M, Yadav A, Gade A** (2009): *Silver nanoparticles as a new generation of antimicrobials*. Biotechnol Adv, **27**, 76–83.
43. **Rao SB, Chetana M, Devi PU** (2005): *Centella asiatica treatment during postnatal period enhances learning and memory in mice*. Physiol Behav, **86**, 449–457.
44. **Rezaee-Asl M, Sabour M, Nikoui V, et al** (2014): *The study of analgesic effects of Leonurus cardiaca L. in mice by formalin, tail flick and hot plate tests*. Int Sch Res Not, **2014**.
45. **Roy A** (2017): *A review on the alkaloids an important therapeutic compound from plants*. IJPB, **3**, 1–9.
46. **Saha S, Guria T, Singha T, et al** (2013): *Evaluation of analgesic and anti-inflammatory activity of chloroform and methanol extracts of Centella asiatica*. Int Sch Res Not, **2013**.
47. **Sarheed O, Ahmed A, Shouqair D, et al** (2016): *Antimicrobial dressings for improving wound healing*. Wound Heal Insights into Anc Challenges; Alexandrescu, V, Ed, 373–398.
48. **Seong M, Lee DG** (2017): *Silver nanoparticles against Salmonella enterica serotype typhimurium: role of inner membrane dysfunction*. Curr Microbiol, **74**, 661–670.
49. **Somchit MN, Sulaiman MR, Zuraini A, et al** (2004): *Antinociceptive and antiinflammatory effects of Centella asiatica*. Indian J Pharmacol, **36**, 377-380.
50. **Tang B, Zhu B, Liang Y, et al** (2011): *Asiaticoside suppresses collagen expression and TGF-β/Smad signaling through inducing Smad7 and inhibiting TGF-βRI and TGF-βRII in keloid fibroblasts*. Arch Dermatol Res, **303**, 563–572.
51. **Widgerow AD, Chait LA, Stals R, et al** (2000): *New innovations in scar management*. Aesthetic Plast Surg, **24**, 227–234.
52. **Wu F, Bian D, Xia Y, et al** (2012): *Identification of major active ingredients responsible for burn wound healing of Centella asiatica herbs*. Evidence-Based Complement Altern Med, **2012**.
53. **Yazgan K** (2020): Ratlarda ammi visnaga L.(diş otu) özütünün ağrı üzerindeki etkisinin hot plate ve tail flick testleriyle araştırılması. Yüksek Lisans Tezi. Kırıkkale Üniversitesi Sağlık Bilimleri Enstitüsü, Kırıkkale.
54. **Yoshida M, Fuchigami M, Nagao T, et al** (2005): *Antiproliferative constituents from Umbelliferae plants VII. Active triterpenes and rosmarinic acid from Centella asiatica*. Biol Pharm Bull, **28**, 173–175.

Use of PCR for detection of *Burkholderia mallei* in Türkiye

Seda EKİCİ[✉,1,a], Orhan DUDAKLI[1,b], Dilek DÜLGER[2,c], Maksut Murat MADEN[1,d], Ayşe DEMİRHAN[1,e]

[1]Veterinary Control Central Research Institute, Ankara, Türkiye; [2]Karabük University, Faculty of Medicine, Department of Medical Microbiology, Karabük, Türkiye

[a]ORCID: 0000-0002-7982-5261; [b]ORCID: 0000-0001-9598-8055; [c]ORCID: 0000-0003-3640-5686; [d]ORCID: 0000-0002-8736-8195
[e]ORCID: 0000-0002-3335-1072

ARTICLE INFO

Article History
Received : 29.12.2021
Accepted : 27.09.2022
DOI: 10.33988/auvfd.1049887

Keywords
Burkholderia mallei
CBRN
Glanders
PCR

✉Corresponding author
seda.ergen@hotmail.com

How to cite this article: Ekici S, Dudaklı O, Dülger D, Maden MM, Demirhan A (2023): Use of PCR for detection of *Burkholderia mallei* in Türkiye. Ankara Univ Vet Fak Derg, 70 (1), 97-100. DOI: 10.33988/auvfd.1049887.

ABSTRACT

Within the scope of the "National Ruam Eradication Project" carried out between 2000-2001, Glanders was eradicated in our country. Unfortunately, 81 horses were culled in Türkiye in December 2019, following the detection of Epidemic in horses in Büyükada. In 2019, Glanders were reported in horses in Uşak and Bolu. No human cases have been reported. Türkiye is at risk for Glanders because of its geography. Therefore, reliable and fastly detection of *Burkholderia mallei* by PCR in a short time will prevent the distribution of unwanted infections that may occur in the future throughout the country. In this study; *Burkholderia mallei* strains isolated from horses were verified and optimized by PCR. The use of PCR for the detection of *Burkholderia mallei* was performed for the first time in our country. It has been concluded that the PCR as a diagnostic method with high reliability and sensitivity safely used together with diagnosis of Glanders.

Chemical Biological, Radiological Nuclear Threats (CBRN) is on the agenda of world health today as they can cause mass deaths by being used as weapons. One of the bacteria that has the potential to be used in biological attacks is *Burkholderia mallei* (*B. mallei)*. It is included in the Bioterrorism Factors and Diseases List (Category B) made by the United States Center for Disease Protection and Control, the List of Important Dangerous Factors of the Biological Weapons Convention and the List of the European Union Bioterrorism Working Group. *B. mallei* is the causative agent of Glanders. Glanders is a systemic and zoonotic infection of equine animals with contagious character, acute and chronic course (20). Glanders is characterized by the formation of purulent nodules and ulcers in the skin, respiratory, and internal organs of patients. The disease can often be transmitted by direct contact, or it can also be transmitted aerogenously. Contamination of the food and water sources is generally seen as a result of the contamination of the environment with the nasal secretions of infected animals (1, 2). The disease follows an acute and chronic course. While it has an acute course in donkeys and mules, it has a chronic form in horses. In humans, in acute events; it progresses with 95% mortality and death occurs within 3 weeks. Treatment is possible with the use of antibiotics (2, 15).

The first information about the presence of Glanders in Türkiye was found in letters written by Veterinarian Godlewsky (9, 19). In these letters, it is mentioned that animals with Glanders are used as long as they can work and then they were released when they were unable to work. This led to the rapid spread of the disease. Glanders, which caused significant damage to the national economy, human and animal health, spread rapidly during the Balkan, I. World and War of Independence showed an epidemic course. As a result of this epidemic, it has been reported that animals infected with the disease are used in the army without health checks (18). In the Public Health Law enacted in 1930 in Türkiye, it is mentioned that the notification of Glanders, the isolation of the sick animals, the transfer of the deceased animals, and the keeping of

culture of the bacteria in the laboratory are prohibited. Until 1999, cases were reported from various places in our country. Within the scope of the "National Ruam Eradication Project" carried out between 2000-2001, the Equidae animals available in our country were tested and the carrier animals were destroyed (25). Isolated cases of Glanders in horses are also reported from time to time in Türkiye.

The aim of the study was to optimize the PCR detection of *B. mallei* against possible infection with Glanders. In this study, 14 isolates isolated between 1985 and 2000 in Veterinary Control Central Research Institute and NH strain were used. The isolates from enriched Dorset-Henley medium were purified in a biosafety level-3 laboratory. For the detection of the *B. mallei*, manufacturer's instructions for High Pure PCR Template Preparation Kit (Roche Diagnostics, Germany) were followed in order to isolate DNA. Primers used for the detection of *B. mallei* are shown in Table 1.

Following that, the primers targeting the 823 bp gene of *B. mallei* used by Merwyn et al. (13) were used in PCR. DNAs were stored at -20 °C. The DNA was stored at -20 °C until analysis.

In this study, the NH strain used in mallein production in our institute was used as a positive control. An optimization study was performed with NH strain used in mallein production in Veterinary Control Central Research Institute to determine the optimal working concentration of synthesized primers. Dilutions $3x10^{1}$ to $3x10^{8}$ of NH strain were prepared. 1 ml of these dilutions were absorbed into the swabs and genomic DNA extracted from each dilution was tested in 5 replicates. Then, PCR process was performed. PCR yielded successful results in all dilutions. This shows us that although there are very few pathogens, the PCR process reliably detects the causative agent. In this way, the disease will be detected in the early period when the clinical symptoms of the disease are not seen and the spread of the disease will be prevented.

According to the results of this study, 50 ng template DNA, 1.0 µM of each primer pairs (BM-4 ve BM-5), 1.25 U of Taq DNA polymerase, 200 µM dNTP, 1.5 mM MgCl, DNase & RNase free water and 1x PCR buffer were arranged in 25 µl reactions. Class-2 laminar cabinet was used for mixing reagents, other buffer liquids and PCR and Isolation. The heat cycle was adjusted as 95°C pre-denaturation for 5 min, 35 cycles at 95°C for 1 min for denaturation, and 60.6 °C for 2 min and 72°C for 2 min. This was followed by 1 cycle at 72°C for 10 min. The reaction mixture was subjected to electrophoresis on 1.2% agarose gel to analyze (Figure 1).

In our study, we performed the DNA extraction and PCR analysis of 14 different samples which were isolated between 1985 and 2000 as *B.mallei* which is a zoonotic and notifiable bacterial dissease causing high mortality in equidae. After the analysis of the results, it is concluded that PCR is a verified method for the detection of *B. mallei*.

Table 1. Primers used in study to amplify the Glander Disease and Amplicon size.

BM-4 5'-CGA TCC TGG TGT GCT CGG CCG_3'	823 bp
BM-5 5'-CGC AGA CCT TCT TCC ATC GCG ATC-3'	823 bp

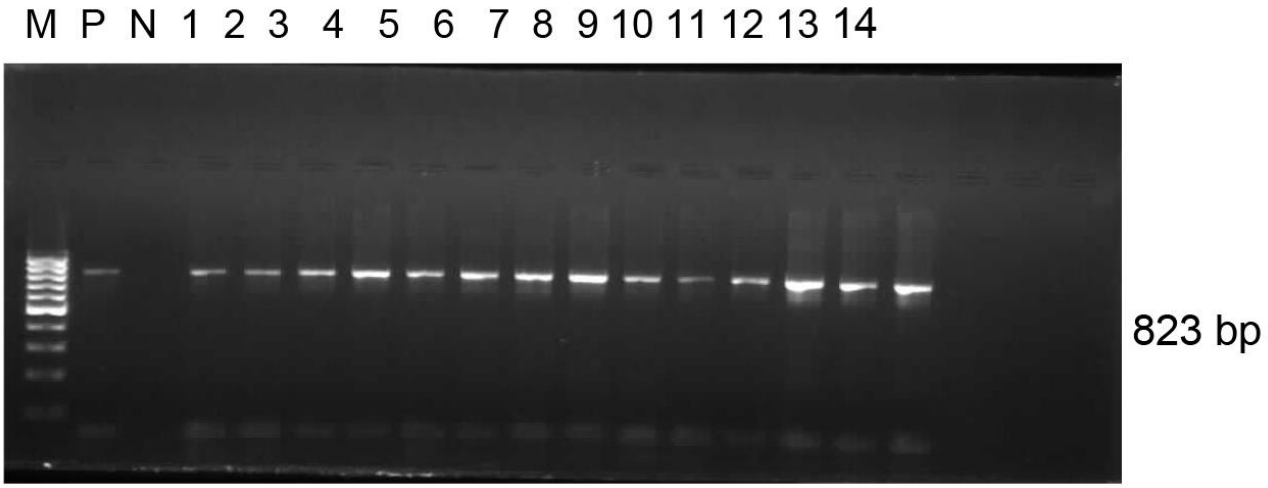

Figure 1. PCR for B mallei strains. Lane M: 100bp ladder; Lane P: Positive control; Lane N: Negative control; Lane 1-14: *B. mallei* isolates.

DOI: 10.33988/auvfd.1049887

Many methods are used in the diagnosis of Glander Disease. Mallein and serological tests are the most important tests in the diagnosis of the disease. Mallein test is a specific and high sensitive test. During the application of this test, intradermo-palpebral or intradermo-cervical injections cause a reaction characterized with swelling of the skin is observed within 1-3 days in infected animals. Intradermic Sauton Mallein produced in our institute is a biological test material accepted and recommended by the OIE (16). Serological tests are Complement Fixation Test (CFT) and Enzyme-Linked Immunosorbent test (ELISA). CFT which has a good sensitivity as a screening test and is able to detect chronically infected glanders carriers. And CFT is prescribed by the World Organisation for Animal Health (OIE) for international trade of equines (17). This method remains difficult to standardise. CFT reliability depends on the choice of antigen and protocol, hence, specificity and sensitivity of the CFT test may vary and yet the sensitivity of this test may range from 62.5% to 100%. In addition to those, the Rose-Bengal plate test is applied in some countries. Specific monoclonal antibodies, molecular methods, western blotting are among the other diagnostic methods used. In the early stages of the Glanders when clinical signs are mild, anamnesis and laboratory diagnoses are not sufficient for the diagnosis of the disease. Therefore, the use of methods such as PCR that are able to detect small numbers of pathogen for the diagnosis of *B mallei* is very important in terms of preventing possible epidemics (3, 6-8, 10, 11, 13, 14, 21, 22).

Molecular methods are used to support and confirm the diagnosis. It is used as a fast, sensitive and reliable diagnostic tool both in diagnosis and verification. Gee et al. (5) used 16S rRNA gene sequencing for rapid identification and differentiation *of Burkholderia pseudomallei* and *B. mallei*. Scholtz et al. (24) used the 989 base pair gene regions of the bacterial flagellar antigen in the Glander Disease epidemic in the United Arab Emirates and the diagnosis of *B. mallei* was made that way. Merwyn et al. (13) successfully optimized *B. mallei* inoculated environmental samples with the primers they designed and detected Glander Disease quickly and reliably. Today, with the rapid advancement of technology, whole genome sequencing of *B. mallei* has been done. Thus, the epidemiology of the disease is tried to be understood. Fonseca et al. (4) identified 2 new genotypes of B. mallei in Brazil by Whole Genome Sequence (WGS). These study results show different introduction events regarding glanders in Brazil, including strains of European origin, in connection with colonization or trade. Singha et al. (23) identified targeting *B. mallei* strains in India and Pakistan by whole genome sequence of 10 *B. mallei* strains with four new markers. In this study, new SNP markers were determined as a result of SNP analysis. Such rapid and distinctive typing tools will contribute to the epidemiological monitoring of *B. mallei* infections in endemic regions of the disease. WGS could help in elucidating the origin of the disease.

Glanders is listed as one of the notifiable diseases by the World Organization for Animal Health (WHO) due to the debilitating disease it causes in both animals and humans. The eradication programs applied against glanders disease, which spreads widely all over the world and causes great losses in equidae, started to give results especially in the first half of the 20th century (17). Today, some outbreaks of Glanders have been reported in Afghanistan, Bangladesh, India, Pakistan (South Asia), Bahrain, Iraq, Syria, Iran, Kuwait and United Arab Emirates (The Middle East), and Brazil (South America) (12). In the last 25 years, a marked increase in outbreaks or cases leading to a putative relapse has been observed (17, 18). It is worth considering that the disease is probably often misdiagnosed and certainly underreported in many countries (18).

Acknowledgements

We would like to express our sincere gratitude to Dr. Cevdet YARALI and Özcan YILDIRIM for their encouragement and support. A publication permit was granted by the Republic of Türkiye Ministry of Agriculture and Forestry with the document dated 27.10.2021 and numbered E-71037622-825.03.01- 3187884.

Financial Support

This research received no grant from any funding agency/sector.

Conflict of Interest

The authors declared that there is no conflict of interest.

Author Contributions

ES, OD, DD and DA conceived and planned the experiments. ES and OD carried out the experiments. ES, OD and DD planned and carried out the simulations. ES, OD, DD and DA contributed to the interpretation of the results. ES took the lead in writing the manuscript. All authors provided critical feedback and helped shape the research, analysis and manuscript.

Data Availability Statement

The data supporting this study's findings are available from the corresponding author upon reasonable request.

Ethical Statement

This study does not present any ethical concerns.

Animal Welfare

Not applicable.

References

1. **Cárdenas NC, Galvis JO, Farinati AA, et al** (2019): *Burkholderia mallei: The dynamics of networks and disease transmission*. Transbound Emerg Dis, **66,** 715-728.
2. **Elschner MC, Klaus CU, Liebler-Tenorio E, et al** (2009): *Burkholderia mallei infection in a horse imported from Brazil.* Equine Vet Educ, **21,** 147-150.
3. **Falcao MV, Laroucau K, Vorimore F, et al** (2022). *Molecular characterization of Burkholderia mallei strains isolated from horses in Brazil (2014–2017).* Infection Genetics and Evolution, **99**, 105250.
4. **Fonseca Júnior AA, Pinto CA, Alencar CA, et al** (2021): *Validation of three qPCR for the detection of Burkholderia mallei in equine tissue samples.* Arch Microbiol, **203,** 3965–3971.
5. **Gee JE, Sacchi CT, Glass MB, et al** (2003): *Use of 16S rRNA gene sequencing for rapid identification and differentiation of Burkholderia pseudomallei and B. mallei.* J Clin Microbiol, **41,** 4647-4654.
6. **Gilling DH, Luna VA, Pfugradt C** (2014): *The identification and differentiation between Burkholderia mallei and Burkholderia pseudomallei using one gene pyrosequencing.* Int Sch Res Notices, **2,** 109583.
7. **Girault G, Wattiau P, Saqib M, et al** (2018): *High-resolution melting PCR analysis for rapid genotyping of Burkholderia mallei.* Infect Genet Evol, **63,** 1–4.
8. **Ghori MT, Khan MS, Khan JA, et al** (2018): *Molecular detection of Burkholderia mallei in nasal swabs from draught horses with signs of respiratory tract infection.* J Anim Plant Sci, **28,** 1717-1724.
9. **Godlewsky S** (1972): Türkiye'de Veteriner Hekimlik (19'uncu Yüzyıl Ortalarında). Çev. Nihal Erk. Ankara Univ Vet Fak Yayınları, 281.
10. **Hornstra H, Pearson T, Georgia S, et al** (2009): *Molecular epidemiology of glanders, Pakistan.* Emerg Infect Dis, **15,** 2036–2039.
11. **Khan I, Wieler LH, Melzer F, et al** (2013): *Glanders in animals: A review on epidemiology, clinical presentation, diagnosis and countermeasures.* Transbound Emerg Dis, **60,** 204–221.
12. **Laroucau K, Aaziz R, Vorimore F, et al** (2021): *A genetic variant of Burkholderia mallei detected in Kuwait: Consequences for the PCR diagnosis of glanders.* Transbound Emerg Dis, **68,** 960-963.
13. **Merwyn S, Kumar S, Agarwal GS, et al** (2010): *Evaluation of PCR, DNA hybridization and immunomagnetic separation-PCR for detection of burkholderia mallei in artificially inoculated environmental samples.* Ind J Mic, **50,** 172-178.
14. **Najafpour R, Mosavari N, Tadayon K, et al** (2015): *Optimization of variable number tandem repeat (VNTR) analysis in the classical PCR machines for typing of Burkholderia mallei.* J Microbiol, **8,** 190-199.
15. **Neubauer H, Sprague LD, Zacharia R, et al** (2005): *Serodiagnosis of Burkholderia mallei infections in horses: state-of-the-art and perspectives.* J Vet Med B, **52,** 201-205.
16. **OIE** (2018): Chapter 2.5.11: Glanders and melioidosis. In: Manual of Diagnostic Tests and Vaccines for Terrestrial Animals. Available at: http://www.oie.int/fileadmin/Home/eng/Health_standards/tahm/2.05.11_GLANDERS.pdf (Accessed January 25, 2021).
17. **OIE** (2020): Chapter 3.5.11: Glanders and melioidosis. In: Manual of Diagnostic Tests and Vaccines for Terrestrial Animals. Available at: https://www.oie.int/fileadmin/Home/eng/Health_standards/tahm/3.05.11_GLANDERS.pdf. (Accessed May 21, 2021).
18. **Osmanağaoğlu Ş, Melikoğlu B** (2009): *Türkiye'de Ruam hastalığı eradikasyon çalışmalarına tarihsel bir bakış açısı.* Kafkas Univ Vet Fak Derg, **15,** 331-337.
19. **Öztürk R, Başağaç RT** (2002): *Veteriner hekimliği tarihinde iz bırakanlar Hüdai-Ahmet-Kemal Cemil.* Türk Vet Hek Birl Derg, **2,** 54-56.
20. **Pakdemirli A, Dülger D** (2021): *Tarihsel bir biyolojik ajan ve KBRN açısından önemi: Ruam (Glanders) "Burkholderia mallei".* Etlik Vet Mikrobiyol Derg, **32,** 1-7.
21. **Saxena A, Pal V, Tripathi NK, et al** (2019): *Development of a rapid and sensitive recombinase polymerase amplification-lateral flow assay for detection of Burkholderia mallei.* Transbound Emerg Dis, **66,** 1016-1022.
22. **Shanmugasundaram K, Singha H, Saini S, et al** (2022): 16S rDNA and ITS Sequence Diversity of Burkholderia mallei Isolated from Glanders-Affected Horses and Mules in India (2013–2019). Current Microbiology, **79**, 1-13.
23. **Singha H, Vorimore F, Saini S, et al** (2021): *Molecular epidemiology of Burkholderia mallei isolates from India (2015–2016): New SNP markers for strain tracing.* Infect Genet Evol, **95,** 105059.
24. **Scholz HC, Joseph M, Tomasso H, et al** (2006): *Detection of the reemerging agent Burjholderia mallei in a recent outbreak of glanders in the United Arab Emirates by a newly flip- based polymerase chain reaction assay.* Diagn Microbiol Infect Dis, **54,** 241-247.
25. **Torba TA** (2020): *Burkholderia mallei: Ruam Hastalığı/Burkholderia mallei: Glanders.* ESTÜDAM Halk Sağl Derg, **5,** 353-361.

Cutaneous clear cell adnexal carcinoma in two dogs: cytological and immunohistochemical evaluation

Mehmet Fatih BOZKURT[1,a], Muhammad Nasir BHAYA[1,b,✉], Alper NİŞANCI[2,c]

[1]Afyon Kocatepe University, Faculty of Veterinary Medicine, Department of Pathology, Afyonkarahisar, Türkiye; [2]Petcode Animal Hospital, Ankara, Türkiye

[a]ORCID: 0000-0002-1669-0988; [b]ORCID: 0000-0001-7696-3039; [c]ORCID: 0000-0002-5771-5280

ARTICLE INFO

Article History
Received : 12.04.2022
Accepted : 20.09.2022
DOI: 10.33988/auvfd.1102050

Keywords
Clear cell adnexal carcinoma
Dog
Psammoma bodies
Tumor

✉Corresponding author
dr.muhammadnasir399@gmail.com

How to cite this article: Bozkurt MF, Bhaya MN, Nişancı A (2023): Cutaneous clear cell adnexal carcinoma in two dogs: cytological and immunohistochemical evaluation. Ankara Univ Vet Fak Derg, 70 (1), 101-105. DOI: 10.33988/auvfd.1102050.

ABSTRACT

In this study, cases of cutaneous clear cell adnexal carcinoma were diagnosed on the right forepaw of a 6-year-old female dog and on the right hind paw of an 8-year-old male dog. On the cytological examination, scattered cell groups were seen on the hemorrhagic background, whose cytoplasmic borders could hardly be distinguished. Although the cells showed marked pleomorphism, but were generally oval, round, or spindle-shaped. Anisokaryosis, karyomegaly, and one or more prominent nucleoli were noted in the nuclei. Pseudoinclusions were found in some cell nuclei. Histologically, it was centrally necrotic, expansive growth consisting of lobular areas in the dermis. The neoplastic cells consisted of oval round-shaped epithelioid cells with clear cytoplasm showing marked anisocytosis, anisorkaryosis and karyomegaly. Nuclei were oval or round in shape with prominent nucleoli. Cystic changes and calcified areas in layers (psammoma bodies) were noted in these areas. Few mitoses were found. In the immunohistochemical examination, tumor cells were positive for vimentin, S-100, MART1 (Melan A), and cytokeratin (MNF116) and negative for glial fibrillary acidic protein (GFAP) and smooth muscle actin (SMA). Based on these findings and results, the tumors were diagnosed as canine clear cell adnexal carcinoma. According to the literature review, this is the first case in which we found psammoma bodies and nuclear pseudo inclusions on microscopic examination of canine cutaneous clear cell adnexal carcinoma.

Canine cutaneous clear cell adnexal carcinoma is one of the rare tumors of dogs and has no differentiation between apocrine, sebaceous and follicular cells (11). First report of this tumor has been published in 1978 with the name of clear cell hidradenocarcinoma in dogs (5). The other reported name of this tumor is follicular stem cell carcinoma (7). Clear cells having vacuolated cytoplasm are the main histopathological findings related to this tumor. Epithelial stem cells of cutaneous region are the main origin for the development of this tumor (7, 11). Other canine cutaneous tumors including balloon cell melanoma, sebaceous carcinoma, clear cell trichoblastoma (12), and clear cell basal carcinoma reveal similarities with the cutaneous clear cell adnexal carcinoma in dogs (3, 4). Schulman et al. (11) have reported this tumor with the name of clear cell adnexal carcinoma for the first time and they proposed that clear cell hidradenocarcinoma and follicular stem cell carcinoma are the same tumors. Mean age of 7 years for the development of this tumor has been reported in dogs. Epithelial or follicular stem cells are the main origin of tumor because the positivity of cytokeratin and vimentin has been reported in different studies (7, 11). The purpose of this study was to evaluate cytological, histopathological and immunohistochemical features of canine cutaneous clear cell adnexal carcinoma and according to literature research, this is the first case in which we found psammoma bodies and nuclear pseudoinclusions on microscopic examination.

Two dogs of 6 and 8 years of old were brought at the Petcode Animal Hospital, Ankara for the examination of swollen masses on right forepaw and right hind paw (Fig 1). Cytological slides were prepared with the help of fine needle aspiration method and Wright stain was performed. After that excisional procedure was performed for the

Figure 1. Macroscopic presentation of tumor at right forepaw.

removal of tumor from the right forelimb and right hind limb of dogs. The excisional biopsy was preserved in 10% buffered formalin solution. Later it was sent Pathology laboratory of Afyon Kocatepe University, Afyonkarahisar for the histopathological and immunohistochemical examination.

After cutting and routine processing of tissues, suitable sections of 4µ were taken on slides. Hematoxylin and eosin stain was performed for the histopathological examination. Immunohistochemical evaluation was done for the confirmation of cellular origin tumor. For this staining process, the slides were deparaffinized in xylene. The clearing of tissues was done in graded alcohol solutions. Quenching of endogenous enzymes was performed by treating the tissues with 3% solution of hydrogen peroxide in methanol. After the antigen retrieval primary antibodies of vimentin, S-100, cytokeratin, GFAP and SMA were dropped on the tissues. The detail of primary antibodies for immunohistochemical evaluation is given in Table 1. After overnight incubation secondary antibodies were dropped on the tissues. Special humidity chamber was used for the incubation of slides on room temperature. ABC kit (TA-125-UDX, UltraVision Polyvalent HRP Kit, LabVision / ThermoScientific-USA) was used. Biotinylated IgG was dropped and was incubated at room temperature for 1 hour. Peroxidase conjugated avidin was used and allowed to react for 30 minutes at 37 ° C. Slides were washed with buffer solution and tissues were treated with red colored AEC (TA-060-HA, AEC Substrate System, LabVision / ThermoScientific-US) peroxidase substrate. After completion of reaction, the slides were taken into distilled water and counter stained with Mayer's hematoxylin. Slides were covered with coverslips using aqueous adhesive medium and examined under a light microscope (Zeiss Axio Lab.A1 Microscope - AxioCam ICc 5 Camera).

Table 1. The detail of antibodies used in immunohistochemical analysis of canine clear cell adnexal carcinoma.

Primary antibody	Detail of primary antibodies	Species
Cytokeratin (MNF116)	Santa Cruz, SC-58830	Mouse
Vimentin	Abcam, 3B4, ab28028	Mouse
S100	Thermo Fisher Scientific, RB-1805-A	Rabbit
MART1 (Melan A) (Ab-4)	Thermo Scientific, MS-799-P1	Mouse
SMA	Dako M0851	Mouse
GFAP	Thermo Scientific, RB-087	Rabbit

Cytological examination revealed scattered cell groups with clear cytoplasm borders on the hemorrhagic background. Although the cells showed marked pleomorphism, but were generally oval, round or spindle-shaped. Anisokaryosis, karyomegaly and one or more prominent nucleoli were noted in the nuclei. Pseudoinclusions were found in some cell nuclei (Fig 2 A-B). Histopathological examination showed that tumor was centrally necrotic, expansive growth consisting of lobular areas in the dermis. The neoplasic cells consisted of oval round shaped epithelioid cells with clear cytoplasm showing marked anisocytosis and anisorkaryosis. Their nuclei were oval or round in shape with prominent nucleoli. Cystic changes and calcified areas in layers (psammoma bodies) were noted in the areas. Few mitoses were found (Fig 2 C-D).

DOI: 10.33988/auvfd.1102050

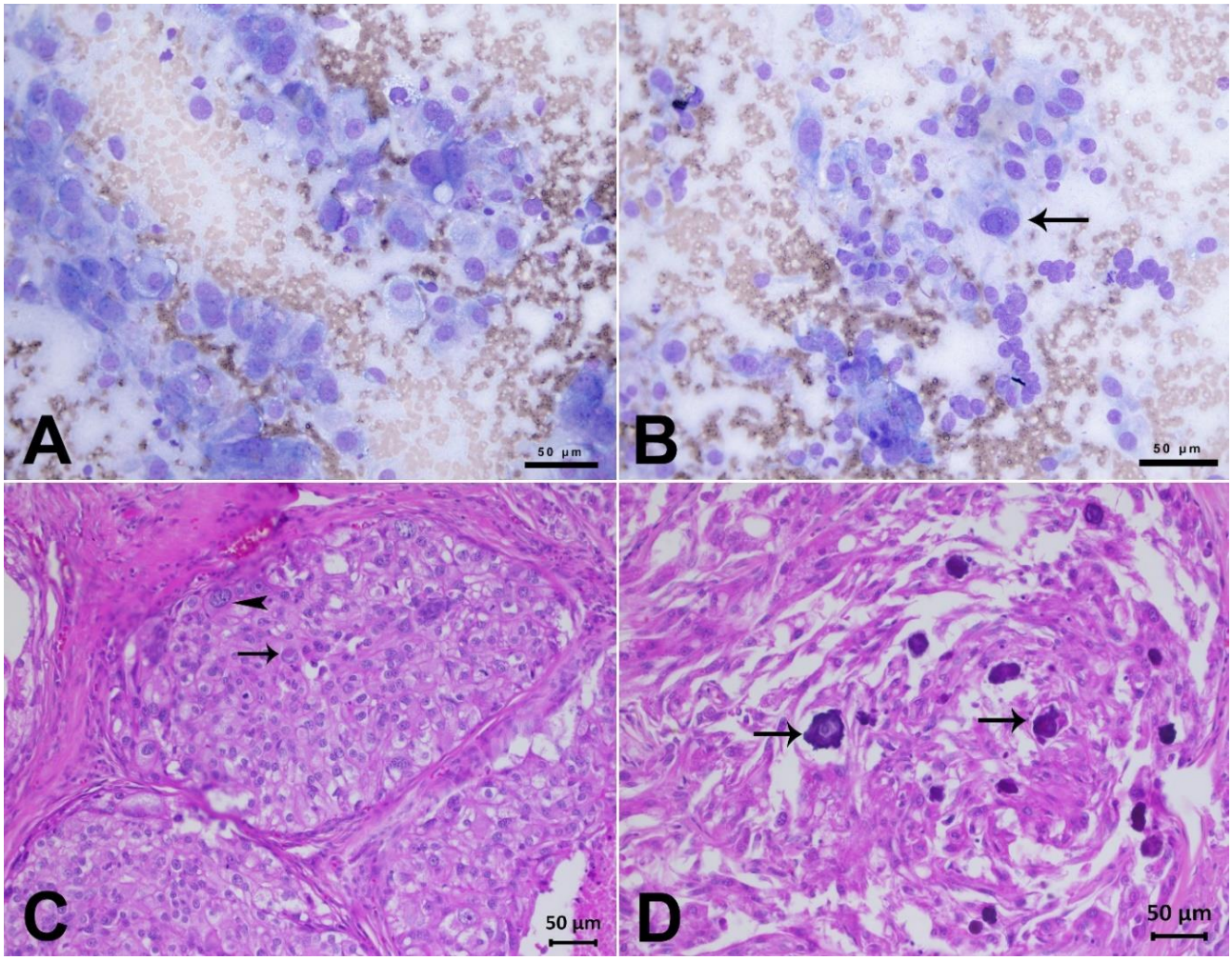

Figure 2. Cytological (A-B) and histopathological (C-D) images of the case (Scale bars=50 µm). **A-B.** Prominent and multi-nucleated oval nucleated, oval or round cytoplasm showing anisocytosis, anisokaryosis, karyomegaly and pseudoinclusion body (shown with arrow in B) (Wright's Stain). **C.** The neoplasic cells consisted of oval round shaped epithelioid cells with clear cytoplasm showing marked anisocytosis, anisorkaryosis , karyomegaly (arrow head) and psuedoinclusion (arrow) in lobular areas (H&E). **D.** some mineralization (psammoma bodies, shown with arrows) in neoplastic areas (H&E).

For immunohistochemical examination vimentin, cytokeratin, MART1, S-100, GFAP and SMA markers were used. Multifocal positivity with vimentin (Fig 3A), strong positivity especially of basal cells with cytokeratin (Fig 3B), diffuse positivity with MART1 (Fig 3C), and nuclear and cytoplasmic positivity with S-100 (Fig 3D) were evaluated. GFAP and SMA revealed no positivity.

In this study we have evaluated the cytological, histopathological and immunohistochemical features of canine cutaneous clear cell adnexal carcinoma. Cellular pleomorphism, loosely arranged oval to polygonal neoplastic cells with cytoplasmic projections and pink colored inclusions have been reported in previous cytological study (9). The criteria for malignancy was significant anisocytosis, anisokaryosis, pleomorphism, multinucleation, karyomegaly, and atypical mitotic figures (9). Cytological results of this study were also similar to the previously reported study. The presence of cytoplasmic pseudoinclusions has been evaluated during cytological examination in this report that was not found in previous studies. Pleomorphic neoplastic cells with clear cytoplasm, multinucleation of oval to polygonal cells has been reported in different studies (9, 11, 13). Histopathological results of this study revealed similar findings like previous studies. The difference from the previous studies in histopathological findings was the presence of psammoma bodies in this tumor. For the confirmation of diagnosis of canine cutaneous clear cell adnexal carcinoma, staining of different markers including cytokeratin, vimentin, Melan A, S-100 and smooth muscle actin has been reported. The positive results of vimentin, cytokeratin, S-100 and Melan A and negative results of smooth muscle actin have been evaluated in these studies (9, 11, 13). The immunohistochemical results of this study were found similar to the results of previous studies.

The differential diagnosis of canine cutaneous clear cell adnexal carcinoma with the other cutaneous tumors is really important. Cytokeratin could not be positive for the

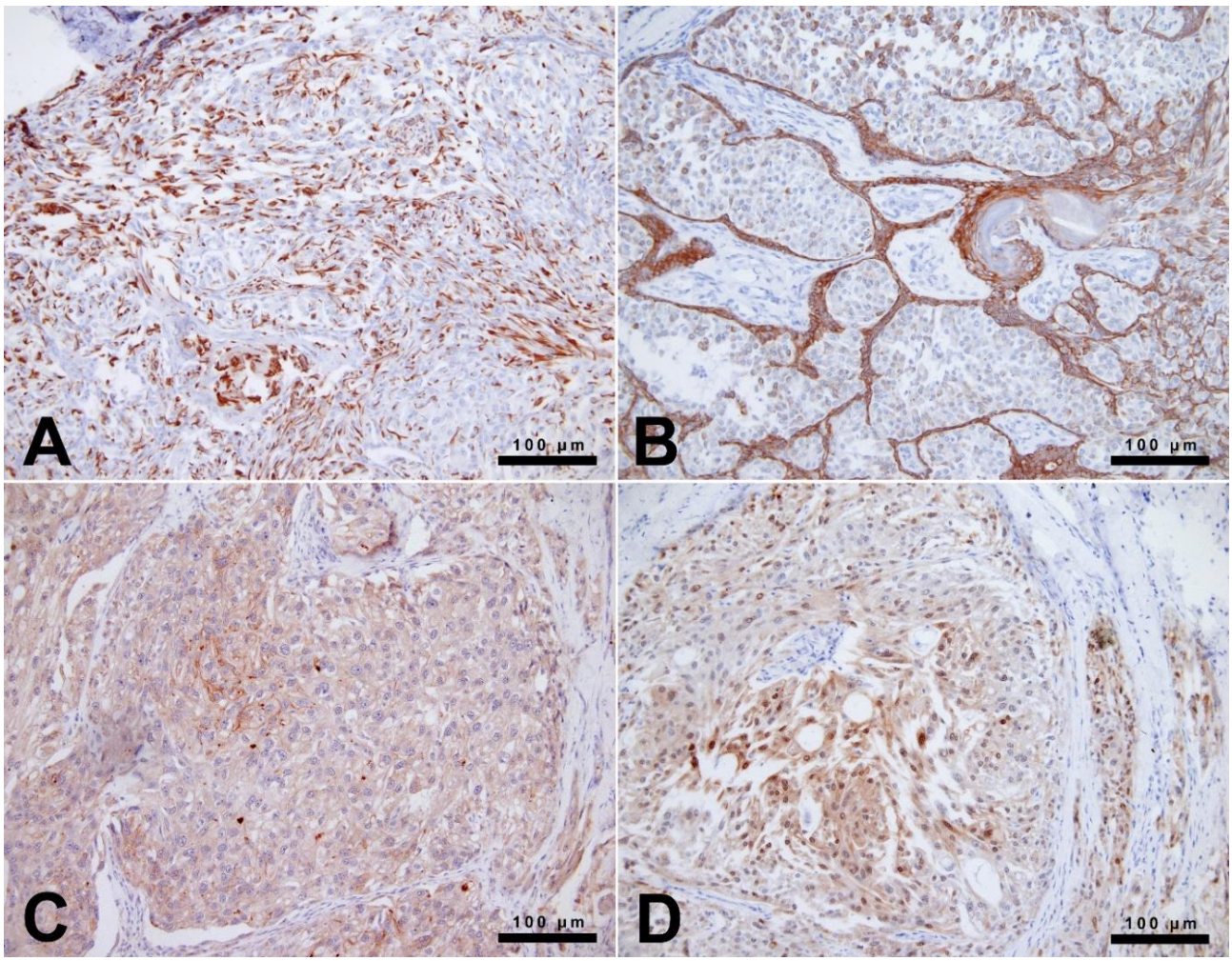

Figure 3. Immunohistochemical images of the case (Scale bar=100 µm). **A.** Multifocal positivity with vimentin. **B.** Strong positivity especially of basal cells with cytokeratin. **C.** Diffuse positivity with MART1. **D.** Nuclear and cytoplasmic positivity with S-100.

balloon cell melanoma and also it shows junctional activities that were not found in this report (11, 13). Positivity of Melan A and lack of sebaceous cells differentiation revealed that this is not a sebaceous carcinoma (4, 11). Epidermal contiguity has been found in clear cell basal carcinoma and it was not found in this report (3, 4). The negative result of smooth muscle actin is a consistent result with the previous studies (7, 11, 13). Liposarcoma has special features and it only shows the positivity of cytokeratin (11). Immunohistochemical results of this study were consistent with the correct diagnosis of cutaneous clear cell carcinoma in dogs. Psammoma bodies have normally been reported in different studies of meningioma in dogs (6, 8, 14) and cats (10). The positivity of vimentin and S-100 in meningioma (1, 2, 8) like clear cell adnexal carcinoma has also been reported. The presence of psammoma bodies in meningioma and clear cell adnexal carcinoma may have correlation. Future investigations have required to find out the correlation between the cells of origin of tumors.

Canine cutaneous clear cell adnexal carcinoma is a rare tumor and this study evaluated the cytological, histopathological and immunohistochemical features of this tumor. The presence of pseudoinclusions and psammoma bodies during microscopical examination were the interesting findings that have not been reported in previous studies.

Financial support

This research received no grant from any funding agency/sector.

Conflict of Interest

The authors declared that there is no conflict of interest.

Author Contributions

Diagnose, Investigation, Writing-Reviewing and Editing are made by MFB and MNB. Clinical evulation contributed by AN.

Data Availability Statement

The data supporting this study's findings are available from the corresponding author upon reasonable request.

Ethical Statement

There was no need of any ethical report for this study.

Animal Welfare

Not applicable.

References

1. **Adamo PF, Cantile C, Steinberg H** (2003): *Evaluation of progesterone and estrogen receptor expression in 15 meningiomas of dogs and cats*. Am J Vet Res, **64**, 1310-1318.
2. **Barnhart KF, Wojcieszyn J, Storts RW** (2002): *Immunohistochemical staining patterns of canine meningiomas and correlation with published immunophenotypes*. Vet Pathol, **39**, 311-321.
3. **Goldschmidt MH, Dunstan RW, Stannard AA, et al** (1998): Histological Classification of Epithelial and Melanocytic Tumors of the Skin of Domestic Animals. 2nd ser, vol. 3, Armed Forces Institute of Pathology, Washington, DC.
4. **Gross TL, Ihrke PJ, Walder EJ, et al** (2005): Skin Diseases of the Dog and Cat. 2nd ed., Blackwell Publishing, Oxford.
5. **Jabara AG, Finnie JW** (1978): *Four cases of clear-cell hidradenocarcinomas in the dog*. J Comp Pathol, **88**, 525-532.
6. **Latouche EL, Arena CB, Ivey JW, et al** (2018): *High-frequency irreversible electroporation for intracranial meningioma: a feasibility study in a spontaneous canine tumor model.* Technol Cancer Res Treat, **17**, 1533033818785285.
7. **Mikaelian I, Wong V** (2003): *Follicular stem cell carcinoma: Histologic, immunohistochemical, ultrastructural, and clinical characterization in 30 dogs.* Vet Pathol, **40**, 433-444.
8. **Montoliu P, Anor S, Vidal E, et al** (2006): *Histological and immunohistochemical study of 30 cases of canine meningioma*. J Comp Pathol, **135**, 200-207.
9. **Piviani M, Sánchez MD, Patel RT** (2012): *Cytologic features of clear cell adnexal carcinoma in 3 dogs.* Vet Clin Pathol, **41**, 405-411.
10. **Ramos-Vara JA, Miller MA, Gilbreath E, et al** (2010): *Immunohistochemical detection of CD34, E-cadherin, claudin-1, glucose transporter 1, laminin, and protein gene product 9.5 in 28 canine and 8 feline meningiomas.* Vet Pathol, **47**, 725-737.
11. **Schulman FY, Lipscomb TP, Atkin TJ** (2005): *Canine cutaneous clear cell adnexal carcinoma: histopathology, immunohistochemistry, and biologic behavior of 26 cases*. J Vet Diagnostic Investig, **17**, 403-411.
12. **Sharif M, Reinacher M** (2006): *Clear cell trichoblastomas in two dogs*. J Vet Med Ser A Physiol Pathol Clin Med, **53**, 352-354.
13. **Yasuno K, Nishiyama S, Suetsugu F, et al** (2009): *Shirota K. Cutaneous clear cell adnexal carcinoma in a dog: special reference to cytokeratin expression*. J Vet Med Sci, **71**, 1513-1517.
14. **Zimmerman KL, Bender HS, Daniel Boon G, et al** (2000): *A comparison of the cytologic and histologic features of meningiomas in four dogs.* Vet Clin Pathol, **29**, 29-34.

Microbial Biofilms in Veterinary Medicine

Fadime KIRAN[1,a,✉], Başar KARACA[1,2,b], Ali Furkan ERDOĞAN[3,c]

[1]Ankara University, Faculty of Science, Department of Biology, Ankara, Türkiye; [2]Turku University, Institute of Dentistry, Department of Periodontology, Turku, Finland; [3]Ankara University, Faculty of Veterinary Medicine, Department of Surgery, Ankara, Türkiye

[a]ORCID: 0000-0002-4536-2959; [b]ORCID: 0000-0001-6943-8965; [c]ORCID: 0000-0002-2646-8002

ARTICLE INFO

Article History
Received : 03.04.2022
Accepted : 13.06.2022
DOI: 10.33988/auvfd.1097786

Keywords
Biofilm
Diagnosis
Infection
Treatment
Veterinary medicine

✉Corresponding author
fkiran@science.ankara.edu.tr

How to cite this article: Kıran F, Karaca B, Erdoğan AF (2023): Microbial Biofilms in Veterinary Medicine. Ankara Univ Vet Fak Derg, 70 (1), 107-114. DOI: 10.33988/auvfd.1097786.

ABSTRACT

Microbial biofilms defined as extremely complex ecosystems are considered clinically important for humans. However, the concept and significant roles of microbial biofilms in the progression of disease have seriously lagged in veterinary medicine, when compared with human medicine. Although the importance of biofilms in animal health is just beginning to emerge, limited studies have paid attention that microbial biofilms are clinically important in the field of veterinary medicine, and lead to serious economic losses. In this review, the importance of microbial biofilms causing high economic losses in the livestock industry has been highlighted. Besides, the concept of microbial biofilm, their role in the pathogenesis of the animal diseases, as well as diagnosis approaches and possible therapeutic strategies needed to overcome their detrimental effects in veterinary medicine, have been discussed.

Introduction to microbial biofilms

In the early years of microbiology, microorganisms were mainly characterized as planktonic or freely floating cells. However, scientific observations have dramatically shown that the predominant form of microbial growth is in biofilms that attach to the surface of living and nonliving materials, in an almost irreversible manner (16). Today, biofilm is generally identified as an accumulation of microbial communities which are enclosed in an extracellular matrix (11). According to the recent international consensus statement (23) biofilm is defined as "A structured community of microbes with genetic diversity and variable gene expression (phenotype) that creates behaviors and defenses used to produce unique infections (chronic infection)". Biofilms are characterized by significant tolerance to antibiotics and biocides while remaining protected from host immunity.

Microbial biofilm formation is considered as a complex process with the inclusion of a cascade of molecular, biochemical and physiological events that depend on the type of microorganism, the surface, and environmental factors (1). The multistage development of mature biofilm begins with the primary adhesion between the microorganisms and the abiotic or biotic surfaces. Following the reversible attachment (i), bacteria and biotic surfaces express multiple adhesins factors and receptors for specific adherence (ii). They form aggregates and microcolonies, differentiate by the production of extracellular matrix (iii), and finally, the maturation of biofilms occurs by the attachment of additional microorganisms (iv) (Figure 1). The matrix consists of extracellular polymeric compounds including polysaccharides, proteins, DNA, and lipids, and protects the bacteria from extreme and depleted environments and antimicrobials, and gives mechanical stability (30, 43). Within biofilms, bacterial cells are sheltered against different adverse environmental conditions such as ultraviolet light radiation, osmotic changes, pH variability, dehydration, antimicrobial drugs, disinfectants, and host immune responses (40). Besides, the bacteria in the microenvironment of the biofilm matrix can deploy cell to cell communication by a signal system called quorum sensing (QS) through the production of

autoinducers (48). With QS mechanisms, microbial populations in the biofilm matrix coordinate their behaviors and gain advantages compared to planktonic cells (5).

The planktonic microorganisms have precisely been of value in strategies to combat diseases. However, recent studies have shown that microorganisms in biofilms show differences from their planktonic counterparts in terms of behavior, structure, and physiology (43). In addition, biofilms reduced the ability of the antimicrobials to get access to the microorganisms and make them resistant against certain antimicrobials.

The importance of microbial biofilms in animal health

With the increasing role of microbial biofilms in natural environments, it is not surprising that they are responsible for infection in both humans and animals. The Centre for Disease Control and Prevention (CDC) has suggested that 65% of bacterial infections in humans are related with microbial biofilms (2). The National Institutes of Health (NIH) revealed that of among all microbial and chronic infections, 65% and 80% are associated with biofilm formation, respectively (28). Due to the different husbandry and living conditions of animals, the risk of infection as well as biofilm formations presumably much greater in animal species than in humans. Biofilms have been also linked with numerous infectious diseases in animals, including chronic wounds, periodontal diseases, mastitis, and Salmonellosis (Figure 1). In addition to their direct effect, they also have significant indirect effects on the industries (1, 11).

Dental biofilms in oral health: Dental/oral biofilms are one of the most studied microbial biofilms in humans which is responsible for dental caries and periodontal diseases. As in humans, the oral microbiota of animals is structured in a variety of aerobic, facultative, or strictly anaerobic bacteria (61). Dysbiosis of oral microbiota leads to oral infections caused by dental plaques/biofilm bacteria which are highly prevalent in periodontal disease, soft tissue infections, and dental caries (59). Among oral infections, dental caries is a rare occurrence in pet animals (61). However, periodontal diseases as a chronic bacterial infection caused by microbial biofilms of mixed-species are one of the most common diseases of adult dogs and cats, and effect up to 80% of animals (31, 61). According to the American Veterinary Dental College, it is estimated that the majority of pets show symptoms of dental or periodontal diseases starting with dental biofilms, by three years of age. The formation of dental biofilm in the oral cavity of animals is a multi-stage process and mostly related to microorganisms in the oral cavity. *Porphyromonas cangingivalis* and oral protozoa such as *Entamoeba gingivalis* and *Trichomonas tenax* are the most common cariogenic microorganisms in canine dental biofilms which play an important role in canine periodontal disease (31). Borsanelli et al. (8) indicated that the significant antagonistic interactions between the *Petrimonas* spp., *Porphyromonas* spp., *Prevotella*spp., and *Fusobacterium* spp. species in the oral microbiota of shep are the key factors for dental biofilm associated with ovine periodontitis. An interesting data obtained by Perez- Serrano et al. (44) showed that dental biofilm can be considered as a source and reservoir of antibiotic resistance genes (ARG) and can be shared between humans and pets living in a household. Their results showed that dogs seem to play an important role in the transference of ARG, and the children appear to be the most affected.

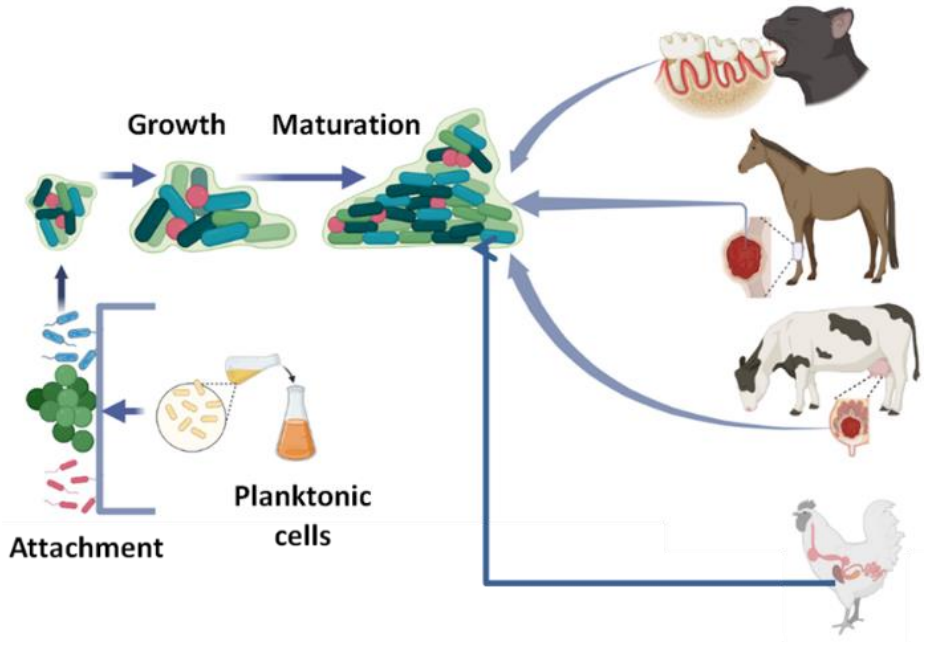

Figure 1. Schematic representation of the stages of microbial biofilm formation and its implications in the veterinary medicine. Figure created with BioRender.com (accessed on 26 March 2022).

DOI: 10.33988/auvfd.1097786

As with humans, dental biofilms in animals are highly important not only for oral health but also for their overall health. In addition to tooth loss, biofilm linked infections in the oral cavity may relate to various local consequences such as oral-nasal fistula, perioendo abscess, pathologic fracture because of chronic periodontal loss which weakens the bone in affected areas, inflammation close to the orbit which potentially leads to blindness, oral cancer and chronic osteomyelitis (61). The implications of "broken mouth" periodontitis especially affect the sheep grazed on rough pasture, and involves periodontal infection of the incisor teeth. In addition to being a painful condition, it reduces the efficiency of grazing of sheep and consequently leads to economic problems for sheep farmers (59).

Evidence is emerging that biofilm-related periodontal infections are also associated with serious systemic diseases, in animals. Therefore, the microbial and matrix composition of dental biofilms and their mechanisms in animals is now considered important to understand their role in animal diseases. However, comparable studies of dental biofilms in animals are relatively limited, despite the fact that similar infections also occur in the case of humans.

Biofilms in chronic wounds: In humans, microbial biofilms related to wound infections lead to chronic inflammation and delayed management (30). Although there are many biofilm-related researches conducted in animal models including rodents, rabbits, pigs, dogs, horses, etc., limited studies have been directly carried out for the determination of the clinical importance of microbial biofilms in the field of veterinary medicine. However, similar to humans, animals suffer from chronic wounds which are the common sites for biofilm formation in veterinary clinics (30). Recent limited studies have been identified the prevalence of microbial biofilms in wounds of dogs, cats, and horses. Nevertheless, their significance and the factors that modulate and stimulate their formation are still unknown (33).

In veterinary medicine, horses are particularly at risk from chronic non-healing wounds of the lower limb similar to venous leg ulcers seen in humans (55). The first study which identified the microbial biofilms in the chronic wounds of horses was carried out by Cochrane et al. (12). In a recent experimental wound model of equine with bacterial inoculation, Jorgensen et al. (29) showed that microbial biofilms have a negative impact on wound healing of distal limb wounds but not another part of the body wounds. Although there are no investigations focused on the effect of microbial biofilms for wound healing of horses in the literature (30), the presence of biofilms in equine wounds partly explains the reluctance of many lower limb wounds to heal. The prevalence of biofilm in traumatic wounds of horses makes them important due to the non-healing limb wounds leading to well-documented welfare and economic concerns (58). In addition to horses, the first report of microbial biofilms in dog chronic wounds has been reported by Swanson et al. (54). A 4-year-old spayed female Mastiff was evaluated for the treatment of chronic non-healing pressure wounds, and biofilm reformation was prevented by treatment with antimicrobials. Although the microbial composition of biofilms in chronic wound infections of animals is still unclear, the majority of the microorganisms in chronic wounds of dogs were found belonging to the *Propionibacteriaceae*, *Porphyromonadaceae*, *Deinococcaceae*, *Nocardiaceae*, *Methylococcaceae*, and *Alteromonadaceae* which may not be cultured by conventional microbiological methods under laboratory conditions (33).

In addition to the direct effect of biofilms on wound infections, the formation of biofilms on surgical implants has also a major role in chronic wound infection, in veterinary medicine (34). Based on the initial researches of microbial biofilms in wounds or on surgical implants, the role of microbial biofilm in wound management is dependent on various factors, mainly the wound bed and its microenvironment. However, additional knowledge is still needed to investigate the prevalence and etiology of biofilms in animal chronic wounds.

Mastitis and microbial biofilms: Mastitis is one of the most important and multi-factorial disease affecting many species of animals including sheep, pigs, dogs, cats, goats, and horses. Bovine mastitis defined as an inflammation of the udder generally caused by microbial biofilm-related infection has a high incidence, worldwide (21). Besides, it is responsible for major economic losses on dairy farms with decreasing in milk production, increasing in health care costs, and leading to serious public health considerations (6, 21).

Bovine mastitis is characterized by the infection of the mammary gland epithelium. In the pathogenesis of mastitis, biofilm formation is also considered another important virulent factor and also a selective advantage for mastitis-causing pathogens such as *Staphylococcus aureus*, *S. epidermidis*, *S. uberis*, and *S. dysgalactiae*. In addition to staphylococci, coliforms, enterococci, and streptococci are also the common isolated genus from cows which suffer from mastitis (53). During the last decade, over 200 studies have been published focused on the *in vitro* biofilm forming potential of bovine mastitis pathogens, especially to *S. aureus*, on their molecular mechanism to form a biofilm, and their potential treatments (41). However, the main role of microbial biofilms in the pathogenesis of bovine mastitis is still unclear. To investigate their actual role in bovine mastitis,

in vivo studies of biofilms in infected udders have to be carried out. Overall, it is considered very important to understand the role of biofilm in bovine mastitis to apply the best control strategies in veterinary medicine. It has to be also the main necessity in order to reduce economic problems in the dairy global market, and to ensure milk safety and quality, as well as animal welfare.

Salmonella biofilms in poultry: Salmonellosis is an infection caused by different serotypes of *Salmonella* spp. live in the intestinal tracts of domestic animals, and cause ranging in the severity of symptoms such as diarrhea and enteritis to systemic syndrome (42). As an emerging zoonotic bacterial threat in the poultry industry, the infection of *Salmonella* spp. leads to important global public health problems (26). *Salmonella*-contaminated animal-derived food products resulted in 3% of the bacterial food-borne disease in all around the world, with approximately 80 million infections and 155.000 deaths, per year (3, 18, 35). According to the Interagency Food Safety Analytics Collaboration (27), 14% of outbreaks of Salmonellosis are estimated to be related with chicken meat and egg, which are contaminated by chicken intestinal contents (9, 45). In addition to public health concerns, Salmonellosis affects meat and egg production and results in a huge economic loss in the poultry industry (39).

Although it consists of more than 2500 serologically different variants or serotypes, *Salmonella enteritidis* and *Salmonella typhimurium* are the most common serotypes isolated from Salmonellosis outbreaks and infected poultry products (7, 20). *Salmonella* infection is transmitted horizontally and vertically in poultry, with high incidence in one-day-old chicks (51), and the contamination with these bacteria in poultry-derived meat/eggs products can occur at multiple stages along the food chain (17, 39). *Salmonella* strains often exist not only as planktonic cells but also in biofilms formed on various surfaces (50). *Salmonella* spp. are able to adhere to abiotic and biotic surfaces and form biofilms. The formation of biofilm may lead to a direct interaction between the contaminated of food products in food processing environments (39). Approximately, 50% of the *Salmonella* strains isolated on poultry farms were able to produce biofilms (37). The biofilms formed by *Salmonella* strains provide them more resistance to antimicrobials, chemical, physical and mechanical stresses, and host immune systems (42), thus playing an important role in the survival of planktonic cells under unsuitable conditions, such as poultry farms and slaughterhouses (56). Therefore, special attention must be paid to the prevention and management of Salmonellosis (39). Since biofilms protect the bacteria from antimicrobial agents, sanitizers, as well as other environmental factors (4), *Salmonella* biofilms, represent a major problem, especially in the feed and food industry (dairy, fish, and meat industry) (50). As a consequence of the importance of biofilm-forming *Salmonella* spp., combating *Salmonella* infections gains importance not only for the public health but also for the poultry industry. Therefore, the multi-factorial and complex phenomenon of the biofilm formation has to be identified under laboratory and, *in vivo* conditions as well as in farm environments (42). Moreover, current approaches are still necessary to develop a control strategy to eradicate the biofilm formed by *Salmonella* spp.

***Medical device-associated biofilms*:** Medical devices can be suitable abiotic surfaces for biofilm formation of various microbial species (15). However, there are relatively few studies on biofilm infections from medical devices in the field of veterinary medicine. According to a study, catheterized dogs developed urinary tract infections more frequently than non-catheterized dogs and *Escherichia coli*, *Proteus mirabilis*, *Pseudomonas*, *Enterococcus*, and *Klebsiella* species were commonly described in catheter-related infections in domestic cats and dogs (10).

Peritoneal dialysis is a procedure that has been used for many years in dogs with acute and chronic renal failure. Not surprisingly, *S. aureus* and *S. epidermidis*, which are commonly isolated in catheter-related biofilm infections, are also present in peritoneal catheters used in the treatment of animals. This is because staphylococci that migrate into the catheter from the skin microbiota, and can form biofilms on the catheter surface (38, 46). It is highly possible to encounter *Pseudomonas*, *S. aureus*, coagulase-negative staphylococci, and meticillin-resistant Gram-positive bacteria, which are also common in humans with catheter-associated bloodstream infections as well as in animals (25). In addition to these medical devices associated with biofilm, polyurethane or silicone surfaces of gastronomy tubes that are essential for animals if they can no longer feed themselves, are suitable environments for the bacterial adherence. Various Gram-positive and Gram-negative bacteria can form biofilms in the lumen of these tubes (60).

Diagnosis of microbial biofilms

Diagnosis of biofilms in animals is very complicated due to the complex lifestyle of planktonic cells, the lack of evident clinical signs, and the requirements for advanced methods (30). Numerous approaches based on different methods have been developed for the phenotypic, biochemical and genotypic analysis of biofilm formation. These techniques aim to determine the viability of microorganisms (quantification of viable cells) and to analyze the components of biofilm matrix and biomass

DOI: 10.33988/auvfd.1097786

(39). For the phenotypic identification of biofilm-producing strains, the most common methods are based on microtitre-plate analysis (13). Macroscopic and quantitative estimation of bacterial biofilm on different surfaces can be determined by crystal violet staining assay, and the Congo red agar test (19) which lead to direct analysis of the colonies and the detection of slime-forming strains and non-slime-forming strains (39).

It is also challenging to achieve an accurate diagnosis of the heterogenetic distribution of bacteria in biofilms through the conventional culture and isolation methods. Standard microbiological culture techniques can allow to detect only the culturable microorganisms but not the unculturable ones. To detect the microorganism composition of the biofilms, molecular techniques including RT-PCR (Real-Time Polymerase Chain Reaction), 16S ribosomal ribonucleic acid (rRNA) gene sequencing, next gene sequencing (NGS) give deeper information. However, they are not considered as the gold standards from the point of biofilm detection. When bacterial infection progresses to biofilm, there is an urgency to develop more accurate diagnostic tools for analyzing the biofilm biomass (14). Considering this, scanning electron microscopy (Figure 2), confocal laser microscopy, and its combination with fluorescent in situ hybridization using different probes can be successfully used in the detection of microbial biofilms (47, 49). In addition to optical imaging techniques, nuclear and ultrasonic imaging techniques and their combination with other methods have been explored in order to detect and quantify early and mature microbial biofilms (14). However, microbial biofilm detection still possesses a challenge for the scientific community. Potential diagnostic markers which able to utilize the difference between planktonic and biofilm cells, are still needed.

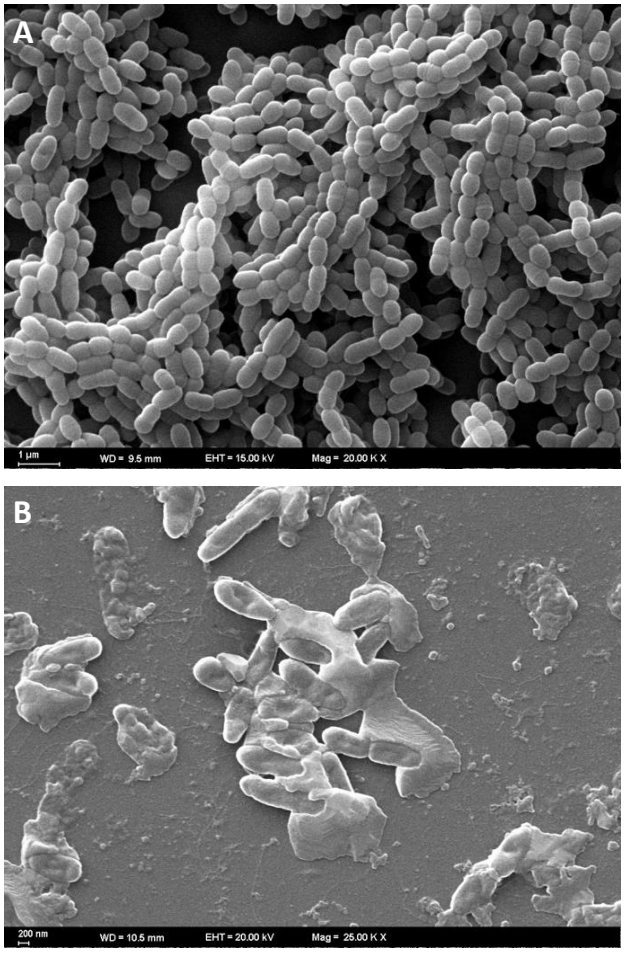

Figure 2. Scanning electron microscopy micrographs of biofilm formation by *Streptococcus mutans* (a, cariogenic pathogen related with dental biofilm progress), and *Pseudomonas aeuroginosa* (b, pathogen related with wound infections).

Novel strategies to control microbial biofilms

Microbial biofilms are highly resistant to antimicrobial drugs (antibiotics, disinfectants, or antifungals) as well as the host immune response when compared to free-flowing planktonic bacteria. Although antimicrobial drugs often eliminate the planktonic cells that are released from the matrix, they have minimal effects on eradicating microbial biofilm that are formed (52). This is because that antimicrobial agent cannot gain access to the pathogens due to the impermeable nature of the biofilm extracellular matrix. This situation makes their treatment increasingly problematic (1, 14). Therefore, an effective treatment has to aim for the complete eradication of microbial biofilm of the pathogenic bacteria, not only to their planktonic form. Thus, alternative and effective strategies play a pivotal role to reach better animal health and bio-safety in veterinary medicine.

Natural or synthetic substances such as chlorhexidine, polyethylemine, silver, nitric oxide, honey, plant extracts, probiotics, matrix-degrading enzymes, are in use as potential antibiofilm treatments (14, 24, 30, 49). Since the QS is a key regulatory system in the pathogenesis of various bacterial infections, applications of these compounds targeted the blocking of QS mechanisms may also provide novel strategies to combat with microbial biofilms (48). Novel therapeutic applications include the combination of conventional antimicrobial agents with ultrasound devices, electric current, phage therapy, or drug delivery systems (1). Ultrasounds enhance the bactericidal activity of the antimicrobials through their passage of non-invasive acoustic energy waves from the skin to the site of biofilm. The electromagnetic impulse increases the antimicrobial activity of cationic agents against bacterial biofilms (32). Although it is not commonly applied in veterinary biofilm therapeutics, phage therapy has the potential for the hydrolyzation and degradation of the extracellular matrix of biofilms (57). With the drug delivery system,

antimicrobials are incorporated into nano-carriers such as phosphatidylcholine or polyamidoamine, and display their mechanisms by prolonging the effect of the active molecules which is delivered to the appropriate action site (32). Another approach for microbial biofilm treatment especially in chronic wounds is using debridements combined with other antibiofilm strategies, although there are no specific guidelines exist for animals (36).

Despite intense researches in animal models, the optimal antibiofilm treatment in veterinary science has not yet been identified. The use of new technologies as a treatment strategy can provide useful tools in veterinary medicine for the control of biofilm infections, in the future.

Conclusions

Considering the prevalence of microbial biofilms formed by microorganisms in different part of ecosystems in all over the world, it is not surprising that they are one of the main contributors causing serious medical complications in humans and animals. In the light of scientific knowledge that microbial biofilm formation is responsible for many infectious diseases affecting humans, the effect of microbial biofilms in veterinary medicine should not be ignored. Most of the biofilm-based infections are related with animal injuries, oral health, and mastitis cases which are similar to that of humans. It is also known that more than 50% of human biofilm infections are zoonotic origin. Despite the limited number of the studies focused on the importance of biofilm in veterinary medicine, their results highlight the need to develop an eradication treatment and preventive plan to combat the biofilm development in animals. Without effective diagnostic and treatment protocols for veterinary biofilms, their impact will remain a significant challenge. Therefore, additional researches are still needed to unravel the mystery of microbial biofilms in veterinary medicine.

Conflicts of interest

The authors declared that there is no conflict of interest.

Data Availability Statement

The data supporting this study's findings are available from the corresponding author upon reasonable request.

References

1. **Abdullahi UF, Igwenagu E, Mu'azu A, et al** (2016): *Intrigues of biofilm: A perspective in veterinary medicine.* Vet World, **9**, 12-18.
2. **Batz MB, Hoffmann S, Morris JG** (2012): *Ranking the disease burden of 14 pathogens in food sources in the United States using attribution data from outbreak investigations and expert elicitation.* J Food Protect, **75**, 1278-1291.
3. **Bell RL, Cao G, Allard MW, et al** (2012): Salmonella Newport contamination of produce: Ecological, genetic, and epidemiological aspects. 155-173. In: Monte AS, De Santos PE (Eds), *Salmonella*: Classification, Genetics and Disease Nova, New York.
4. **Beshiru A, Igbinosa IH, Igbinosa EO** (2018*): Biofilm formation and potential virulence factors of* Salmonella *strains isolated from ready-to-eat shrimps.* PLoS ONE, **13**, e0204345.
5. **Bjarnsholt T, Givskov M** (2006): *The role of quorum sensing in the pathogenicity of the cunning aggressor Pseudomonas aeruginosa.* Anal Bioanal Chem, **387**, 409-414.
6. **Borawski P, Pawlewicz A, Parzonko A, et al** (2020): *Factors shaping cow's milk production in the EU.* Sustainability, **12**, 420.
7. **Borges KA, Furian TQ, de Souza SN, et al** (2018): *Biofilm formation by Salmonella Enteritidis and Salmonella Typhimurium isolated from avian sources is partially related with their in vivo pathogenicity.* Microb Path, **118**, 238-241.
8. **Borsanelli AC, Athayde FRF, Agostinho SD, et al** (2021): *Dental biofilm and its ecological interrelationships in ovine periodontitis.* J Med Microbiol, **70**, PMID: 34313584.
9. **Braden CR** (2006): *Salmonella enterica serotype Enteritidis and eggs: a national epidemic in the United States.* Clin Infect Dis, **43**, 512-517.
10. **Bubenik LJ, Hosgood GL, Waldron DR, et al** (2007): *Frequency of urinary tract infection in catheterized dogs and comparison of bacterial culture and susceptibility testing results for catheterized and noncatheterized dogs with urinary tract infections.* J American Vet Med Assoc, **231,** 893-899.
11. **Choudhary P, Singh S, Agarwal V** (2020): Microbial biofilms. 1-11. In: Dincer S (Ed), Bacterial biofilms. IntechOpen, London.
12. **Cochrane CA, Freeman K, Woods E, et al** (2009): *Biofilm evidence and the microbial diversity of horse wounds.* Can J Microbiol, **55**, 197-202.
13. **Christensen GD, Simpson WA, Younger JJ, et al** (1985): *Adherence of coagulase-negative Staphylococci to plastic tissue culture plates: a quantitative model for the adherence of Staphylococci to medical device.* J Clin Microbiol, **22**, 996-1006.
14. **Cruz A, Condinho M, Carvalho B, et al** (2021): *The two weapons against bacterial biofilms: Detection and treatment.* Antibiotics, **10**, 1482-1503.
15. **Donlan RM** (2001): *Biofilms and device-associated infections.* Emerg Infec Dis, **7**, 277-281.
16. **Donlan RM** (2002): *Biofilms: microbial life on surfaces.* Emerg Infect Dis, **8**, 881-890.
17. **Dookeran MM, Baccus-Taylor GS, Akingbala JO, et al** (2012): *Transmission of Salmonella on broiler chickens and carcasses from production to retail in Trinidad and Tobago.* J Agr Biodiv Res, **1**, 78-84.
18. **Eng SK, Pusparajah P, Mutalib NSA, et al** (2015): *Salmonella: a review on pathogenesis, epidemiology and antibiotic resistance.* Front Life Sci, **8**, 284-293.
19. **Freeman DJ, Falkiner FR, Keane CT** (1989): *New method for detecting slime production by coagulase negative staphylococci.* J Clin Pathol, **42**, 872-874.

20. **Gast R** (2008): Salmonella infection. 619-642. In: Saif Y, Fadly A, Glisson J, et al (Eds.), Diseases of poultry, Blakwell, Iowa.
21. **Gomes F, Saavedra MJ, Henriques M** (2016): *Bovine mastitis disease/pathogenicity: evidence of the potential role of microbial biofilms.* Pathog Dis,**74**, 1-7.
22. **Gómez-Suárez C, Busscher H, van der Mei H** (2001): *Analysis of bacterial detachment from substratum surfaces by the passage of air-liquid interfaces.* App Environ Microbiol, **67**, 2531-2537.
23. **Haesler E, Swanson T, Ousey K, et al** (2019): *Clinical indicators of wound infection and biofilm: Reaching international consensus.* J Wound Care, **28**, 1-4.
24. **Hawas S, Verderosa AD, Totsika M** (2022): *Combination therapies for biofilm inhibition and eradication: A comparative review of laboratory and preclinical studies.* Front Cell Infect Microbiol, **12**, 850030.
25. **Hooper SJ, Percival SL, Cochrane CA, et al** (2011): Biofilms and implication in medical devices in humans and animals. 191-203. In: Biofilms and Veterinary Medicine, Springer, Berlin, Heidelberg.
26. **Hossain MJ, Attia Y, Ballah FM, et al** (2021): *Zoonotic significance and antimicrobial resistance in Salmonella in poultry in Bangladesh for the period of 2011–2021*. Zoonotic Dis, **1**, 3-24.
27. **IFSAC** (2017): Foodborne illness source attribution estimates for 2013 for *Salmonella*, *Escherichia coli* O157, *Listeria monocytogenes*, and *Campylobacter* using multi-year outbreak surveillance data. United States. USDAFSIS, GA and D.C: U.S. Department of Health and Human Services, CDC, FDA.
28. **Jamal M, Wisal A, SaadiaA, et al** (2018): *Bacterial biofilm and associated infections.* J Chinese Med Assoc, **81**, 7-11.
29. **Jørgensen E, Bay L, Skovgaard LT, et al** (2019): *An equine wound model to study effects of bacterial aggregates on wound healing.* Adv Wound Care, **8**, 487-498.
30. **Jørgensen E, Bjarnsholt T, Jacobsen S** (2021): *Biofilm and equine limb wounds.* Animals, **11**, 2825-2840.
31. **Kačírová J, Maďar M, Štrkolcová G, et al** (2020): Dental biofilm as etiological agent of canine periodontal disease. 1-17. In: Dincer S (Ed), Bacterial biofilms. IntechOpen, London.
32. **Kasimanickam RK, Ranjan A, Asokan GV, et al** (2013): *Prevention and treatment of biofilms by hybrid and nanotechnologies.* Int J Nanomed, **8**, 2809-2819.
33. **König LM, Klopfleisch R, Höper D, et al** (2014): *Next generation sequencing analysis of biofilms from three dogs with postoperative surgical site infection.* Int Sch Res Not, 1-5.
34. **König LM, Klopfleisch R, Kershaw O, et al** (2015): *Prevalence of biofilms on surgical suture segments in wounds of dogs, cats, and horses.* Vet Pathol, **52**, 295-297.
35. **Majowicz SE, Musto J, Scallan E, et al** (2010*): International Collaboration on Enteric Disease "Burden of Illness" Studies. The global burden of nontyphoidal Salmonella gastroenteritis.* Clin Infect Dis, **50**, 882-889.
36. **Malone M, Swanson T** (2017): *Biofilm-based wound care: The importance of debridement in biofilm treatment strategies.* Br J Community Nurs, **22**, 20-25.
37. **Marin C, Hernandez A, Lainez M** (2009): *Biofilm development capacity of Salmonella strains isolated in poultry risk factors and their resistance against disinfectants.* Poultry Sci, **88**, 424-431.
38. **McDermid KP, Morek DW, Olson ME, et al** (1993): *A porcine model of Staphylococcus epidermidis catheter-associated infection.* J Infec Dis, **168**, 897-903.
39. **Merino L, Procura F, Fernando T, et al** (2017): *Biofilm formation by Salmonella sp. in the poultry industry: Detection, control and eradication strategies.* Food Res Int, **24**, 1-11.
40. **Nilsson RE, Ross T, Bowman JP** (2011): *Variability in biofilm production by Listeria monocytogenes correlated to strain origin and growth conditions.* Int J Food Microbiol, **150**, 14-24.
41. **Pedersen RR, Krömker V, Bjarnsholt T, et al** (2021): *Biofilm research in bovine mastitis.* Front Vet Sci, **8**, 656810.
42. **Peng M, Salaheen S, Almario JA, et al** (2016): *Prevalence and antibiotic resistance pattern of Salmonella serovars in integrated crop livestock farms and their products sold in local markets.* Environ Microbiol,**18**, 1654-1665.
43. **Percival SL, Malic S, Cruz H, et al** (2011): Introduction to biofilms. 129-142. In: Percival S, Knottenbelt D,Cochrane C (Eds), Biofilms and Veterinary Medicine. Springer, Berlin.
44. **Pérez-Serrano RM, Domínguez-Pérez RA, Ayala-Herrera JL, et al** (2020): *Dental plaque microbiota of pet owners and their dogs as a shared source and reservoir of antimicrobial resistance genes.* J Glob Antimicrob Resist, **21**, 285-290.
45. **Pires SM, Vieira SR, Hald T, et al** (2014): *Source attribution of human Salmonellosis: an overview of methods and estimates.* Foodborne Pathog Dis, **11**, 667-676.
46. **Read RR, Eberwein P, Dasgupta MK, et al** (1989): *Peritonitis in peritoneal dialysis: bacterial colonization by biofilm spread along the catheter surface.* Kidney Int, **35**, 614-621.
47. **Relucenti M, Familiari G, Donfrancesco O, et al** (2021): *Microscopy methods for biofilm Imaging: Focus on SEM and VP-SEM.* Pros Con Biol, **10**, 51.
48. **Schillaci D, Vitale M** (2012): *Biofilm related to animal health, zoonosis and food transmitted diseases: Alternative targets for antimicrobial strategy?* J Microbial Biochem Technol, **4**, 7-10.
49. **Sevin S, Karaca B, Haliscelik O, et al** (2021): *Postbiotics secreted by Lactobacillus sakei EIR/CM-1 isolated from cow milk microbiota, display antibacterial and antibiofilm activity against ruminant mastitis-causing pathogens.* Ital J Anim Sci, **20**, 1302-1316.
50. **Shatila F, Yaşa I, Yalçın HT** (2021): *Biofilm formation by Salmonella enterica strains.* Curr Microbiol**, 78,** 1150-1158.
51. **Shivaprasad HL, Methner PA** (2013): Salmonella infections in the domestic fowl. 162-192. In: Barrow PA, Methner U (Eds.), Salmonellain Domestic Animals (2nd ed.), CABI, Boston, Massachusetts.
52. **Stewart PS, Franklin MJ** (2008): *Physiological heterogeneity in biofilms.* Nat Rev Microbiol, **6**, 199-210.

53. **Smulski S, Gehrke M, Libera K, et al** (2020): *Effects of various mastitis treatments on the reproductive performance of cows.* BMC Vet Res, **16**, 99-109.
54. **Swanson EA, Freeman LJ, Seleem MN, et al** (2014): *Biofilm-infected wounds in a dog.* J Am Veter Med Assoc, **244**, 699-707.
55. **Theoret CL** (2004): *Wound repair in the horse: problems and proposed innovative solutions.* Clin Tech Equine Prac, **3**, 134-140.
56. **Wang H, Ye K, Wei X, et al** (2013): *Occurrence, antimicrobial resistance and biofilm formation of Salmonella isolates from a chicken slaughter plant in China*. Food Cont, **33**, 378-384.
57. **Weiling FU, Forster T, Mayer O, et al** (2010): *Bacteriophage cocktail for the prevention of biofilm formation by Pseudomonas aeruginosa on catheters in an* in vitro *model system.* Antimicrob Agents Chemother, **54**, 397-404.
58. **Westgate SJ, Percival SL, Knottenbelt DC, et al** (2011): *Microbiology of equine wounds and evidence of bacterial biofilms.* Vet Microbiol, **150**, 152-159.
59. **Williams DW, Lewis MAO, Percival SL, et al** (2011): Role of biofilms in the oral health of animals.129-142. In: Percival S, Knottenbelt D,Cochrane C (Eds), Biofilms and Veterinary Medicine. Springer, Berlin.
60. **Wortinger A** (2006): *Care and use of feeding tubes in dogs and cats.* J American Animal Hosp Assoc, **42**, 401-406.
61. **Zambori C, Tirziu E, Nichita I, et al** (2012): *Biofilm implication in oral diseases of dogs and cats.* Anim Sci Biotechnol, **45**, 208-212.

Instruction to Authors

1. The Journal of the Faculty of Veterinary Medicine, Ankara University is a peer-reviewed general veterinary medical journal being published 4 times a year and its abbreviation is "Ankara Univ Vet Fak Derg".
2. The language of the journal is English.
3. Original research articles, reviews, case reports and short communications on all aspects of veterinary science, which had not been previously published elsewhere in whole or in part except abstract not exceeding 250 words, are published in the journal. Review articles are only be submitted by invitation.
4. Manuscripts (including footnotes, references, figure legends, and tables) should be prepared with the following attributes: 12-point Times New Roman, double-space typed, 3-cm ample margins, sequential line numbering, and A4 page size. Page numbers should also be written on the top-middle of each page except first page. Manuscripts including figures and tables should not be exceeding 30 pages for original research articles, 30 pages for review articles, 15 pages for case reports and short communications.
5. The manuscripts have to be submitted online from this web page: "vetjournal.ankara.edu.tr". Once a manuscript has been submitted electronically via online system, the order of authorship (including adding or removing authors) cannot be changed.
6. Original research articles and case reports must be prepared in the following order: title, author/s, address, abstract, key words, introduction, materials and methods, results, discussion and conclusion, acknowledgement, and references. Sub divisions of introduction, materials and methods, results, and discussion and conclusion should not be placed in short communications. Acknowledgement should be limited to only technical support.
   Title should be short and clear, and be written with small letters. Explanation/s regarding the study should be indicated as footnotes.
   Author/s should be indicated as first and last name. Last name/s should be written with capital letters.
   Abstract should be written as a single paragraph not exceeding 250 words.
   Keywords up to 5 words should be written alphabetically.
   Introduction limited to 2 pages should include the literature review related to study. The purpose/s and hypothesis of study should be indicated in the last paragraph of introduction.
   Materials and Methods should be brief, clear, and without unnecessary details. Type of research (descriptive, observation, experimental, case-control, follow-up etc.), characteristics of subjects, inclusion and exclusion criteria, sampling method if it was used in conjunction with the data collection phase, and reason for sampling method without probability if it was used should be indicated. Sample size and its calculation method, power value if calculated, and censored and missing numbers should be indicated. Statistical analysis and its software applications should be indicated.
   Results should be explained briefly. Information stated in tables or figures should not be repeated in the text.
   Subheadings should be typed with italic and second subheadings should be typed with normal fonts in both materials and methods and results sections. Subheadings in italics should be placed at the beginning of the paragraph. Images should be at least 1920 x 1280 dpi resolutions. Tables and figures should be placed into separate sheets as a last part of manuscript.
   Abbreviations, **symbols ant units:** Abbreviations should be placed in parenthesis next to word/s written first time and then they should be used as abbreviations in the text i.e., Canine Transmissible Venereal Tumor (CTVT). Genus and species names in Latin should be indicated with italic font. All measurements must be indicated according to Systeme Internationale (SI) units.
   Discussion and Conclusion should include the interpretation of present study results with other study results indicated in reference list.
   Reference list should be numbered alphabetically. Each reference should be ordered with author's name in black, parenthesized publication year in normal, title in italic, and short name of journal and page numbers in normal and its volume number in black font. The periodicals must be abbreviated according to "Periodical Title Abbreviations: By Abbreviation". For references with more than 3 authors, only the first 3 authors should be listed, followed by "et al." In the text, references must be cited with number, and if name of author was indicated, just last name should be written before the reference number. In a single sentence, numbers of references should be limited to 5 ordered from small to higher number.
   The following is the style used for common types of references:
   For article:
   Sandstedt K, Ursing J (1991): *Description of the Campylobacter upsaliensis previously known as CNW group*. Syst Appl Microbiol, **14**, 39-45.
   Sandstedt K, Ursing J, Walder M (1983): *Thermotolerant Campylobacter with no or weak catalase activity isolated from dogs*. Curr Microbiol, **8**, 209-213.
   Lamont LA, Bulmer BJ, Sisson DD, et al. (2002): *Doppler echocardiographic effects of medetomidine on dynamic left ventricular outflow tract obstruction in cats.* J Am Vet Med Assoc, **221**, 1276-1281.
   For book:
   Falconer DS (1960): Introduction to Quantitative Genetics. Oliver and Boyd Ltd, Edinburgh.
   For book chapter:
   Bahk J, Marth EH (1990): Listeriosis and Listeria monocytogenes. 248-256. In: DO Cliver (Ed), Foodborne Diseases. Academic Press, San Diego.
   Electronic material should be placed with access date.
   Li G., Hart A, Gregory J (1998): Flokülasyona hız gradyanı etkisi. Available at http://www.server.com/projects/paper2.html. (Accessed May 20, 2004)
   Mail address of corresponding author should be placed at the end of manuscript.
7. Manuscript with copyright release form signed by all authors should be submitted to: "Ankara Üniversitesi Veteriner Fakültesi Dekanlığı, Yayın Alt Komitesi, 06110 Ankara, Türkiye". Conditions regarding for authorship was explained in the copyright release form. Publication process regarding evaluation of manuscript is at the discretion of the Editor. Acceptance or denial decision regarding manuscript will be sent to corresponding author. Manuscript that was not accepted for publication will not be returned to corresponding author.
8. Studies based on animal experiments should include an approval statement of Ethical Committee in the materials and methods section of manuscript. A copy of Ethical Committee Certificate must be sent to Editor for accepted manuscript for publication so that manuscript can be printed in the journal.
9. Veterinary Journal of Ankara University uses double-blind review procedure, which both the reviewer and author identities are concealed from each other throughout process. Authors approve to submit their manuscript in compliance with the double-blind review policy.
10. Authors are responsible for the article published in the journal.
11. Studies comparing products with trade name are not interest of this journal.
12. Any materials or products used in the study should not include their trade names.

Copyright Release

Authorship depends on following 3 conditions.

1. Individuals should make a substantial contribution to the conception and design of the study, the acquisition of the data used in the study, or the analysis and interpretation of that data.
2. Individuals should involve in drafting or revising the manuscript critically for important intellectual content.
3. Individuals should have an opportunity to approve subsequent revisions of the manuscript, including the version to be published.

All 3 conditions must be met. Acquisition of funding, collection of data, or general supervision of the research team does not, alone, justify authorship.

For multi-institutional studies, the individual who headed the study should be listed as an author, along with individuals who provided assistance with pathological and statistical analyses and any other individual who had a substantial impact on the study design or made a unique contribution to the study.

The undersigned authors release "Ankara Üniversitesi Veteriner Fakültesi Dergisi" from all responsibility concerning the manuscript entitled;

Title of manuscript: .....

.....

.....

upon its submission to the publishing commission of "Ankara Üniversitesi Veteriner Fakültesi Dergisi".

The undersigned author/s warrant that the article is original, is not under consideration by another journal, has not been previously published as whole or in part except abstract not exceeding 250 words, any permission necessary to publish it in the above mentioned journal has been obtained and provided to the "Ankara Üniversitesi Veteriner Fakültesi Dergisi". We sign for and accept responsibility for releasing this material.

Copyright to the above article is hereby transferred to "Ankara Üniversitesi Veteriner Fakültesi Dergisi", effective upon acceptance for publication.

Must be signed by all author/s

Authors names & titles	Signature	Date
.....		
.....		
.....		
.....		
.....		

Address for correspondence:

.....

.....

.....

Ankara Üniversitesi Veteriner Fakültesi Dergisi

ISSN 1300-0861 • E-ISSN 1308-2817 Volume 70 • Number 1 • Year 2023

Ankara Univ Vet Fak Derg - vetjournal.ankara.edu.tr - Open Acsess